# FINITE ELEMENT STRESS ANALYSIS OF PIPE BENDS USING DOUBLY CURVED SHELL ELEMENTS

by

RAGHUNATHA NATARAJAN, B.Sc.(Engg) Hons., M.Tech.

A Thesis submitted for the award of the
Degree of Doctor of Philosophy in the
Faculty of Engineering, London University.

Department of Mechanical Engineering,
City and Guilds College,
Imperial College of Science and Technology,
University of London.

April, 1971.

## ABSTRACT

Many accurate calculation methods have been evolved for analysing the flexibility of pipeline systems but the flexibility and stress factors of the curved pipes have not been theoretically derived taking into account the effect of the pipes and flanges to which they are normally attached. The calculation of these factors including the effect of attached pipes and flanges has been carried out using curved shell finite elements.

A doubly curved quadrilateral shell finite element has been developed for the analysis of thin shells of arbitrary geometry. The solution of the resulting large number of unknowns has been discussed briefly.

Three different shapes of this curved shell element, two orders of isoparametric three dimensional elements and a ring element with assumed displacement functions in the form of trigonometric functions have been considered in the solution of the problem of a 90 deg-bend under in-plane moment. These results have been compared with a known numerical solution to determine their accuracy. The solution computer times and core storage necessary while solving the pipe bend problem have also been recorded.

A comparison of the quartic type of curved shell elements with some other curved shell elements to be found in the literature has also been presented.

The effect of the end conditions on bends has been studied by analysing 90 deg-bends under in-plane moments with the ends terminated by tangents or with a tangent on one end and a rigid flange on the other. The quartic shell element model has been found to be the most

suitable for these calculations. Various bend angles with straight pipes as end restraints have also been studied.

Consideration is given to the application of the results of this investigation to the design of piping systems.

ACKNOWLEDGEMENTS

I would like to acknowledge with gratitude the valuable guidance, help and encouragement from my supervisor, Dr. J.A. Blomfield.

I would also like to thank the Computer Staff at Imperial College for their co-operation.

Grateful acknowledgement is made to the British Council and the Indian Institute of Technology, New Delhi who made it possible for me to work on this project under the Colombo Plan Fellowship.

R. Natarajan.

London

April 1971.

CONTENTS


| | | Page No. |
|---|---|---|
| ABSTRACT | | 2 |
| ACKNOWLEDGEMENTS | | 4 |
| CONTENTS | | 5 |
| NOMENCLATURE | | 8 |
| INTRODUCTION | | 11 |
| CHAPTER 1 | Review of Finite Element Method Applied to General Shell Structures | 15 |
| CHAPTER 2 | Theory of a Thin Doubly Curved Shell Element | 19 |
| 2.1 | Introduction | 19 |
| 2.2 | Description of The Basic Theory of The Element | 20 |
| 2.2.1 | Geometry | 20 |
| 2.2.2 | Displacement Field | 23 |
| 2.2.3 | Shell Assumptions | 26 |
| 2.2.4 | Convergence Criteria | 26 |
| 2.2.5 | Shape Functions of Middle Surface | 27 |
| 2.3 | Stiffness Formulation | 27 |
| 2.3.1 | Strain Displacement Relations | 27 |
| 2.3.2 | Stress Strain Relations | 32 |
| 2.3.3 | Stiffness Matrix | 33 |
| 2.3.4 | Economical Use of Elasticity Matrix | 34 |
| 2.4 | Stress Matrix | 34 |
| 2.5 | Consistent Force Matrix | 35 |
| CHAPTER 3 | Assembly and The Solution of The Equilibrium Equations | 37 |
| 3.1 | Practical Aspect of The Computer Algorithms | 38 |
| 3.1.1 | Block Diagram | 40 |
| 3.2 | Techniques to Economise the Computer Solution Time | 41 |

Page No.


| | | |
|---|---|---|
| CHAPTER 4 | Stress Analysis of Curved Tubes Under In-plane Moment | 42 |
| 4.1 | Proposed Finite Element Analysis | 43 |
| 4.2 | Statement of The Analysed Problem | 44 |
| 4.3 | Analysis Using Three Dimensional Elements | 45 |
| 4.3.1 | Comparison of Different Orders of Gaussian Quadrature Formulae | 47 |
| 4.4 | Analysis Using Doubly Curved Shell Elements | 48 |
| 4.4.1 | Comparison of Different Orders of Gaussian Quadrature Formulae | 49 |
| 4.4.2 | Comparison of Quadratic, Cubic and Quartic Shell Elements | 52 |
| 4.5 | Study of Quartic Shell Elements | 53 |
| 4.6 | Analysis Using a Ring Element | 53 |
| 4.7 | Flexibility and Stress Factors | 55 |
| CHAPTER 5 | Comparison of Results of the Curved Shell Element with Few Other Existing Shell Elements | 58 |
| 5.1 | Comparison with a Shallow Shell Element | 58 |
| 5.2 | Comparison with a Curved Triangular Element | 60 |
| 5.3 | Summary of Quartic Element Versus Other Curved Elements | 61 |
| CHAPTER 6 | Stress Analysis of Pipe Bend Structures With Shell Finite Elements | 63 |
| 6.1 | Introduction | 63 |
| 6.2 | Finite Element Idealisation of the Problem | 64 |
| 6.3 | 90 Degree Bend With Ends Terminated by Tangents | 65 |

| | | Page No. |
|---|---|---|
| 6.4 | 180 Degree Bend With Ends Terminated by Tangents | 69 |
| 6.5 | Variation In Flexibility and Stress Factors With Arc Lengths of Bends | 70 |
| 6.6 | 90 Degree Bend With A Straight Section on One End and Flange on the Other | 72 |
| 6.6.1 | Note On a 90 Degree Bend With Both Ends Terminated By Flanges | 73 |
| 6.7 | Reversed 90 Degree Bends | 74 |
| 6.8 | Discussion of Results and Design Considerations | 75 |
| CHAPTER 7 | Conclusions and Recommendations for Future Work | 80 |
| REFERENCES | | 84 |
| APPENDICES | | |
| APPENDIX A | Theory of Isoparametric Three-Dimensional Element | 90 |
| APPENDIX B | Shape Functions for Three-Dimensional Isoparametric Elements | 103 |
| APPENDIX C | Shape Functions for Curved Shell Elements | 106 |
| APPENDIX D | Computer Program Listing Used for the Solution of Pipe Bend Problems | 109 |
| APPENDIX E | Shape Functions for A Ring Element | 162 |
| APPENDIX F | Moment Calculation | 164 |
| APPENDIX G | Calculation of Flexibility | 166 |
| TABLES 3.1 and 3.2 | | 167 |
| TABLE 6.1 | | 168 |
| FIGURES | | 169 |

## NOMENCLATURE

| | |
|---|---|
| $[\ ]$ | Rectangular Matrix |
| $\{\ \}$ | Column Matrix |
| $[BR]^T$ | Transpose of [BR] |
| $\vec{A}$ | Vector A |
| $\hat{A}$ | Unit vector A |
| $\vec{A} \times \vec{B}$ | Vector product of the two vectors A and B |
| $\vec{A} \cdot \vec{B}$ | Scalar product of the two vectors A and B |
| a | Radius of bend |
| b | Pipe bore radius |
| Det[J] | Determinant of J matrix |
| dV | Elemental volume of an element |
| dA | Elemental area on the surface of the element |
| E | Modulus of Elasticity |
| $\{F_i\}$ | Vector of element nodal forces |
| I | Second moment of Inertia of pipe cross-section |
| [J] | Jacobian Matrix |
| [K] | Stiffness Matrix |
| K | Flexibility factor |
| $\ell$ | Length of tangent pipes attached to ends of a bend |
| M | Applied in-plane moment on a bend |
| $N_i$ | Interpolation coefficients, functions of $\xi$ and $\eta$ |
| r | Radius of point of bend mid wall relative to axis of revolution |
| t | Thickness of the shell element |
| [TR] | Transformation matrix between $\delta_i$ and $\delta R_i$ |
| $u_x$, $u_y$, $u_z$ | Displacements in x, y and z directions |
| $u_\xi$, $u_\eta$, $u_\zeta$ | Displacements in $\xi$, $\eta$ and $\zeta$ directions |

| | |
|---|---|
| $x, y, z$ | Global cartesian coordinate system, right handed |
| $x', y', z'$ | Element local rectangular coordinate system |
| $\alpha_i, \beta_i$ | Rotations of nodal normal vector about $\hat{v}_{2i}$ and $-\hat{v}_{1i}$ |
| $\gamma_{x'y'}$, $\gamma_{x'z'}$, $\gamma_{y'z'}$ | Shearing strains in the local coordinates |
| $\gamma = b/a$ | Ratio, bore radius to pipe radius. |
| $\{\delta_i\}$ | Vector of element nodal deflections in global directions |
| $\{\delta R_i\}$ | Vector of element nodal deflection in $\xi$, $\eta$ and $\zeta$ directions |
| $\varepsilon_{x'}, \varepsilon_{y'}$ | Strains in the local x' and y' directions |
| $\eta^*$ | A ratio, flexibility factor/$\hat{\sigma}$ |
| $[\theta_i] = [\hat{v}_{1i}, \hat{v}_{2i}, \hat{v}_{3i}]$ | Three mutually perpendicular unit vectors at any node i |
| $\theta$ | Angle between radius r and normal to shell middle surface, $\theta$ = O at intrados |
| $\lambda = at/b^2$ | Pipe factor |
| $\nu$ | Poisson's ratio |
| $\xi, \eta, \zeta$ | Natural non-dimensional coordinates, right handed |
| $\sigma_\xi, \sigma_\eta$ | Normal stress along $\xi$ and $\eta$ direction |
| $\sigma_{x'}, \sigma_{y'}$ | Normal stress in the local x', y' directions |
| $\hat{\sigma} = (I/Mb)\bar{\sigma}$ | Maximum equivalent stress factor |
| $\bar{\sigma}$ | Equivalent stress |
| $\tau_{\xi\eta}$, $\tau_{\eta\zeta}$, $\tau_{\zeta\xi}$ | Shear stresses |
| $\tau_{x'y'}$, $\tau_{x'z'}$, $\tau_{y'z'}$ | Shearing stresses in the local coordinate system |

| | |
|---|---|
| $\phi$ | Function to be extrapolated, may be displacements or coordinates |
| $\psi$ | Angle around pipe bend |

# INTRODUCTION

Various calculation methods have been developed so that in designing the layout of pipe lines, sufficient flexibility can be provided to accommodate thermal expansion without inducing excessive stresses. The basis of all the different methods of flexibility analysis is to consider the pipe line as a structure with displacements imposed at the various anchor points, these being equal and opposite to the expansion which would occur if the ends of the pipe line were not fixed. The pipe line consists of straight or tangent lengths of pipe and sections of curved pipe usually known as pipe bends. While simple bending theory may be directly applied to the straight lengths, the behaviour of curved pipe subjected to bending is more complex, providing a greater flexibility but involving higher stresses than indicated by simple theory [57]. This is taken into account in most methods of piping flexibility analysis by the use of flexibility factors relating the flexibility of the curved pipe to that obtained in a straight pipe of the same arc length and cross-section and subjected to the same bending moment. In a similar way, stress intensification factors are used to give the maximum stresses in terms of that calculated by simple bending theory.

The literature relating to the elastic stress analysis of pipe bends is extensive and references [41] and [42] contain a comprehensive survey for the so-called 'long radius bend' (pipe mid-wall radius b small compared with bend radius a). Due to the more varied requirements of modern technology more sharply curved pipes have been increasingly used which have required a more accurate evaluation of pipe line stresses. Turner and Ford [46] published a theory for in-plane bending which eliminated many of the simplifying assumptions previously

made. More recently Jones [43] extended Von Kármán's analysis to analyse short radius bends under in-plane moment. The effect of pressure was included in the analysis by Kafka and Dunn [58] and by Rodabaugh and George [59]. Smith [60] applied the Turner and Ford method of analysis to out-of-plane bending of a curved tube.

All these theoretical results were limited because of the various approximations and assumptions made during the formulation and solution of the problem. Hence it would be desirable to employ a new approach that could combine all the significant effects needed for the analysis of curved tubes, including the effects of end constraints. Moreover the experimental results presented in reference [53] show clearly that for a 90° bend with flanges the theory that does not account for the end effects can overestimate the flexibility and stress intensification factors by a factor of 2 or more. It was also concluded in reference [53] that, when the end effects were important, then the flexibility of the bend also depends on the total bend angle of the elbow, which is not predicted by the usual theory.

On the basis of such experimental evidence, it would be important to employ a general approach that would be valid for any tube bore and bend radius and would account for all end effects.

Now that the digital computers are more readily available, numerical methods of solution have become the preferred method for solution for many structural problems. Furthermore rigorous piping flexibility analyses of the more complex configurations are now possible.

It is described in this thesis how the finite element displacement method has been used to analyse curved tubes with end constraints.

The finite element method is a completely general approach for the solution of problems in continuum mechanics and was introduced in the fifties [1] [2]. This method was first applied to the solution of

plane stress problems [3] and subsequently was extended to the analysis of axisymmetric solids and plate bending problems [4]. Since then there has been a concurrent and rapid development of electronic computers, matrix methods and finite element techniques. Several important conferences have been devoted exclusively to these subjects [5] [6]. The first textbooks have appeared [7] [8] and a fairly general formulation of the finite element method in stress analysis can be obtained from references [9] and [10].

A formulation for a curved arbitrary shape of shell was developed by Ahmad [28]. In the work to be described (Chapter 2) the procedure for calculating the stiffness coefficients has been modified so that the element is suitable for analysing thin shell structures. By prescribing different degrees of polynomials for displacements in the element, higher order elements can be generated. Three different orders of this element have been considered.

A computer program based on a simplified version of the Front Solution Method [32] has been developed so that it applies to general shell structural problems.

The accuracy of these three orders of elements has been compared, by applying each of them to a problem of a curved pipe subjected to an in-plane moment, and hence an economical element chosen. The accuracy of this chosen curved shell element has been further compared with other types of curved shell elements. A complete ring element using trigonometric functions to represent the displacements and geometry has also been developed and its accuracy compared with the curved shell element. This study of the curved pipe has also been helpful in obtaining information about the performance of the adopted solution technique. The same pipe bend problem was also solved using isoparametric three dimensional elements so that an idea can be obtained of

the accuracy that can be achieved if these elements are used in solving shell structural problems.

A program has been developed, using the curved shell elements and the adopted version of the Front Solution technique, to analyse curved pipes of different included angles and end restraints. This has been used to study the effects of end constraints, such as tangent pipes and flanges, on the flexibility and stress factors of the curved pipes. This has been done for a 90° bend subjected to in-plane bending for a range of $\lambda$ (pipe factor = $at/b^2$) values. Curved pipes of different included angles have been analysed in order to study the effect of the total angle of bend on the flexibility and stress factors. Further a study was conducted to find whether the flexibility factor of a bend depends on the type of loading and the ratio $\gamma$ (b/a = bore radius/ pipe radius). The movement of the location of the maximum stress concentration around the circumference of the pipe due to end constraints has also been studied.

A comparison of the theoretically predicted flexibility and stress factors with some published experimental values has been made.

The results from these studies have been analysed and conclusions have been reached so that piping-flexibility analysis procedures can be improved.

# CHAPTER 1

## REVIEW OF FINITE ELEMENT METHOD APPLIED TO GENERAL SHELL STRUCTURES

The widespread use of thin shell structures has created a need for a systematic method of analysis which can adequately account for arbitrary geometric form and boundary conditions as well as ~~arbitrary~~ general types of loading. Classical thin shell theory yields differential equations of equilibrium or continuity whose complexity depends greatly on the shell geometry and whose solution is a function of the geometric position of the boundary and the type of force or displacement quantity which must be satisfied there. Hence, the complications caused by geometry and boundary conditions together with variable thickness, variable material properties, discontinuities in the shell surface and general loading disqualify the classical approach as a systematic method of analysis for most real problems. With the aid of a digital computer different numerical procedures such as finite difference and numerical integration methods have been suggested for more general shell shapes. These methods are, however, still limited to special shell geometries.

The finite element method, which was introduced in the fifties, is a completely general approach for the solution of problems in stress analysis. During the last few years great efforts have been made to solve shell problems by the finite element displacement method. This analysis can be attempted by two methods. The first method applies to shells of revolution and a variety of different shell elements have been published [11] [12] [13].* The second method consists of the idealisation of the continuous surface as an assemblage of discrete curved elements.

---

* Numbers in brackets [ ] indicate references.

A simple type of element under the latter method is a planar element. The bending behaviour of such an element is accounted for by plate flexure considerations, the membrane behaviour by including plane-stress stiffness. The membrane action and the bending action are uncoupled within each element. The use of flat plate elements for analysis of shells was first presented in [14] and [15]. Clough and Johnson [16] used the constant strain triangular element and a fully compatible nine-degree of freedom plate bending triangular element to show that excellent solutions can be obtained with reasonable mesh refinements. However, for shells having complex straining it was necessary to employ very fine subdivisions in order to achieve the desired accuracy. Thus for a shell structure the geometric discretization errors introduced by using planar elements must be considered. The use of refined planar elements may prove advantageous [17] [18] for shell structures with smooth geometries. However, for shells with complex geometries the discretization errors may offset the benefit of such a refined element. Curved elements would enable the shell geometries to be more accurately matched.

Very little has been published about curved shell elements. This is mainly due to the difficulties encountered in providing for the rigid body displacements. Utku [19] has proposed an element stiffness matrix for a shallow triangular element using linear functions to represent the displacements and reducing geometrical idealisation errors by taking into account average curvatures of the middle surface. Connor and Brebbia [20] have developed a stiffness matrix for a thin shallow shell element of rectangular plan. The displacement patterns do not contain all the rigid body displacements of a curved shell element. On the same lines, that is, explicitly including the coupling between membrane and bending effects by using shallow shell theory to

relate strains and displacements [20], Ford [21] developed a higher order shallow shell element. In reference [22] a shallow cylindrical shell element has been developed accounting for the rigid body displacement using trigonometric functions. Dupuis and Goël [23] have formulated using tensor notations, a shallow shell element representing rigid body displacements. The representation of the true rigid body displacement is violated when numerical integration is used for calculating the stiffness coefficients, but the representation improves as the mesh size is made finer. Argyris [24] has published a doubly curved triangular shell element representing rigid body motions exactly and satisfying interelement compatibility.

In the late sixties, Irons and others have developed [25] the so-called Iso-parametric element families for two and three dimensional analysis in conjunction with numerical integration [26]. A comprehensive description of the elements developed is available in references [9] and [10]. This study has been extended to axisymmetric shells of revolution [27] and arbitrary thick shell elements [28]. The thick shell element is fully compatible and rigid body displacements are also represented truly. Further this numerically integrated element approximates the geometry better and includes the effect of shear deformations. It is also possible, in this formulation, to develop higher order elements, by placing larger numbers of nodes on the surfaces of an element.

The finite element displacement method, so far described, is today well-known and proved to be superior to the equilibrium method, particularly in solving structural problems. However great difficulties are sometimes encountered in this method, particularly in the field of shells. To overcome some of the difficulties element characteristics have been evaluated by the combination of variational principles and different boundary continuity conditions. Pian [31] has indicated the alterna-

tive schemes. The development of mixed models for plates and shells have also been discussed in references [29] and [30].

A curved thin shell element has been developed, in Chapter 2, on the lines similar to that in reference [28] for the analysis of pipe bends. The accuracy of this thin shell element has been compared, in Chapter 5, with the elements described in references [21] and [24].

# CHAPTER 2

# THEORY OF A THIN DOUBLY CURVED SHELL ELEMENT

## 2.1 Introduction

The basic concept of the finite element method is the idealisation of the continuum as an assemblage of discrete structural elements. The idealisation governs the type of element which must be used in the solution. The shell structural analysis can be attempted using the curvilinear isoparametric three-dimensional elements coupled with numerical integration as shown in Appendix A. With a straightforward use of the three-dimensional concept, however, certain difficulties will be encountered. In the first place the retention of three degrees of freedom at each node leads to large stiffness coefficients for relative displacements along an edge corresponding to the shell thickness. This presents numerical problems and inevitably leads to ill-conditioned equations when shell thicknesses become small compared with the other dimensions in the element. The second factor is the use of several nodes across the shell thickness ignores the well-known ~~fact~~ assumption that the normals to the middle surface remain straight after deformation. Thus an unnecessary high number of degrees of freedom has to be carried, involving penalties of computer time.

Overcoming the difficulties of using a three-dimensional element, an arbitrary thin doubly curved shell element has been formulated on the lines of Ahmad's thick shell element [28]. This numerically integrated shell element is a fully compatible one with rigid body modes included so that there is monotonic convergence and global equilibrium satisfaction. Further it includes the effect of shear deformation. By a judicious definition of unique orthogonal axes at the nodal points, the five degrees of freedom at each nodal point, three translations and

two rotations, have certain physical meaning which allows the boundary conditions to be defined exactly.

The specific advantages of the present element over that of Ahmad's, when used in thin shell structural analysis ~~have been~~ Will be pointed out, whilst outlining the present theory.

## 2.2 Description of the Basic Theory of the Element

### 2.2.1 Geometry

The actual shell surface has been merely subdivided into a specified number of regions (elements) resulting in a doubly curved element. For such a typical shell element, the external faces are curved, while the sections across the thickness are generated by straight lines. The geometry of the elements is defined by the nodal coordinates specified and the shape functions used. For example if the coordinates of the nodes on the mid-surface and the thickness of the element at these nodal points are specified, then the element can represent any warped surface depending on the number of nodes on any edge.

Let $\xi,\eta$ be two curvilinear coordinates in the middle plane of a shell element and $\zeta$ a linear coordinate in the thickness direction varying between -1 and +1 on the respective faces of the element as shown in Figure 2.1(b).

The relationship between the cartesian coordinates and the curvilinear coordinates, which has to be established, will be written as

$$\begin{Bmatrix} x \\ y \\ z \end{Bmatrix} = \sum N_i(\xi,\eta) \begin{Bmatrix} x_i \\ y_i \\ z_i \end{Bmatrix}_{\text{mid-surface}} + \sum N_i(\xi,\eta) \frac{\zeta}{2} \vartheta_{3i} t_i \qquad (2.1)$$

where $i = 1$ to $n$, where $n$ is the total number of nodes and $N_i$ are functions

of $\xi$ and $\eta$ only, taking a value of unity at the node i and zero at all other nodes, and discussed later. $t_i$ is the thickness of the element at node i and given as

$$t = \Sigma N_i t_i \tag{2.2}$$

For any value of $\xi$, $\eta$ and $\zeta$, the x, y and z coordinates can be found once the functions $N_i$ are known. As the x, y and z coordinates have been defined parametrically in terms of $\xi$, $\eta$ and $\zeta$, the side faces of an element can be parabolically, cubically or quartically curved as well as warped according as the element is of the type shown in Figures 2.1, 2.2 or 2.3 respectively. These are the three types of elements that will be used in the analysis later.

To satisfy the continuity at interfaces, it is necessary for x, y and z to be uniquely defined over the sides of the element by the coordinates of the nodes on that side only. Since $N_i$ for nodes not on that face is zero, the variation of coordinates on that side for both elements will be identical.

$\hat{v}_{3i}$ is a unit vector normal to the middle surface as defined by the approximating polynomial

$$\begin{Bmatrix} x \\ y \\ z \end{Bmatrix} = \Sigma N_i \begin{Bmatrix} x_i \\ y_i \\ z_i \end{Bmatrix}_{\substack{\text{mid-} \\ \text{surface}}} \tag{2.3}$$

at the node i and calculated with the help of the tangential vectors along $\xi$ and $\eta$ directions in the middle surface at node i, rather than defining it by the top and bottom coordinates of the normal at the node i as in reference [28].

In the former case the coordinates of the mid-surface node and local thickness is required as input data, that is, only four quantities, whereas in the latter case six quantities are required. It is clear that this is an advantage in the case of thin shells in which the mid-surface is defined rather than the inner and outer surface.

Unique Orthogonal Axes Including Normal Vector At Any Node

Let $\hat{v}_{1i}$ and $\hat{v}'_{2i}$ be the unit vectors on the middle surface along $\xi$ and $\eta$ directions respectively at the node i on the face $\eta = +1$ or $-1$ (Figure 2.4). If the position vector of any point i on the middle surface is given by

$$M = \hat{i}\, x + \hat{j} y + \hat{k} z \tag{2.4}$$

where $\hat{i}$, $\hat{j}$ and $\hat{k}$ are the unit vectors along x, y and z directions respectively, then

$$\hat{v}_{1i} = \hat{i}\,\frac{\partial x}{\partial \xi} + \hat{j}\,\frac{\partial y}{\partial \xi} + \hat{k}\,\frac{\partial z}{\partial \xi} \Bigg/ \sqrt{\left(\frac{\partial x}{\partial \xi}\right)^2 + \left(\frac{\partial y^2}{\partial \xi}\right) + \left(\frac{\partial z}{\partial \xi}\right)^2} \tag{2.5}$$

and

$$\hat{v}'_{2i} = \hat{i}\,\frac{\partial x}{\partial \eta} + \hat{j}\,\frac{\partial y}{\partial \eta} + \hat{k}\,\frac{\partial z}{\partial \eta} \Bigg/ \sqrt{\left(\frac{\partial x}{\partial \eta}\right)^2 + \left(\frac{\partial y}{\partial \eta}\right)^2 + \left(\frac{\partial z}{\partial \eta}\right)^2} \tag{2.6}$$

The normal vector to the middle surface at this node can then be found by the vector product of $\hat{v}_{1i}$ and $\hat{v}'_{2i}$ and given by

$$\hat{v}_{3i} = \frac{\hat{v}_{1i} \times \hat{v}'_{2i}}{\sin \chi} \tag{2.7}$$

where $\chi$ is the angle between $\hat{v}_{1i}$ and $\hat{v}'_{2i}$ and is easily obtained from the scalar product of $\hat{v}_{1i}$ and $\hat{v}'_{2i}$ vectors and given as

$$\cos \chi = \hat{v}_{1i} \cdot \hat{v}'_{2i} \tag{2.8}$$

If $\hat{v}_{2i}$ is taken as a unit vector ~~parallel to $\hat{v}'_{2i}$ and~~ perpendicular to $\hat{v}_{3i}$ and $\hat{v}_{1i}$ then

$$\hat{v}_{2i} = \hat{v}_{3i} \times \hat{v}_{1i} \tag{2.9}$$

Thus $$[\theta_i] = [\hat{v}_{1i}, \hat{v}_{2i}, \hat{v}_{3i}] \tag{2.10}$$

constitute three unique mutually perpendicular unit vectors at the node i with $\hat{v}_{3i}$ vector normal to the middle surface and $\hat{v}_{1i}$ and $\hat{v}_{2i}$ acting respectively along and normal to the face $\eta = +1$ or $-1$.

Similarly on the face $\xi = +1$ or $-1$ at any node j, $\hat{v}_{2j}$ is taken along $\eta$ direction and $\hat{v}_{3j}$ normal to the middle plane.

### 2.2.2 Displacement Field

Since in shell theory all parameters are usually defined in terms of middle surface variables only, it is now necessary to define the variation of the global displacement components $u_x$, $u_y$ and $u_z$ in terms of the nodal displacements $(u_x, u_y, u_z)_i$ and two rotations $(\alpha,\beta)_i$ of the nodal normal vector $\hat{v}_{3i}$ about $\hat{v}_{2i}$ and $-\hat{v}_{1i}$ respectively (Figure 2.4). The same functions $N_i$ as in expression 2.1 can again be used to obtain the variation of displacements within the element, thus assuring compatibility of displacements at interfaces of the elements.

We can now write

$$\begin{Bmatrix} u_x \\ u_y \\ u_z \end{Bmatrix} = \Sigma N_i \begin{Bmatrix} u_x \\ u_y \\ u_z \end{Bmatrix}_i + \Sigma N_i \zeta \frac{t_i}{2} [\hat{v}_{1i} \hat{v}_{2i}] \begin{Bmatrix} \alpha \\ \beta \end{Bmatrix}_i \tag{2.11}$$

Thus at each node i, there are five components of variables, given as

$$\{\delta_i\} = \begin{Bmatrix} u_x \\ u_y \\ u_z \\ \alpha \\ \beta \end{Bmatrix}_i \tag{2.12}$$

The above definition of $\hat{v}_{1i}$ and $\hat{v}_{2i}$ means that the rotations $\alpha$ and $\beta$ can be interpreted physically as the local rotations on any element edge forming the boundary of the structure. This is not possible when these vectors are defined with respect to the global coordinates as in reference [28] unless additional transformations are made.

Comparing equation 2.11 with 2.1, it is seen that the definition of the coordinates is more general than that of the displacements but includes it as a special case. Hence the elements are of Superparametric type in distinction to Isoparametric elements as described in Appendix A.

Arranging expression 2.11 in the matrix form, we have

$$\begin{Bmatrix} u_x \\ u_y \\ u_z \end{Bmatrix} = \begin{bmatrix} N_1 & 0 & 0 & N_1\zeta\frac{t_1}{2}\hat{v}_{1x_1} & N_1\zeta\frac{t_1}{2}\hat{v}_{2x_1} & - & - & - \\ 0 & N_1 & 0 & N_1\zeta\frac{t_1}{2}\hat{v}_{1y_1} & N_1\zeta\frac{t_1}{2}\hat{v}_{2y_1} & - & - & - \\ 0 & 0 & N_1 & N_1\zeta\frac{t_1}{2}\hat{v}_{1z_1} & N_1\zeta\frac{t_1}{2}\hat{v}_{2z_1} & - & - & - \end{bmatrix}$$

$$\begin{bmatrix} N_i & 0 & 0 & N_i\zeta\frac{t_i}{2}v_{1x_i} & N_i\zeta\frac{t_i}{2}v_{2x_i} & - & - & - \\ 0 & N_i & 0 & N_i\zeta\frac{t_i}{2}v_{1y_i} & N_i\zeta\frac{t_i}{2}v_{2y_i} & - & - & - \\ 0 & 0 & N_i & N_i\zeta\frac{t_i}{2}v_{1z_i} & N_i\zeta\frac{t_i}{2}v_{2z_i} & - & - & - \end{bmatrix}$$

$$* \begin{Bmatrix} u_{x_1} \\ u_{y_1} \\ u_{z_1} \\ \alpha_1 \\ \beta_1 \\ \vdots \\ u_{x_i} \\ u_{y_i} \\ u_{z_i} \\ \alpha_i \\ \beta_i \\ \vdots \end{Bmatrix}$$

$$= [N] \quad \{\delta\}^e \tag{2.13}$$

where [N] is the shape function matrix

$\hat{v}_{1x_i}$ is the component of unit vector $\hat{v}_{1i}$ along x direction

etc.

### 2.2.3 Shell Assumptions

(1) Normals to the deformed surface remain straight and inextensible when deformed but not necessary normal.

(2) Stresses normal to the mid-surface are assumed small enough to be neglected.

Thus the shell element is allowed to experience shear deformations and at the same time avoiding unnecessary number of degrees of freedom across the thickness, if a three-dimensional element is used in its place.

### 2.2.4 Convergence Criteria

For the convergence of finite element analysis, the two criteria to be satisfied [7] are

1) the assumed displacements must be continuous over each element and across element boundaries.

2) any required state of constant strain can be adequately reproduced on the element.

It has already been pointed out that the displacement compatibility is achieved by the definition of the shape functions. The most vital states of constant strain, that is, the states of zero strain - the rigid body motions - remain available as for the Isoparametric case. The only degeneracy introduced constrains the points along the nodal normals to remain in a straight line and inextensible, a condition automatically present in a case of true rigid body motion.

Invariance of the element stiffness is obtained since it has been formulated using local natural non-dimensional coordinates.

### 2.2.5 Shape Functions of Middle Surface

From expressions 2.1 and 2.11, it was seen that with $\zeta = 0$ on the middle surface, a two-dimensional curved surface defined by coordinates $\xi,\eta$ could be easily mapped into a three-dimensional cartesian space. The given middle surface of an element is taken to be represented by anyone of the three, two-dimensional curved spaces, illustrated in Figure 2.5 depending on the order of elements required. It is well known that for the first kind of elements the functions are parabolic, for the second cubic, and for the third quartic, in $\xi$ and $\eta$ and thus the curved mid-surface of the shell element can take up a parabolic, cubic or quartic form respectively. The shape function expressions for these three types [38] are given in Appendix C.

## 2.3 Stiffness Formulation

Having defined the geometry and displacement field in a shell element, we can now proceed to the various relations necessary for calculating its stiffness matrix.

### 2.3.1 Strain Displacement Relations

Since expression 2.11 relates the global displacements $u_x$, $u_y$, $u_z$ to the curvilinear coordinates, the derivatives of these displacements with respect to the global coordinates, required for the definition of strains at any point in the element, are given by a matrix relation:

$$\begin{bmatrix} \frac{\partial u_x}{\partial x} & \frac{\partial u_y}{\partial x} & \frac{\partial u_z}{\partial x} \\ \frac{\partial u_x}{\partial y} & \frac{\partial u_y}{\partial y} & \frac{\partial u_z}{\partial y} \\ \frac{\partial u_x}{\partial z} & \frac{\partial u_y}{\partial z} & \frac{\partial u_z}{\partial z} \end{bmatrix} = [J]^{-1} \begin{bmatrix} \frac{\partial u_x}{\partial \xi} & \frac{\partial u_y}{\partial \xi} & \frac{\partial u_z}{\partial \xi} \\ \frac{\partial u_x}{\partial \eta} & \frac{\partial u_y}{\partial \eta} & \frac{\partial u_z}{\partial \eta} \\ \frac{\partial u_x}{\partial \zeta} & \frac{\partial u_y}{\partial \zeta} & \frac{\partial u_z}{\partial \zeta} \end{bmatrix} \tag{2.14}$$

where [J] is the Jacobian matrix, defined as

$$[J] = \begin{bmatrix} \frac{\partial x}{\partial \xi} & \frac{\partial y}{\partial \xi} & \frac{\partial z}{\partial \xi} \\ \frac{\partial x}{\partial \eta} & \frac{\partial y}{\partial \eta} & \frac{\partial z}{\partial \eta} \\ \frac{\partial x}{\partial \zeta} & \frac{\partial y}{\partial \zeta} & \frac{\partial z}{\partial \zeta} \end{bmatrix} \tag{2.15}$$

The Jacobian matrix can be obtained explicitly from the expression 2.1 which will differ numerically from the corresponding Jacobian in reference [28] because of the different definitions used for the vector $\hat{v}_{3i}$.

To be consistent with the second shell assumption stated in Section 2.2.3, we have to neglect the strain in a direction normal to the surface at all points. This necessitates the transformation of the global derivatives of displacements to the derivatives along local axes x', y', z', the directions of which are shown in Figure 2.6. The local directions are defined so as to be consistent with the definitions of $\hat{v}_{1i}$, $\hat{v}_{2i}$ and $\hat{v}_{3i}$ given by equation 2.10.

This local set of orthogonal axes are created as follows at the point under consideration:

Let $\vec{x}'$ and $\vec{y}^*$ be vectors tangent to a local membrane surface located at a distance $\zeta$ = constant from the mid-surface and along $\xi$ and $\eta$ directions respectively. Then a vector $\vec{z}'$ normal to the local membrane surface is obtained by the vector product of $\vec{x}'$ and $\vec{y}^*$ vectors and given by

$$\vec{z}' = \vec{x}' \times \vec{y}^* \tag{2.16}$$

Further if $\hat{y}'$ is a unit vector ~~parallel to $\hat{y}^*$ and~~ perpendicular to $\hat{x}'$ and $\hat{z}'$ at the point of interest, then

$$\hat{y}' = \hat{z}' \times \hat{x}' \tag{2.17}$$

and thus they form the three mutually perpendicular axes with $\hat{z}'$ normal to the membrane surface at the point. It is of interest to note that $\hat{v}_1$, $\hat{v}_2$, $\hat{v}_3$ defined by equation 2.10 are the values of $\hat{x}'$, $\hat{y}'$ and $\hat{z}'$ on the mid-surface.

Hence a matrix of unit vectors in x', y', z' directions is constructed as: (which is in fact the direction cosine matrix)

$$[\theta] = [\hat{x}', \hat{y}', \hat{z}']$$

or

$$[\theta] = \begin{bmatrix} \cos(xx') & \cos(xy') & \cos(xz') \\ \cos(yx') & \cos(yy') & \cos(yz') \\ \cos(zx') & \cos(zy') & \cos(zz') \end{bmatrix} \tag{2.18}$$

where cos(xx') is the cosine of the angle between global x axis and local x' axis. The global derivatives of $u_x$, $u_y$ and $u_z$ are now transformed

to the derivatives along local orthogonal system by the following operation:

$$\begin{bmatrix} \frac{\partial u_{x'}}{\partial x'} & \frac{\partial u_{y'}}{\partial x'} & \frac{\partial u_{z'}}{\partial x'} \\ \frac{\partial u_{x'}}{\partial y'} & \frac{\partial u_{y'}}{\partial y'} & \frac{\partial u_{z'}}{\partial y'} \\ \frac{\partial u_{x'}}{\partial z'} & \frac{\partial u_{y'}}{\partial z'} & \frac{\partial u_{z'}}{\partial z'} \end{bmatrix} = [\theta]^T \begin{bmatrix} \frac{\partial u_x}{\partial x} & \frac{\partial u_y}{\partial x} & \frac{\partial u_z}{\partial x} \\ \frac{\partial u_x}{\partial y} & \frac{\partial u_y}{\partial y} & \frac{\partial u_z}{\partial y} \\ \frac{\partial u_x}{\partial z} & \frac{\partial u_y}{\partial z} & \frac{\partial u_z}{\partial z} \end{bmatrix} [\theta] \tag{2.19}$$

For the model taken, the total strain at any point [34] within the element is defined in the local orthogonal x', y', z' system as:

$$\{\varepsilon'\} = \begin{Bmatrix} \varepsilon_{x'} \\ \varepsilon_{y'} \\ \gamma_{x'y'} \\ \gamma_{x'z'} \\ \gamma_{y'z'} \end{Bmatrix} = \begin{Bmatrix} \partial u_{x'}/\partial x' \\ \partial u_{y'}/\partial y' \\ \partial u_{x'}/\partial y' + \partial u_{y'}/\partial x' \\ \partial u_{z'}/\partial x' + \partial u_{x'}/\partial z' \\ \partial u_{z'}/\partial y' + \partial u_{y'}/\partial z' \end{Bmatrix} \tag{2.20}$$

It is seen that the normal strain $\varepsilon_{z'}$ at the point under consideration has been neglected as required. From the matrix expression 2.19, by selecting proper terms, the local strains can be explicitly determined. This leads us to the definition of strain displacement matrix, given by:

$$\{\varepsilon'\} = [B'] \begin{Bmatrix} \{\delta_1\} \\ \{\delta_2\} \\ . \\ . \\ \{\delta_i\} \\ . \\ . \end{Bmatrix} ; \qquad \{\delta_i\} = \begin{Bmatrix} u_x \\ u_y \\ u_z \\ \alpha \\ \beta \end{Bmatrix}_i \tag{2.21}$$

With the definition of the three unit vectors $\hat{v}_{1i}$, $\hat{v}_{2i}$ and $\hat{v}_{3i}$ at any node i, - expression 2.10 - acting along and normal to a face and perpendicular to the mid-surface respectively, it is possible to define the known boundary conditions exactly for each element since usually in shell problems they are given along and normal to a side. This is made possible by transforming the global displacements at the nodes into displacements along the vectors given by equation 2.10.

The transformation matrix of displacements at a node i is given by

$$\begin{bmatrix} u_x \\ u_y \\ u_z \end{bmatrix}_i = [\Theta_i] \begin{bmatrix} u_\xi \\ u_\eta \\ u_\zeta \end{bmatrix}_i \tag{2.22}$$

where $[\Theta_i]$ is given by equation 2.10

$u_\xi$ is the displacement along local $\xi$ direction

$u_\eta$ is the displacement along local $\eta$ direction

and $u_\zeta$ is the normal displacement.

This transformation matrix has already been formed while defining the displacement field and hence no extra computation is necessary at this stage. Again it is seen that the present formulation ~~varies~~ differs from that given in reference [28].

Since the displacements have now been taken along the local directions at each node, the [B'] matrix given by equation 2.21 is to be modified. Hence

$$\{\varepsilon'\} = [BR'] \begin{Bmatrix} \{\delta R_1\} \\ \{\delta R_2\} \\ \vdots \\ \{\delta R_i\} \\ \vdots \end{Bmatrix} \quad ; \quad \{\delta R_i\} = \begin{Bmatrix} u_\zeta \\ u_\eta \\ u_\xi \\ \alpha \\ \beta \end{Bmatrix}_i \tag{2.23}$$

$$\text{and} \quad [BR'] = [B'] \, [TR] \tag{2.24}$$

[TR] being the complete transformation matrix defined by expression 2.22. Thus [BR'] is the modified strain displacement matrix used in the stiffness calculations.

### 2.3.2 Stress Strain Relations

The stresses $\{\sigma'\}$ along local orthogonal directions are related to the corresponding strains $\{\varepsilon'\}$ by elasticity matrix [D'].

Thus

$$\{\sigma'\} = \begin{Bmatrix} \sigma_{x'} \\ \sigma_{y'} \\ \tau_{x'y'} \\ \tau_{x'z'} \\ \tau_{y'z'} \end{Bmatrix} = [D'] \, \{\varepsilon'\} \tag{2.25}$$

[D'] matrix for an isotropic material can be written as

$$[D'] = \frac{E}{1-\nu^2} \begin{bmatrix} 1 & \nu & 0 & 0 & 0 \\ & 1 & 0 & 0 & 0 \\ & & \frac{1-\nu}{2} & 0 & 0 \\ \text{symmetric} & & & \frac{1-\nu}{2} & 0 \\ & & & & \frac{1-\nu}{2} \end{bmatrix} \tag{2.26}$$

in which E and $\nu$ are the Young's Modulus and Poisson's ratio respectively of the material.

### 2.3.3 Stiffness Matrix

The stiffness matrix is defined as

$$[K]^e = \int_V [BR']^T [D'] [BR'] \, dV \tag{2.27}$$

in which matrices [BR'] and [D'] were defined in the earlier section. Since [BR'] in the above integral is a functionof $\xi$, $\eta$ and $\zeta$, the elemental volume is also rewritten using the standard expression

$$dV = \text{Det}[J] \cdot d\xi \, d\eta \, d\zeta \tag{2.28}$$

The integrations are carried out numerically using Gaussian Quadrature formulae. Hence

$$[K]^e = \sum_{q=1}^{n^3} K_q [BR']^T [D'] [BR'] \text{Det}[J]_q \tag{2.29}$$

where q is the Gaussian sampling point at which values of the functions are calculated, and $K_q$ is the product of the three weight coefficients at this point. The stiffness matrices for the three orders of elements considered are calculated using a program written in Fortran IV and included in Appendix D. Again the decision of which order of rule to be used for these shell elements will be discussed in detail in Chapter 4.

The assembly of element stiffness coefficients and the solution for the local nodal displacements follow the method of the Front Solution as described in Chapter 3.

### 2.3.4 Economical Use of Elasticity Matrix

The elasticity matrix for an isotropic material was given in expression 2.26 and since it is a matrix of full rank, operations similar to that adopted in three-dimensional elements [37] cannot be performed. Instead if the non-zero terms in the elasticity matrix are alone used in calculating the stiffness coefficients, certain amount of saving in central processor time of the computer is possible. This is included in the present formulation of the element stiffness matrix. The actual saving in central processor time was about 10% while solving a pipe bend problem with 32 quadratic shell elements.

## 2.4 Stress Matrix

Once the nodal displacements have been calculated, the five local stresses at a nodal point can be evaluated from

$$\{\sigma'\} = [D'] [BR'] \{\delta R\} \tag{2.30}$$

calculating the [BR'] matrix at the nodal points in the usual way [7]. Because of the definition of local orthogonal axes, the above components

of direct stresses are the ones usually presented in pipe bend problems. So no further stress transformations are required for comparison with the existing results.

## 2.5 Consistent Force Matrix

An element can either be subjected to constant or variable pressures. If {g} is the magnitude of pressure on an infinitesimal area dA then the consistent nodal forces are given by the standard expression A.35 with the nodal force components as:

$$\{F_i\} = \begin{Bmatrix} F_x \\ F_y \\ F_z \\ M_\alpha \\ M_\beta \end{Bmatrix}_i \tag{2.31}$$

and [N] is given by expression 2.13. The calculations of consistent nodal forces for two cases of applied loads are discussed below.

(a) Surface Distributed Pressure

If P is the magnitude of constant pressure on an infinitesimal area dA on the middle surface of the element, using the expression A.35 with

$$d\vec{A} = \begin{Bmatrix} \partial A_x \\ \partial A_y \\ \partial A_z \end{Bmatrix} = \begin{Bmatrix} \frac{\partial x}{\partial \xi} \\ \frac{\partial y}{\partial \xi} \\ \frac{\partial z}{\partial \xi} \end{Bmatrix} \times \begin{Bmatrix} \frac{\partial x}{\partial \eta} \\ \frac{\partial y}{\partial \eta} \\ \frac{\partial z}{\partial \eta} \end{Bmatrix} \tag{2.32}$$

and matrix [N] from expression 2.13 after putting $\zeta = 0$ in it, the

nodal equivalent loads can be evaluated.

(b) Distributed Pressure On One of The Faces of The Element

Let a pressure P be acting on an infinitesimal area dA on the face $\xi = -1$ of the shell element. Using again the expression A.35, the consistent loads are calculated with the definition for [N] from expression 2.13 and $\vec{dA}$ as

$$\vec{dA} = \begin{Bmatrix} \partial A_x \\ \partial A_y \\ \partial A_z \end{Bmatrix} = \begin{Bmatrix} \frac{\partial x}{\partial \eta} \\ \frac{\partial y}{\partial \eta} \\ \frac{\partial z}{\partial \eta} \end{Bmatrix} \times \begin{Bmatrix} \frac{\partial x}{\partial \zeta} \\ \frac{\partial y}{\partial \zeta} \\ \frac{\partial z}{\partial \zeta} \end{Bmatrix} \qquad (2.33)$$

# CHAPTER 3

## ASSEMBLY AND THE SOLUTION OF THE EQUILIBRIUM EQUATIONS

The stiffness matrix K of the complete assemblage relates the nodal loads F acting on the structure to the corresponding nodal displacements $\delta$ by

$$K\delta = F \tag{3.1}$$

The stiffness matrix, may be characterized in general as

1) symmetric
2) banded
3) positive definite
4) sparsely populated.

Algorithms which utilize either iterative methods or direct methods for the solution of equations with these properties are well known. Earlier applications of the finite element procedure were based predominately on iterative methods in which property 4 was utilized so that the solution could be obtained while working entirely in the high speed core memory. In the more recent years, however, direct solutions based on Gaussian elimination have become the preferred solution [16] procedure due to their overall economy and ease of applicability.

In the Band Solution under these methods, given the bandwidth, an efficient equation solving technique is to retain in core only a triangle of coefficients whose side lengths equal the bandwidth. This triangle effectively moves diagonally downwards as the elimination proceeds. Usually the band is sparsely filled and frequently the bandwidth varies from one position to another.

With the explosive development of the finite element technique, a development comparable only with the growth of computing power itself, it becomes necessary to develop elements with more degrees of freedom. Whereas simple elements have corner nodes, these elements have nodes along their edges or on the faces of three-dimensional elements. Thus the dimension of [K] which is equal to the number of degrees of freedom of the structure is very large and the matrix [K] cannot be fully assembled and stored in core. The Front Solution [32] technique is suitable for equations arising out of such elements. Since in the present analysis, elements are of the type mentioned above, this solution technique has been adopted.

A Front Solution is a means of solving a large banded, sparse matrix using Gaussian elimination process. Due to sparseness of the coefficient matrix, only a small amount of the matrix has to be calculated before forward elimination of a variable corresponding to a row. After the elimination process, data pertaining to the variable is stored on a file and the row is freed. Consequently the total core required for this method is very small compared to the conventional methods.

A variable becomes active on its first appearance and is eliminated immediately after its last. Thus before an element is introduced, the active variables cut the structure into two independent parts or 'substructures'. After assembly and reduction of the coefficients arising from this element, the new set of active variables again cut the structure into two parts. The 'front' composed of nodes separating the substructures advances thus, an element at a time.

## 3.1 Practical Aspect of The Computer Algorithms

The program for the front solution method given in reference [32] was not used but a program based on a description contained in reference [39] was programmed and developed independently. The present program

was made much simpler than reference [32] by excluding the book-keeping procedures necessary for changing the loading pattern and mesh pattern, which usually is not an essential part of research oriented programs.

Suitably partitioning the equation 3.1 as

$$\left[\begin{array}{c|c} M_{KN} & M_U \\ \hline M_U^T & M_{UN} \end{array}\right] \left\{\begin{array}{c} \delta_{KN} \\ \hline \delta_{UN} \end{array}\right\} = \left\{\begin{array}{c} F_{UN} \\ \hline F_{KN} \end{array}\right\} \qquad (3.2)$$

where $\delta_{KN}$ and $\delta_{UN}$ are known (prescribed) and unknown nodal variables. The corresponding unknown and known generalised forces are $F_{UN}$ and $F_{KN}$. Expansion of 3.2 gives

$$M_{KN}\ \delta_{KN} + M_U\ \delta_{UN} = F_{UN}$$

and

$$M_U^T\ \delta_{KN} + M_{UN}\ \delta_{UN} = F_{KN}$$

Re-ordering

$$M_{UN}\ \delta_{UN} = F_{KN} - M_U^T\ \delta_{KN} \qquad (3.3)$$

and

$$F_{UN} = M_U\ \delta_{UN} + M_{KN}\ \delta_{KN} \qquad (3.4)$$

From equation 3.3 the unknown nodal variables can be calculated by an extension of Gaussian elimination process with the modified right-hand side vector $F_{KN} - M_U^T\ \delta_{KN}$. In the backward elimination stage, as the elements of $\delta_{UN}$ are explicitly known, the unknown reactions $F_{UN}$ can also be found.

### 3.1.1 Block Diagram

A brief description of the flow diagram (Figure 3.1) is given here. The complete computer program for analysing pipe bend problems using curved shell elements described in Chapter 2 and the Front Solution method described as above, has been written in Fortran IV and given as Appendix D.

In the routine INIAL, element numbers, the nicknames (that is, degrees of freedom) of all variables in each element, and the prescribed nicknames, are fed in for the whole structure as input data. Using this, in the same routine, two scalars NUNKVA (the largest number of unknown variables or rows of $M_{UN}$ in expression 3.2 which is required at any one time) and NKNVA (the corresponding value for $M_{KN}$ in expression 3.2) are determined and several areas are defined, allocated and initialised if necessary.

The main program NAMAIN calls one by one the elements in ascending order along with the loading and geometrical data. This call is effected through FEM (element stiffness routine), STFTR and FORWAD.

STFTR calls the element stiffness routine to calculate the lower diagonal stiffness coefficients and the corresponding stress matrices at the nodal points. These are stored in a tape file and used again if geometrically similar elements are present in the structure. Then the element stiffness coefficients are distributed in the proper areas of $M_{KN}$, $M_U^T$ and $M_{UN}$ in the expression 3.2.

FORWAD writes on another tape file the row corresponding to a completed nodal variable (which will not appear any more) and modifies the rest of the coefficients in expression 3.2. Thus the frontal process alternates between accumulation of element coefficients (assembly) and elimination. BACKWD reads back, in order, the data stored on file for nodal variables and calculates the unknowns.

## 3.2 Techniques to Economise The Computer Solution Time

### Block Storage

As has already been mentioned, in this solution method, as soon as an equation is complete, it is stored and a new equation from the next element takes its place. Storage on magnetic tape or disc can occur immediately after each equation has been completed or after several equations have been completed, temporarily storing them in a buffer area in fast core. A study of it was conducted with a block of 10 equations and the resulting solution times are given in Table 3.1.

It should be noted here thata very high percentage of peripheral processor time has been saved mainly because the BACKSPACE-READ-BACKSPACE motion of the tape has been done for a block of equations instead ~~of~~ for an individual equation during backward substitution.

### Computation of Stiffness Matrix

In most structures many of the elements are identical in size and shape and only their positions in the structure are different. It is often possible to take advantage of this fact and form the stiffness matrix once only. An idea of computing time gained in this process is given in Table 3.2.

A problem of circular cylinder with internal pressure under end constraints has been solved using quadratic shell elements. The cylinder was divided into a number of rings and the stiffnesses of the elements in the first ring alone were calculated and stored on a tape and used for the rest of the rings. This was compared with the problem solved after calculating the stiffness for all elements.

It is seen that even though the stiffnesses of only 8 elements out of total 64 elements have been calculated, the time saved is only of the order of 100 seconds since most of the solution time has been taken by forward ~~and backward~~ elimination and back substitution.

# CHAPTER 4

## STRESS ANALYSIS OF CURVED TUBES UNDER IN-PLANE MOMENT

General pipe-line layouts, may experience changes in their free lengths due to an applied load or due to changes in temperature of the fluids they are conveying. It is normal practice to absorb the expansion of the straight pipe-line by an expansion bend or curved pipe. The loads acting on the curved pipe could be in-plane bending, out-of-plane bending, torsion and pressure. It is well known that the forces and deflections in a curved pipe are not those predicted by simple Bernoulli-Euler bending theory and it is more flexible than a straight pipe. Von Kármán in 1911 presented explanations for this phenomenon.

Since then various analytical methods of solution have been used to solve the governing differential equations for the in-plane bending of curved tubes. Von Kármán's analysis itself was subsequently extended in many papers. References [41] and [42] contain a comprehensive literature survey of the early work and more recently Jones [43] considered tubes with a large tube-to-bend-radius ratio.

A different approach, based on the differential equations of shell theory, was presented by Reissner [44] and was later used by Clark and Reissner [45]. Turner and Ford [46] used equations similar to those of thin shell theory.

All these methods were based upon some form of series expansion containing varying degrees of approximations. The governing equations were also solved directly without analytical approximations using numerical methods by Blomfield [40]. In this chapter the finite element method, which has a completely general approach for the solution of problems in stress analysis, has been utilized in the analyses of these curved tubes.

Since a different numerical solution of the governing differential equations of this problem, using Predictor-corrector step-by-step method, is available [40], the accuracy of the finite elements used in the present analysis and their associated problems have also been studied.

## 4.1 Proposed Finite Element Analysis

A theoretical study of two types of elements, three-dimensional curved elements and doubly curved shell elements was presented in Appendix A and Chapter 2 respectively. In each type, it is possible to generate a family of elements by choosing higher and higher degree of polynomials to represent element displacements and geometry. Thus there are two alternate approaches in the finite element procedure. In the first approach, for both types of elements under study, a relatively simple representation of the stiffness properties is utilized and by mesh refinement (i.e. increasing the number of subdivisions) the accuracy achieved can be studied, while in the second approach an improved representation of element properties is utilized which generally requires a less refined mesh. Hence a decision has to be made regarding the approach suitable for solving curved pipe problems using the two types of elements. At the same time, since all these elements are numerically integrated ones, the order of Gaussian formula necessary for each type of elements, while solving shell structural problems, has to be decided.

The geometrical proportions of the pipe bends are usually expressed in terms of a non-dimensional factor $\lambda = at/b^2$ called the Pipe Factor. In the present analysis a right-angle bend, having a value of $\lambda$ equal to 0.1458, with the assumption of plane sections remaining plane, is studied under in-plane moment. The computing times (RUN compiler on the CDC 6600 at London University) for analysing the above problem using

different types of elements are also given, which helps to make an economical decision with regard to the choice of an element. Further, these computing times might help to compare the performance of the Front Solution method as adopted here, with other solution methods. The criterion chosen to determine the accuracy of solution is a direct comparison of this with the existing numerical solution obtained using Predictor-Corrector step-by-step method [40] with 74 step-lengths.

Having decided the order of shell elements suitable, the number of such elements required to represent adequately a right-angle bend is studied. The flexibilities of this bend for a range of $\lambda$ values are calculated, after computing the corresponding applied moment. These results are compared with those given in references [40] and [46].

An element, in the form of a ring, with displacements varying in a trigonometric function is attempted and the results are compared with those of the curved shell element.

## 4.2 Statement of The Analysed Problem

A curved tube with constant radius of curvature can be considered as a sector of a closed toroidal shell of revolution. The deformations of such a sector due to a pure moment applied in the plane perpendicular to the axis of revolution are analysed with the assumption

$$U_{\psi} = k\, r\, \psi \tag{4.1}$$

where

$$k = \frac{\Delta\psi}{\psi} \tag{4.2}$$

$U_{\psi}$ is the displacement along meridional direction of the tube

and

$$r = a - b \cos\theta \tag{4.3}$$

$\psi$, $\Delta\psi$, and $\theta$ are as shown in Fig. 4.1. The points along the $\psi$ direction

at which $\theta$ is zero are denoted as at intrados, whereas those at $\theta = \pi$ are at extrados. Using the above assumption for $U_\psi$ and a consistent shell theory it has been proved [40] that this is a problem of axi-symmetrically loaded shell of revolution and the rotation of shell mid-surface in the $\psi$ direction is given by

$$\phi_\psi = k \cos \theta \, . \, \psi \qquad (4.4)$$

Hence it is enough if a sector of the 90 degree bend is analysed by prescribing the boundary displacements and rotations, as given by the expressions 4.1 and 4.4, to represent the problem.

The dimensions of the curved pipe and the build up, for example, of quadratic shell elements to represent the structure, are shown in Figure 4.2. This problem has been analysed using different orders of curved shell elements and three-dimensional elements.

## 4.3 Analysis Using Three-Dimensional Elements

As mentioned before, two orders of Isoparametric three-dimensional elements have been used in the analysis.

i) Element with quadratic variation of the displacements along an edge and

ii) Element with cubic variation of displacements along an edge. The derivation of the corresponding element stiffness matrix is given in Appendix A.

Since the boundary conditions in shell structural problems are usually specified along and perpendicular to a face of an element, the displacements at any nodal point have been transformed from cartesian system into a local system of axes. This local system is as shown in Figure 4.3.

Expression A.13 gives the element stiffness with displacements referenced to a rectangular cartesian system. At a typical node i, these rectangular cartesian displacements $u_x$, $u_y$ and $u_z$ are related to the displacements along local directions by:

$$\begin{Bmatrix} u_x \\ u_y \\ u_z \end{Bmatrix}_i = \begin{bmatrix} -\cos\theta \sin\psi & \sin\theta \sin\psi & \cos\psi \\ -\cos\theta \cos\psi & \sin\theta \cos\psi & -\sin\psi \\ \sin\theta & \cos\theta & 0 \end{bmatrix}_i \begin{Bmatrix} u'_x \\ u'_y \\ u'_z \end{Bmatrix}_i \qquad (4.5)$$

where

$u'_x$ is the displacement normal to the surface

$u'_y$ is the displacement along circumferential direction

and $u'_z$ is the displacement along meridional direction as shown in Figure 4.3.

Now the stiffness matrix can be transformed with displacements referenced to local system by:

$$[K]^e = \int_V [TR]^T [B]^T [D] [B] [TR] \, dV \qquad (4.6)$$

where [TR] is the transformation matrix made up by the expressions 4.5 at all nodes of an element.

The stresses have been first computed based on the cartesian system and then transformed also along the local directions for easier interpretaion of stress distribution.

The longitudinal stress factors on the inside and outside surfaces of the bend, obtained using quadratic elements, are plotted in Figure 4.4. Figure 4.5 shows the corresponding meridional stress factors. Similarly the results obtained using cubic elements are plotted in Figures 4.6 and 4.7. In all these Figures the corresponding curve due to the

other numerical solution is also given, for comparison.

As the number of quadratic elements is doubled, an improvement in the stress distributions is noticed from Figures 4.4 and 4.5. But from Figures 4.6 and 4.7, it is clearly seen that a much better correlation with the numerical solution exists, when cubic elements are used.

Table 4.1 gives the computer central processor times and necessary computer core for solving the pipe bend problem using the above two types of elements,

Table 4.1

Central Processor Time And Core Required. (RUN Compiler)

| Type of Element | Total Number of Elements | Total Number of Nodes | Cental Processor Time | Approximate Core | Remarks |
|---|---|---|---|---|---|
| Quadratic | 16 | 192 | 350 secs | 45,000 | Results shown in |
| | 32 | 384 | 761 secs | | Figures 4.4 & 4.5 |
| Cubic | 8 | 160 | 441 secs | 70,000 | Results shown in |
| | 16 | 320 | approx. 1000 secs | | Figures 4.6 & 4.7 |

### 4.3.1 Comparison of Different Orders of Guassian Quadrature Formulae

Since the element stiffness matrix, as indicated in Appendix A, is calculated numerically using Gaussian quadrature formulae, a decision has to be made as to which order of approximation formulae it is necessary to use. An attempt therefore has been made to find the optimum number of integration points, while solving the pipe bend problem. The results for a cubic element, better suited for shell structural analysis, are shown in Table 4.2.

Table 4.2

Central Processor Time For Solution Using Cubic Three-Dimensional Elements

Total number of elements = 16

Total number of nodes = 320.

| Case Number | Integration rule over Surface | Integration rule through Thickness | Central Processor Time (RUN Compiler) (secs) | Remarks |
|---|---|---|---|---|
| 1 | 4 by 4 | 4 | Approx. 1000 | Stress distributions plotted in Figs. 4.6 and 4.7 |
| 2 | 4 by 4 | 3 | 795 | Results same as in case 1 |
| 3 | 3 by 3 | 3 | 619 | Results same as in case 1 |
| 4 | 4 by 4 | 2 | 690 | Large variation from case 1 |

From a comparison of stress distributions, obtained in different cases, a 3 x 3 x 3 rule will be sufficient for a cubic element. It is to be noted here that, from theoretical considerations of the Gauss quadrature formula, for a polynomial of degree three two sampling points are more than sufficient. But from practical considerations, a higher order rule is necessary as proved above.

## 4.4 Analysis Using Doubly Curved Shell Elements

Three different degrees of shell elements have been used, namely quadratic, cubic and quartic, in the analysis. Their shape functions and

the corresponding formulation of stiffness matrix were given in detail in Chapter 2. Since it is obvious that shell elements will be better suited for shell structural analysis than three-dimensional elements, they have been considered in detail here.

### 4.4.1 Comparison of Different Orders Of Gaussian Quadrature Formulae

In these shell elements as well, Guassian quadrature formulae are used to calculate the stiffness coefficients. Various orders of approximation formulae have been tried on these shell elements while solving the same pipe bend problem and the optimum is chosen.

The results of the computing times for quadratic, cubic and quartic shell elements are given correspondingly in Tables 4.3, 4.4 and 4.5. The resulting stress distributions are also plotted and compared with the existing numerical solution.

Table 4.3

Central Processor Time For Solution Using Quadratic Shell Elements

Total number of elements = 32

Total number of nodes = 160

| Case Number | Integration rule over Surface | Integration rule through Thickness | Central Processor Time (RUN Compiler) (secs) | Remarks |
|---|---|---|---|---|
| 1 | 4 by 4 | 2 | 235 | Stress distribution plotted in Figs. 4.8 and 4.9 |
| 2 | 3 by 3 | 2 | 193 | Results same as in case 1 |
| 3 | 2 by 2 | 2 | 157 | Stresses vary by 10% compared to case 1 |

Table 4.4

Central Processor Time For Solution Using Cubic Shell Elements

Total number of elements = 24

Total number of nodes = 192

| Case Number | Integration Rule Over Surface | Integration Rule Through Thickness | Cental Processor Time (RUN Compiler) (secs) | Remarks |
|---|---|---|---|---|
| 1 | 4 by 4 | 2 | 372 | Stress distribution plotted in Figs. 4.10 and 4.11 |
| 2 | 3 by 3 | 2 | 295 | Results same as in case 1 |

Table 4.5

Central Processor Time For Solution Using Quartic Shell Elements

Total number of elements = 12

Total number of nodes = 144

| Case Number | Integration Rule Over Surface | Integration Rule Through Thickness | Central Processor Time (RUN Compiler) (secs) | Remarks |
|---|---|---|---|---|
| 1 | 4 by 4 | 2 | 350 | Stress distributions plotted in Figs. 4.12 and 4.13 |
| 2 | 3 by 3 | 2 | 280 | Large variations compared to case 1 |

So far it has been shown how the central processor time varies with different orders of integration formulae applied over the surface of the elements. To show how the central processor time varies with the order of integration rule through the thickness, tests have been conducted using quadratic elements. The central processor computing times are given in Table 4.6.

Table 4.6

Central Processor Time For Solution

Total number of elements = 32

Total number of nodes = 104

| Case Number | Integration Rule Over Surface | Integration Rule Through Thickness | Central Processor Time (RUN Compiler) (secs) | Remarks |
|---|---|---|---|---|
| 1 | 4 by 4 | 4 | 358 | Stress distributions are same |
| 2 | 4 by 4 | 2 | 254 | |

Thus with the knowledge of computing times for solving a typical pipe bend problem and comparing the resulting stress distributions with that obtained using another numerical method, it is possible to conclude that when quadratic or cubic shell elements are used for analysing shell structures a 3 x 3 x 2 Gaussian quadrature rule would suffice. On the other hand if quartic elements are used, a 4 x 4 x 2 rule is necessary.

### 4.4.2 Comparison of Quadratic, Cubic and Quartic Shell Elements

For this type of analysis, a general program for calculating the stiffness matrix has been written, which only requires the specification of the order of shell elements to be used in the problem. For all these elements the optimum Gaussian quadrature formula, as decided in the earlier section, has been used.

In Table 4.7, the computing times and core necessary, for the solution of pipe bend problem using different orders of shell elements, are given.

Table 4.7

| Type of Element | Total Number of Elements | Total Number of Nodes | Central Processor Time (RUN Compiler) (secs) | Approximate Core | Remarks |
|---|---|---|---|---|---|
| Quadratic | 16 | 80 | - | 40,000 | Stresses shown in Figs. 4.8 and 4.9 |
| | 32 | 160 | 193 | | |
| Cubic | 16 | 128 | 189 | 45,000 | Stresses shown in Figs. 4.10 and 4.11 |
| | 24 | 192 | 295 | | |
| Quartic | 6 | 72 | 111 | 53,000 | Stresses shown in Figs. 4.12 and 4.13 |
| | 8 | 96 | 227 | | |
| | 12 | 144 | 350 | | |

It can be seen that the cubic elements give results which are closer to the existing numerical solution than the quadratic elements for approximately the same central processor time and half the number of elements.

Further the eight quartic elements give a result in less central processor time comparable to the 24 cubic elements. Quartic elements also show a faster rate of convergence (i.e. improved accuracy with decreasing mesh size). There would appear therefore to be a significant advantage in using the highest order element available.

## 4.5 Study of Quartic Shell Elements

It has been shown that the quartic shell elements consume less time for a given accuracy in stress distributions for the pipe bend problem. Therefore it was decided to use quartic elements for further study of pipe bend problems.

So far only a sector of the curved pipe has been analysed, to study the stress distributions in a 90° bend, due to symmetry of the problem. From the stress distributions shown in Figures 4.12 and 4.13 for different number of elements around the circumference, it was found that eight was the optimum number for a bend having a value of $\lambda$ as 0.1 and above. For bends with lower pipe factors this optimum increased to twelve. If a full 90 degree bend is to be analysed, it will be necessary to use more than one sector. Figures 4.14 and 4.15 show the stress distributions at any cross section of a 90 degree bend subjected to in-plane moment, for different numbers of rings (i.e. sectors) used to idealise the bend. From these results it could be concluded that sufficiently accurate stress distributions in a 90 degree bend are obtained, if it is idealised by four rings.

## 4.6 Analysis Using A Ring Element

The stress distributions on pipe bends, presented earlier in this Chapter, suggest that it may be possible to represent this variation by trigonometric series. So a ring element, with the variation of displacements or geometry along the circumference described by trigonometric

series and the longitudinal variation by polynomials, has been developed to solve the pipe bend problem.

For example in a 10 nodal ring element, as shown in Figure 4.16, the extrapolation formula is taken as

$$\begin{aligned}\phi &= \alpha_1 + \alpha_2 \cos \pi\eta + \alpha_3 \sin \pi\eta + \alpha_4 \cos 2\pi\eta + \alpha_5 \sin 2\pi\eta \\ &+ \alpha_6\xi + \alpha_7\xi \cos \pi\eta + \alpha_8\xi \sin \pi\eta + \alpha_9\xi \cos 2\pi\eta \\ &+ \alpha_{10}\xi \sin 2\pi\eta \end{aligned} \tag{4.7}$$

These 10 constants can be evaluated in terms of nodal variables

$$\text{or} \qquad \phi = \sum_{1}^{10} N_i \phi_i \tag{4.8}$$

where $N_i$ are the shape functions given in Appendix E.

These shape function expressions are substituted in expression 2.1 and 2.11 and the stiffness matrix calculated as before. The same pipe bend problem, has been analysed using a ring element which has any odd number of nodes along the circumference and four such rings of nodes along the longitudinal direction.

Since the problem of a curved pipe under in-plane moment is symmetrical about the plane in which the moment is applied, half of the previous full ring element is enough for this analysis. Hence a program to calculate the stiffness of such elements, with any odd number of nodes along the circumference and four such rings of nodes along the longitudinal direction has been written. The shape functions for such an element, as shown in Figure 4.17, with 20 nodes are also given in Appendix E.

Using this element also, the same pipe bend problem has been solved. The resulting stress distributions are compared with those obtained

(i) using a full ring element

and (ii) using four quartically curved shell elements in Figures 4.18 and 4.19. The stress distributions due to a half ring element are better than those of the quartic elements. But the disadvantage of the ring element is due to the size of the stiffness matrix, which is quite large, compared to that of a quartic element.

## 4.7 Flexibility And Stress Factors

The flexibility factor, K, for a curved smooth pipe, under an in-plane bending moment M is defined as follows (Fig. 4.1).

If the bend and a straight piece of pipe of the same length and cross-sectional dimensions as the bend are both loaded over their entire lengths by constant in-plane bending moments, M, of equal magnitude, the flexibility factor K,

= relative rotation of the end sections of the bend/ relative rotation of the end sections of the straight pipe (4.9)

(or) $$\frac{d\psi}{\psi} = K \cdot \frac{Ma}{EI} \qquad (4.10)$$

where I is the second moment of area of the wall cross-section.

The applied moment M is calculated as shown in Appendix F.

Stress factor is a dimensionless term defined as

$$\text{Actual stress in bend} = (\text{Stress Factor}) * \frac{Mb}{I} \qquad (4.11)$$

Using the optimum number of elements, based on stress considerations, a sector of the 90 degree bend subjected to an in-plane moment has been

analysed for a range of $\lambda$ values. The applied moment corresponding to the prescribed displacements has been computed in all these cases. Using expression 4.10 the corresponding flexibility factor has been calculated. It was found that an increase in number of elements above the optimum value, did not affect the value of flexibility factor. The dimensions of the bends and the calculated flexibility factors are given in Table 4.8. Further in Table 4.8 for one particular value of $\lambda$, for which the numerical solution exists [40], the flexibility factors are compared. The difference in the values may be due to the component of shear deflection that has been included in the finite element solution.

Table 4.8

Flexibility Factors

| Mean radius of bend axis a | Pipe bore radius b | Wall Thickness t | Pipe factor $\lambda$ | Flexibility Factor K | |
|---|---|---|---|---|---|
| | | | | Finite Element | Predictor Corrector Step-by-step Method |
| 10.0 | 5.0 | 0.5 | 0.2 | 8.0 | - |
| 10.5 | 5.662 | 0.444 | 0.1458 | 10.85 | 11.15 |
| 10.0 | 5.0 | 0.25 | 0.1 | 16.2 | - |
| 10.0 | 5.0 | 0.125 | 0.05 | 32.3 | - |

Figure 4.20, for the flexibility factor plotted with respect to the pipe factor, predicts the distribution similar to that given by Turner and Ford's theoretical calculations [46] except the values are slightly lower for higher values of $\lambda$.

The maximum transverse stress factors on the inside and outside surfaces are plotted in Figure 4.21 for the above two methods. The internal transverse stress factors compare favourably whereas the external transverse stress factors predicted by the finite element are lower than those by the other method.

Figures 4.4 to 4.14 show that the stress distributions predicted by the finite element method are identical with the existing numerical results [40]. Further they also show, for all orders of elements considered, there is monotonic convergence to a solution as the number of elements is increased.

Thus the present finite element method is as good as the existing analytical and numerical methods for solution of curved pipe problems. The added advantage to the finite element method is that it is possible and easy to extend the analysis so that different end effects on the bend can also be studied.

# CHAPTER 5

## COMPARISON OF RESULTS OF THE CURVED SHELL ELEMENT WITH FEW OTHER EXISTING SHELL ELEMENTS

Any numerical process is by its very nature approximate. The approximation may range from the curtailment of significant digits (round off) to various physical idealisations introduced into the process of solution. In the last chapter it was shown, that using the curved shell elements developed here, an accurate solution of shell structural problems can be obtained ~~and~~ that compares well with the solution obtained by another numerical method.

In this chapter, the accuracy of two types of elements, one being a shallow shell element and the other an arbitrarily curved shell element, is compared with the present quartic shell element using the few numerical results published.

### 5.1 Comparison With A Shallow Shell Element

The analysis of shells by the finite element method has been attempted in the past, by two methods. The first method applies to shells of revolution. The second consists in splitting the shell into flat finite elements [7, 16, 47]. The bending behaviour of such an element is accounted for by plate flexure considerations, the membrane behaviour by including plane-stress and the coupling between membrane and bending by resolution of force and displacement at the nodal points of the structure. More recently the coupling between membrane and bending effects has been explicitly included, using shallow shell theory to relate strains and displacements [20].

On these lines Ford [21] has developed a triangular shell element, using a compatible plate element [48] and linear functions to represent

the in-plane displacements. Koiter's shell theory [20] specialised for shallow shells was used for the strain displacement relations. This element has 24 degrees of freedom and does not represent rigid body motions exactly. Further using these elements the curved shell middle surface is idealised by polyhedron surfaces.

The problem of a torus under internal pressure was attempted using these shallow shell elements and the results were presented in reference [21]. Due to symmetry of the problem only a sector of the complete torus was analysed with elements distributed over half of the symmetrical shell as shown in Figure 5.1. The convergence of this finite element can be studied from the results of this problem given for two different meshes - one being a 20° segment with 44 triangular elements and the other being a more refined mesh of 10 degree segment with 34 elements. These results are compared with those using quartic curved shell elements in Figure 5.2 (for the normal displacement), Figure 5.3 and Figure 5.4 (for the stress resultants). The quartic element distribution is shown in Figure 5.1.

There is no exact solution, for comparison with these finite element solutions, to this seemingly straight forward problem. One solution, however, available is that given by Kalnins [49], who used what he called a multisegment integration method in solving the relevant shell equations and these results are also shown in Figures 5.2, 5.3 and 5.4.

From the study of these results, it is evident that the rate of convergence, when shallow shell elements are used, is slow, whereas rapid convergence is obtained with the quartic shell elements. Further acceptable results can be obtained by using as few as four quartic elements. The agreement of the curved shell element solution with Kalnin's values appears excellent, particularly the peak values, when compared to the quality of results associated with the finely meshed shallow shell elements.

## 5.2 Comparison With A Curved Triangular Element

Argyris and Scharpf [24] have developed a curved triangular arbitrary shell element (SHEBA type) satisfying compatibility between elements and no straining under rigid body displacements. In SHEBA 6 element, with the application of homogeneous triangular coordinates and taking a complete polynomial of fifth order in it to connect the three global cartesian displacements to the kinematic freedoms at the nodes, interelement compatibility is achieved. At the vertices the three displacements and their first and second derivatives are prescribed. In addition the first tangential derivatives normal to the edges are introduced for all displacements at the three intermediate points on the edges. Thus these elements have 63 degrees of freedom whereas a quartic element has 85 degrees of freedom. The displacements and rotations at the nodes in quartic elements have certain physical meaning which is not true in SHEBA elements. Further in SHEBA elements the mapping of the surface in global cartesian coordinates based on the corresponding nodal geometrical data is done obeying the same rule of transformation as the displacements ensuring zero strains under rigid body motions. It is worth remembering at this point that the present curved quartic shell element represents rigid body motions exactly as well as satisfying interelement compatibility. Just as SHEBA allows a close modelling of the idealised structure to the actual geometry [50], so can the quartic element represent curved edges.

To check the accuracy of this element one of the examples attempted was the analysis of a thin circular cylinder under a radial line load as shown in Figure 5.5. The results were presented in reference [50]. These results were checked using an analytical solution given by Flügge [51]. Symmetry permitted the analysis of one slice and the element

distribution is also shown in Figure 5.5. The radial displacement thus obtained is compared in Figure 5.6 with those from using quartic curved shell elements. Corresponding value of the analytical solution by Flügge is also presented, for a basis of comparison between the two finite element solutions. In Figure 5.7 the longitudinal bending stress is plotted along a generator for quartic shell elements and compared with Flügge's result.

The agreement of quartic shell element solution with Flügge's values appears excellent. Further use of quartic shell elements instead of SHEBA elements in shell structural analysis, provides greater accuracy with lesser degrees of freedom. This is evident from the results of the above example in which one quartic shell element with 85 degrees of freedom gave an acceptable accuracy of results when compared to seven SHEBA 6 elements with total of 207 degrees of freedom.

## 5.3 Summary of Quartic Element Versus Other Curved Elements

In both examples, the quartic shell finite element solution was found to compare favourably with the distribution and magnitude of the corresponding analytical solution. Further quartic elements when compared with the other two shell elements considered here, gave better accuracy in shell structural problems with fewer elements. This point is further supported by the results shown in reference [47] for the problem of thin circular cylinder under a radial line load analysed by triangular plate elements whose membrane and bending deformations were approximated by cubic polynomial functions. The solution for the radial displacement presented shows that for a favourable agreement with analytical solution, very fine mesh was necessary.

Thus it may be concluded from these examples and as well as from the analysis of pipe bends in the previous chapter, the quartic shell

element is, for the analysis of arbitrary shell structures, an excellent element.

# CHAPTER 6

## STRESS ANALYSIS OF PIPE BEND STRUCTURES WITH SHELL FINITE ELEMENTS

### 6.1 Introduction

All the previous theoretical analyses of curved pipes, a review of which is given in Chapter 4, were limited since all the significant effects needed for the analysis, including the effects of end constraints are not considered. Moreover, the experimental results presented in reference [53] show clearly that for a 90 degree bend the flexibility and stress concentration factors depend on the type of loading, the addition of constraints such as tangent pipes, flanges. It is also shown in the same reference that, the flexibility of the bend also depends on the total angle of the bend, which is not predicted by the usual theory.

Hence it can be concluded that it would be important to devise a method of analysis of curved tubes that would be valid for any tube and bend radii and would account for all end effects. Kalnins [54] extended his multisegment method of direct numerical integration and analysed a 90 degree bend with ends restrained by straight pipes. The theoretical stress distributions compared favourably with the experimental results.

In this chapter finite element method, in conjunction with doubly curved shell elements, has been used for calculations of stress intensification and flexibility factors of right-angle bends having values of $\lambda$ between 0.05 and 0.5 under an in-plane moment.

In order to determine the effects of usual types of end constraints on the values of flexibility factors, results have been computed with the ends of the bends terminated by the following:

(a) Straight sections (or tangent pipes), of the same diameter and wall thickness as the material in the curved tube.

(b) A straight section on one end and a rigid flange at the other.

To study how the flexibility will differ with different arc lengths, bends of different included angles with the same end restraints have been analysed. This finite element analysis has been further extended to study the behaviour of two 90 degree bends when they are connected together such that they are loaded in opposite directions. In the following sections results, after the computation of different problems, are presented.

The calculation of the stresses and deflections in pipe bends is mainly as a means to the end of designing such members safely and economically. Hence the conclusions, that could be used for design purposes are given at the end.

## 6.2 Finite Element Idealisation of The Problem

It was concluded in Chapter 4 with the study of different orders of curved shell elements, quartic type elements were best suited for analysing pipe bend problems. Further if these elements were used to model a closed ring and these rings were used to idealise the curved pipe, the number of elements required per ring and the number of such rings required, were estimated for a reasonably accurate representation of stresses.

Symmetry permits the analysis of one half of the pipe structure and a representative finite element idealisation, with quartic shell elements, of a 90 degree bend with ends terminated by tangents, is shown in Figure 6.1.

The flange end condition is simulated by prescribing zero displacements and rotations to the nodes at that section. By restricting only the longitudinal displacement of the nodes at the end section of a tangent pipe, the effect of a very long straight pipe is provided.

The consistent nodal loads have been evaluated as described in Section 2.5 with the longitudinal bending stress distribution, calculated using the simple bending formula, as the pressure distribution over the side of the corresponding elements. Using the transformation matrix (expression 2.10), these loads calculated along the global directions, have been transformed into loads acting along the local directions.

The stiffness formulation of elements, assembly and the solution of the equations, take up the usual form and the nodal displacements and stresses have been evaluated.

As a good measure of the computational accuracy of the analysis, the external applied moment corresponding to the computed stresses, has been calculated and checked with the original applied moment.

## 6.3 90 Degree Bend With Ends Terminated By Tangents

The finite element idealisation of this problem and the number of elements required to represent the bend adequately were indicated in the earlier section. The consistent nodal forces corresponding to an in-plane moment are applied at the free end of one tangent pipe, whereas the desired end restraints are prescribed to the free end of the other tangent pipe. The lengths of the two tangent pipes are taken as the same.

Short radius 90 degree bends (the midwall pipe radius is not negligible compared to the bend radius) with pipe factor $\lambda$ ranging from 0.05 to 0.5 have been analysed. Most of the bends considered have the ratio $\frac{1}{\gamma}$ (radius of bend to midwall radius of pipe) of the order two. In one case a long radius thick bend has also been considered. The dimensions of these bends are given in Table 6.1.

From a preliminary analysis of this type of problem the maximum length of an element, used to represent the tangent pipes, was found to

be of the order of two inches per element per ring. Further it was also noticed,with the dimensions of bends taken, that a length of 40 inches to 60 inches of the tangent pipe was required for the assumed load distribution to represent a pure moment.

To study in advance the effect on the bend due to a flange attached to the free end of a tangent pipe, the conditions corresponding to either a flange or a long tangent pipe ~~are~~ were applied to the free end of the tangent pipe. From a comparative study of the stresses and deflections in the bend, in these two problems, it was concluded that this flange did not have any effect on the bend.

These conclusions, arrived at from an initial study of the problem, have also been used as a datum for the rest of the pipe bend analysis.

To study the amount of restraining effects due to tangent pipes on the bend, flexibility of the bend under these conditions has to be calculated. The flexibility factor for a bend was defined in Chapter 4 and given by expression 4.10. This definition is acceptable if sections of the bend remain plane before and after deformation. From an analysis of the computed deflections, end sections of the bend are found to be warped and ~~they are~~ that is no ~~more~~ longer in a plane after deformation. So an alternative consistent definition of the flexibility of a bend is to be adopted and given in Appendix G.

Figure 6.2 shows the original shape of the centre line of a pipe structure analysed and compares the computed shape with the assumed one. The value of flexibility factor at different sections along the length of the tangent pipe has been calculated and plotted in Figure 6.3 showing that the sections near the bend are much more flexible and the sections warped more than one would normally expect. From Figure 6.2, it is pointed out that the assumed deflections and the computed deflections are the same at the free end as well as at the junctions of bend and tangent pipes. Thus knowing the flexibility of individual components

in a pipe system, the effects of one on the other can be studied.

The deflections of the pipe structure have been computed for a range of λ values. The length of tangents in all cases have been taken equal to that required for load effects to die out. Since in the present finite element analysis, one end cross-section of the pipe structure, at which the consistent loads were specified, is free to warp whereas the other end section is constrained to move according to the desired end conditions, flexibility of both tangent pipes have been calculated. It was found for all λ, the value of flexibility factor of the tangent pipe, with one of its ends restrained, was very nearly equal to one. With bends of λ equal to 0.15 and over, the free end cross-section of the other tangent pipe was very nearly in a plane and remained circular. For this case ~~At the same instance~~ the calculated flexibility of this tangent pipe was also equal to one. For lower pipe factors, as the length of this tangent pipe was increased, the corresponding value of flexibility factor approached one ~~with~~ without ~~practically~~ ~~not~~ changing the magnitude of the bend flexibility. Hence a critical length of the tangent pipes is defined such that the flexibility of the tangent pipe, having a free end, is unity and the free end section remains plane and circular so that the end conditions existing in practice are reproduced. For very low pipe factors, as expected, the flexibility of the free-end -tangent pipe approached one rather slowly and the critical length was twice that required for the load effects to die out.

Figure 6.4 shows the distribution of flexibility factor of the bend with respect to the pipe factor (λ). For a consistent comparison, the corresponding distribution in the case of 90 degree bends, with no end restraints and with the plane sections remaining plane assumption, is also shown.

The stresses have been computed, on the inside and outside surfaces, along the longitudinal and circumferential directions on both surfaces, at the nodal points. It was found in all bends analysed here that the maximum stress was occurring on the inside surface at the central cross-section at around 85 degrees from the intrados along the hoop direction. Following the usual practice, the non-dimensional stress factors $\sigma/(Mb/I)$ have been calculated and the plots of maximum transverse stress factors on the inside and outside surfaces of the bends are shown in Figure 6.5 for different values of $\lambda$. The various experimental results for the stress factors are also shown in the same figure.

To show the versatility of the shell finite elements in solving pipe structures under in-plane bending, results have been computed for two pipe systems, one representing a short radius thin pipe [41] and the other a long radius thick pipe [55]. The results have been compared with the experimental results available in those references. The results of computations are shown in Figures 6.6 to 6.8 in which comparisons have been made with the corresponding experimental results.

Two types of applied loads, one a pure moment throughout the length of the pipe structure and the other, a technique of applying a bending moment which increases linearly with distance from the line of loading, the maximum bending moment therefore occurring at the central section, have been used to analyse the pipe systems to show different flexibility and stress concentration factors exist for different types of applied loads. The applied load in the latter case, has a shear component and the present finite element includes the effect of shear on the deflections of the pipe structure which normally the other theories neglect. The flexibility of the bends, under a load of linearly varying moment, have been calculated using the expression given in reference [41]. The flexibility and the maximum transverse stress factors of the bends, for

the above two types of loads, are plotted with respect to pipe factor in Figures 6.10 and 6.11 respectively.

In reference [43], Jones analysed the in-plane bending of short radius curved pipe bend by extending Von Kármán's original theory and concluded that the stresses in and flexibility of curved pipe bends are virtually independent of the ratio $\gamma$ (b/a) and depend almost entirely on the pipe factor $\lambda$. To check this, computations have been done on 90 degree bends for two different ratios of $\gamma$ but having the same value of $\lambda$. The results of flexibility and maximum transverse stress factors are shown again in Figures 6.10 and 6.11 respectively.

## 6.4 180 Degree Bends With Ends Terminated By Tangents

The experimental results published in reference [53] and the discussion on it by Markl in the same reference, indicated that 180 degree bends were more flexible than 90 degree bends, which again the existing theories cannot predict. To study this characteristic quantitatively for a value of $\gamma$, 180 degree bends with the ends terminated by tangent pipes and having values of $\lambda$ between 0.1 and 0.2 have been analysed under an in-plane moment.

The same procedures as for right-angle bends, have been adopted in finite element idealisation of the problem and calculations of flexibility of tangent pipes and bends. Figure 6.12 compares, over a range of $\lambda$, the flexibility of 180 degree bends with 90 degree bends when both these curved pipes have been subjected to the same end restraints, that produced by tangent pipes.

The effect of increased flexibility in 180 degree bends over 90 degree bends was not felt while defining the critical tangent length for bends with pipe factor 0.15 and over. But when the value of $\lambda$ was 0.1, the critical tangent pipe length was nearly twice the corresponding value in the right-angle bend.

The maximum stress in the bend was occurring at the central section on the inside surface along the hoop direction at about 90 degrees from intrados. Figure 6.13 shows the variation of maximum transverse stress factor with $\lambda$ on the inside surface and compares it with the corresponding results obtained for 90 degree bends.

Thus from Figures 6.12 and 6.13, a measure of the error, in assuming that 90 degree and 180 degree bends behave identically, can be obtained.

## 6.5 Variation In Flexibility And Stress Factors With Arc Lengths Of Bends

The flexibility of bends, other than and below 90° as their included angle, are predicted assuming a linear relationship exists between the flexibility of a straight pipe and the flexibility of the corresponding 90° bend. This prediction is based on the assumption that the maximum flexibility occurs in a curved pipe, when it includes an angle of 90° and the minimum value occurs when the included angle is zero (straight pipe). For pipes curved over more than 90 degrees, the flexibility is assumed to be the same as that of the corresponding 90 degree bend, which was proved to be incorrect in the earlier section. Moreover in the communications on reference [46], Vigness and Pardue stated that as the bend length is decreased, the point of maximum stress shifts thus producing increasing discrepancies between theory and measurements. The effects of bend angles on flexibility and stress factors as well as its effect on the point of maximum stress in the bend, are studied in this section.

Bends of different included angles ranging from 10 degrees to 75 degrees but of same pipe factor and $\gamma$ have been analysed. To be consistent, the ends of these bends are also constrained by straight tangents as well as loaded by an in-plane moment. The finite element analysis and the consequent calculations of flexibility factors, take

the usual form. For all bends, the calculated value of flexibility factor of tangent pipes was one, whereas the critical length of these pipes varied from 72 inches for a 10 degree bend to 48 inches for a 75 degree bend. A curve between bend angle and the corresponding bend flexibility is plotted in Figure 6.14 for a pipe factor of 0.1. To extend this analysis over a range of pipe factors, as well as to compare a small angle bend with that of a 90 degree bend, computations, as before, have been done on a 30 degree bend for different values of $\lambda$. The calculated flexibilities of this bend are compared with the 90 degree bend in Figure 6.12. With the results in Figure 6.12, a curve between bend angle and the corresponding flexibility, can be plotted for each different value of $\lambda$ considered as shown in Figure 6.14. A study of Figure 6.14 also shows, for any particular length of the bend, how the bend flexibility will vary with the pipe factor.

From a study of maximum stresses in bends of different arc lengths but of same pipe factor, it was concluded that the maximum stress occurred at the centre of the bend on the inside surface along the hoop direction for a 90 degree bend but moved towards the intrados, reaching a point which is at an angle of 75 degrees from intrados, for a 30 degree bend. If the bend angle was further reduced, the maximum stress moved to the intrados at the outside surface along the longitudinal direction, thus behaving more like a straight pipe.

Similar behaviour in the movement of maximum stress was observed in a 30 degree bend as the value of $\lambda$ was increased from 0.1 to 0.2. This behaviour was not present in 90 degree bends.

Figure 6.15 shows the distribution of maximum transverse stress factor with arc length of the bend for a pipe factor of 0.1.

## 6.6 90 Degree Bend With A Straight Section On One End And Flange On The Other

The experimental results presented in reference [53] also show that the flanges produce greater restraint on the bend than that due to straight tangent pipes. Moreover little is known theoretically how the flexibility of and stresses in the bend will be affected by varying the end constraints. Hence in this section results are computed for an in-plane moment on a 90 degree bend, with one end terminated by a straight pipe as before whereas to the other end, a flange is attached. The results are compared with the corresponding values obtained for a 90 degree bend with the ends of the bend terminated by tangents.

The finite element idealisation has been done as before, and the displacements and rotations of the flanged end of the bend fixed. With the computed results the flexibility of the curved pipe and the tangent have been calculated in the usual manner. These flexibility factors also are plotted in Figure 6.12 to show how the rigid flanges produce a greater lowering of these factors than that produced by the tangent pipes themselves. It was also noticed that due to an effect of the flange end condition, flexibility of the tangent pipe approached one rather slowly even for bends with values of $\lambda$ as 0.2.

From the computed results of the stresses in the bend it was noticed that the maximum value occurred at the flanged end section along the longitudinal direction. But the experimental results and the consequent conclusions arrived at in reference [53] were based on the stress factors at the centre of the bend. The present analysis further showed that at the central bend cross-section, the maximum longitudinal and transverse stresses were not occurring at the same point. Hence a necessity of determining 'equivalent stresses' arises.

Using the more accepted theory of yielding - the Shear Strain Energy Theory (von Mises) - the equivalent stress $\bar{\sigma}$ is given by [56]

$$\bar{\sigma}^2 = \frac{1}{2}[(\sigma_\xi - \sigma_\eta)^2 + \sigma_\xi^2 + \sigma_\eta^2] + 3[\tau_{\xi\eta}^2 + \tau_{\eta\zeta}^2 + \tau_{\zeta\xi}^2] \quad (6.1)$$

where $\sigma_\xi$ and $\sigma_\eta$ are the normal stresses

and $\tau_{\xi\eta}$ etc. are the shear stresses.

Further the equivalent stress factor is defined by $\hat{\sigma} = (\frac{I}{Mb})\ \bar{\sigma}$ (6.2)

The maximum equivalent stress occurring at the flanged end section, for different pipe factors has been calculated and it was noticed that this maximum moved from extrados to a point which is at 90 degrees from intrados, as the value of $\lambda$ decreased from 0.2 to 0.05.

At central cross-section of the bend, a local maximum of equivalent stress factors exists. The position of this maximum also changed from intrados to a point about 90 degrees from intrados, with decreasing pipe factors.

### 6.6.1 Note on A 90 Degree Bend With Both Ends Terminated By Flanges

This problem was attempted by fixing one end of the bend and applying the consistent nodal forces on to

(a) a short cylindrical element with its material having a large value of modulus of elasticity compared to that of the bend and attached to the other free end of the bend.

(b) a short cylindrical element made of the same material as the bend but of wall thickness five times that of the bend wall and attached to the bend as before.

(c) the end of the bend itself.

In all these cases, the flange conditions on the applied load end, were not reproduced properly. The resulting stress distribution was not regular. This may be due to assumed linear distribution of stresses - for moment - as applied force. From the solution of other pipe bend problems, it was seen that this had an effect on the stresses. This

could be solved, by applying equivalent displacement and force boundary conditions at the free end of the bend, so that the net effect is a moment. This of course requires modification in the solution routine and was not attempted.

## 6.7 Reversed 90 Degree Bends

A more general pipe structural problem, with two right-angle bends of same radii of curvature, is set up as shown in Figure 6.17 and solved for the load of an in-plane bending moment using the present finite element method. In addition to showing the general applicability of this method in solving pipe structural problems, this helps to study the amount of restraining effect of one bend on the other when both are attached together as in Figure 6.17. To form a general design conclusion, this problem has been solved for a range of $\lambda$ values but all of the same $\gamma$.

The finite element idealisation and the solution of this problem take the usual form. From the computed results it was seen that the cross-section about which the whole problem is antisymmetric did not remain plane after deformation. Hence to calculate the flexibility of the pipe system, the two bends are assumed to act as one part of the structure. With this assumption and the computed deflections of the centre of pipe structure, the flexibility factors of the bends and tangent pipes have been calculated as in the case of a single right-angle bend. Flexibility factors of the two tangent pipes were found to be one and as assumed, the flexibility of the two bends were the same even though they were loaded in opposite directions. The flexibility values of the bends are again plotted in Figure 6.12 so that the restraint produced in the present case on the bend, can be compared with those due to the tangent pipe and flange.

The maximum stress for all cases was found to be at the inside surface of the central cross-section of the bend at around 85 degrees from intrados along the hoop direction. Figure 6.13 shows the variation of maximum transverse stress factor in the bend with pipe factor and compares with the corresponding curve for a 90 degree bend with ends terminated by straight pipes.

## 6.8 Discussion of Results And Design Considerations

The numerical method adopted here, has been shown valid for short and long radius bends having values of $\lambda$ between 0.05 and 0.5. In addition this method has been found well suited for analysing curved pipes with different end restraints and arc lengths. The computational accuracy of this method has been found excellent, since in all cases analysed, the computed moment agrees within 1% of the applied moment.

The computed flexibilities of curved pipes, with the assumption of sections remaining plane before and after deformation, compared favourably with those obtained by Turner and Ford [46]. The computed flexibility factors of the bends with end effects were not compared with the corresponding experimental results. This is because, the computed results showed that the sections of the bend were actually warped after deformation, whereas in general, they are assumed to be plane while calculating these factors from experimental measurements. Further these results are scattered. The maximum stress factors, on the other hand, have been compared with the experimental results. In the case of bends with straight tangents as end restraints, the computed maximum transverse stress factors fit well with the experimental scatter of results shown in reference [46].

From design considerations the first yield of the material is assumed as the critical condition and with the help of Von Mises yield

criterion the individual stresses are related to some readily measured yield value of the material. The yield value of the material is usually taken as that obtained in a simple tensile test and denoted as $\sigma_o$. Thus the equivalent stress $\bar{\sigma}$ is calculated using expression 6.1 and yield would have occurred if

$$\bar{\sigma}^2 > \sigma_o^2$$

Based on the above theory, the distribution of maximum equivalent stress with pipe factor is shown in Figure 6.16 for

a) a 90 degree bend with tangents as end restraints

b) a 30 degree bend with tangents as end restraints

and c) a 90 degree bend with ends terminated by tangent on one end and a rigid flange at the other.

The following conclusions are arrived at, after an analysis of the results of short radius tubes presented in the earlier sections. These are applicable to bending problems and other operating stresses, such as those from internal pressure, are additional.

(1) The assumption of sections in a curved pipe remain plane after deformation is not valid and hence a different consistent way, other than that so far generally used in experimental study, has been adopted for the definition of the flexibility of components in the pipe structure.

(2) The end effects, on a 90 degree bend, due to straight pipes reduce the bend flexibility by 20%. This is a ~~considerable~~ significant amount from the design point and assumed negligible in the literature so far available.

In this pipe configuration, a flange attached to the end of a tangent pipe does not produce any change in the flexibility of the bend.

(3) With the same end restraints to a curved pipe, different flexibility and stress concentration factors exist for different types of

applied loads. Further, for the same type of applied loads and end conditions, the flexibility and stress concentration factors of a 90 degree bend are found to increase by 10% as the ratio $\gamma$ (b/a) is decreased from 1/2 to 1/3. Thus the position is complicated, however, in that the deflections are not functions of just $\lambda$, but also of the pipe dimensions not grouped into the one parameter $\lambda$. So large number of different flexibility factors exist and pertinent values of the flexibility factors are taken, whenever comparison is attempted.

(4) To get a better understanding of the behaviour of these bends at low pipe factors, a ratio $\eta^*$ was defined by Turner and Ford in reference [46] and given as $\eta^* = K/\hat{\sigma}$. This is plotted, with the results of the present analysis, for 90 degree and 30 degree bends with the ends of both bends terminated by tangents, in Figure 6.18 and shows that maximum flexibility per unit stress is obtained at low values of $\lambda$. Further it shows that for low values of pipe factor, maximum flexibility per unit stress is obtained using small arc bends.

(5) In a 180 degree bend, with it's ends terminated by tangents, the peak transverse stress and the flexibility are about 15% more than the corresponding values in a 90 degree bend. This conforms with the conclusion arrived from experimental results in reference [53]. Markl also points out in the discussion of the above paper that he has observed a similar trend in his experiments as well.

(6) From Figure 6.14 it is seen that the assumption of linear variation of the flexibility factor with bend angle will be in great error for bends with low pipe factors. For example a 60 degree bend with $\lambda$ equal to 0.1 is found 30% more flexible than usually assumed. For low values of $\lambda$ this discrepancy increases to 65%.

If the arc length is reduced by 66% from 90 degrees, the flexibility and the equivalent stress reduce by about 40%. Thus the expecta-

tion that the flexibility would differ with different arc lengths is true.

(7) When a flange replaces one of the tangent end restraints in a 90 degree bend, for higher values of $\lambda$, flexibility factor of the bend is reduced by 40%. The effect is more pronounced at low pipe factors as is evident from the fact that at $\lambda$ equal to 0.05, the flexibility is reduced by 65%. Further under these end restraints, the ratio flexibility per unit equivalent stress is half of that in the case of the bend with tangents as end restraints as shown in Figure 6.18.

Thus for restraints by flanges, the end effect is much more pronounced than that produced by tangents.

The maximum equivalent stress factor at the centre of bend is also reduced by 30% to 60%. The conclusions based on the experiments in reference [53] show that a flange reduces the stress factor by 25% to 40%. The difference between the present analysis and that given in reference [53], may be due to the fact that in the latter case the conclusions were based on the longitudinal stress factors.

From Figure 6.12 for the flexibility factors and Figure 6.16 for equivalent stresses, it is clear that it will be difficult to lay any approximate rule for evaluating the effects of flanges on the bend.

(8) The arc length affects the position of maximum equivalent stress as is evident from the fact that for a small angle bend, it is near the intrados and for a right-angle bend, it moves to a point which is at an angle of 90 degrees from intrados. Similar effect is present in small arc bends when the pipe factor is decreased.

Addition of a rigid flange on one end alone, causes shifting of the maximum equivalent stress around the circumference of the pipe, only for the bends with high values of $\lambda$. This is evident from the fact that for a pipe factor of 0.2, the addition of a flange moves the maximum equivalent stress to intrados from a point which is at an angle

of 90 degrees from intrados.

(9) From Figures 6.12 and 6.13, it is concluded that when two bends of equal radii are connected together at one end in opposite directions, the flexibility and stress concentration factors are reduced by 10% to 15% from the corresponding values in a single right-angle bend, whereas if they are connected in the same sense (180 degree bend), the factors are increased by 15%.

Thus the end effects on the bend can be classified in an ascending order as that due to restraint by tangent pipe, reversed bend and flange.

From these conclusions it is evident that a general design criterion is difficult to be formed. But if the design of a bend is first based on the values given in Figures 6.12 and 6.16, obtained with tangents as its end restraints, then by taking proper safety factor on the basis of the conclusions reached above, bend with other end restraints can be designed. Further from the above conclusions, it is possible to predict the point of maximum stress in curved tubes with different arc lengths and end restraints.

# CHAPTER 7

## CONCLUSIONS AND RECOMMENDATIONS FOR FUTURE WORK

A method of analysis well-suited for pipe bends as a special class of general three-dimensional shell problem has been presented. This method which combines the curved shell finite-element formulation of the equilibrium problem with the simplified version of the Front Solution procedure, provides a means of solving pipe bend problems accounting for all end effects. The use of a consistent definition of the nodal degrees of freedom in the doubly curved thin shell element developed allows exact representation of the general shell structural boundary conditions. Further, a smaller amount of input data is required in this development of the element compared to that given in reference [27].

The solutions of the problem of a curved pipe under in-plane moment using three different ~~shapes~~ orders of this curved shell element and two different orders of isoparametric three-dimensional elements showed that the highest order of element available in each type was more economical for a given degree of accuracy. As anticipated the three-dimensional elements took more computer time and core than shell elements, sometimes as high as 100%, for the solution of shell structural problems with a given accuracy. The ring element was found to be quite promising in solving the pipe bend problem and more effort is required to reduce the size of the stiffness matrix of this element. The optimum number of integration points required, while calculating stiffness coefficients for the different elements used, has been given as a guide line for future users of these elements. A mass of information such as computer solution times, core necessary etc. has been given so that if similar data are available for other types of elements and for other solution

methods, a comparative study of different elements as well as of different solution techniques will be possible.

The stress distributions in a curved pipe under in-plane moment obtained using shell elements agreed well with the existing numerical solution and demonstrated the accuracy to which the stresses can be predicted using the adopted finite element displacement model. The computed flexibility and stress intensification factors in a 90 degree-bend subjected to in-plane moment over a range of pipe factors ($\lambda$) were also found to agree favourably with the known numerical solutions.

The examples presented in Chapter 5 showed that the quartic element solutions gave excellent approximations to various other analytical solutions. Further it was found that acceptable results could be obtained with a few quartic elements, for the example considered, whereas a very fine mesh was required when flat shell or shallow shell elements were used. When compared with SHEBA 6 elements, the same order of accuracy has been obtained using quartic elements but with fewer degrees of freedom representing the structure. Thus an adequate representation of a complex situation by very few elements holds a promise of cheap and simple design modification and is an essential step in this computer aided design age.

Since the quartic shell elements can allow for shear deformations, this will certainly improve the accuracy in analysing structures where shear strains may not be negligible. Even though the quadrilateral element developed can adequately represent curved edges, a curved triangular element on these lines is necessary to deal with some special problems.

The results of a study performed to determine the effects of constraints at the ends of the bends showed that the sections in the bend were warped. With a consistent definition for the flexibility, it was seen that even if the bends in a piping system are separated far apart

by straight pipes, the tangents produce a considerable reduction in the flexibility and stress factors of the bend. It was also evident that the addition of constraints such as flanges at the ends of the bend greatly increases the bending rigidity. From a study of bends with various included angles, it was seen that the relation between the flexibility factor and arc length of the bend is not linear. Further it was found that the flexibility factors are not functions of just $\lambda$ but also of the pipe dimensions not grouped into one parameter $\lambda$. The amount of these effects on the flexibility and stress factors of the bend has been given in Chapter 6 so that it can be absorbed into general design practice.

From a study of the two 90 deg-bends connected together in reversed directions, their flexibility factors were found reduced still further than those with straight tangents welded at their ends. Hence if bends in a piping system are connected closely, then under these conditions their flexibility factors have to be computed.

Thus the present design of pipeline systems have to be modified by taking into account the factors discussed above.

Even though the bends were analysed for in-plane moment loading, with a few modifications, the developed program can effectively deal with other cases of loading such as out-of-plane bending, torsion and pressure.

The effect of short tangent pipes attached to the bends can be studied if the applied moment is represented by equivalent displacements of the nodes at the load-end-cross-section. This will also help to study directly the bend with rigid flanges at both ends.

Larger and more practical problems can be solved in a matter of minutes with the help of improved, faster compilers in the computer (such as FTN on the CDC 6600 at London University). The output may be in reams and reams of paper. Hence effective visual interpretation will

be of great help in avoiding the errors in input as well as to sort out the output. Further, if the stress contours are plotted on developed shell surfaces, it opens a way for engineering optimisation by structural modifications.

Since a completely general approach for the solution of curved pipe problems is now available, some carefully controlled experiments are needed in order to verify the theoretical results.

In situations where the normal stresses do not vary linearly across the shell thickness, a need to develop a suitable system combining the five-degree freedom shell with the three-degree freedom solid exists. This is not entirely straight-forward but it is promising to note that the Front Solution technique can effectively solve problems of this nature.

## REFERENCES


(1) Argyris, J.H., "Energy Theorems and Structural Analysis", Aircraft Eng. 26, 1954, 27, 1955.

(2) Turner, M.J., Clough, R.W., Martin, H.C. and Topp, L.J., "Stiffness and Deflection Analysis of Complex Structures", J. Aeronaut. Sci. 23, No.9, 1956.

(3) Clough, R.W., "The Finite Element in Plane Stress Analysis", Proceedings, 2nd ASCE Conf. on Electronic Computation, Pittsburgh, Pa., September 1960.

(4) Clough, R.W., "The Finite Element Method in Structural Mechanics", Stress Analysis, Zienkiewicz, O.C., Holister, G.S., John Wiley & Sons Ltd., 1965.

(5) Przemieniecki, J.S., et al., "Proceedings of Conference on Matrix Methods in Structural Mechanics", Wright-Patterson Air Force Base, Ohio, 1965.

(6) Second Conference on "Matrix Methods in Structural Mechanics", Wright-Patterson Air Force Base, Ohio, 15-17, Oct. 1968.

(7) Zeinkiewicz, O.C., "The Finite Element Method in Structural and Continuum Mechanics", McGraw Hill, 1967.

(8) Przemieniecki, J.S., "Theory of Matrix Structural Analysis", McGraw Hill, 1968.

(9) Finite Element Methods in Stress Analysis, Ed. by Holand, I., and Bell, K., TAPIR - Norway 1969.

(10) Finite Element Techniques in Structural Mechanics, Ed. by Tottenham, H., and Brebbia, C. Proceedings of A Seminar At The University of Southampton, April 1970.

(11) Popov, E.P., Penzien, J. and Lee, Z.A., "Finite Element Solution for Axisymmetric Shells", J. Eng. Mech. Div., Proc. ASCE, Vol.90, No. EM5, Oct. 1964.

(12) Jones, R.E. and Strome,D.R., "A Survey of Analysis of Shells by the Displacement Method", Proc. Conf. on Matrix Methods in Structural Mechanics, AFFL-TR-66-80, 1965.

(13) Jones, R.E., and Strome, D.R., "Direct Stiffness Method Analysis of Shells of Revolution Utilizing Curved Elements", AIAA Journal, Vol. 4, No.9, September 1966.

(14) Zienkiewicz, O.C., and Cheung, Y.K., "Finite Element Method of Analysis for Arch Dam Shells and Comparison with Finite Difference Procedures", Proceedings of Symposium on Theory of Arch Dams, Southampton Univ., 1964 (Pergamon Press 1965).

(15) Clough, R.W. and Tocher, J.L., "Analysis of Thin Arch Dams by the Finite Element Method", Proceedings of Symposium on Theory of Arch Dams, Southampton Univ., 1964.(Pergamon Press, 1965).

(16) Clough, R.W. and Johnson, C.P., "A Finite Element Approximation for the Analysis of Thin Shells", Int. J. Solids Structures, Vol.4, 1968.

(17) Carr, A.J., "A Refined Finite Element Analysis of Thin Shell Structures Including Dynamic Loadings", Ph.D. Thesis, University of California, Berkeley, 1967.

(18) Johnson, C.P., "The Analysis of Thin Shells by a Finite Element Procedure", SEL Report, No.67-22, University of California, Berkeley, 1967.

(19) Utku, S., "Stiffness Matrices for Thin Triangular Elements of Nonzero Gaussian Curvature",AIAA Vol.5, No.9, September 1967.

(20) Connor, J.J. and Brebbia, C., "Stiffness Matrix for Shallow Rectangular Shell Element", Journal of the Engineering Mechanics. Division, ASCE, Vol. 93, No.5, October 1967.

(21) Ford, R., "TRIF - A triangular Finite Element for Shell Structure", C.E.G.B. Report RD/C/N359, April 1969.

(22) Megärd, G., "Planar and Curved Shell Elements", Published in "Finite Element Methods in Stress Analysis". Ed. by I. Holland and K. Bell, Tapir, Trondheim, Norway, 1969.

(23) Dupuis, G., and Goël, J.J., "A Curved Finite Element For Thin Elastic Shells", Technical Report No.4, Division of Engineering, Brown University, Providence, R.I., December 1969.

(24) Argyris, J.H. and Scharpf, D.W., "The SHEBA Family of Shell Elements for the Matrix Displacement Method", Aeronaut. J. Royal Aeronaut. Soc., Vol. 72, Oct. 1968.

(25) Irons, B.M. and Zienkiewicz, O.C., "The Isoparametric Finite Element Systems - A New Concept in Finite Element Analysis". Conf. - Recent Advances in Stress Analysis, J.B.C.S.A., Royal Aero. Soc., London, March 1968.

(26) Irons, B.M., "Numerical Integration Applied to the Finite Element Methods". Conf. on Use of Digital Computers in Structural Engineering, University of Newcastle, 1966.

(27) Ahmad, S., Irons, B.M., and Zienkiewicz, O.C., "Curved Thick Shell and Membrane Elements with Particular Reference to Axisymmetric Problems", 2nd Conf. on Matrix Methods in Structural Mechanics, Wright-Patterson Air Force Base, Ohio, 1968.

(28) Ahmad, S., Irons, B.M., and Zienkiewicz, O.C., "Analysis of Thick and Thin Shell Structures with General Curved Elements (with special reference to arch dams)". Int. J. Num. Meth. Eng., Vol. 2, July 1970.

(29) Connor, J., "Mixed Models for Plates", Chapter 5 in "Finite Element Techniques in Structural Mechanics". Proceedings of a Seminar at The University of Southampton April 1970, Ed. by H. Tottenham and C. Brebbia.

(30) Connor, J., "Mixed Models for Shells", Chapter 7 in "Finite Element Techniques in Structural Mechanics", Proceedings of A Seminar at the University of Southampton April 1970, Ed. by H. Tottenham and C. Brebbia.

(31) Pian, T.H. and Tong, P., "Basis of Finite Element Methods for Solid Continua", Int. J. for Numerical Methods in Engineering, Vol. 1, No. 1, 1969.

(32) Irons, B.M., "A Frontal Solution Program for Finite Element Analysis", Int. J. Numerical Methods in Engineering, Vol. 2, 1970.

(33) Ergatoudis, I., Irons, B.M. and Zienkiewicz, O.C., "Curved, Isoparametric, Quadrilateral Elements for Finite Element Analysis", Int. J. Solids Structure, Vol. 4, 1968.

(34) Timoshenko, S. and Goodier, J.N., "Theory of Elasticity", McGraw-Hill (1951).

(35) Conte, S.D., "Elementary Numerical Analysis", McGraw-Hill (1965).

(36) Kopal, Z., "Numerical Analysis", Chapman and Hall, London (1955).

(37) Irons, B.M., "Economical Computer Techniques for Numerically Integrated Finite Elements", Int. J. Numerical Methods in Engineering, Vol. 1, 1969.

(38) Ergatoudis, J., "Isoparametric Finite Elements in Two and Three Dimensional Analysis", Ph.D. Thesis, University of Wales, Swansea, 1968.

(39) Iron, B.M., "The GSS Front Solution", Systems and Programming Specifications 0021, Rolls-Royce Ltd., England.

(40) Blomfield, J.A., "The Elastic-Plastic Behaviour of Pipe Bends Subjected to Cyclic Loading", Ph.D. Thesis, London University, 1970.

(41) Gross, N. and Ford, H., "The Flexibility of Short-Radius Pipe Bends", Proc. I. Mech. E., (B), V. 1B, 1952-53.

(42) Gross, N., "Experiments on Short-Radius Pipe Bends", Proc. I. Mech. E. (B), V. 1B, 1952-53.

(43) Jones, N., "In Plane Bending of A Short-Radius Curved Pipe Bend", J. Eng. Ind., May 1967.

(44) Reissner, E., "On Bending of Curved Thin-Walled Tubes", Proc. Nat. Acad. Sci., U.S., Vol. 35, 1949.

(45) Clark, R., and Reissner, E., "Bending of Curved Tubes", Advances in Applied Mechanics, Vol. 2, Academic Press, N.Y.

(46) Turner, C.E. and Ford H., "Examination of The Theories for Calculating the Stresses in Pipe Bends Subjected to In-Plane Bending," Proc. of The Institution of Mech. Enggs, London, Vol.171, No.15, 1957.

(47) Prince, N. and Rashid, Y.R., "Structural Analysis of Shell Intersections", Paper presented at Ist. Int. Conf. on Pressure Vessel Technology, Delft, Netherlands, Oct. 1969.

(48) Ford, R., "TRIB- A Triangular Finite Element for Plate Flexture", C.E.G.B. Report RD/C/N188, Sept. 1968.

(49) Kalnins, A., "Analysis of Shells of Revolution Subjected to Symmetrical and Non-Symmetrical Loads", Jr. of App. Mech., Sept. 1964.

(50) Argyris, J.H., "The Impact of the Digital Computer on Engineering Sciences - Part (I)", The Aeronautical Journal of the Royal Aeronautical Society, Vol. 74, Jan. 1970.

(51) Flügge, W., "Stresses in Shells", Springer, Berlin - Göttingen - Heidelberg - New York, 1966.

(52) Timoshenko, S. and Woinowsky-Krieger, S., "Theory of Plates and Shells", Engineering Societies Monographs, McGraw-Hill Book Co., Inc., New York, 2nd edition, 1959.

(53) Pardue, T.E., and Vigness, I., "Properties of Thin Walled Curved Tubes of Short-Bend Radius", Trans. ASME, Vol. 73, 1951, pp. 77-87.

(54) Kalnins, A., "Stress Analysis of Curved Tubes", Paper presented at Ist Int. Conf. on Pressure Vessel Tech., Delft, Netherlands, Oct. 1969.

(55) Smith, R.T., and Ford, H., "Experimental Study of the Flexibility of a Full Scale Two Dimensional Steam Pipeline", Jr. Mechanical Engg Science, Vol. 4, No.3, 1962, pp. 270-286.

(56) Ford, H., "Advanced Mechanics of Materials", (1963), Longmans.

(57) Von Kármán, T., "Über die Formanderung dunnwandiger Rohre insbesonders federnder Ansgleichrohe," Zeitschrift VDI, Vol. 55, 1911.

(58) Kafka, P.G. and Dunn, M.B., "Stiffness of Curved Circular Tubes with Internal Pressure", Trans. A.S.M.E., V. 78, June 1956.

(59) Rodabaugh, E.C. and George, H.H., "Effect of Internal Pressure on Flexibility and Stress-Intensification Factors of Curved Pipe or Welding Elbows", Trans. A.S.M.E., V.79, No.4, May 1957.

(60) Smith, R.T., "Theoretical Analysis of the Stresses in Pipe Bends Subjected to Out-of-Plane Bending", J. Mech. Eng. Sci., V.9, No.2, 1967.

# APPENDIX A

## Theory of Isoparametric Three-Dimensional Element

### Isoparametric Elements

All practical problems in fact are three-dimensional though in many cases two-dimensional representations give adequate approximations with a considerably reduced effort. At the same time there is no mathematical complication in the addition of the third dimension. The Three-Dimensional elements which have been programmed and used in this thesis are the Isoparametric elements. The 'Isoparametric' concept [33] that is to use the same interpolation functions for both the coordinates and the unknowns, facilitates the formulation of curved elements.

The important step, as in the case of all finite elements, is to choose a shape function prescribing the variation of displacements (or coordinates) in terms of appropriate nodal values. Shape functions should also be (1) continuous within the element and across interelement boundaries and (2) they can reproduce conditions of constant strain exactly. In most cases these are derived from a suitable polynomial. The polynomial is chosen so that the displacements along the edges are linear, parabolic, cubic and so on, giving a unique variation of displacements in terms of the nodal values on that edge. The number of terms in the polynomial usually equals the number of nodes in the element.

Let $\phi$ be the quantity to be interpolated, this may be a coordinate, x, y, z, a displacement $u_x$, $u_y$, $u_z$, the temperature or any other quantity prescribed over the element, in terms of its nodal values.

For instance in a typical three-dimensional element with n nodes, the coordinates are given by

$$\phi = \alpha_1+\alpha_2 x + \alpha_3 y + \alpha_4 z + \ldots + \alpha_n x^4 y^3 z^5 \qquad (A.1)$$

or $$\phi(x,y,z) = [M(x,y,z)][\alpha] \quad (A.2)$$

where $$[M] = [1,x,y,z, \ldots, x^4y^3z^5] \quad (A.3)$$

and $$[\alpha]^T = [\alpha_1,\alpha_2, \ldots, \alpha_n] \quad (A.4)$$

By substituting the coordinates of each node,

$$\phi_i = [C][\alpha] \quad (A.5)$$

where C is a square matrix of constant terms. If Det[C] $\neq$ 0

$$[\alpha] = [C]^{-1} \phi_i \quad (A.6)$$

Therefore

$$\phi(x,y,z) = M(x,y,z)\ C^{-1}\ \phi_i \quad (A.7)$$

$$= \Sigma N_i\ \phi_i \quad (A.8)$$

Where $N_i$ is the Interpolation shape function taking a value of unity at the node i and zero at all other nodes.

Using precisely the same polynomial terms but now with the local natural non-dimensional $\xi$, $\eta$ and $\zeta$ coordinates, with a range of +1 and -1 within such elements, instead of the x,y and z, the general shape elements as in Figure A.2 can be formulated.

The basic shape of the sides of these elements are straight and since the more general shaped elements are derived from this, these are called 'Parent' elements. The Parent element is a cube of base 2, with the cartesian system oxyz as its reference and shown in Figure A.1. Two types of elements have been used in the investigation. In the first type the displacements vary parabolically along an edge and the corresponding position of the nodes is shown in Figure A.2(a). In the other

they vary cubically as shown in Figure A.2(b). The corresponding shape functions are given in Appendix B.

Convergence Criteria

To ensure convergence to the correct solution by finer mesh subdivision, there are three requirements which the assumed displacement functions must satisfy [7]:

(1) The assumed displacements must be continuous over each element and across element boundaries.

(2) Rigid body movements should be possible without straining.

(3) Any required state of constant strain can be adequately reproduced on the element.

To satisfy the continuity of displacements along the interfaces, it is necessary for $u_x$, $u_y$ and $u_z$ to be uniquely defined over the face of the element by the displacements of the nodes in that face only. The $N_i$ for nodes not on that face are zero, therefore the variation of displacements on that face, for both elements is identical.

With regard to the second and third conditions which are closely related, a constant strain and rigid body motion are associated with

$$u_x = a + bx + cy + dz \tag{A.9}$$

where a, b, c and d are arbitrary constants (with similar requirements for $u_y$ and $u_z$). Thus

$$\begin{aligned} u_x &= a + bx + cy + dz \\ &= N_1 u_{x_1} + N_2 u_{x_2} + \ldots \\ &= N_1(a + bx_1 + cy_1 + dz_1) + N_2(a + bx_2 + cy_2 + dz_2) \\ &\quad \ldots. \end{aligned}$$

$$= a(N_1 + N_2 + \ldots) + b(N_1x_1 + N_2x_2 + \ldots) +$$

$$c(N_1y_1 + N_2y_2 + \ldots) + d(N_1z_1 + N_2z_2 + \ldots) \qquad (A.10)$$

which is an identity by virtue of the definition of the coordinates x, y and z and

$$N_1 + N_2 + \ldots = 1 \qquad (A.11)$$

This last statement must be true as the coordinates have to be defined uniquely for any nodal values. Thus, for example, the element size decreases to zero and $x_1 \to x_2 \to x_3$ etc. $\to$ A. Thus also for any internal point $x \to A$ and substituting we have

$$A = N_1A + N_2A + \ldots \qquad (A.12)$$

which verifies the previous assertion.

Elements formulated in natural coordinates $\xi$, $\eta$, $\zeta$ have invariant properties, that is, their force displacement relations are independent of the external reference system.

Stiffness Formulation

The formulation of displacement model element characteristics such as stiffness etc. are available in the finite element text [7]. The stiffness matrix of an element is defined, for instance, as

$$[K]^e = \int_V [B]^T [D] [B] \, dV \qquad (A.13)$$

in which the [B] matrix relates the strains $\{\varepsilon\}$ to the element nodal displacements

$$\{\varepsilon\} = [B] \{\delta\}^e \qquad (A.14)$$

and [D] is the elasticity matrix giving stress-strain relationship

$$\{\sigma\} = [D]\{\varepsilon\} \tag{A.15}$$

The strains $\{\varepsilon\}$ can be obtained once the displacements at any point within the element are defined.

In the case of three-dimensional elements, the element nodal displacements vector is

$$\{\delta\}^e = \begin{Bmatrix} \{\delta_1\} \\ \{\delta_2\} \\ \vdots \\ \{\delta_i\} \\ \vdots \end{Bmatrix} \quad \text{where} \quad \{\delta_i\} = \begin{Bmatrix} u_x \\ u_y \\ u_z \end{Bmatrix}_i \tag{A.16}$$

and the interpolation formula is of the form given in expression A.8.

To calculate the strains, derivatives of the displacements with respect to x, y and z are needed, but the displacements are given as functions of $\xi$, $\eta$ and $\zeta$. The logical step is to convert the $\xi$, $\eta$ and $\zeta$ derivatives of $\phi$

$$\begin{Bmatrix} \frac{\partial\phi}{\partial\xi} \\ \frac{\partial\phi}{\partial\eta} \\ \frac{\partial\phi}{\partial\zeta} \end{Bmatrix} = \begin{bmatrix} \frac{\partial N_1}{\partial\xi}, & \frac{\partial N_2}{\partial\xi}, & \cdots \\ \frac{\partial N_1}{\partial\eta}, & \frac{\partial N_2}{\partial\eta}, & \cdots \\ \frac{\partial N_1}{\partial\zeta}, & \frac{\partial N_2}{\partial\zeta}, & \cdots \end{bmatrix} \begin{Bmatrix} \phi_1 \\ \phi_2 \\ \cdot \\ \cdot \\ \cdot \end{Bmatrix} \tag{A.17}$$

or in shorthand form

$$\begin{Bmatrix} \frac{\partial\phi}{\partial\xi} \\ \frac{\partial\phi}{\partial\eta} \\ \frac{\partial\phi}{\partial\zeta} \end{Bmatrix} = [DE]\{\phi^e\} \tag{A.18}$$

into x, y and z derivatives using the chain rule.

In matrix form

$$\begin{Bmatrix} \frac{\partial\phi}{\partial\xi} \\ \frac{\partial\phi}{\partial\eta} \\ \frac{\partial\phi}{\partial\zeta} \end{Bmatrix} = \begin{bmatrix} \frac{\partial x}{\partial\xi} & \frac{\partial y}{\partial\xi} & \frac{\partial z}{\partial\xi} \\ \frac{\partial x}{\partial\eta} & \frac{\partial y}{\partial\eta} & \frac{\partial z}{\partial\eta} \\ \frac{\partial x}{\partial\zeta} & \frac{\partial y}{\partial\zeta} & \frac{\partial z}{\partial\zeta} \end{bmatrix} \begin{Bmatrix} \frac{\partial\phi}{\partial x} \\ \frac{\partial\phi}{\partial y} \\ \frac{\partial\phi}{\partial z} \end{Bmatrix} = [J] \begin{Bmatrix} \frac{\partial\phi}{\partial x} \\ \frac{\partial\phi}{\partial y} \\ \frac{\partial\phi}{\partial z} \end{Bmatrix} \qquad \text{(A.19)}$$

where [J] is the Jacobian matrix.

This transformation can be inverted and substituted in expression A.18 to give

$$\begin{Bmatrix} \frac{\partial\phi}{\partial x} \\ \frac{\partial\phi}{\partial y} \\ \frac{\partial\phi}{\partial z} \end{Bmatrix} = [J]^{-1} [DE] \{\phi\}^e = [DEXYZ] \{\phi\}^e \qquad \text{(A.20)}$$

Substituting $u_x$, $u_y$ and $u_z$ in turn for $\phi$ in A.20 yields

$$\begin{bmatrix} \frac{\partial u_x}{\partial x} & \frac{\partial u_y}{\partial x} & \frac{\partial u_z}{\partial x} \\ \frac{\partial u_x}{\partial y} & \frac{\partial u_y}{\partial y} & \frac{\partial u_z}{\partial y} \\ \frac{\partial u_x}{\partial z} & \frac{\partial u_y}{\partial z} & \frac{\partial u_z}{\partial z} \end{bmatrix} = [DEXYZ] \begin{bmatrix} u_{x_1} & u_{y_1} & u_{z_1} \\ u_{x_2} & u_{y_2} & u_{z_2} \\ u_{x_3} & u_{y_3} & u_{z_3} \\ \cdot & \cdot & \cdot \\ \cdot & \cdot & \cdot \end{bmatrix} \qquad \text{(A.21)}$$

The strain displacement relations [34] are given as

$$\begin{Bmatrix} \varepsilon_x \\ \varepsilon_y \\ \varepsilon_z \\ \gamma_{xy} \\ \gamma_{yz} \\ \gamma_{xz} \end{Bmatrix} = \begin{Bmatrix} \partial u_x/\partial x \\ \partial u_y/\partial y \\ \partial u_z/\partial z \\ \partial u_x/\partial y + \partial u_y/\partial x \\ \partial u_y/\partial z + \partial u_z/\partial y \\ \partial u_z/\partial x + \partial u_x/\partial z \end{Bmatrix} \tag{A.22}$$

Thus knowing the nodal displacements, the strains at any point in an element, are given in the matrix form as

$$\begin{Bmatrix} \varepsilon_x \\ \varepsilon_y \\ \varepsilon_z \\ \gamma_{xy} \\ \gamma_{yz} \\ \gamma_{zx} \end{Bmatrix} = \begin{bmatrix} A(1,1) & 0 & 0 & A(1,2) & 0 & 0 & - & - \\ 0 & A(2,1) & 0 & 0 & A(2,2) & 0 & - & - \\ 0 & 0 & A(3,1) & 0 & 0 & A(3,2) & - & - \\ A(2,1) & A(1,1) & 0 & A(2,2) & A(1,2) & 0 & - & - \\ 0 & A(3,1) & A(2,1) & 0 & A(3,2) & A(2,2) & - & - \\ A(3,1) & 0 & A(1,1) & A(3,2) & 0 & A(1,2) & - & - \end{bmatrix} * \begin{Bmatrix} u_{x_1} \\ u_{y_1} \\ u_{z_1} \\ u_{x_2} \\ u_{y_2} \\ u_{z_2} \\ \vdots \\ \cdot \end{Bmatrix} \tag{A.23}$$

where matrix [A] ≡ [DEXYZ], used for simplicity sake.

Thus expression A.23 defines the [B] matrix in the basic expression A.14. Remembering that [B] is a function of $\xi$, $\eta$ and $\zeta$, the element of volume in the integration for the stiffness must also be transformed as

$$dx\ dy\ dz = \text{Det}\ [J]\ d\xi\ d\eta\ d\zeta \tag{A.24}$$

The limits of integration also change and the stiffness is given by

$$[K]^e = \int_{-1}^{+1}\int_{-1}^{+1}\int_{-1}^{+1} [B]^T\ [D]\ [B]\ \text{Det}\ [J]\ d\xi\ d\eta\ d\zeta \tag{A.25}$$

[D], the elasticity matrix for an isotropic material is given as

$$[D] = \frac{E}{(1+\nu)(1-2\nu)} \begin{bmatrix} (1-\nu) & \nu & \nu & 0 & 0 & 0 \\ & (1-\nu) & \nu & 0 & 0 & 0 \\ & & (1-\nu) & 0 & 0 & 0 \\ & & & \left(\frac{1-2\nu}{2}\right) & 0 & 0 \\ & \text{Symmetric} & & & \left(\frac{1-2\nu}{2}\right) & 0 \\ & & & & & \left(\frac{1-2\nu}{2}\right) \end{bmatrix} \tag{A.26}$$

where E is the Young's Modulus and $\nu$, the Poisson's ratio for the material.

The assembly of the stiffness equations and their subsequent solution is performed by a version of the 'Front Solution' as described in Chapter 3.

Numerical Integration

Numerical integration facilitates the speedy formulation and programming of a complicated element like the curved three-dimensional elements, for which closed form integration is complicated, in a relatively short time.

The expressions to be integrated over the volume of an element, as given in equation A.25, are functions of $\xi$, $\eta$ and $\zeta$ which take values between +1 and -1. Since the limits of integration are +1 to -1 for such expressions, they are ideally suited for the Gaussian Quadrature formulae [35].

Gauss Quadrature

The approximation with n sampling points is exact for a polynomial f(x) of degree less than or equal to (2n + 1). In numerical integration the definite integral $\int_{-1}^{+1} f(x)\,dx$ is replaced by the summation $\Sigma\, C_j f(a_j)$ (j = 1 to n) where $C_j$ is the weight coefficient, $f(a_j)$ the value of the function at the specified point $a_j$ and n the number of Gauss points used. The 'C' and 'a' values for n = 2 to n = 512 can be found in reference [36].

Three-Dimensional Elements

To integrate over the volume of the element, the standard operation

$$\int_{-1}^{+1} f(\xi)\,d\xi = \sum_{j=1}^{n} C_j\, f(a_j) \qquad \text{(A.27)}$$

is used three times. So in this case

$$[K] = \sum_{q=1}^{n^3} K_q\, [B]^T\, [D]\, [B]\, \mathrm{Det}[J]_q \qquad \text{(A.28)}$$

where q is the Gaussian sampling point at which the values of the functions are calculated, and $K_q$ is the product of the three weight coefficients at this point.

The decision as to which order of approximation formulae is necessary in these types of elements is made, by comparing the solution using these

elements with that obtained by other methods. This has been explained in detail in Chapter 4.

Economical Use of Elasticity Matrix

For a cubic three-dimensional element, the stiffness is a 96 x 96 matrix and created by numerical integration. Matrix multiplications are seldom an efficient process and a little sophistication in the integration process is desirable, particularly in the three-dimensional elements. This was suggested by Irons [37] and is included in the present formulation of the element stiffness matrix.

The stiffness matrix is given by

$$K = \sum_{V} [B]^T [D] [B] \qquad (A.29)$$

where [B] can be written as

$$[B] = \begin{bmatrix} 1 & 0 & 0 & 0 & 0 & 0 & 0 & 0 & 0 \\ 0 & 0 & 0 & 0 & 1 & 0 & 0 & 0 & 0 \\ 0 & 0 & 0 & 0 & 0 & 0 & 0 & 0 & 1 \\ 0 & 0 & 0 & 0 & 0 & 1 & 0 & 1 & 0 \\ 0 & 0 & 1 & 0 & 0 & 0 & 1 & 0 & 0 \\ 0 & 1 & 0 & 1 & 0 & 0 & 0 & 0 & 0 \end{bmatrix} * \begin{bmatrix} \{Q_1\} & 0 & 0 & \{Q_2\} & 0 & 0 \\ 0 & \{Q_1\} & 0 & 0 & \{Q_2\} & 0 \\ 0 & 0 & \{Q_1\} & 0 & 0 & \{Q_2\} \end{bmatrix} \text{ etc.}$$

$$\text{(or)} \qquad [B] = [H] [Q] \qquad (A.30)$$

where

$$\{Q_i\} = \begin{Bmatrix} DEXYZ(1,i) \\ DEXYZ(2,i) \\ DEXYZ(3,i) \end{Bmatrix} \quad (A.31)$$

The stiffness matrix now takes the form

$$K = [Q]^T [H]^T [D] [H] [Q] \quad (A.32)$$

(or)

$$K = [Q]^T [P] [Q] \quad (A.33)$$

where $$[P] = [H]^T [D] [H] \quad (A.34)$$

which can be taken out of the integration.

Taking advantage of the zeros in [Q] matrix, the stiffness can be calculated using equation A.33.

The number of multiplications while calculating the full stiffness matrix for a quadratic element at a Gaussian point, using the old system is 23760, which reduces to 13230 while using the method suggested above. Further the computer time is also halved.

Equivalent Nodal Forces

In general a continuum is loaded by surface or body forces acting on a finite area or volume. For the finite element method these loads must be converted into consistent nodal forces and given by the standard expression

$$\{F\}^e = \int_V [N]^T \{g\} \, d(vol) \quad (A.35)$$

where $\{g(x,y,z)\}$ is a vector expression representing the applied load and [N] is the shape function matrix.

Surface Distributed Pressure

Let the pressure P be the load applied on an infinitesimal element of area dA on the face $\zeta = -1$ of a three-dimensional element. The pressure P can be uniform or of any other function. The element of volume is replaced by the element of area dA as the integration is to be performed only over a face.

Hence the expression for the equivalent nodal forces takes the form

$$\{F\}^e = \int_A [N]^T P \, dA \tag{A.36}$$

where

$$\{F\}^e = [F_1, F_2, \ldots]^T \tag{A.37}$$

and the equivalent nodal forces and

$$\{F_i\} = \begin{Bmatrix} U_x \\ U_y \\ U_z \end{Bmatrix}_i \tag{A.38}$$

the nodal components of force in the x, y and z directions.

dA, the element of area is the vector product

$$dA = \vec{\partial\xi} \times \vec{\partial\eta} \tag{A.39}$$

(or)

$$dA = \begin{Bmatrix} \frac{\partial x}{\partial \xi} \\ \frac{\partial y}{\partial \xi} \\ \frac{\partial z}{\partial \xi} \end{Bmatrix} \times \begin{Bmatrix} \frac{\partial x}{\partial \eta} \\ \frac{\partial y}{\partial \eta} \\ \frac{\partial z}{\partial \eta} \end{Bmatrix} d\xi \, d\eta$$

$$= \begin{Bmatrix} \partial A_x \\ \partial A_y \\ \partial A_z \end{Bmatrix} \tag{A.40}$$

Hence the equivalent nodal forces are given by

$$\{F_i\} = \int_{-1}^{+1}\int_{-1}^{+1} N_i \begin{bmatrix} 1 & 0 & 0 \\ 0 & 1 & 0 \\ 0 & 0 & 1 \end{bmatrix} P \begin{Bmatrix} \partial A_x \\ \partial A_y \\ \partial A_z \end{Bmatrix} d\xi\, d\eta \tag{A.41}$$

The integration is again evaluated numerically.

Stress Calculation

Once the nodal displacements have been determined by the solution of the overall 'structural' type equations, the stresses at any point within an element can be found knowing the [B] matrix at that point and given by

$$\{\sigma(\xi,\eta,\zeta)\} = [D]\ [B(\xi,\eta,\zeta)]\ \{\delta\}^e \tag{A.42}$$

The matrix product [D] [B] sometimes is referred to as the stress matrix.

The stresses along the global directions are calculated at the nodal points and if at a point, many elements meet, the stresses are averaged.

# APPENDIX B

## Shape Functions For Three-Dimensional Isoparametric Elements

### Quadratic Element

The following polynomial for $\phi$, representing a coordinate or displacement, ensures a parabolic variation along the edges.

$$\begin{aligned} = \; & \alpha_1 + \alpha_2\xi + \alpha_3\eta + \alpha_4\zeta + \alpha_5\xi\eta + \alpha_6\eta\zeta + \alpha_7\zeta\xi + \alpha_8\xi\eta\zeta + \alpha_9\xi^2 \\ & + \alpha_{10}\eta^2 + \alpha_{11}\zeta^2 + \alpha_{12}\xi^2\eta + \alpha_{13}\xi^2\zeta + \alpha_{14}\xi\eta^2 + \alpha_{15}\eta^2\zeta \\ & + \alpha_{16}\eta\zeta^2 + \alpha_{17}\xi\zeta^2 + \alpha_{18}\xi^2\eta\zeta + \alpha_{19}\xi\eta^2\zeta + \alpha_{20}\xi\eta\zeta^2 \end{aligned} \tag{B.1}$$

There are 20 nodal values from which the 20 constants can be evaluated (Figure A.3) and the explicit expressions for shape functions are

$$\begin{aligned} 8N_1 &= (1-\xi)(1-\eta)(1+\zeta)(-\xi-\eta+\zeta-2) \\ 4N_2 &= (1-\xi)(1-\eta^2)(1+\zeta) \\ 8N_3 &= (1-\xi)(1+\eta)(1+\zeta)(-\xi+\eta+\zeta-2) \\ 4N_4 &= (1-\xi^2)(1+\eta)(1+\zeta) \\ 8N_5 &= (1+\xi)(1+\eta)(1+\zeta)(\xi+\eta+\zeta-2) \\ 4N_6 &= (1+\xi)(1-\eta^2)(1+\zeta) \\ 8N_7 &= (1+\xi)(1-\eta)(1+\zeta)(\xi-\eta+\zeta-2) \\ 4N_8 &= (1-\xi^2)(1-\eta)(1+\zeta) \\ 4N_9 &= (1-\xi)(1-\eta)(1-\zeta^2) \\ 4N_{10} &= (1-\xi)(1+\eta)(1-\zeta^2) \\ 4N_{11} &= (1+\xi)(1+\eta)(1-\zeta^2) \\ 4N_{12} &= (1+\xi)(1-\eta)(1-\zeta^2) \\ 8N_{13} &= (1-\xi)(1-\eta)(1-\zeta)(-\xi-\eta-\zeta-2) \\ 4N_{14} &= (1-\xi)(1-\eta^2)(1-\zeta) \end{aligned} \tag{B.2}$$

$$
\begin{aligned}
8N_{15} &= (1-\xi)(1+\eta)(1-\zeta)(-\xi+\eta-\zeta-2) \\
4N_{16} &= (1-\xi^2)(1+\eta)(1-\zeta) \\
8N_{17} &= (1+\xi)(1+\eta)(1-\zeta)(\xi+\eta-\zeta-2) \\
4N_{18} &= (1+\xi)(1-\eta^2)(1-\zeta) \\
8N_{19} &= (1+\xi)(1-\eta)(1-\zeta)(\xi-\eta-\zeta-2) \\
4N_{20} &= (1-\xi^2)(1-\eta)(1-\zeta)
\end{aligned}
\qquad \text{(B.2)}
$$

Cubic Element

The chosen polynomial for $\phi$ is, $\phi$ = 20 terms of the Quadratic Element +

$$\alpha_{21}\xi^3 + \alpha_{22}\eta^3 + \alpha_{23}\zeta^3 + \alpha_{24}\xi^3\eta\zeta + \alpha_{25}\xi\eta^3\zeta + \alpha_{26}\xi\eta\zeta^3 + \alpha_{27}\xi^3\eta +$$

$$\alpha_{28}\xi^3\zeta + \alpha_{29}\xi\eta^3 + \alpha_{30}\eta^3\zeta + \alpha_{31}\xi\zeta^3 + \alpha_{32}\eta\zeta^3 \qquad \text{(B.3)}$$

Using the 32 nodal values, the expressions for the shape functions are (Figure A.3)

$$
\begin{aligned}
64N_1 &= (1-\xi)(1-\eta)(1+\zeta)\{9(\xi^2+\eta^2+\zeta^2)-19\} \\
64N_2 &= 9(1-\eta^2)(1-\xi)(1-3\eta)(1+\zeta) \\
64N_3 &= 9(1-\eta^2)(1-\xi)(1+3\eta)(1+\zeta) \\
64N_4 &= (1-\xi)(1+\eta)(1+\zeta)\{9(\xi^2+\eta^2+\zeta^2)-19\} \\
64N_5 &= 9(1-\xi^2)(1-3\xi)(1+\eta)(1+\zeta) \\
64N_6 &= 9(1-\xi^2)(1+3\xi)(1+\eta)(1+\zeta) \\
64N_7 &= (1+\xi)(1+\eta)(1+\zeta)\{9(\xi^2+\eta^2+\zeta^2)-19\} \\
64N_8 &= 9(1-\eta^2)(1+\xi)(1+3\eta)(1+\zeta) \\
64N_9 &= 9(1-\eta^2)(1+\xi)(1-3\eta)(1+\zeta) \\
64N_{10} &= (1+\xi)(1-\eta)(1+\zeta)\{9(\xi^2+\eta^2+\zeta^2)-19\} \\
64N_{11} &= 9(1-\xi^2)(1+3\xi)(1-\eta)(1+\zeta) \\
64N_{12} &= 9(1-\xi^2)(1-3\xi)(1-\eta)(1+\zeta)
\end{aligned}
\qquad \text{(B.4)}
$$

$$64N_{13} = 9(1-\zeta^2)(1+3\zeta)(1-\xi)(1-\eta)$$

$$64N_{14} = 9(1-\zeta^2)(1+3\zeta)(1-\xi)(1+\eta)$$

$$64N_{15} = 9(1-\zeta^2)(1+3\zeta)(1+\xi)(1+\eta)$$

$$64N_{16} = 9(1-\zeta^2)(1-3\zeta)(1+\xi)(1-\eta)$$

$$64N_{17} = 9(1-\zeta^2)(1-3\zeta)(1-\xi)(1-\eta)$$

$$64N_{18} = 9(1-\zeta^2)(1-3\zeta)(1-\xi)(1+\eta)$$

$$64N_{19} = 9(1-\zeta^2)(1-3\zeta)(1+\xi)(1+\eta)$$

$$64N_{20} = 9(1-\zeta^2)(1-3\zeta)(1+\xi)(1-\eta)$$

$$64N_{21} = (1-\xi)(1-\eta)(1-\zeta)\{9(\xi^2+\eta^2+\zeta^2)-19\}$$

$$64N_{22} = 9(1-\eta^2)(1-\xi)(1-3\eta)(1-\zeta)$$

$$64N_{23} = 9(1-\eta^2)(1-\xi)(1+3\eta)(1-\zeta)$$

$$64N_{24} = (1-\xi)(1+\eta)(1-\zeta)\{9(\xi^2+\eta^2+\zeta^2)-19\}$$

$$64N_{25} = 9(1-\xi^2)(1-3\xi)(1+\eta)(1-\zeta)$$

$$64N_{26} = 9(1-\xi^2)(1+3\xi)(1+\eta)(1-\zeta)$$

$$64N_{27} = (1+\xi)(1+\eta)(1-\zeta)\{9(\xi^2+\eta^2+\zeta^2)-19\}$$

$$64N_{28} = 9(1-\eta^2)(1+\xi)(1+3\eta)(1-\zeta)$$

$$64N_{29} = 9(1-\eta^2)(1+\xi)(1-3\eta)(1-\zeta)$$

$$64N_{30} = (1+\xi)(1-\eta)(1-\zeta)\{9(\xi^2+\eta^2+\zeta^2)-19\}$$

$$64N_{31} = 9(1-\xi^2)(1+3\xi)(1-\eta)(1-\zeta)$$

$$64N_{32} = 9(1-\xi^2)(1-3\xi)(1-\eta)(1-\zeta)$$

APPENDIX C

## Shape Functions For Curved Shell Elements

Quadratic Element (Figure 2.5a)

The polynomial for $\phi$, which can be a coordinate or displacement of the midsurface of the shell element, is chosen as

$$\phi = \alpha_1 + \alpha_2\xi + \alpha_3\eta + \alpha_4\xi^2 + \alpha_5\xi\eta + \alpha_6\eta^2 + \alpha_7\xi^2\eta + \alpha_8\xi\eta^2 \tag{C.1}$$

such that the function varies parabolically along an edge. The eight constants are derived from the eight nodal values of the element. The shape functions are given as

$$\begin{aligned}
N_1 &= \tfrac{1}{4}(-1+\xi\eta+\xi^2+\eta^2-\xi^2\eta-\xi\eta^2) \\
N_2 &= \tfrac{1}{2}(1-\xi-\eta^2+\xi\eta^2) \\
N_3 &= \tfrac{1}{4}(-1-\xi\eta+\xi^2+\eta^2+\xi^2\eta-\xi\eta^2) \\
N_4 &= \tfrac{1}{2}(1+\eta-\xi^2-\xi^2\eta) \\
N_5 &= \tfrac{1}{4}(-1+\xi\eta+\xi^2+\eta^2+\xi^2\eta+\xi\eta^2) \\
N_6 &= \tfrac{1}{2}(1+\xi-\eta^2-\xi\eta^2) \\
N_7 &= \tfrac{1}{4}(-1-\xi\eta+\xi^2+\eta^2-\xi^2\eta+\xi\eta^2) \\
N_8 &= \tfrac{1}{2}(1-\eta-\xi^2+\xi^2\eta)
\end{aligned} \tag{C.2}$$

Cubic Element (Figure 2.5b)

$$\phi = \text{a complete cubic} + \alpha_{11}\xi^3\eta + \alpha_{12}\xi\eta^3 \tag{C.3}$$

The shape functions are given by

$$
\begin{aligned}
N_1 &= \frac{1}{32}(1-\xi)(1-\eta)\{-10+9(\xi^2+\eta^2)\} \\
N_2 &= \frac{9}{32}(1-\xi)(1-\eta^2)(1-3\eta) \\
N_3 &= \frac{9}{32}(1-\xi)(1-\eta^2)(1+3\eta) \\
N_4 &= \frac{1}{32}(1-\xi)(1+\eta)\{-10+9(\xi^2+\eta^2)\} \\
N_5 &= \frac{9}{32}(1-\xi^2)(1-3\xi)(1+\eta) \\
N_6 &= \frac{9}{32}(1-\xi^2)(1+3\xi)(1+\eta) \\
N_7 &= \frac{1}{32}(1+\xi)(1+\eta)\{-10+9(\xi^2+\eta^2)\} \\
N_8 &= \frac{9}{32}(1+\xi)(1-\eta^2)(1+3\eta) \\
N_9 &= \frac{9}{32}(1+\xi)(1-\eta^2)(1-3\eta) \\
N_{10} &= \frac{1}{32}(1+\xi)(1-\eta)\{-10+9(\xi^2+\eta^2)\} \\
N_{11} &= \frac{9}{32}(1-\xi^2)(1+3\xi)(1-\eta) \\
N_{12} &= \frac{9}{32}(1-\xi^2)(1-3\xi)(1-\eta)
\end{aligned}
\qquad (C.4)
$$

Quartic Element (Figure 2.5c)

This element has 17 nodes with one internal node at $\xi = 0$, $\eta = 0$. The chosen polynomial for $\phi$ is

$$\phi = \text{complete quartic} + \alpha_{16}\xi^4\eta + \alpha_{17}\xi\eta^4 \qquad (C.5)$$

The shape functions are given by

$$
\begin{aligned}
N_1 &= \frac{1}{12}(1-\xi)(1-\eta)\{4[\xi(1-\xi^2)+\eta(1-\eta^2)]+3\xi\eta\} \\
N_2 &= -\frac{4}{3}\eta(1-\eta^2)(\frac{1}{2}-\eta)(1-\xi) \\
N_3 &= 2(\frac{1}{4}-\eta^2)(1-\eta^2)(1-\xi)-\frac{1}{2}(1-\xi^2)(1-\eta^2) \\
N_4 &= \frac{4}{3}\eta(1-\eta^2)(\frac{1}{2}+\eta)(1-\xi) \\
N_5 &= \frac{1}{12}(1-\xi)(1+\eta)\{4[\xi(1-\xi^2)-\eta(1-\eta^2)]-3\xi\eta\}
\end{aligned}
\qquad (C.6)
$$

$$N_6 = -\frac{4}{3}\xi(1-\xi^2)(\frac{1}{2}-\xi)(1+\eta)$$

$$N_7 = 2(\frac{1}{4}-\xi^2)(1-\xi^2)(1+\eta)-\frac{1}{2}(1-\xi^2)(1-\eta^2)$$

$$N_8 = \frac{4}{3}\xi(1-\xi^2)(\frac{1}{2}+\xi)(1+\eta)$$

$$N_9 = \frac{1}{12}(1+\xi)(1+\eta)\{-4[\xi(1-\xi^2)+\eta(1-\eta^2)]+3\xi\eta\}$$

$$N_{10} = \frac{4}{3}\eta(1-\eta^2)(\frac{1}{2}+\eta)(1+\xi)$$

$$N_{11} = 2(\frac{1}{4}-\eta^2)(1-\eta^2)(1+\xi)-\frac{1}{2}(1-\xi^2)(1-\eta^2)$$

$$N_{12} = -\frac{4}{3}\eta(1-\eta^2)(\frac{1}{2}-\eta)(1+\xi)$$

$$N_{13} = \frac{1}{12}(1+\xi)(1-\eta)\{-4[\xi(1-\xi^2)-\eta(1-\eta^2)]-3\xi\eta\}$$

$$N_{14} = \frac{4}{3}\xi(1-\xi^2)(\frac{1}{2}+\xi)(1-\eta)$$

$$N_{15} = 2(\frac{1}{4}-\xi^2)(1-\xi^2)(1-\eta)-\frac{1}{2}(1-\xi^2)(1-\eta^2)$$

$$N_{16} = -\frac{4}{3}\xi(1-\xi^2)(\frac{1}{2}-\xi)(1-\eta)$$

$$N_{17} = (1-\xi^2)(1-\eta^2)$$

APPENDIX D

## Listing of the Computer Program

```
C*****************************************************************
C         PROGRAMMED AND DEVELOPED BY -- R.NATARAJAN. IMPERIAL COLLEGE
C         PROGRAMME TO CALCULATE DEFLECTIONS AND STRESS IN CURVED PIPE
C         SUBJECTED TO IN-PLANE MOMENT.
C         DOUBLY CURVED THIN SHELL ELEMENTS USED IN THE SOLUTION.
C         THE ANALYSIS INCLUDE THE END EFFECTS DUE TO TANGENTS AND FLA
C*****************************************************************
      PROGRAM NAMAIN(INPUT,OUTPUT,TAPE5=INPUT,TAPE6=OUTPUT,TAPE1,
     1TAPE2,TAPE3,TAPE4,TAPE7)
      INTEGER ELPOSN,ELNODE,PRENIC,UNKNIC,ELVEC
      REAL KNOMAT,KNORHS
      INTEGER AA
      DIMENSION HED(8)
      COMMON/TRANS/D(17),Q(17),XM(17),YM(17),ZM(17),T(17),V1X(17),
     1V1Y(17),V1Z(17),V2X(17),V2Y(17),V2Z(17),V3X(17),V3Y(17),V3Z(17)
     2TRIN(17,3,3),P(17)
      COMMON/S8/ XG(4),CG(4),XGZ(2),CGZ(2),DI(5,5)
      COMMON/S6/ ELNODE(110,87),RHSRED(1,85)
      COMMON/S1/ PREDEF(1,500)
      COMMON/S2/ PRENIC(1,500),UNKNIC(1,181),KNONIC(2,35),UNRHS(1,35)
     2KNORHS(1,181),ELVEC(1,85),ELPOSN(2,85),KNOMAT(1,800),
     3UNKMAT(1,18000),UNCLE(181,35)
      COMMON/C1/ NUNKVA,NKNVA,NOSTR,NCELNO,NCELN1,NTOTAL,NPRDEF,NT,
     1NELEM,NFREE,NNELM,NODTOT,NUNKV1,NKNVA1
      COMMON/C2/ N,IEL,NLG,NREC,NTREC
      COMMON/NO/NRING1,NRING2,NRING3,NELEM1,NELEM2,NELEM3,NEPR,NRING
      COMMON/NSTR/ NODSTR,IGAUST
      COMMON/DM/ E,PR,COMM1
      COMMON/GV/ RM,GR,PI
      COMMON/COM/ ANGLE,THIK
      COMMON/COC/ CLEN
      REWIND 1
      REWIND 2
      REWIND 3
      REWIND 4
C
C        READ DATA
C
      READ(5,5003) NELFM,NELTO
 5003 FORMAT(3I5)
      DO 6 I=1,4
    6 READ(5,7) XG(I),CG(I)
      DO 5 I=1,2
    5 READ(5,7) XGZ(I),CGZ(I)
    7 FORMAT(2F10.0)
      READ(5,5000) HED
      READ(5,5002) NNELM,NEPR,NRING1,NRING2,NRING3
 5002 FORMAT(5I5)
 5000 FORMAT(8A10)
 5001 FORMAT(1H1,8A10///)
      NELEM1=NEPR*NRING1
      NELEM2=NEPR*NRING2
      NELEM3=NEPR*NRING3
      READ(5,11) ANGLE,GR,RM,THIK,CLEN
   11 FORMAT(5F10.0)
C
```

```
C         AUTOMATIC MESH GENERATION AND BOUNDARY CONDITIONS TO REPRESEN
C         THE GIVEN PIPE BEND PROBLEM
C         CALCULATION OF THE TWO SCALERS NUNKVA AND NKNVA
C
      CALL VALUE
      CALL INIAL
      DO 40 I=1,NOSTR
      DO 40 K=1,NPRDEF
   40 PREDEF(I,K)=0.0
      CALL PRDF
C
C         WRITE DATA
C
      WRITE(6,5001) HED
      WRITE(6,103)
  103 FORMAT(1X,*GAUSS ABSC AND COEFF*)
      WRITE(6,104) ((XG(I),CG(I)),I=1,4)
      WRITE(6,104) ((XGZ(I),CGZ(I)),I=1,2)
  104 FORMAT(2E16.8)
      WRITE(6,2000)
 2000 FORMAT(14H ELNODE TABLED///)
      DO 2001 I=1,NELEM
      WRITE(6,2002) I,(ELNODE(I,J),J=2,NCELNO,5)
 2001 CONTINUE
 2002 FORMAT(I5/,12(3X,I7))
      WRITE(6,41)
   41 FORMAT(1X,*PRESCRIBED DEFLECTIONS*)
      WRITE(6,44) ((PREDEF(I,J),J=1,NPR DEF),I=1,NOSTR)
   44 FORMAT(12F10.6)
   42 FORMAT(12I10)
      WRITE(6,43)
   43 FORMAT(1X,*CORROSPONDING NICK NAMES*)
      WRITE(6,42) ((PRENIC(I,J),J=1,NPR DEF),I=1,NOSTR)
C
C         CALCULATIONS OF QUANTITIES TO DEFINE AREAS REQUIRED
C
      NCELNO=NFREE*NNELM+1
      NCELN 1=NCELNO-1
      NT=NFREE*NODTOT
      NTOTAL=NKNVA+NUNKVA
      NUNKV1=(NUNKVA*(NUNKVA+1)/2)
      NKNVA1=(NKNVA*(NKNVA+1)/2)
      NTREC=NTOTAL+1
      NREC=0
      NLG=0
C
C         WRITING THE ABOVE QUANTITIES
C
      WRITE(6,3000) NELEM,NFREE,NNELM,NPR DEF,NOSTR,NUNKVA,NKNVA,
     1NODTOT,PGAUS,NCELNO,NCELN1,NT,NTOTAL,NUNKV1,NKNVA1
 3000 FORMAT(1X,*NUMBER OF ELEMENTS(NELEM)=*I5/
     11X,*NUMBER OF DEGREE OF FREEDOM(NFREE)=*I5/
     21X,*NUMBER OF NODES PER ELEMENT(NNELM)=*I5/
     41X,*NUMBER OF PRESCRIBED DEFLECTION(NPRDEF)=*I5/
     51X,*NUMBER OF STRESSING CASE(NOSTR)=*I5/
     61X,*NUMBER OF UNKNOWN VARIABLE AT ONE TIME(NUNKVA)=*I5/
     71X,*NUMBER OF KNOWN VARIABLE AT ONE TIME(NKNVA)=*I5/
     81X,*TOTAL NUMBER OF NODES IN THE STRUCTURE(NODTOT)=*I5/
     91X,*NUMBER OF GAUSS POINTS IN EPSI AND ETA DIRECTION(PGAUS)=*I5/
```

```
     21X,*NUMBER OF COLUMS IN ELNODE MATRIX(NCELNO)=*I5/
     31X,*NUMBER OF COLUMS IN ELNODE MATRIX MINUS ONE(NCELN1)=*I5/
     41X,*TOTAL NUMBER OF DEGREES OF FREEDOM OF THE STRUCTURE(NT)=*I5
     51X,*TOTAL SIZE OF MATRIX REQUIRED FOR SOLUTION(NTOTAL)=*I5/
     61X,*SIZE OF UNKNOWN MATRIX(NUNKV1)=*I5/
     71X,*SIZE OF KNOWN MATRIX(NKNVA1)=*I5//)
C
C         ERROR DETECTION
C
      IF(NUNKVA.GT.181) GO TO 3001
      IF(NKNVA.GT.35) GO TO 3001
      GO TO 3002
 3001 WRITE(6,3003)
 3003 FORMAT(1X,* PROGRAM HALTED DUE TO LESS SPECIFIED DIMENSION*)
      STOP
 3002 CONTINUE
C
C         INITIALISATION
C
      DO 300 I=1,NCELN 1
  300 ELVEC(1,I)=0
      DO 310 I=1,2
      DO 310 J=1,NCELN 1
  310 ELPOSN(I,J)=0
      DO 320 J=1,NUNKV1
  320 UNKMAT(1,J)=0.0
      DO 330 J=1,NUNKVA
  330 UNKNIC(1,J)=0
      DO 340 I=1,NUNKVA
      DO 340 J=1,NKNVA
  340 UNCLE(I,J)=0.0
      DO 350 J=1,NKNVA1
  350 KNOMAT(1,J)=0.0
      DO 360 I=1,2
      DO 360 J=1,NKNVA
  360 KNONIC(I,J)=0
      DO 370 I=1,NOSTR
      DO 370 J=1,NUNKVA
  370 KNORHS(I,J)=0.0
      DO 38 K=1,NKNVA
   38 UNRHS(1,K)=0.0
C
C         FORWARD  ELEMINATION
C         LOOP ----  1001 ---  IS FOR EACH ELEMENT
C
      PI=3.14159
      DO 1001 N=NELFM,NELTO
      WRITE(6,3010) N
 3010 FORMAT(1X,*ELEMENT NUMBER=*I5)
C
C         ROUTINE TO GENERATE COORDINATES OF EACH ELEMENT
C
      IF(ELNODE(N,87).EQ.1) GO TO 401
      IF(ELNODE(N,87).EQ.2) GO TO 402
      GO TO 410
  401 CALL COCYL1
      GO TO 410
  402 CALL COBEND
  410 CONTINUE
```

```
      CALL TRAN
C
C         MODULUS OF ELASTICITY AND POISSONS RATIO
C
      E=1.0
      PR=0.3
C
C         CALCULATE CONSISTENT LOADS IN LOCAL DIRECTIONS
C
      DO 496 I=1,NCELN1
  496 RHSRED(1,I)=0.0
      IF(N.LE.NEPR) CALL LOAD
      WRITE(6,3020)
 3020 FORMAT(1X,*LOAD VECTOR FOR THIS ELEMENT*)
      WRITE(6,3021)
 3021 FORMAT(8X,*FORCE ALONG NORM*,8X,*FORCE ALONG ETA *,
     18X,*FORCE ALONG EPS1*,8X,*MOMENT ALONG ETA*,
     28X,*MOMENT ALONG EPSI*)
      WRITE(6,3030) (RHSRED(1,I),I=1,NCELN1)
 3030 FORMAT(5(8X,E16.8))
C
C         START OF ROUTINE TO FILL UP UNKNIC,KNONIC,KNORHS,ELPOSN
C
      DO 500 J=2,NCELNO
      JM1=J-1
  500 ELVEC(1,JM1)=ELNODE(N,J)
      DO 510 J=2,NCELNO
      JM1=J-1
      AA=IABS(ELNODE(N,J))
C
C         TO CHECK IN UNKNOWN NICK NAME
C
      DO 520 K=1,NUNKVA
      IF(UNKNIC(1,K).EQ.AA) GO TO 530
  520 CONTINUE
C
C         TO CHECK IN KNOWN NICK NAME
C
      DO 540 L=1,NKNVA
      IF(KNONIC(1,L).EQ.AA) GO TO 550
  540 CONTINUE
C
C         TO CHECK IN PRESCRIBED DEFLECTION
C
      DO 560 M=1,NPRDEF
      IF(PRENIC(1,M).EQ.AA) GO TO 570
  560 CONTINUE
C
C         IF NOT INSERT IN UNKNOWN NICK NAME
C
      DO 580 NN=1,NUNKVA
      IF(UNKNIC(1,NN).EQ.0) GO TO 590
  580 CONTINUE
  590 UNKNIC(1,NN)=ELNODE(N,J)
      KNORHS(1,NN)=RHSRED(1,JM1)
      ELPOSN(1,JM1)=NN
      ELPOSN(2,JM1)=0
      GO TO 510
  530 UNKNIC(1,K)=ELNODE(N,J)
```

```
      KNORHS(1,K)=KNORHS(1,K)+RHSRED(1,JM1)
      ELPOSN(1,JM1)=K
      ELPOSN(2,JM1)=0
      GO TO 510
  550 KNONIC(1,L)=ELNODE(N,J)
       ELPOSN(1,JM1)=L
      ELPOSN(2,JM1)=1
      GO TO 510
  570 DO 610 MM=1,NKNVA
      IF(KNONIC(1,MM).EQ.0) GO TO 620
  610 CONTINUE
  620 KNONIC(1,MM)=ELNODE(N,J)
      KNONIC(2,MM)=M
      ELPOSN(1,JM1)=MM
      ELPOSN(2,JM1)=1
      GO TO 510
  510 CONTINUE
C
C         CALL A ROUTINE TO DISTRIBUTE THE ELEMENT STIFFNESS MATRIX
C         IN PROPER AREAS OF THE MAIN MATRIX
C
      CALL STFTR
C
C         CALL A ROUTINE TO ELEMINATE THE COMPLETED NICKNAMES
C
      CALL FORWAD
 1001 CONTINUE
C
C         CALL A ROUTINE FOR BACK SUBSTITUTION AND CALCULATE
C         THE UNKNOWNS
C
      CALL BACKWD
C
C         CALL A ROUTINE TO CALCULATE NODAL STRESS
C
      CALL STRESS
 7003 STOP
      END
```

```
      SUBROUTINE STFTR
      INTEGER ELPOSN,ELNODE,PRENIC,UNKNIC,ELVEC
      REAL KNOMAT,KNORHS
      INTEGER AJ
      COMMON/S2/ PRENIC(1,500),UNKNIC(1,181),KNONIC(2,35),UNRHS(1,35)
     2KNORHS(1,181),ELVEC(1,85),ELPOSN(2,85),KNOMAT(1,800),
     3UNKMAT(1,18000),UNCLE(181,35)
      COMMON/C1/ NUNKVA,NKNVA,NOSTR,NCELNO,NCELN1,NTOTAL,NPRDEF,NT,
     1NELEM,NFREE,NNELM,NODTOT,NUNKV1,NKNVA1
      COMMON/S4/ SK(3655)
      COMMON/C2/ N,IEL,NLG,NREC,NTREC
      COMMON/NO/NRING1,NRING2,NRING3,NELEM1,NELEM2,NELEM3,NEPR,NRING
      COMMON/RN/ NAME
      COMMON/S6/ ELNODE(110,87),RHSRED(1,85)
C
C        THIS ROUTINE CALLS THE ELEMENT STIFFNESS MATRIX GENERATION R
C        THE STIFFNESS COFFICIENTS OF THE ELEMENT ARE STORED IN A
C        TAPE UNIT AND USED WHEN A GEOMETRICALLY SIMILAR ELEMENT IS
C        PRESENT IN THE STRUCTURE
C
      NCSK=NCELN1*(NCELN1+1)/2
      NAME=ELNODE(N,87)
      GO TO (30,31,32) NAME
   30 IF(N.LE.NEPR) GO TO 50
      GO TO 51
   50 CALL FEM
      WRITE(3)
     1(SK(I),I=1,NCSK)
      GO TO 3
   51 DO 52 I=2,NRING1
      IF(N.LE.(I*NEPR)) GO TO 53
      GO TO 52
   53 NI=(I-1)*NEPR
      GO TO 54
   52 CONTINUE
   54 NJ=N-NI
      IF(NJ.EQ.1) REWIND 3
      READ(3)
     1(SK(I),I=1,NCSK)
      GO TO 3
   31 NB=N-NELEM1
      IF(NB.LE.NEPR) GO TO 1
      GO TO 2
    1 CALL FEM
      WRITE(4)
     1(SK(I),I=1,NCSK)
      GO TO 3
    2 DO 4 I=2,NRING2
      IF(NB.LE.(I*NEPR)) GO TO 5
      GO TO 4
    5 NI=(I-1)*NEPR
      GO TO 6
    4 CONTINUE
    6 NJ=NB-NI
      IF(NJ.EQ.1) REWIND 4
      READ(4)
```

```
     1(SK(I),I=1,NCSK)
      GO TO 3
   32 NC=N-NELEM1-NELEM2
      DO 62 I=1,NRING3
      IF(NC.LE.(I*NEPR)) GO TO 63
      GO TO 62
   63 NI=(I-1)*NEPR
      GO TO 64
   62 CONTINUE
   64 NJ=NC-NI
      IF(NJ.EQ.1) REWIND 3
      READ(3)
     1(SK(I),I=1,NCSK)
    3 CONTINUE
C
C         ROUTINE TO DISTRIBUTE ELEMENT STIFFNESS MATRIX IN
C         UNKMAT,KNOWN AND UNCLE MATRICES ( MAIN MATRIX)
C
      DO 900 I=1,NCELN1
      I1=ELPOSN(1,I)
      I2=ELPOSN(2,I)
      DO 900 J=1,NCELN1
      IF(J.GE.I) GO TO 901
      IS=J+(I*(I-1)/2)
      GO TO 902
  901 IS=I+(J*(J-1)/2)
  902 CONTINUE
      J1=ELPOSN(1,J)
      J2=ELPOSN(2,J)
      IF(I2.EQ.0) GO TO 810
C
C         TO FILL KNOWN MATRIX  IF NICK NAME IS IN KNONIC
C
      IF(J2.EQ.0) GO TO 900
      IF(J1.GT.I1) GO TO 900
      IJ=(I1*(I1-1)/2)+J1
      KNOMAT(I,IJ)=KNOMAT(1,IJ)+SK(IS)
      GO TO 900
C
C         TO FILL UNCLE AND UNKMAT WHEN NICKNAME IS AN UNKNOWN ONE
C
  810 IF(J2.EQ.1) GO TO 830
      GO TO 840
  830 UNCLE(I1,J1)=UNCLE(I1,J1)+SK(IS)
      GO TO 900
  840 IF(J1.GT.I1) GO TO 900
      IJ=(I1*(I1-1)/2)+J1
      UNKMAT(1,IJ)=UNKMAT(1,IJ)+SK(IS)
  900 CONTINUE
      RETURN
      END
```

```
      SUBROUTINE FORWAD
      INTEGER ELPOSN,ELNODE,PRENIC,UNKNIC,ELVEC
      REAL KNOMAT,KNORHS
      INTEGER COPRDE
      COMMON/S1/ PREDEF(1,500)
      COMMON/S3/ COMP(305)
      COMMON/C1/ NUNKVA,NKNVA,NOSTR,NCELNO,NCELN1,NTOTAL,NPRDEF,NT,
     1NELEM,NFREE,NNELM,NODTOT,NUNKV1,NKNVA1
      COMMON/S2/ PRENIC(1,500),UNKNIC(1,181),KNONIC(2,35),UNRHS(1,35),
     2KNORHS(1,181),ELVEC(1,85),ELPOSN(2,85),KNOMAT(1,800),
     3UNKMAT(1,18000),UNCLE(181,35)
      COMMON/C2/ N,IEL,NLG,NREC,NTREC
      COMMON/BR/ BUF(10,271),IBUF(10,4)
      COMMON/BUFR/ RHS,NIC,LP1,LP2,NPOSN
C
C        ROUTINE FOR MODIFYING ELEMENTS IN MAIN MATRIX FOR A COMPLETED
C        UNKNOWN NICKNAME
C
      DO 100 IM=1,NCELN1
      IF(ELVEC(1,IM).LT.0) GO TO 101
      GO TO 100
  101 I=ELPOSN(1,IM)
      IF(ELPOSN(2,IM).EQ.1) GO TO 210
C
C        STORING COMPLETED ROW IN AN AUXILIARY ROW MATRIX -- COMP--
C
  110 I1=I+NKNVA
      I11=I*(I-1)/2
      DO 120 J=1,NKNVA
  120 COMP(J)=UNCLE(I,J)
      DO 130 J1=1,I
      IJ1=I11+J1
      MJ1=NKNVA+J1
  130 COMP(MJ1)=UNKMAT(1,IJ1)
      IP1=I+1
      IF(IP1.GT.NUNKVA) GO TO 141
      DO 140 I2=IP1,NUNKVA
      IJ2=(I2*(I2-1)/2)+I
      MI2=NKNVA+I2
  140 COMP(MI2)=UNKMAT(1,IJ2)
  141 CONTINUE
C
C        MODIFY KNOMAT MATRIX
C
      DO 150 I4=1,NKNVA
      II2=I4*(I4-1)/2
      CMP=COMP(I4)/COMP(I1)
      DO 150 J4=1,I4
      IJ4=II2+J4
  150 KNOMAT(1,IJ4)=KNOMAT(1,IJ4)-CMP*COMP(J4)
C
C        MODIFY UNCLE MATRIX
C
      DO 160 I5=1,NUNKVA
      MI5=I5+NKNVA
      CMP=COMP(MI5)/COMP(I1)
```

```
      DO 160 J5=1,NKNVA
  160 UNCLE(I5,J5)=UNCLE(I5,J5)-CMP*COMP(J5)
C
C         MODIFY UNKMAT MATRIX
C
      DO 170 I6=1,NUNKVA
      II3=I6*(I6-1)/2
      MI6=I6+NKNVA
      CMP=COMP(MI6)/COMP(I1)
      DO 170 J6=1,I6
      MJ6=J6+NKNVA
      IJ6=II3+J6
  170 UNKMAT(I,IJ6)=UNKMAT(1,IJ6)-CMP*COMP(MJ6)
C
C         RELEASE THE STORED EQUATION SPACE
C
      DO 420 J=1,NKNVA
  420 UNCLE(I,J)=0.0
      DO 430 J1=1,I
      IJ1=II1+J1
  430 UNKMAT(1,IJ1)=0.0
      IF(IP1.GT.NUNKVA) GO TO 441
      DO 440 I2=IP1,NUNKVA
      IJ2=(I2*(I2-1)/2)+I
  440 UNKMAT(1,IJ2)=0.0
  441 CONTINUE
C
C         STORING REQUIRED DATA IN A BUFFER AREA
C
      NIC=IABS(UNKNIC(1,I))
      RHS=KNORHS(1,I)
      LP1=ELPOSN(1,IM)
      LP2=ELPOSN(2,IM)
      NPOSN=0
      CALL BUFFER
C
C         MODIFY RIGHT HAND SIDE
C
      RHSK=KNORHS(1,I)
      RHK=RHSK/COMP(I1)
      DO 180 I7=1,NKNVA
  180 UNRHS(1,I7)=UNRHS(1,I7)-COMP(I7)*RHK
      DO 190 I8=1,NUNKVA
      MI8=I8+NKNVA
  190 KNORHS(1,I8)=KNORHS(1,I8)-COMP(MI8)*RHK
      KNORHS(1,I)=0.0
C
C         UNKNIC IS MADE ZERO
C
      UNKNIC(1,I)=0
      GO TO 100
C
C         ROUTINE FOR COMPLETED KNOWN NICKNAMES
C         STORING COMPLETED ROW TERMS OF KNOMAT IN AUXILARY MATRIX CO
C
  210 II1=(I*(I-1)/2)
      DO 220 J1=1,I
      IJ1=II1+JI
      COMP(J1)=KNOMAT(1,IJ1)
```

```
  220 KNOMAT(1,IJ1)=0.0
      IF(I.EQ.NKNVA) GO TO 240
C
C         STORING COMPLETED COLUM TERMS OF KNOMAT
C
      IP1=I+1
      DO 230 I2=IP1,NKNVA
      IJ2=(I2*(I2-1)/2)+I
      COMP(I2)=KNOMAT(1,IJ2)
  230 KNOMAT(1,IJ2)=0.0
C
C         STORING COMPLETED COLUM TERMS OF UNCLE
C
  240 DO 250 I3=1,NUNKVA
      MI3=NKNVA+I3
      COMP(MI3)=UNCLE(I3,I)
  250 UNCLE(I3,I)=0.0
C
C         FINDING THE VALUE OF PRESCRIBED DEFLECTION(PREKNW)
C         CORROSPONDING TO THE COMPLETED NICKNAMES
C
      COPRDE=KNONIC(2,I)
      PREKNW=PREDEF(1,COPRDE)
C
C         MODIFY THE UNKNOWN RHS EXCEPT THE COMPLETED RHS
C
      DO 260 I4=1,NKNVA
      IF(I4.EQ.I) GO TO 260
      UNRHS(1,I4)=UNRHS(1,I4)-COMP(I4)*PREKNW
  260 CONTINUE
C
C       MODIFY THE KNOWN RHS
C
      DO 270 I5=1,NUNKVA
      MI5=NKNVA+I5
  270 KNORHS(1,I5)=KNORHS(1,I5)-COMP(MI5)*PREKNW
C
C         STORING REQUIRED DATA IN A BUFFER AREA
C
      NIC=IABS(KNONIC(1,I))
      RHS=UNRHS(1,I)
      LP1=ELPOSN(1,IM)
      LP2=ELPOSN(2,IM)
      NPOSN=KNONIC(2,I)
      CALL BUFFER
C
C         RESET FOR NEXT ELEMENT
C
      KNONIC(1,I)=0
      KNONIC(2,I)=0
      UNRHS(1,I)=0.0
  100 CONTINUE
      IF(N.EQ.NELEM) GO TO 1002
      GO TO 1003
 1002 IF(NLG.EQ.0) GO TO 1003
      WRITE(1)
     1NLG,((BUF(I,J),I=1,NLG),J=1,NTREC),((IBUF(I,J),I=1,NLG),J=1,4)
      NREC=NREC+1
 1003 CONTINUE
```

```
RETURN
END
```

```
      SUBROUTINE BACKWD
      INTEGER ELPOSN,ELNODE,PRENIC,UNKNIC,ELVEC
      REAL KNOMAT,KNORHS
      INTEGER U1
      COMMON/S1/ PREDEF(1,500)
      COMMON/S2/ PRENIC(1,500),UNKNIC(1,181),KNONIC(2,35),UNRHS(1,35),
     2KNORHS(1,181),ELVEC(1,85),ELPOSN(2,85),KNOMAT(1,800),
     3UNKMAT(1,18000),UNCLE(181,35)
      COMMON/C1/ NUNKVA,NKNVA,NOSTR,NCELNO,NCELN1,NTOTAL,NPRDEF,NT,
     1NELEM,NFREE,NNELM,NODTOT,NUNKV1,NKNVA1
      COMMON/S3/ COMP(305)
      COMMON/S5/ U1(5000),U2(5000)
      COMMON/BR/ BUF(10,271),IBUF(10,4)
      COMMON/C2/ N,IEL,NLG,NREC,NTREC
C
C         INITIALISATION
C
      WRITE(6,2)
    2 FORMAT(30X,*CALCULATED REACTIONS*)
      DO 202 I=1,NKNVA
      DO 202 J=1,2
  202 KNONIC(J,I)=0
      DO 203 I=1,NUNKVA
  203 UNKNIC(1,I)=0
      DO 1 M=1,NUNKVA
    1 KNORHS(1,M)=0.0
      DO 20 M1=1,NT
      U1(M1)=0
      U2(M1)=0.0
   20 CONTINUE
      DO 400 I=1,NODTOT
      DO 500 J=1,NFREE
      J1=NFREE-J
      I1=NFREE*I-J1
      U1(I1)=I*100+J*10
  500 CONTINUE
  400 CONTINUE
C
C         READ BACK THE STORED DATA IN BLOCKS IN A REVERSED ORDER
C
      DO 10 L=1,NREC
      BACK SPACE 1
      READ(1)
     1NLG,((BUF(I,J),I=1,NLG),J=1,NTREC),((IBUF(I,J),I=1,NLG),J=1,4)
      LG=NLG
  300 DO 4 I=1,NTOTAL
    4 COMP(I)=BUF(LG,I)
      I=NTOTAL+1
      RHS=BUF(LG,I)
      LP1=IBUF(LG,1)
      LP2=IBUF(LG,2)
      NIC=IBUF(LG,3)
      NPOSN=IBUF(LG,4)
      LG=LG-1
C
C         CHECK WHETHER  FNIC  IS IN  KNONIC
```

```
C
      IF(LP2.EQ.1) GO TO 110
      GO TO 140
C
C        IF  FNIC  IS IN  KNONIC  MULTIPLY  KNOMAT WITH  PREDEF
C
  110 ANS1=0.0
      KNONIC(1,LP1)=NIC
      KNONIC(2,LP1)=NPOSN
      DO 120 I2=1,NKNVA
      NPOSN=KNONIC(2,I2)
      IF(NPOSN.EQ.0) GO TO 120
  210 ANS1=ANS1+COMP(I2)*PREDEF(1,NPOSN)
  120 CONTINUE
C
C        THEN MULTIPLY UNCLE WITH UNKDEF NOW STORED IN KNOWN RHS
C
      ANS2=0.0
      DO 130 I3=1,NUNKVA
      MI3=I3+NKNVA
  130 ANS2=ANS2+COMP(MI3)*KNORHS(1,I3)
C
C        FINDING THE CORROSPONDING UNKNOWN REACTION
C
      ANS=ANS1+ANS2-RHS
      WRITE(6,1000) NIC,ANS
 1000 FORMAT(19H REACTION AT NODE  I10,2X,5H IS  E16.8)
C
C        TO FIND THE UNKNOWN DEFL IF  FNIC  IS NOT IN  KNONIC
C        TO ALSO FIND THE ROW IT OCCUPIES DURING FORWARD ELIMINATION
      GO TO 200
  140 UNKNIC(1,LP1)=NIC
      I5=LP1
      IM5=I5-1
      IP5=I5+1
      IN5=I5+NKNVA
C
C        UNCLE IS MULTIPLIED WITH KNOWN DISPLACEMENTS
C
  160 ANS1=0.0
      DO 170 I6=1,NKNVA
      NPOSN=KNONIC(2,I6)
      IF(NPOSN.EQ.0) GO TO 170
  220 ANS1=ANS1+COMP(I6)*PREDEF(1,NPOSN)
  170 CONTINUE
C
C        UNKMAT IS MULTIPLIED WITH UNKNOWN DISPL NOW KNOWN AND STORED
C        IN KNORHS --- EXCEPT THE DIAGONAL TERM
C
      ANS2=0.0
      IF(IM5.EQ.0) GO TO 181
      DO 180 I7=1,IM5
      MI7=NKNVA+I7
  180 ANS2=ANS2+COMP(MI7)*KNORHS(1,I7)
  181 ANS3=0.0
      IF (IP5.GT.NUNKVA) GO TO 191
      DO 190 I8=IP5,NUNKVA
      MI8=NKNVA+I8
  190 ANS3=ANS3+COMP(MI8)*KNORHS(1,I8)
```

```
  191 CONTINUE
      KNORHS(1,I5)=(RHS-ANS1-ANS2-ANS3)/COMP(IN5)
C
C         WRITING THE UNKNOWN DISPLACEMENTS
C
      UNDEFL=KNORHS(1,I5)
      DO 410 J=1,NT
      IF(NIC.EQ.U1(J)) GO TO 420
  410 CONTINUE
  420 U2(J)=UNDEFL
  200 IF(LG.EQ.0) GO TO 101
      GO TO 300
  101 BACK SPACE 1
   10 CONTINUE
      DO 430 J=1,NPRDEF
      DEFL=PREDEF(1,J)
      NIC=PRENIC(1,J)
      DO 440 JJ=1,NT
      IF(NIC.EQ.U1(JJ)) GO TO 441
  440 CONTINUE
  441 U2(JJ)=DEFL
  430 CONTINUE
      MPRINT=0
      DO 1701 J=1,NT,5
      J1=J+1
      J2=J+2
      J3=J+3
      J4=J+4
      IF(MPRINT.GT.0) GO TO 401
      WRITE(6,1601)
 1601 FORMAT(1H1,10X,*NODE*,4X,*DISPL ALONG NORM*,5X,*DISPL ALONG ETA*
     14X,*DISPL ALONG EPSI*,2X,*ROTATION ABOUT ETA*,2X,
     22X,*ROTATION ABOUT EPSI*)
      MPRINT=50
  401 MPRINT=MPRINT-1
      WRITE(6,1700) U1(J),U2(J),U2(J1),U2(J2),U2(J3),U2(J4)
 1700 FORMAT(I16,5(4X,E16.8))
 1701 CONTINUE
      RETURN
      END
```

```
      SUBROUTINE FEM
C     ****************************************************************
C     PROGRAMME TO CALCULATE STIFFNESS OF AN ARBITRARY THIN
C     SHELL ELEMENT
C     ****************************************************************
      COMMON/NO/NRING1,NRING2,NRING3,NELEM1,NELEM2,NELEM3,NEPR,NRING
      COMMON/STRS/ V1(17),V2(17),V3(2),IS(4,5),NE,NNS,NCM,NE2
      COMMON/C1/ NUNKVA,NKNVA,NOSTR,NCELNO,NCELN1,NTOTAL,NPRDEF,NT,
     1NELEM,NFREE,NNELM,NODTOT,NUNKV1,NKNVA1
      COMMON/FE1/JAC(3,3),IJAC(3,3),DE(3,153),JDE(3,153),DUD(3,85),
     1DVD(3,85),DWD(3,85),L(3,3),F1(85),F2(85),F3(85),S1(85),S2(85),
     2S3(85),T1(85),T2(85),T3(85),B(5,85),DB(5,85)
      COMMON/FE2/ BR(5,85)
      COMMON/C2/ N,IEL,NLG,NREC,NTREC
      COMMON/S4/ SK(3655)
      COMMON/S8/ XG(4),CG(4),XGZ(2),CGZ(2),DI(5,5)
      COMMON/NSTR/ NODSTR,IGAUST
      COMMON/TRANS/D(17),Q(17),XM(17),YM(17),ZM(17),T(17),V1X(17),
     1V1Y(17),V1Z(17),V2X(17),V2Y(17),V2Z(17),V3X(17),V3Y(17),V3Z(17),
     2TRIN(17,3,3),P(17)
      COMMON/SHP/G,H,QXM,QYM,QZM,PXM,PYM,PZM,QXTB,QYTB,QZTB,PXTB,PYTB,
     1PZTB,DXTB,DYTB,DZTB,DT
      COMMON/DM/E,PR,COMM1
      REAL JAC,IJAC,JDE,L,LDUDX,LDVDX,LDWDX,LDUDY,LDVDY,LDWDY,
     1LDUDZ,LDVDZ,LDWDZ,VJAC,MVJAC
      NCSK=NCELN1*(NCELN1+1)/2
      WRITE(6,303)
  303 FORMAT(4X,*X-COORDINATE*,4X,*Y-COORDINATE*,4X,*Z-COORDINATE*)
      WRITE(6,701) (XM(I),YM(I),ZM(I),I=1,NNELM)
  701 FORMAT(3E16.8)
      COMM1=E/(1.-PR*PR)
      COMM=SQRT(COMM1)
      D1=COMM
      D12=COMM*PR
      D2=COMM*SQRT(1.-PR*PR)
      D3=COMM*SQRT((1.-PR)/2.)
      D4=COMM*SQRT((1.-PR)/2.4)
      DO 200 I=1,NCSK
  200 SK(I)=0.0
C*******NUMERICAL INTEGRATION LOOP
      DO 1000 IG=1,4
      G=-XG(IG)
      DO 1000 JG=1,4
      H=XG(JG)
      IF(NNELM.EQ.8) GO TO 1
      IF(NNELM.EQ.12) GO TO 2
      CALL SHAP17
      GO TO 3
    1 CALL SHAP8
      GO TO 3
    2 CALL SHAP12
    3 CONTINUE
      DO 1000 KG=1,2
      F=XGZ(KG)
C         CALCULATION OF JACOBIAN MATRIX AND ITS INVERSE
```

```
      DO 9 I=1,3
      DO 9 J=1,3
      JAC(I,J)=0.0
    9 IJAC(I,J)=0.0
      JAC(1,1)=QXM+F*0.5*QXTB
      JAC(1,2)=QYM+F*0.5*QYTB
      JAC(1,3)=QZM+F*0.5*QZTB
      JAC(2,1)=PXM+F*0.5*PXTB
      JAC(2,2)=PYM+F*0.5*PYTB
      JAC(2,3)=PZM+F*0.5*PZTB
      JAC(3,1)=0.5*DXTB
      JAC(3,2)=0.5*DYTB
      JAC(3,3)=0.5*DZTB
C        VJAC IS DETERMINANT OF JACOBIAN MATRIX
C        IJAC IS INVERSE JACOBIAN MATRIX
      VJAC=JAC(1,1)*(JAC(2,2)*JAC(3,3)-JAC(2,3)*JAC(3,2))-
     1JAC(1,2)*(JAC(2,1)*JAC(3,3)-JAC(2,3)*JAC(3,1))+
     2JAC(1,3)*(JAC(2,1)*JAC(3,2)-JAC(2,2)*JAC(3,1))
      IJAC(1,1)=(JAC(2,2)*JAC(3,3)-JAC(3,2)*JAC(2,3))/VJAC
      IJAC(1,2)=-(JAC(1,2)*JAC(3,3)-JAC(3,2)*JAC(1,3))/VJAC
      IJAC(1,3)=(JAC(1,2)*JAC(2,3)-JAC(2,2)*JAC(1,3))/VJAC
      IJAC(2,1)=-(JAC(2,1)*JAC(3,3)-JAC(3,1)*JAC(2,3))/VJAC
      IJAC(2,2)=(JAC(1,1)*JAC(3,3)-JAC(3,1)*JAC(1,3))/VJAC
      IJAC(2,3)=-(JAC(1,1)*JAC(2,3)-JAC(2,1)*JAC(1,3))/VJAC
      IJAC(3,1)=(JAC(2,1)*JAC(3,2)-JAC(2,2)*JAC(3,1))/VJAC
      IJAC(3,2)=-(JAC(1,1)*JAC(3,2)-JAC(1,2)*JAC(3,1))/VJAC
      IJAC(3,3)=(JAC(1,1)*JAC(2,2)-JAC(2,1)*JAC(1,2))/VJAC
C******** DERIVATIVES OF GLOBAL DIS. W.R.T. LOCAL COORDINATES
      DO 10 I=1,3
      DO 10 J=1,NCM
   10 DE(I,J)=0.0
      DO 11 I=1,NNELM
      I1=I+NNELM
      I2=I+2*NNELM
      I3=I+3*NNELM
      I4=I+4*NNELM
      I5=I+5*NNELM
      I6=I+6*NNELM
      I7=I+7*NNELM
      I8=I+8*NNELM
      QFT=Q(I)*F*0.5*T(I)
      PFT=P(I)*F*0.5*T(I)
      DFT=D(I)*0.5*T(I)
      DE(1,I)=Q(I)
      DE(1,I1)=QFT*V1X(I)
      DE(1,I2)=QFT*V2X(I)
      DE(1,I3)=Q(I)
      DE(1,I4)=QFT*V1Y(I)
      DE(1,I5)=QFT*V2Y(I)
      DE(1,I6)=Q(I)
      DE(1,I7)=QFT*V1Z(I)
      DE(1,I8)=QFT*V2Z(I)
      DE(2,I)=P(I)
      DE(2,I1)=PFT*V1X(I)
      DE(2,I2)=PFT*V2X(I)
      DE(2,I3)=P(I)
      DE(2,I4)=PFT*V1Y(I)
      DE(2,I5)=PFT*V2Y(I)
      DE(2,I6)=P(I)
```

```
      DE(2,I7)=PFT*V1Z(I)
   12 DE(2,I8)=PFT*V2Z(I)
      DE(3,I1)=DFT*V1X(I)
      DE(3,I2)=DFT*V2X(I)
      DE(3,I4)=DFT*V1Y(I)
      DE(3,I5)=DFT*V2Y(I)
      DE(3,I7)=DFT*V1Z(I)
   13 DE(3,I8)=DFT*V2Z(I)
   11 CONTINUE
C******** DERIVATIVES OF GLOBAL DIS. W.R.T. GLOBAL COORDINATES
      DO 21 I=1,3
      DO 21 J=1,NCM
      JDE(I,J)=0.0
      DO 21 K=1,3
   21 JDE(I,J)=JDE(I,J)+IJAC(I,K)*DE(K,J)
C******** ARRANGING ABOVE DERIVATIVES IN PROPER ORDER
      DO 30 J=1,3
      DO 30 I=1,NCELN1
      DUD(J,I)=0.0
      DVD(J,I)=0.0
   30 DWD(J,I)=0.0
      DO 60 J=1,3
      I=1
      I1=1
   31 DUD(J,I1)=JDE(J,I)
      I1=I1+5
      I=I+1
       IF(I.EQ.NNELM+1) GO TO 32
      GO TO 31
   32 I1=4
   33 DUD(J,I1)=JDE(J,I)
      I1=I1+5
      I=I+1
      IF(I.EQ.2*NNELM+1) GO TO 34
      GO TO 33
   34 I1=5
   35 DUD(J,I1)=JDE(J,I)
      I1=I1+5
      I=I+1
      IF(I.EQ.3*NNELM+1) GO TO 36
      GO TO 35
   36 CONTINUE
      I1=2
   41 DVD(J,I1)=JDE(J,I)
      I1=I1+5
      I=I+1
      IF(I.EQ.4*NNELM+1) GO TO 42
      GO TO 41
   42 I1=4
   43 DVD(J,I1)=JDE(J,I)
      I1=I1+5
      I=I+1
      IF(I.EQ.5*NNELM+1) GO TO 44
      GO TO 43
   44 I1=5
   45 DVD(J,I1)=JDE(J,I)
      I1=I1+5
      I=I+1
      IF(I.EQ.6*NNELM+1) GO TO 46
```

```
      GO TO 45
   46 CONTINUE
      I1=3
   51 DWD(J,I1)=JDE(J,I)
      I1=I1+5
      I=I+1
      IF(I.EQ.7*NNELM+1) GO TO 52
      GO TO 51
   52 I1=4
   53 DWD(J,I1)=JDE(J,I)
      I1=I1+5
      I=I+1
      IF(I.EQ.8*NNELM+1) GO TO 54
      GO TO 53
   54 I1=5
   55 DWD(J,I1)=JDE(J,I)
      I=I+1
      I1=I1+5
      IF(I.EQ.9*NNELM+1) GO TO 56
      GO TO 55
   56 CONTINUE
   60 CONTINUE
      DO 61 I=1,3
      DO 61 J=1,3
   61 L(I,J)=0.0
      AGEN=SQRT(JAC(1,1)*JAC(1,1)+JAC(1,2)*JAC(1,2)+JAC(1,3)*JAC(1,3))
      BGEN=SQRT(JAC(2,1)*JAC(2,1)+JAC(2,2)*JAC(2,2)+JAC(2,3)*JAC(2,3))
      ACOS=(JAC(1,1)*JAC(2,1)+JAC(1,2)*JAC(2,2)+JAC(1,3)*JAC(2,3))/
     1(AGEN*BGEN)
      ASIN=SQRT(1.-ACOS*ACOS)
      VNI=(JAC(1,2)*JAC(2,3)-JAC(1,3)*JAC(2,2))/(AGEN*BGEN*ASIN)
      VNJ=(JAC(1,3)*JAC(2,1)-JAC(1,1)*JAC(2,3))/(AGEN*BGEN*ASIN)
      VNK=(JAC(1,1)*JAC(2,2)-JAC(1,2)*JAC(2,1))/(AGEN*BGEN*ASIN)
      VETAI=(VNJ*JAC(1,3)-VNK*JAC(1,2))/AGEN
      VETAJ=(VNK*JAC(1,1)-VNI*JAC(1,3))/AGEN
      VETAK=(VNI*JAC(1,2)-VNJ*JAC(1,1))/AGEN
      L(1,1)=JAC(1,1)/AGEN
      L(2,1)=JAC(1,2)/AGEN
      L(3,1)=JAC(1,3)/AGEN
      L(1,2)=VETAI
      L(2,2)=VETAJ
      L(3,2)=VETAK
      L(1,3)=VNI
      L(2,3)=VNJ
      L(3,3)=VNK
C******** CALCULATION OF LOCAL DERIVATIVES
      DO 71 I=1,NCELN1
      F1(I)=DUD(1,I)*L(1,1)+DVD(I,I)*L(2,1)+DWD(1,I)*L(3,I)
      F2(I)=DUD(1,I)*L(1,2)+DVD(1,I)*L(2,2)+DWD(1,I)*L(3,2)
      F3(I)=DUD(1,I)*L(1,3)+DVD(1,I)*L(2,3)+DWD(1,I)*L(3,3)
      S1(I)=DUD(2,I)*L(1,1)+DVD(2,I)*L(2,1)+DWD(2,I)*L(3,1)
      S2(I)=DUD(2,I)*L(1,2)+DVD(2,I)*L(2,2)+DWD(2,I)*L(3,2)
      S3(I)=DUD(2,I)*L(1,3)+DVD(2,I)*L(2,3)+DWD(2,I)*L(3,3)
      T1(I)=DUD(3,I)*L(1,1)+DVD(3,I)*L(2,1)+DWD(3,I)*L(3,1)
      T2(I)=DUD(3,I)*L(1,2)+DVD(3,I)*L(2,2)+DWD(3,I)*L(3,2)
      T3(I)=DUD(3,I)*L(1,3)+DVD(3,I)*L(2,3)+DWD(3,I)*L(3,3)
   71 CONTINUE
C******** B MATRIX
      DO 80 I=1,NCELN1
```

```
      B(1,I)   =F1(I)*L(1,1)+S1(I)*L(2,1)+T1(I)*L(3,1)
      B(2,I)   =F2(I)*L(1,2)+S2(I)*L(2,2)+T2(I)*L(3,2)
      B(3,I)   =F1(I)*L(1,2)+S1(I)*L(2,2)+T1(I)*L(3,2)
     1         +F2(I)*L(1,1)+S2(I)*L(2,1)+T2(I)*L(3,1)
      B(4,I)   =F2(I)*L(1,3)+S2(I)*L(2,3)+T2(I)*L(3,3)
     1         +F3(I)*L(1,2)+S3(I)*L(2,2)+T3(I)*L(3,2)
      B(5,I)   =F3(I)*L(1,1)+S3(1)*L(2,1)+T3(1)*L(3,1)
     1         +F1(I)*L(1,3)+S1(I)*L(2,3)+T1(I)*L(3,3)
   80 CONTINUE
C******** B MATRIX MODIFIED TO BR MATRIX SO THAT THE NODAL DISPLACEME
C******* ARE IN THE CHOSEN LOCAL DIRECTIONS
      DO 89 I=1,5
      DO 89 J=1,NCELN1
      BR(I,J)=0.0
   89 CONTINUE
      DO 91 I=1,5
      N1=0
      J=0
   92 J=J+1
      N1=N1+1
      IF(N1.EQ.NNELM+1) GO TO 93
      J1=J+1
      J2=J+2
      J3=J+3
      J4=J+4
      BR(I,J)=B(I,J)*V3X(N1)+B(I,J1)*V3Y(N1)+B(I,J2)*V3Z(N1)
      BR(I,J1)=B(I,J)*V2X(N1)+B(I,J1)*V2Y(N1)+B(I,J2)*V2Z(N1)
      BR(I,J2)=B(I,J)*V1X(N1)+B(I,J1)*V1Y(N1)+B(I,J2)*V1Z(N1)
      BR(I,J3)=B(I,J3)
      BR(I,J4)=B(I,J4)
      J=J4
      GO TO 92
   93 CONTINUE
   91 CONTINUE
      MVJAC=VJAC*CG(IG)*CG(JG)*CGZ(KG)
C******** CALCULATION OF STIFFNESS MATRIX
      DO 110 K=1,NCELN1
      DB(1,K)=D1*BR(1,K)+D12*BR(2,K)
      DB(2,K)=D2*BR(2,K)
      DB(3,K)=D3*BR(3,K)
      DB(4,K)=D4*BR(4,K)
      DB(5,K)=D4*BR(5,K)
  110 CONTINUE
      DO 120 I=1,NCELN1
      DO 120 J=1,I
      I1=J+(I*(I-1)/2)
      DO 120 K=1,5
  120 SK(I1)=SK(I1)+DB(K,I)*DB(K,J)*MVJAC
 1000 CONTINUE
C******* CALL ROUTINE TO CALCULATE STRESS MATRIX AT NODAL POINTS
      CALL FEM2
      RETURN
      END
```

```
      SUBROUTINE SHAP8
      COMMON/TRANS/D(17),Q(17),XM(17),YM(17),ZM(17),T(17),V1X(17),
     1V1Y(17),V1Z(17),V2X(17),V2Y(17),V2Z(17),V3X(17),V3Y(17),V3Z(17),
     2TRIN(17,3,3),P(17)
      COMMON/SHP/G,H,QXM,QYM,QZM,PXM,PYM,PZM,QXTB,QYTB,QZTB,PXTB,PYTB,
     1PZTB,DXTB,DYTB,DZTB,DT
C
C         SHAPE FUNCTIONS AND THEIR DERIVATIVES FOR A QUADRATIC ELEMENT
C
      H2=H*H
      G2=G*G
C
C         SHAPE FUNCTION MATRIX --D -
C
C
C
C         DERIVATIVE OF SHAPE FUN. W.R.T. EPSI
C
C
C         DERIVATIVE OF SHAPE FUNCTION W.R.T. ETA
C
      GH=G*H
      G2H=G2*H
      H2G=H2*G
      HG=-1.+G2+H2
      G2G=2.*G
      H2H=2.*H
      G22=G2G*H
      D(1)=0.25*(HG+GH-G2H-H2G)
      D(2)=0.5*(1.-G-H2+H2G)
      D(3)=0.25*(HG-GH+G2H-H2G)
      D(4)=0.5*(1.+H-G2-G2H)
      D(5)=0.25*(HG+GH+G2H+H2G)
      D(6)=0.5*(1.+G-H2-H2G)
      D(7)=0.25*(HG-GH-G2H+H2G)
      D(8)=0.5*(1.-H-G2+G2H)
      Q(1)=0.25*(H+G2G-G22-H2)
      Q(2)=0.5*(-1.+H2)
      Q(3)=0.25*(-H+G2G+G22-H2)
      Q(4)=0.5*(-G2G-G22)
      Q(5)=0.25*(H+G2G+G22+H2)
      Q(6)=-Q(2)
      Q(7)=0.25*(-H+G2G-G22+H2)
      Q(8)=0.5*(-G2G+G22)
      P(1)=0.25*(G+H2H-G2-G22)
      P(2)=0.5*(-H2H+G22)
      P(3)=0.25*(-G+H2H+G2-G22)
      P(4)=0.5*(1.-G2)
      P(5)=0.25*(G+H2H+G2+G22)
      P(6)=0.5*(-H2H-G22)
      P(7)=0.25*(-G+H2H-G2+G22)
      P(8)=-P(4)
      CALL SHAPE
      RETURN
      END
```

```
      SUBROUTINE SHAP12
      COMMON/TRANS/D(17),Q(17),XM(17),YM(17),ZM(17),T(17),V1X(17),
     1V1Y(17),V1Z(17),V2X(17),V2Y(17),V2Z(17),V3X(17),V3Y(17),V3Z(17),
     2TRIN(17,3,3),P(17)
      COMMON/SHP/G,H,QXM,QYM,QZM,PXM,PYM,PZM,QXTB,QYTB,QZTB,PXTB,PYTB,
     1PZTB,DXTB,DYTB,DZTB,DT
C
C        SHAPE FUNCTIONS AND THEIR DERIVATIVES FOR A CUBIC ELEMENT
C
      A=1.-G
      B=1.-H
      A1=1.+G
      B1=1.+H
      C=-10.+9.*(G*G+H*H)
      A2=1.+3.*G
      A3=1.-3.*G
      B2=1.+3.*H
      B3=1.-3.*H
      A4=1.-G*G
      B4=1.-H*H
      V1=1./32.
      V2=9./32.
      A5=18.*G
      B5=18.*H
      D(1)=V1*A*B*C
      D(2)=V2*A*B4*B3
      D(3)=V2*A*B4*B2
      D(4)=V1*A*B1*C
      D(5)=V2*A4*A3*B1
      D(6)=V2*A4*A2*B1
      D(7)=V1*A1*B1*C
      D(8)=V2*A1*B4*B2
      D(9)=V2*A1*B4*B3
      D(10)=V1*A1*B*C
      D(11)=V2*A4*A2*B
      D(12)=V2*A4*A3*B
      Q(1)=V1*(-B*C+A*B*A5)
      Q(2)=-V2*B4*B3
      Q(3)=-V2*B4*B2
      Q(4)=V1*B1*(-C+A*A5)
      Q(5)=V2*B1*(-2.*G*A3-3.*A4)
      Q(6)=V2*B1*(-2.*G*A2+3.*A4)
      Q(7)=V1*(B1*C+A1*B1*A5)
      Q(8)=V2*B4*B2
      Q(9)=V2*B4*B3
      Q(10)=V1*(B*C+A1*B*A5)
      Q(11)=V2*B*(-2.*G*A2+3.*A4)
      Q(12)=V2*B*(-2.*G*A3-3.*A4)
      P(1)=V1*A*(-C+B*B5)
      P(2)=V2*A*(-2.*H*B3-B4*3.)
      P(3)=V2*A*(-2.*H*B2+B4*3.)
      P(4)=V1*A*(C+B1*B5)
      P(5)=V2*A4*A3
      P(6)=V2*A4*A2
      P(7)=V1*A1*(C+B1*B5)
      P(8)=V2*A1*(-2.*H*B2+3.*B4)
```

```
P(9)=V2*A1*(-2.*H*B3-B4*3.)
P(10)=V1*A1*(-C+B*B5)
P(11)=-V2*A4*A2
P(12)=-V2*A4*A3
CALL SHAPE
RETURN
END
```

```
      SUBROUTINE SHAP17
      COMMON/TRANS/D(17),Q(17),XM(17),YM(17),ZM(17),T(17),V1X(17),
     1V1Y(17),V1Z(17),V2X(17),V2Y(17),V2Z(17),V3X(17),V3Y(17),V3Z(17),
     2TRIN(17,3,3),P(17)
      COMMON/SHP/G,H,QXM,QYM,QZM,PXM,PYM,PZM,QXTB,QYTB,QZTB,PXTB,PYTB,
     1PZTB,DXTB,DYTB,DZTB,DT
C
C        SHAPE FUNCTIONS AND THEIR DERIVATIVES FOR A QUARTIC ELEMENT
C
      A1=1.+G
      A2=1.-G
      A3=A1*A2
      A4=0.5+G
      A5=0.5-G
      B1=1.+H
      B2=1.-H
      B3=B1*B2
      B4=0.5-H
      B5=0.5+H
      C1=1./12.
      C2=4./3.
      A6=G*A3
      B6=H*B3
      A3B=0.5*A3*B3
      A1B=3.*G*H
      A7=1.-3.*G*G
      A8=G*(1.-H*H)
      A9=2.*G*G
      B7=1.-3.*H*H
      B8=H*(1.-G*G)
      B9=2.*H*H
      D(1)=C1*A2*B2*(4.*(A6+B6)+A1B)
      D(2)=-C2*B6*B4*A2
      D(3)=2.*B4*B5*B3*A2-A3B
      D(4)=C2*B6*B5*A2
      D(5)=C1*A2*B1*(4.*(A6-B6)-A1B)
      D(6)=-C2*A6*A5*B1
      D(7)=2.*A4*A5*A3*B1-A3B
      D(8)=C2*A6*A4*B1
      D(9)=C1*A1*B1*(-4.*(A6+B6)+A1B)
      D(10)=C2*B6*B5*A1
      D(11)=2.*B4*B5*B3*A1-A3B
      D(12)=-C2*B6*B4*A1
      D(13)=C1*A1*B2*(-4.*(A6-B6)-A1B)
      D(14)=C2*A6*A4*B2
      D(15)=2.*A4*A5*A3*B2-A3B
      D(16)=-C2*A6*A5*B2
      D(17)=2.*A3B
      Q(1)=C1*B2*((-4.*(A6+B6)-A1B)+A2*(4.*A7+3.*H))
      Q(2)=C2*B6*B4
      Q(3)=-2.*B4*B5*B3+A8
      Q(4)=-C2*B6*B5
      Q(5)=C1*B1*((-4.*(A6-B6)+A1B)+A2*(4.*A7-3.*H))
      Q(6)=-C2*B1*(A3*A5-A9*A5-A6)
      Q(7)=2.*B1*(-2.*A6-2.*G*A4*A5)+A8
      Q(8)=C2*B1*(A3*A4-A9*A4+A6)
```

```
Q(9)=C1*B1*((-4.*(A6+B6)+A1B)+A1*(-4.*A7+3.*H))
Q(10)=C2*B6*B5
Q(11)=2.*B4*B5*B3+A8
Q(12)=-C2*B6*B4
Q(13)=C1*B2*((-4.*(A6-B6)-A1B)+A1*(-4.*A7-3.*H))
Q(14)=C2*B2*(A3*A4-A9*A4+A6)
Q(15)=2.*B2*(-2.*A6-2.*G*A4*A5)+A8
Q(16)=-C2*B2*(A3*A5-A9*A5-A6)
Q(17)=-2.*A8
P(1)=C1*A2*((-4.*(A6+B6)-A1B)+B2*(4.*B7+3.*G))
P(2)=-C2*A2*(B3*B4-B9*B4-B6)
P(3)=2.*A2*(-2.*B6-2.*H*B4*B5)+B8
P(4)=C2*A2*(B3*B5-B9*B5+B6)
P(5)=C1*A2*((4.*(A6-B6)-A1B)+B1*(-4.*B7-3.*G))
P(6)=-C2*A6*A5
P(7)=2.*A4*A5*A3+B8
P(8)=C2*A6*A4
P(9)=C1*A1*((-4.*(A6+B6)+A1B)+B1*(-4.*B7+3.*G))
P(10)=C2*A1*(B3*B5-B9*B5+B6)
P(11)=2.*A1*(-2.*B6-2.*H*B4*B5)+B8
P(12)=-C2*A1*(B3*B4-B9*B4-B6)
P(13)=C1*A1*((4.*(A6-B6)+A1B)+B2*(4.*B7-3.*G))
P(14)=-C2*A6*A4
P(15)=-2.*A4*A5*A3+B8
P(16)=C2*A6*A5
P(17)=-2.*B8
CALL SHAPE
RETURN
END
```

```
      SUBROUTINE SHAPE
      COMMON/TRANS/D(17),Q(17),XM(17),YM(17),ZM(17),T(17),V1X(17),
     1V1Y(17),V1Z(17),V2X(17),V2Y(17),V2Z(17),V3X(17),V3Y(17),V3Z(17),
     2TRIN(17,3,3),P(17)
      COMMON/SHP/G,H,QXM,QYM,QZM,PXM,PYM,PZM,QXTB,QYTB,QZTB,PXTB,PYTB,
     1PZTB,DXTB,DYTB,DZTB,DT
      COMMON/C1/ NUNKVA,NKNVA,NOSTR,NCELNO,NCELN1,NTOTAL,NPRDEF,NT,
     1NELEM,NFREE,NNELM,NCDTOT,NUNKV1,NKNVA1
C******** CALCULATION OF AMID AND AGEN FOR THE ELEMENT AT ANY POINT
      DT=0.0
      QXM=0.0
      QYM=0.0
      QZM=0.0
      QXTB=0.0
      QYTB=0.0
      QZTB=0.0
      PXM=0.0
      PYM=0.0
      PZM=0.0
      PXTB=0.0
      PYTB=0.0
      PZTB=0.0
      DXTB=0.0
      DYTB=0.0
      DZTB=0.0
      DO 4 I=1,NNELM
      QXM=QXM+Q(I)*XM(I)
      QYM=QYM+Q(I)*YM(I)
      QZM=QZM+Q(I)*ZM(I)
      DT=DT+D(I)*T(I)
      PXM=PXM+P(I)*XM(I)
      PYM=PYM+P(I)*YM(I)
      PZM=PZM+P(I)*ZM(I)
      QXTB=QXTB+Q(I)*V3X(I)*T(I)
      QZTB=QZTB+Q(I)*V3Z(I)*T(I)
      QYTB=QYTB+Q(I)*V3Y(I)*T(I)
      PXTB=PXTB+P(I)*V3X(I)*T(I)
      PYTB=PYTB+P(I)*V3Y(I)*T(I)
      PZTB=PZTB+P(I)*V3Z(I)*T(I)
      DXTB=DXTB+D(I)*V3X(I)*T(I)
      DYTB=DYTB+D(I)*V3Y(I)*T(I)
      DZTB=DZTB+D(I)*V3Z(I)*T(I)
    4 CONTINUE
      RETURN
      END
```

```
      SUBROUTINE TRAN
      COMMON/TRANS/D(17),Q(17),XM(17),YM(17),ZM(17),T(17),V1X(17),
     1V1Y(17),V1Z(17),V2X(17),V2Y(17),V2Z(17),V3X(17),V3Y(17),V3Z(17),
     2TRIN(17,3,3),P(17)
      DIMENSION JAC(3,3),IJAC(3,3)
      COMMON/STRS/ V1(17),V2(17),V3(2),IS(4,5),NE,NNS,NCM,NE2
      COMMON/C1/ NUNKVA,NKNVA,NOSTR,NCELNO,NCELN1,NTOTAL,NPRDEF,NT,
     1NELEM,NFREE,NNELM,NODTOT,NUNKV1,NKNVA1
      COMMON/SHP/G,H,QXM,QYM,QZM,PXM,PYM,PZM,QXTB,QYTB,QZTB,PXTB,PYTB,
     1PZTB,DXTB,DYTB,DZTB,DT
      REAL JAC,IJAC
C
C        ROUTINE TO CALCULATE THE DISPLACEMENT TRANSFORMATION MATRIX
C        AT EACH NODE
C
      DO 100 I1=1,NNELM
      G=V1(I1)
      H=V2(I1)
      IF(NNELM.EQ.8) GO TO 1
      IF(NNELM.EQ.12) GO TO 2
      CALL SHAP17
      GO TO 3
    1 CALL SHAP8
      GO TO 3
    2 CALL SHAP12
    3 CONTINUE
      AMID=SQRT(QXM*QXM+QYM*QYM+QZM*QZM)
      BMID=SQRT(PXM*PXM+PYM*PYM+PZM*PZM)
      COSMID=(QXM*PXM+QYM*PYM+QZM*PZM)/(AMID*BMID)
      SINMID=SQRT(1.-COSMID*COSMID)
      V1X(I1)=QXM/AMID
      V1Y(I1)=QYM/AMID
      V1Z(I1)=QZM/AMID
      V3X(I1)=(QYM*PZM-QZM*PYM)/(AMID*BMID*SINMID)
      V3Y(I1)=(QZM*PXM-QXM*PZM)/(AMID*BMID*SINMID)
      V3Z(I1)=(QXM*PYM-QYM*PXM)/(AMID*BMID*SINMID)
      V2X(I1)=V3Y(I1)*V1Z(I1)-V3Z(I1)*V1Y(I1)
      V2Y(I1)=V3Z(I1)*V1X(I1)-V3X(I1)*V1Z(I1)
      V2Z(I1)=V3X(I1)*V1Y(I1)-V3Y(I1)*V1X(I1)
C
C        INVERSE OF THE ABOVE MATRIX
C
      JAC(1,1)=V3X(I1)
      JAC(1,2)=V2X(I1)
      JAC(1,3)=V1X(I1)
      JAC(2,1)=V3Y(I1)
      JAC(2,2)=V2Y(I1)
      JAC(2,3)=V1Y(I1)
      JAC(3,1)=V3Z(I1)
      JAC(3,2)=V2Z(I1)
      JAC(3,3)=V1Z(I1)
      VJAC=JAC(1,1)*(JAC(2,2)*JAC(3,3)-JAC(2,3)*JAC(3,2))-
     1JAC(1,2)*(JAC(2,1)*JAC(3,3)-JAC(2,3)*JAC(3,1))+
     2JAC(1,3)*(JAC(2,1)*JAC(3,2)-JAC(2,2)*JAC(3,1))
      IJAC(1,1)=(JAC(2,2)*JAC(3,3)-JAC(3,2)*JAC(2,3))/VJAC
      IJAC(1,2)=-(JAC(1,2)*JAC(3,3)-JAC(3,2)*JAC(1,3))/VJAC
```

```
      IJAC(1,3)=(JAC(1,2)*JAC(2,3)-JAC(2,2)*JAC(1,3))/VJAC
      IJAC(2,1)=-(JAC(2,1)*JAC(3,3)-JAC(3,1)*JAC(2,3))/VJAC
      IJAC(2,2)=(JAC(1,1)*JAC(3,3)-JAC(3,1)*JAC(1,3))/VJAC
      IJAC(2,3)=-(JAC(1,1)*JAC(2,3)-JAC(2,1)*JAC(1,3))/VJAC
      IJAC(3,1)=(JAC(2,1)*JAC(3,2)-JAC(2,2)*JAC(3,1))/VJAC
      IJAC(3,2)=-(JAC(1,1)*JAC(3,2)-JAC(1,2)*JAC(3,1))/VJAC
      IJAC(3,3)=(JAC(1,1)*JAC(2,2)-JAC(2,1)*JAC(1,2))/VJAC
      DO 11 I=1,3
      DO 11 J=1,3
   11 TRIN(I1,I,J)=IJAC(I,J)
  100 CONTINUE
      RETURN
      END
```

```
      SUBROUTINE INIAL
      REAL KNOMAT,KNORHS
      INTEGER AA,A,B
      INTEGER ELPOSN,ELNODE,PRENIC,UNKNIC,ELVEC
      COMMON/S6/ ELNODE(110,87),RHSRED(1,85)
      COMMON/S2/ PRENIC(1,500),UNKNIC(1,181),KNONIC(2,35),UNRHS(1,35),
     2KNORHS(1,181),ELVEC(1,85),ELPOSN(2,85),KNOMAT(1,800),
     3UNKMAT(1,18000),UNCLE(181,35)
      COMMON/C1/ NUNKVA,NKNVA,NOSTR,NCELNO,NCELN1,NTOTAL,NPRDEF,NT,
     1NELEM,NFREE,NNELM,NODTOT,NUNKV1,NKNVA1
      DIMENSION A(500),B(500)
      COMMON/NO/NRING1,NRING2,NRING3,NELEM1,NELEM2,NELEM3,NEPR,NRING
C
C        CALCULATING NUMBER OF KNOWN VARIBLES AND UNKNOWN VARIBLES
C        APPEARING AT ONE TIME
C
      NFREE=5
      NOSTR=1
      NFREE1=NFREE-1
      NCELNO=NFREE*NNELM+1
      CALL NODE
      DO 70 I=1,500
      A(I)=0
   70 B(I)=0
      NUNKVA=0
      NKNVA=0
      DO 80 I=1,NELEM
      DO 200 J=2,NCELNO
      AA=IABS(ELNODE(I,J))
C
C        TO CHECK WHETHER NICKNAME IS IN  A  OR  B  ALREDY
C
      DO 90 K=1,500
      IF(A(K).EQ.AA) GO TO 100
      IF(B(K).EQ.AA) GO TO 110
   90 CONTINUE
      GO TO 120
  100 A(K)=ELNODE(I,J)
      GO TO 210
  110 B(K)=ELNODE(I,J)
      GO TO 210
C
C        TO CHECK WHETHER NICKNAME IS IN  PRENIC  IF SO STORE IN  B
C
  120 DO 130 K=1,NOSTR
      DO 130 L=1,NPRDEF
      IF(AA.EQ.PRENIC(K,L)) GO TO 140
  130 CONTINUE
      GO TO 170
  140 DO 150 M=1,500
      IF(B(M).EQ.0) GO TO 160
  150 CONTINUE
  160 B(M)=ELNODE(I,J)
      GO TO 210
C
C        IF IT IS NOT IN  A  OR  B OR PRENIC STORE IT IN  A
```

```
C
  170 DO 180 N=1,500
      IF(A(N).EQ.0) GO TO 190
  180 CONTINUE
  190 A(N)=ELNODE(I,J)
  210 IF(J.EQ. NCELNO) GO TO 220
  200 CONTINUE
  220 DO 230 II=1,500
      III=501-II
      IF(A(III).NE.0) GO TO 240
  230 CONTINUE
  240 IF(III.GT.NUNKVA) NUNKVA=III
      DO 250 JJ=1,500
      IF(A(JJ).LT.0) A(JJ)=0
  250 CONTINUE
      DO 260 KK=1,500
      KK1=501-KK
      IF(B(KK1).NE.0) GO TO 270
  260 CONTINUE
  270 IF(KK1.GT.NKNVA) NKNVA=KK1
      DO 280 LL=1,500
      IF(B(LL).LT.0) B(LL)=0
  280 CONTINUE
   80 CONTINUE
      WRITE(6,1000) NUNKVA,NKNVA
   30 FORMAT(6I5)
   20 FORMAT (F10.0)
   60 FORMAT(F10.0)
 1000 FORMAT(27H NO OF UNKNOWN AT ONE TIME=I5,
     126H NO OF KNOWN AT ONE TIME =I5)
      RETURN
      END
```

```
      SUBROUTINE NODE
      INTEGER C,A
      INTEGER ELPOSN,ELNODE,PRENIC,UNKNIC,ELVEC
      REAL KNOMAT,KNORHS
      COMMON/STRS/ V1(17),V2(17),V3(2),IS(4,5),NE,NNS,NCM,NE2
      DIMENSION C(2000)
      COMMON/S6/ ELNODE(110,87),RHSRED(1,85)
      COMMON/NO/NRING1,NRING2,NRING3,NELEM1,NELEM2,NELEM3,NEPR,NRING
      COMMON/S2/ PRENIC(1,500),UNKNIC(1,181),KNONIC(2,35),UNRHS(1,35),
     2KNORHS(1,181),ELVEC(1,85),ELPOSN(2,85),KNOMAT(1,800),
     3UNKMAT(1,18000),UNCLE(181,35)
      COMMON/C1/ NUNKVA,NKNVA,NOSTR,NCELNO,NCELN1,NTOTAL,NPRDEF,NT,
     1NELEM,NFREE,NNELM,NODTOT,NUNKV1,NKNVA1
C
C         ROUTINE FOR AUTOMATIC MESH GENERATION FOR PIPE BEND PROBLEMS
C
      NRING=NRING1+NRING2+NRING3
      NELEM=NRING*NEPR
      IJ=NELEM*NNELM
      DO 8 I=1,IJ
      C(I)=0
    8 CONTINUE
      DO 1 I=1,NNELM
    1 C(I)=I
      A=NNELM
      DO 200 N1=1,NRING
      DO 100 N2=1,NEPR
      N=NEPR*(N1-1)+N2
      M=NNELM*(N-1)
      L=NNELM*(N-2)
      K=NNELM*(N-NEPR-1)
      IF(N.EQ.1) GO TO 100
      IF(N.EQ.((N1-1)*NEPR+1)) GO TO 300
      DO 30 I=1,NNS
      I1=IS(4,I)
      J1=IS(2,I)
   30 C(M+I1)=C(L+J1)
      IF(N.GT.NEPR) GO TO 300
      IF(N.EQ.N1*NEPR) GO TO 1001
      GO TO 302
  301 ML=NNELM*(N-NEPR)
      DO 31 I=1,NNS
      I1=IS(2,I)
      J1=IS(4,I)
   31 C(M+I1)=C(ML+J1)
  302 CONTINUE
 1001 CONTINUE
      DO 3 I=1,NNELM
      IF(C(M+I).EQ.0) GO TO 4
      GO TO 3
    4 A=A+1
      C(M+I)=A
    3 CONTINUE
      IF(N.LE.NEPR) GO TO 100
  300 CONTINUE
      DO 32 I=1,NNS
```

```
      I1=IS(1,I)
      J1=IS(3,I)
   32 C(M+I1)=C(K+J1)
      IF(N.EQ.N1*NEPR) GO TO 1002
      GO TO 402
  401 ML=NNELM*(N-NEPR)
      DO 33 I=1,NNS
      I1=IS(2,I)
      J1=IS(4,I)
   33 C(M+I1)=C(ML+J1)
  402 CONTINUE
 1002 CONTINUE
      DO 10 I=1,NNELM
      IF(C(M+I).EQ.0) GO TO 11
      GO TO 10
   11 A=A+1
      C(M+I)=A
   10 CONTINUE
  100 CONTINUE
  200 CONTINUE
      NODTOT=A
  700 DO 500 I=1,IJ
      N=IJ+1-I
      IF(C(N).EQ.A) GO TO 600
  500 CONTINUE
  600 A=A-1
      C(N)=-C(N)
      IF(A.EQ.0) GO TO 800
      GO TO 700
  800 DO 810 I=1,IJ
      IF(C(I).GT.0) GO TO 820
      GO TO 830
  820 C(I)=100*C(I)+10
      GO TO 810
  830 C(I)=100*C(I)-10
  810 CONTINUE
      DO 636 I=1,NELEM
      DO 636 J=1,NCELNO
  636 ELNODE(I,J)=0
      DO 60 I=1,NELEM
      ELNODE(I,1)=I
      K1=2
      DO 60 L=1,NNELM
      ELNODE(I,K1)=C(NNELM*(I-1)+L)
      IF(ELNODE(I,K1).GT.0) GO TO 504
      GO TO 502
  504 DO 501 J=1,4
      K2=K1+J
  501 ELNODE(I,K2)=ELNODE(I,K1)+J*10
      GO TO 60
  502 DO 503 J=1,4
      K2=K1+J
  503 ELNODE(I,K2)=ELNODE(I,K1)-J*10
   60 K1=K1+5
      DO 310 I=1,NELEM1
  310 ELNODE(I,87)=1
      N1=NELEM1+1
      N2=NELEM1+NELEM2
      N3=N2+1
```

```
      DO 311 I=N1,N2
  311 ELNODE(I,87)=2
      IF(N3.GT.NELEM) GO TO 313
      DO 312 I=N3,NELEM
  312 ELNODE(I,87)=3
  313 CONTINUE
C
C       ROUTINE TO GENERATE THE NICK NAMES OF THE NODES WITH PRESCRI
C       DISPLACEMENTS AND ROTATIONS
C
      NJ=(NRING-1)*NEPR+1
      J=0
      NN=NNS-1
      DO 101 I=1,NJ,NEPR
      DO 35 IJ=1,NN
       J=J+1
      I1=IS(4,IJ)
      I2=5*I1-2
      I3=5*I1+1
      PRENIC(1,J)=ELNODE(I,I2)
      J=J+1
      PRENIC(1,J)=ELNODE(I,I3)
   35 CONTINUE
  101 CONTINUE
      DO 105 I=NEPR,NELEM,NEPR
      DO 37 IJ=1,NN
      J=J+1
      I1=IS(2,IJ)
      I2=5*I1-2
      I3=5*I1+1
      PRENIC(1,J)=ELNODE(I,I2)
      J=J+1
      PRENIC(1,J)=ELNODE(I,I3)
   37 CONTINUE
  105 CONTINUE
      JJ=62
      DO 104 I=1,5
      J=J+1
      PRENIC(1,J)=ELNODE(NJ,JJ)
      JJ=JJ+1
  104 CONTINUE
      DO 102 I=NJ,NELEM
      K=0
      DO 36 I8=2,NNS
      J=J+1
      IJ=NNS-K
      I1=IS(3,IJ)
      I2=5*I1-1
      I3=5*I1
      I4=5*I1-2
      I5=5*I1-3
      I6=5*I1+1
      PRENIC(1,J)=ELNODE(I,I2)
      J=J+1
      PRENIC(1,J)=ELNODE(I,I3)
      J=J+1
      PRENIC(1,J)=ELNODE(I,I4)
      J=J+1
      PRENIC(1,J)=ELNODE(I,I5)
```

```
      J=J+1
      PRENIC(1,J)=ELNODE(I,I6)
      K=K+1
   36 CONTINUE
  102 CONTINUE
      NPRDEF=J
      DO 103 I=1,NPRDEF
  103 PRENIC(1,I)=IABS(PRENIC(1,I))
      RETURN
      END
```

```
      SUBROUTINE FEM2
      COMMON/NO/NRING1,NRING2,NRING3,NELEM1,NELEM2,NELEM3,NEPR,NRING
      COMMON/STRS/ V1(17),V2(17),V3(2),IS(4,5),NE,NNS,NCM,NE2
      COMMON/C1/ NUNKVA,NKNVA,NOSTR,NCELNO,NCELN1,NTOTAL,NPRDEF,NT,
     1NELEM,NFREE,NNELM,NODTOT,NUNKV1,NKNVA1
      COMMON/FE1/JAC(3,3),IJAC(3,3),DE(3,153),JDE(3,153),DUD(3,85),
     1DVD(3,85),DWD(3,85),L(3,3),F1(85),F2(85),F3(85),S1(85),S2(85),
     2S3(85),T1(85),T2(85),T3(85),B(5,85),DB(5,85)
      COMMON/FE2/ BR(5,85)
      COMMON/S8/ XG(4),CG(4),XGZ(2),CGZ(2),DI(5,5)
      REAL JAC,IJAC,JDE,L,LDUDX,LDVDX,LDWDX,LDUDY,LDVDY,LDWDY,
     1LDUDZ,LDVDZ,LDWDZ,VJAC,MVJAC
      COMMON/SHP/G,H,QXM,QYM,QZM,PXM,PYM,PZM,QXTB,QYTB,QZTB,PXTB,PYTB,
     1PZTB,DXTB,DYTB,DZTB,DT
      COMMON/TRANS/D(17),Q(17),XM(17),YM(17),ZM(17),T(17),V1X(17),
     1V1Y(17),V1Z(17),V2X(17),V2Y(17),V2Z(17),V3X(17),V3Y(17),V3Z(17),
     2TRIN(17,3,3),P(17)
      COMMON/DM/E,PR,COMM1
C
C       ROUTINE TO GENERATE THE STRESS MATRIX AT NODAL POINTS ON THE IN
C        AND OUT SIDE SURFACES
C
      DS1=COMM1
      DS2=COMM1*PR
      DS3=COMM1*(1.-PR)/2.
      DS4=COMM1*(1.-PR)/2.4
      DO 700 JG=1,NE
      G=V1(JG)
      H=V2(JG)
      IF(NNELM.EQ.8) GO TO 1
      IF(NNELM.EQ.12) GO TO 2
      CALL SHAP17
      GO TO 3
    1 CALL SHAP8
      GO TO 3
    2 CALL SHAP12
    3 CONTINUE
      DO 700 IG=1,2
      F=V3(IG)
C         CALCULATION OF JACOBIAN MATRIX AND ITS INVERSE
      DO 9 I=1,3
      DO 9 J=1,3
      JAC(I,J)=0.0
    9 IJAC(I,J)=0.0
      JAC(1,1)=QXM+F*0.5*QXTB
      JAC(1,2)=QYM+F*0.5*QYTB
      JAC(1,3)=QZM+F*0.5*QZTB
      JAC(2,1)=PXM+F*0.5*PXTB
      JAC(2,2)=PYM+F*0.5*PYTB
      JAC(2,3)=PZM+F*0.5*PZTB
      JAC(3,1)=0.5*DXTB
      JAC(3,2)=0.5*DYTB
      JAC(3,3)=0.5*DZTB
C         VJAC IS DETERMINANT OF JACOBIAN MATRIX
C         IJAC IS INVERSE JACOBIAN MATRIX
      VJAC=JAC(1,1)*(JAC(2,2)*JAC(3,3)-JAC(2,3)*JAC(3,2))-
```

```
     1JAC(1,2)*(JAC(2,1)*JAC(3,3)-JAC(2,3)*JAC(3,1))+
     2JAC(1,3)*(JAC(2,1)*JAC(3,2)-JAC(2,2)*JAC(3,1))
      IJAC(1,1)=(JAC(2,2)*JAC(3,3)-JAC(3,2)*JAC(2,3))/VJAC
      IJAC(1,2)=-(JAC(1,2)*JAC(3,3)-JAC(3,2)*JAC(1,3))/VJAC
      IJAC(1,3)=(JAC(1,2)*JAC(2,3)-JAC(2,2)*JAC(1,3))/VJAC
      IJAC(2,1)=-(JAC(2,1)*JAC(3,3)-JAC(3,1)*JAC(2,3))/VJAC
      IJAC(2,2)=(JAC(1,1)*JAC(3,3)-JAC(3,1)*JAC(1,3))/VJAC
      IJAC(2,3)=-(JAC(1,1)*JAC(2,3)-JAC(2,1)*JAC(1,3))/VJAC
      IJAC(3,1)=(JAC(2,1)*JAC(3,2)-JAC(2,2)*JAC(3,1))/VJAC
      IJAC(3,2)=-(JAC(1,1)*JAC(3,2)-JAC(1,2)*JAC(3,1))/VJAC
      IJAC(3,3)=(JAC(1,1)*JAC(2,2)-JAC(2,1)*JAC(1,2))/VJAC
C******** DERIVATIVES OF GLOBAL DIS. W.R.T. LOCAL COORDINATES
      DO 10 I=1,3
      DO 10 J=1,NCM
   10 DE(I,J)=0.0
      DO 11 I=1,NNELM
      I1=I+NNELM
      I2=I+2*NNELM
      I3=I+3*NNELM
      I4=I+4*NNELM
      I5=I+5*NNELM
      I6=I+6*NNELM
      I7=I+7*NNELM
      I8=I+8*NNELM
      DFT=D(I)*0.5*T(I)
      PFT=P(I)*F*0.5*T(I)
      QFT=Q(I)*F*0.5*T(I)
      DE(1,I)=Q(I)
      DE(1,I1)=QFT*V1X(I)
      DE(1,I2)=QFT*V2X(I)
      DE(1,I3)=Q(I)
      DE(1,I4)=QFT*V1Y(I)
      DE(1,I5)=QFT*V2Y(I)
      DE(1,I6)=Q(I)
      DE(1,I7)=QFT*V1Z(I)
      DE(1,I8)=QFT*V2Z(I)
      DE(2,I)=P(I)
      DE(2,I1)=PFT*V1X(I)
      DE(2,I2)=PFT*V2X(I)
      DE(2,I3)=P(I)
      DE(2,I4)=PFT*V1Y(I)
      DE(2,I5)=PFT*V2Y(I)
      DE(2,I6)=P(I)
      DE(2,I7)=PFT*V1Z(I)
   12 DE(2,I8)=PFT*V2Z(I)
      DE(3,I1)=DFT*V1X(I)
      DE(3,I2)=DFT*V2X(I)
      DE(3,I4)=DFT*V1Y(I)
      DE(3,I5)=DFT*V2Y(I)
      DE(3,I7)=DFT*V1Z(I)
   13 DE(3,I8)=DFT*V2Z(I)
   11 CONTINUE
C******** DERIVATIVES OF GLOBAL DIS. W.R.T. GLOBAL COORDINATES
      DO 21 I=1,3
      DO 21 J=1,NCM
      JDE(I,J)=0.0
      DO 21 K=1,3
   21 JDE(I,J)=JDE(I,J)+IJAC(I,K)*DE(K,J)
C******** ARRANGING ABOVE DERIVATIVES IN PROPER ORDER
```

```
      DO 30 J=1,3
      DO 30 I=1,NCELN1
      DUD(J,I)=0.0
      DVD(J,I)=0.0
   30 DWD(J,I)=0.0
      DO 60 J=1,3
      I=1
      I1=1
   31 DUD(J,I1)=JDE(J,I)
      I1=I1+5
      I=I+1
       IF(I.EQ.NNELM+1) GO TO 32
      GO TO 31
   32 I1=4
   33 DUD(J,I1)=JDE(J,I)
      I1=I1+5
      I=I+1
      IF(I.EQ.2*NNELM+1) GO TO 34
      GO TO 33
   34 I1=5
   35 DUD(J,I1)=JDE(J,I)
      I1=I1+5
      I=I+1
      IF(I.EQ.3*NNELM+1) GO TO 36
      GO TO 35
   36 CONTINUE
      I1=2
   41 DVD(J,I1)=JDE(J,I)
      I1=I1+5
      I=I+1
      IF(I.EQ.4*NNELM+1) GO TO 42
      GO TO 41
   42 I1=4
   43 DVD(J,I1)=JDE(J,I)
      I1=I1+5
      I=I+1
      IF(I.EQ.5*NNELM+1) GO TO 44
      GO TO 43
   44 I1=5
   45 DVD(J,I1)=JDE(J,I)
      I1=I1+5
      I=I+1
      IF(I.EQ.6*NNELM+1) GO TO 46
      GO TO 45
   46 CONTINUE
      I1=3
   51 DWD(J,I1)=JDE(J,I)
      I1=I1+5
      I=I+1
      IF(I.EQ.7*NNELM+1) GO TO 52
      GO TO 51
   52 I1=4
   53 DWD(J,I1)=JDE(J,I)
      I1=I1+5
      I=I+1
      IF(I.EQ.8*NNELM+1) GO TO 54
      GO TO 53
   54 I1=5
   55 DWD(J,I1)=JDE(J,I)
```

```
      I=I+1
      I1=I1+5
      IF(I.EQ.9*NNELM+1) GO TO 56
      GO TO 55
   56 CONTINUE
   60 CONTINUE
C         STRAIN TRANSFORMATION MATRIX
      DO 61 I=1,3
      DO 61 J=1,3
   61 L(I,J)=0.0
      AGEN=SQRT(JAC(1,1)*JAC(I,1)+JAC(1,2)*JAC(1,2)+JAC(1,3)*JAC(I,3))
      BGEN=SQRT(JAC(2,1)*JAC(2,1)+JAC(2,2)*JAC(2,2)+JAC(2,3)*JAC(2,3))
      ACOS=(JAC(1,1)*JAC(2,1)+JAC(1,2)*JAC(2,2)+JAC(1,3)*JAC(2,3))/
     1(AGEN*BGEN)
      ASIN=SQRT(1.-ACOS*ACOS)
      VNI=(JAC(1,2)*JAC(2,3)-JAC(1,3)*JAC(2,2))/(AGEN*BGEN*ASIN)
      VNJ=(JAC(1,3)*JAC(2,1)-JAC(1,1)*JAC(2,3))/(AGEN*BGEN*ASIN)
      VNK=(JAC(1,1)*JAC(2,2)-JAC(1,2)*JAC(2,1))/(AGEN*BGEN*ASIN)
      VETAI=(VNJ*JAC(1,3)-VNK*JAC(1,2))/AGEN
      VETAJ=(VNK*JAC(1,1)-VNI*JAC(1,3))/AGEN
      VETAK=(VNI*JAC(1,2)-VNJ*JAC(1,1))/AGEN
      L(1,1)=JAC(1,1)/AGEN
      L(2,1)=JAC(1,2)/AGEN
      L(3,1)=JAC(1,3)/AGEN
      L(1,2)=VETAI
      L(2,2)=VETAJ
      L(3,2)=VETAK
      L(1,3)=VNI
      L(2,3)=VNJ
      L(3,3)=VNK
C******** CALCULATION OF LOCAL DERIVATIVES
      DO 71 I=1,NCELN1
      F1(I)=DUD(1,I)*L(1,1)+DVD(1,I)*L(2,1)+DWD(1,I)*L(3,1)
      F2(I)=DUD(1,I)*L(1,2)+DVD(1,I)*L(2,2)+DWD(1,I)*L(3,2)
      F3(I)=DUD(1,I)*L(1,3)+DVD(1,I)*L(2,3)+DWD(1,I)*L(3,3)
      S1(I)=DUD(2,I)*L(1,1)+DVD(2,I)*L(2,1)+DWD(2,I)*L(3,1)
      S2(I)=DUD(2,I)*L(1,2)+DVD(2,I)*L(2,2)+DWD(2,I)*L(3,2)
      S3(I)=DUD(2,I)*L(1,3)+DVD(2,I)*L(2,3)+DWD(2,I)*L(3,3)
      T1(I)=DUD(3,I)*L(1,1)+DVD(3,I)*L(2,1)+DWD(3,I)*L(3,1)
      T2(I)=DUD(3,I)*L(1,2)+DVD(3,I)*L(2,2)+DWD(3,I)*L(3,2)
      T3(I)=DUD(3,I)*L(1,3)+DVD(3,I)*L(2,3)+DWD(3,I)*L(3,3)
   71 CONTINUE
C******** B MATRIX
      DO 80 I=1,NCELN1
      B(1,I)  =F1(I)*L(1,1)+S1(I)*L(2,1)+T1(I)*L(3,1)
      B(2,I)  =F2(I)*L(1,2)+S2(I)*L(2,2)+T2(I)*L(3,2)
      B(3,I)  =F1(I)*L(1,2)+S1(I)*L(2,2)+T1(I)*L(3,2)
     1        +F2(I)*L(1,1)+S2(I)*L(2,1)+T2(I)*L(3,1)
      B(4,I)  =F2(I)*L(1,3)+S2(I)*L(2,3)+T2(I)*L(3,3)
     1        +F3(I)*L(1,2)+S3(I)*L(2,2)+T3(I)*L(3,2)
      B(5,I)  =F3(I)*L(1,1)+S3(I)*L(2,1)+T3(I)*L(3,1)
     1        +F1(I)*L(1,3)+S1(I)*L(2,3)+T1(I)*L(3,3)
   80 CONTINUE
C******** B MATRIX MODIFIED TO BR MATRIX SO THAT THE NODAL DISPLACEME
C******* ARE IN THE CHOSEN LOCAL DIRECTIONS
      DO 89 I=1,5
      DO 89 J=1,NCELN1
      BR(I,J)=0.0
   89 CONTINUE
```

```
      DO 91 I=1,5
      N1=0
      J=0
   92 J=J+1
      N1=N1+1
      IF(N1.EQ.NNELM+1) GO TO 93
      J1=J+1
      J2=J+2
      J3=J+3
      J4=J+4
      BR(I,J)=B(I,J)*V3X(N1)+B(I,J1)*V3Y(N1)+B(I,J2)*V3Z(N1)
      BR(I,J1)=B(I,J)*V2X(N1)+B(I,J1)*V2Y(N1)+B(I,J2)*V2Z(N1)
      BR(I,J2)=B(I,J)*V1X(N1)+B(I,J1)*V1Y(N1)+B(I,J2)*V1Z(N1)
      BR(I,J3)=B(I,J3)
      BR(I,J4)=B(I,J4)
      J=J4
      GO TO 92
   93 CONTINUE
   91 CONTINUE
C******** CALCULATION OF STRESS MATRIX
      DO 101 I=1,5
      DO 101 J=1,NCELN1
  101 DB(I,J)=0.0
      DO 110 J=1,NCELN1
      DB(1,J)=BR(1,J)*DS1+BR(2,J)*DS2
      DB(2,J)=BR(1,J)*DS2+BR(2,J)*DS1
      DB(3,J)=BR(3,J)*DS3
      DB(4,J)=BR(4,J)*DS4
      DB(5,J)=BR(5,J)*DS4
  110 CONTINUE
      WRITE(2) ((DB(I,J),I=1,5),J=1,NCELN1)
  700 CONTINUE
  900 RETURN
      END
```

```
      SUBROUTINE STRESS
      INTEGER U1
      INTEGER ELPOSN,ELNODE,PRENIC,UNKNIC,ELVEC
      REAL KNOMAT,KNORHS
      DIMENSION EQO(500),EQI(500)
      COMMON/S6/ ELNODE(110,87),RHSRED(1,85)
      COMMON/MOM/ SEO(32,5),SEI(32,5)
      COMMON/STRS/ V1(17),V2(17),V3(2),IS(4,5),NE,NNS,NCM,NE2
      COMMON/NO/NRING1,NRING2,NRING3,NELEM1,NELEM2,NELEM3,NEPR,NRING
      COMMON/S5/ U1(5000),U2(5000)
      COMMON/C1/ NUNKVA,NKNVA,NOSTR,NCELNO,NCELN1,NTOTAL,NPRDEF,NT,
     1NELEM,NFREE,NNELM,NODTOT,NUNKV1,NKNVA1
      COMMON/FE1/JAC(3,3),IJAC(3,3),DE(3,153),JDE(3,153),DUD(3,85),
     1DVD(3,85),DWD(3,85),L(3,3),F1(85),F2(85),F3(85),S1(85),S2(85),
     2S3(85),T1(85),T2(85),T3(85),B(5,85),DB(5,85)
      COMMON/NSTR/ NODSTR,IGAUST
      DIMENSION C(85),STRL(5,1),SO(5),SI(5),STSL(32,5),STSS(110,32,5)
      COMMON/S2/ PRENIC(1,500),UNKNIC(1,181),KNONIC(2,35),UNRHS(1,35),
     2KNORHS(1,181),ELVEC(1,85),ELPOSN(2,85),KNOMAT(1,800),
     3UNKMAT(1,18000),UNCLE(181,35)
      EQUIVALENCE (STSS(1,1,1),UNKMAT(1,1))
      REAL L
C
C         ROUTINE TO CALCULATE THE AVERAGE NODAL STRESS
C
      REWIND 2
      REWIND 3
      REWIND 4
      DO 1000 K=1,NEPR
      DO 1000 M=1,NE2
      READ(2)
     1 ((DB(I,J),I=1,5),J=1,NCELN1)
      WRITE(3)
     1 ((DB(I,J),I=1,5),J=1,NCELN1)
 1000 CONTINUE
      IF(ELNODE(NELEM,87).EQ.1) GO TO 1002
      DO 1001 K=1,NEPR
      DO 1001 M=1,NE2
      READ(2)
     1 ((DB(I,J),I=1,5),J=1,NCELN1)
      WRITE(4)
     1 ((DB(I,J),I=1,5),J=1,NCELN1)
 1001 CONTINUE
 1002 CONTINUE
      REWIND 3
      REWIND 4
      DO 21 I=1,NELEM
      DO 21 J=1,NE2
      DO 21 K=1,5
   21 STSS(I,J,K)=0.0
      DO 70 I=1,NELEM
      DO 70 J=2,NCELNO
      ELNODE(I,J)=IABS(ELNODE(I,J))
   70 CONTINUE
C
C         ROUTINE TO CALCULATE STRESSES AT THE NODAL POINTS- ELEMENT
```

```
C          BY ELEMENT
C
      DO 20 LL=1,NELEM
      DO 30 K=2,NCELNO
      DO 40 M=1,NT
      IF(ELNODE(LL,K).EQ.U1(M)) GO TO 50
   40 CONTINUE
   50 KM1=K-1
      C(KM1)=U2(M)
   30 CONTINUE
      NAME=ELNODE(LL,87)
      DO 850 MS=1,NE2
      GO TO (851,852,851) NAME
  851 READ(3)
     1 ((DB(I,J),I=1,5),J=1,NCELN1)
      GO TO 853
  852 READ(4)
     1 ((DB(I,J),I=1,5),J=1,NCELN1)
  853 CONTINUE
      DO 830 I=1,5
      STRL(I,1)=0.0
      DO 830 K=1,NCELN1
  830 STRL(I,1)=STRL(I,1)+DB(I,K)*C(K)
      DO 832 I=1,5
  832 STSS(LL,MS,I)=STRL(I,1)
  850 CONTINUE
      DO 854 I=1,NRING
      IF(LL.EQ.I*NEPR) GO TO 855
  854 CONTINUE
      GO TO 20
  855 REWIND 3
      REWIND 4
   20 CONTINUE
C
C          NODAL STRESSES ARE AVERAGED OUT AND PRINTED
C
      MPRINT=0
      DO 41 NODE=1,NODTOT
      DO 81 I=1,NELEM
      IF((ELNODE(I,82)-10).EQ.NODE*100) GO TO 41
   81 CONTINUE
      DO 42 I=1,5
      SO(I)=0.0
      SI(I)=0.0
   42 CONTINUE
      NJ=0
      DO 31 NEL=1,NELEM
      N=0
      DO 32 I=2,NCELNO,5
      N=N+1
      IF((ELNODE(NEL,I)-10).EQ.NODE*100) GO TO 33
   32 CONTINUE
      GO TO 31
   33 NJ=NJ+1
      N1=2*N-1
      N2=2*N
      DO 34 I=1,5
      SO(I)=SO(I)+STSS(NEL,N1,I)
   34 SI(I)=SI(I)+STSS(NEL,N2,I)
```

```
 31 CONTINUE
    DO 35 I=1,5
    SO(I)=SO(I)/FLOAT(NJ)
 35 SI(I)=SI(I)/FLOAT(NJ)
    NN1=NNS*5
    DO 61 NEL=1,NEPR
    I1=0
    DO 62 I=2,NN1,5
    I1=I1+1
    IF((ELNODE(NEL,I)-10).EQ.NODE*100) GO TO 63
 62 CONTINUE
    GO TO 64
 63 SEO(NEL,I1)=SO(1)
    SEI(NEL,I1)=SI(1)
 64 CONTINUE
 61 CONTINUE
    IF(MPRINT.GT.0) GO TO 400
    WRITE(6,60)
 60 FORMAT(1H1,1X,*NODE*,3X,*SURFACE*,4X,*DIRECT STRS EPSI*,
   14X,*DIRECT STRS ETA *,4X,*SHEAR STS EPSI ETA*,2X,*SHEAR STS ETA
   2TA*,2X,*SHEAR STS EPSI ZETA*)
    MPRINT=25
400 MPRINT=MPRINT-1
    WRITE(6,36) NODE,(SO(I),I=1,5)
 36 FORMAT(I5,3X,*OUTSIDE*,5(4X,E16.8))
    WRITE(6,37) (SI(I),I=1,5)
 37 FORMAT(9X,*INSIDE*,5(4X,E16.8))
    EQO(NODE)=SQRT(0.5*((SO(1)-SO(2))**2+(SO(2))**2+(SO(1))**2)+
   13.*(SO(3)*SO(3)+SO(4)*SO(4)+SO(5)*SO(5)))
    EQI(NODE)=SQRT(0.5*((SI(1)-SI(2))**2+(SI(2))**2+(SI(1))**2)+
   13.*(SI(3)*SI(3)+SI(4)*SI(4)+SI(5)*SI(5)))
 41 CONTINUE
    MPT=0
    DO 301 MP=1,NODTOT
    IF(MPT.GT.0) GO TO 302
    WRITE(6,303)
303 FORMAT(1H1,1X,*NODE*,10X,*EQU STS OUT SIDE*,10X,*EQU STS INSIDE
    MPT=50
302 MPT=MPT-1
    WRITE(6,304) MP,EQO(MP),EQI(MP)
304 FORMAT(I5,10X,E16.8,10X,E16.8)
301 CONTINUE
    CALL MOMENT
    RETURN
    END
```

```
      SUBROUTINE COBEND
      COMMON/D1/ X(17)
      COMMON/STRS/ V1(17),V2(17),V3(2),IS(4,5),NE,NNS,NCM,NE2
      COMMON/COD/ CO(17),CD(17),STE(17),CTE(17),PH(6),PHN(17)
      COMMON/TRANS/D(17),Q(17),XM(17),YM(17),ZM(17),T(17),V1X(17),
     1V1Y(17),V1Z(17),V2X(17),V2Y(17),V2Z(17),V3X(17),V3Y(17),V3Z(17),
     2TRIN(17,3,3),P(17)
      COMMON/NO/NRING1,NRING2,NRING3,NELEM1,NELEM2,NELEM3,NEPR,NRING
      COMMON/C1/ NUNKVA,NKNVA,NOSTR,NCELNO,NCELN1,NTOTAL,NPRDEF,NT,
     1NELEM,NFREE,NNELM,NODTOT,NUNKV1,NKNVA1
      COMMON/C2/ N,IEL,NLG,NREC,NTREC
      COMMON/GV/ RM,GR,PI
      COMMON/COM/ ANGLE,THIK
C
C        ROUTINE TO CALCULATE COORDINATES OF AN ELEMENT LYING IN
C        THE BEND
C
      NB=N-NELEM1
      DO 2 I=1,NRING2
      IF(NB.LE.(I*NEPR)) GO TO 3
      GO TO 2
    3 NI=(I-1)*NEPR
      NR=I
      GO TO 4
    2 CONTINUE
    4 CONTINUE
      DO 1 I=1,NE
    1 CO(I)=X(I)+FLOAT(NB-NI-1)*X(NNS)
      CO(17)=X(17)+FLOAT(NB-NI-1)*X(NNS)
      DO 651 I=1,NNELM
      STE(I)=SIN(CO(I)*PI/180.0)
      CTE(I)=COS(CO(I)*PI/180.0)
      ZM(I)=RM*STE(I)
      CD(I)=RM*CTE(I)
  651 CONTINUE
      DO 654 I=1,NNELM
  654 CD(I)=GR-CD(I)
      PINC=ANGLE/FLOAT(NRING2*(NNS-1))
      DO 104 I=1,NNS
  104 PH(I)=FLOAT(I-1)*PINC
      PH(6)=PH(3)
      DO 105 I=1,NNS
      I1=IS(4,I)
  105 PHN(I1)=(PH(I)+(NR-1)*PH(NNS))*PI/180.0
      PHN(17)=(PH(6)+(NR-1)*PH(NNS))*PI/180.0
      DO 106 I=1,NNS
      I1=IS(1,I)
  106 PHN(I1)=PHN(1)
      DO 107 I=2,NNS
      I1=IS(2,I)
      I2=IS(4,I)
  107 PHN(I1)=PHN(I2)
      I2=IS(4,NNS)
      DO 108 I=1,NNS
      I1=IS(3,I)
  108 PHN(I1)=PHN(I2)
```

```
      DO 120 I=1,NNELM
      SPH=SIN(PHN(I))
      CPH=COS(PHN(I))
      XM(I)=CD(I)*SPH
      YM(I)=CD(I)*CPH
  120  CONTINUE
      RETURN
      END
```

```
      SUBROUTINE COCYL1
      COMMON/GV/ RM,GR,PI
      COMMON/C2/ N,IEL,NLG,NREC,NTREC
      COMMON/C1/ NUNKVA,NKNVA,NOSTR,NCELNO,NCELN1,NTOTAL,NPRDEF,NT,
     1NELEM,NFREE,NNELM,NODTOT,NUNKV1,NKNVA1
      COMMON/NO/NRING1,NRING2,NRING3,NELEM1,NELEM2,NELEM3,NEPR,NRING
      COMMON/COD/ CO(17),CD(17),STE(17),CTE(17),PH(6),PHN(17)
      COMMON/STRS/ V1(17),V2(17),V3(2),IS(4,5),NE,NNS,NCM,NE2
      COMMON/D1/ X(17)
      COMMON/TRANS/D(17),Q(17),XM(17),YM(17),ZM(17),T(17),V1X(17),
     1V1Y(17),V1Z(17),V2X(17),V2Y(17),V2Z(17),V3X(17),V3Y(17),V3Z(17),
     2TRIN(17,3,3),P(17)
      COMMON/COC/ CLEN
C
C        ROUTINE TO CALCULATE COORDINATES OF AN ELEMENT LYING IN
C        THE TANGENT PIPE
C
      DO 2 I=1,NRING1
      IF(N.LE.I*NEPR) GO TO 3
      GO TO 2
    3 NI=(I-1)*NEPR
      NR=I
      GO TO 4
    2 CONTINUE
    4 CONTINUE
      DO 1 I=1,NE
    1 CO(I)=X(I)+FLOAT(N-NI-1)*X(NNS)
      CO(17)=X(17)+FLOAT(N-NI-1)*X(NNS)
      DO 21 I=1,NNELM
      ZM(I)=RM*SIN(CO(I)*PI/180.0)
      YM(I)=(-RM)*COS(CO(I)*PI/180.0)+GR
   21 CONTINUE
      PINC=CLEN/FLOAT(NRING1*(NNS-1))
      DO 104 I=1,NNS
  104 PH(I)=FLOAT(I-1)*PINC
      PH(6)=PH(3)
      DO 105 I=1,NNS
      I1=IS(4,I)
  105 XM(I1)=PH(I)+(NR-1)*PH(NNS)
      XM(17)=PH(6)+(NR-1)*PH(NNS)
      DO 106 I=1,NNS
      I1=IS(1,I)
  106 XM(I1)=XM(1)
      DO 107 I=2,NNS
      I1=IS(2,I)
      I2=IS(4,I)
  107 XM(I1)=XM(I2)
      I2=IS(4,NNS)
      DO 108 I=1,NNS
      I1=IS(3,I)
  108 XM(I1)=XM(I2)
      DO 101 I=1,NNELM
  101 XM(I)=-CLEN+XM(I)
      RETURN
      END
```

```
      SUBROUTINE PRDF
      COMMON/TRANS/D(17),Q(17),XM(17),YM(17),ZM(17),T(17),V1X(17),
     1V1Y(17),V1Z(17),V2X(17),V2Y(17),V2Z(17),V3X(17),V3Y(17),V3Z(17),
     2TRIN(17,3,3),P(17)
      COMMON/D1/ X(17)
      COMMON/S1/ PREDEF(1,500)
      COMMON/COD/ CO(17),CD(17),STE(17),CTE(17),PH(6),PHN(17)
      COMMON/STRS/ V1(17),V2(17),V3(2),IS(4,5),NE,NNS,NCM,NE2
      COMMON/C1/ NUNKVA,NKNVA,NOSTR,NCELNO,NCELN1,NTOTAL,NPRDEF,NT,
     1NELEM,NFREE,NNELM,NODTOT,NUNKV1,NKNVA1
      COMMON/NO/NRING1,NRING2,NRING3,NELEM1,NELEM2,NELEM3,NEPR,NRING
      COMMON/GV/ RM,GR,PI
      COMMON/COM/ ANGLE,THIK
      NEPR=2*NEPR
      PI=3.14159
      DO 401 I=1,NNELM
      T(I)=THIK
401   CONTINUE
      AINC=360.0/FLOAT(NEPR*(NNS-1))
      DO 100 I=1,NNS
100   X(I)=FLOAT(I-1)*AINC
      I2=IS(1,NNS)
      DO 101 I=2,NNS
      I1=IS(2,I)
101   X(I1)=X(I2)
      DO 102 I=1,NNS
      I1=IS(3,I)
      I2=IS(1,I)
102   X(I1)=X(I2)
      I2=IS(1,1)
      DO 103 I=1,NNS
      I1=IS(4,I)
103   X(I1)=X(I2)
      X(17)=X(3)
      NEPR=NEPR/2
      RETURN
      END
```

```
      SUBROUTINE MOMENT
      COMMON/STRS/ V1(17),V2(17),V3(2),IS(4,5),NE,NNS,NCM,NE2
      COMMON/D1/ X(17)
      DIMENSION CO(5),AM(36),A(5),B(5),F(5),AN(4)
      COMMON/NO/NRING1,NRING2,NRING3,NELEM1,NELEM2,NELEM3,NEPR,NRING
      COMMON/GV/ RM,GR,PI
      COMMON/MOM/ SEO(32,5),SEI(32,5)
      COMMON/TRANS/D(17),Q(17),XM(17),YM(17),ZM(17),T(17),V1X(17),
     1V1Y(17),V1Z(17),V2X(17),V2Y(17),V2Z(17),V3X(17),V3Y(17),V3Z(17),
     2TRIN(17,3,3),P(17)
C
C        ROUTINE TO CALCULATE BACK THE APPLIED MOMENT FROM THE COMPUTED
C        STRESS DISTRIBUTIONS
C
      H=T(1)
      DO 100 N=1,NEPR
      DO 1 I=1,NNS
    1 CO(I)=COS((X(I)+FLOAT(N-1)*X(NNS))*(PI/180.0))
      DO 3 I=1,NNS
      A(I)=0.5*(SEO(N,I)+SEI(N,I))
      B(I)=(SEO(N,I)-SEI(N,I))/H
    3 CONTINUE
      DO 4 I=1,NNS
      F(I)=((A(I)+(2.*B(I)*RM))*(H*H*H/12.)+A(I)*RM*RM*H)*CO(I)
    4 CONTINUE
      VAL=(X(2)/2.)*(PI/180.0)
      NNS1=NNS-1
      DO 10 I=1,NNS1
   10 AN(I)=(F(I)+F(I+1))*VAL
      AM(N)=0.0
      DO 11 I=1,NNS1
   11 AM(N)=AM(N)+AN(I)
  100 CONTINUE
       TOT=0.0
      DO 101 I=1,NEPR
  101 TOT=TOT+AM(I)
      WRITE(6,102)
  102 FORMAT(6X,*APPLIED MOMENT*)
      WRITE(6,110) (AM(N),N=1,NEPR)
  110 FORMAT(8E16.8)
      WRITE(6,111) TOT
  111 FORMAT(6X,* TOTAL MOMENT IS *E16.8)
      RETURN
      END
```

```
      SUBROUTINE VALUE
      COMMON/C1/ NUNKVA,NKNVA,NOSTR,NCELNO,NCELN1,NTOTAL,NPRDEF,NT,
     1NELEM,NFREE,NNELM,NODTOT,NUNKV1,NKNVA1
      COMMON/STRS/ V1(17),V2(17),V3(2),IS(4,5),NE,NNS,NCM,NE2
      V3(1)=1.0
      V3(2)=-1.0
      IF(NNELM.EQ.8) GO TO 1
      IF(NNELM.EQ.12) GO TO 2
      GO TO 3
    1 V1(1)=V1(2)=V1(3)=V2(1)=V2(8)=V2(7)=V3(2)=-1.0
      V1(5)=V1(6)=V1(7)=V2(3)=V2(4)=V2(5)=V3(1)=1.0
      V1(4)=V1(8)=V2(2)=V2(6)=0.0
      IS(1,1)=1
      IS(1,2)=2
      IS(1,3)=3
      IS(2,1)=3
      IS(2,2)=4
      IS(2,3)=5
      IS(3,1)=7
      IS(3,2)=6
      IS(3,3)=5
      IS(4,1)=1
      IS(4,2)=8
      IS(4,3)=7
      GO TO 4
    2 CONTINUE
      V1(1)=V1(2)=V1(3)=V1(4)=V2(1)=V2(12)=V2(11)=V2(10)=-1.0
      V1(5)=V1(12)=V2(2)=V2(9)=-1./3.
      V1(6)=V1(11)=V2(3)=V2(8)=1./3.
      V1(7)=V1(8)=V1(9)=V1(10)=V2(4)=V2(5)=V2(6)=V2(7)=1.0
      IS(1,1)=1
      IS(1,2)=2
      IS(1,3)=3
      IS(1,4)=4
      IS(2,1)=4
      IS(2,2)=5
      IS(2,3)=6
      IS(2,4)=7
      IS(3,1)=10
      IS(3,2)=9
      IS(3,3)=8
      IS(3,4)=7
      IS(4,1)=1
      IS(4,2)=12
      IS(4,3)=11
      IS(4,4)=10
      GO TO 4
    3 CONTINUE
      V1(1)=V1(2)=V1(3)=V1(4)=V1(5)=V2(1)=V2(16)=V2(15)=V2(14)=V2(13)=-1
     1.0
      V1(9)=V1(10)=V1(11)=V1(12)=V1(13)=V2(5)=V2(6)=V2(7)=V2(8)=V2(9)=1
     1.0
      V1(6)=V1(16)=V2(2)=V2(12)=-0.5
      V1(8)=V1(14)=V2(4)=V2(10)=0.5
      V1(7)=V1(15)=V2(3)=V2(11)=V1(17)=V2(17)=0.0
      IS(1,1)=1
```

```
      IS(1,2)=2
      IS(1,3)=3
      IS(1,4)=4
      IS(1,5)=5
      IS(2,1)=5
      IS(2,2)=6
      IS(2,3)=7
      IS(2,4)=8
      IS(2,5)=9
      IS(3,1)=13
      IS(3,2)=12
      IS(3,3)=11
      IS(3,4)=10
      IS(3,5)=9
      IS(4,1)=1
      IS(4,2)=16
      IS(4,3)=15
      IS(4,4)=14
      IS(4,5)=13
    4 CONTINUE
      IF(NNELM.EQ.17) GO TO 20
      GO TO 21
   20 NE=NNELM-1
      GO TO 22
   21 NE=NNELM
   22 NNS=(NE/4)+1
      NCM=9*NNELM
      NE2=2*NE
      RETURN
      END
```

```
      SUBROUTINE BUFFER
      COMMON/BR/ BUF(10,271),IBUF(10,4)
      COMMON/BUFR/ RHS,NIC,LP1,LP2,NPOSN
      COMMON/C1/ NUNKVA,NKNVA,NOSTR,NCELNO,NCELN1,NTOTAL,NPRDEF,NT,
     1NELEM,NFREE,NNELM,NODTOT,NUNKV1,NKNVA1
      COMMON/S3/ COMP(305)
      COMMON/C2/ N,IEL,NLG,NREC,NTREC
C
C        ROUTINE IN WHICH THE ROW CORROSPONDING TO THE COMPLETED
C        VARIABLE IS STORED IN A BUFFER AREA
C
      NLG=NLG+1
      DO 1 I=1,NTOTAL
    1 BUF(NLG,I)=COMP(I)
      I=NTOTAL+1
      BUF(NLG,I)=RHS
      IBUF(NLG,1)=LP1
      IBUF(NLG,2)=LP2
      IBUF(NLG,3)=NIC
      IBUF(NLG,4)=NPOSN
      IF(NLG.EQ.10) GO TO 10
      GO TO 20
   10 WRITE(1)
     1NLG,((BUF(I,J),I=1,NLG),J=1,NTREC),((IBUF(I,J),I=1,NLG),J=1,4)
      NREC=NREC+1
      NLG=0
   20 CONTINUE
      RETURN
      END
```

```
      SUBROUTINE LOAD
      COMMON/RAD2/ CRHS(1,85)
      COMMON/LOD/FX(17),FY(17),FZ(17),ALMOM(17),BEMOM(17)
      COMMON/SHP/G,H,QXM,QYM,QZM,PXM,PYM,PZM,QXTB,QYTB,QZTB,PXTB,PYTB,
     1PZTB,DXTB,DYTB,DZTB,DT
      COMMON/GV/ RM,GR,PI
      COMMON/S8/ XG(4),CG(4),XGZ(2),CGZ(2),DI(5,5)
      COMMON/C1/ NUNKVA,NKNVA,NOSTR,NCELNO,NCELN1,NTOTAL,NPRDEF,NT,
     1NELEM,NFREE,NNELM,NODTOT,NUNKV1,NKNVA1
      COMMON/S6/ ELNODE(110,87),RHSRED(1,85)
      COMMON/TRANS/D(17),Q(17),XM(17),YM(17),ZM(17),T(17),V1X(17),
     1V1Y(17),V1Z(17),V2X(17),V2Y(17),V2Z(17),V3X(17),V3Y(17),V3Z(17),
     2TRIN(17,3,3),P(17)
      DIMENSION AREA(6),DAREA(3,1),SHAP(3,85),FO(85)
C
C        ROUTINE TO GENERATE CONSISTENT NODAL LOADS CORROSPONDING TO
C        AN IN-PLANE MOMENT
C
      AM=0.003430866*2.
      SI=T(1)*PI*(RM**3)
      DO 3 I=1,17
      FX(I)=0.0
      FY(I)=0.0
      FZ(I)=0.0
      ALMOM(I)=0.0
      BEMOM(I)=0.0
    3 CONTINUE
      DO 30 I=1,85
   30 FO(I)=0.0
      G=-1.0
      DO 500 IG=1,4
      DO 500 KG=1,2
      H=-XG(IG)
      F=XGZ(KG)
      CALL SHAP17
      AREA(1)=PXM+F*0.5*PXTB
      AREA(2)=PYM+F*0.5*PYTB
      AREA(3)=PZM+F*0.5*PZTB
      AREA(4)=0.5*DXTB
      AREA(5)=0.5*DYTB
      AREA(6)=0.5*DZTB
      DAREA(1,1)=AREA(2)*AREA(6)-AREA(3)*AREA(5)
      DAREA(2,1)=AREA(3)*AREA(4)-AREA(1)*AREA(6)
      DAREA(3,1)=AREA(1)*AREA(5)-AREA(2)*AREA(4)
      DO 10 I=1,17
      J=5*(I-1)+1
      J1=J+1
      J2=J+2
      J3=J+3
      J4=J+4
      SHAP(1,J)=D(I)
      SHAP(1,J1)=0.0
      SHAP(1,J2)=0.0
      SHAP(1,J3)=D(I)*F*0.5*T(I)*V1X(I)
   10 SHAP(1,J4)=D(I)*F*0.5*T(I)*V2X(I)
      DO 11 I=1,17
```

```
      J=5*(I-1)+2
      J1=J-1
      J2=J+1
      J3=J+2
      J4=J+3
      SHAP(2,J1)=0.0
      SHAP(2,J)=D(I)
      SHAP(2,J2)=0.0
      SHAP(2,J3)=D(I)*F*0.5*T(I)*V1Y(I)
   11 SHAP(2,J4)=D(I)*F*0.5*T(I)*V2Y(I)
      DO 12 I=1,17
      J=5*(I-1)+3
      J1=J-2
      J2=J-1
      J3=J+1
      J4=J+2
      SHAP(3,J1)=0.0
      SHAP(3,J2)=0.0
      SHAP(3,J)=D(I)
      SHAP(3,J3)=D(I)*F*0.5*T(I)*V1Z(I)
   12 SHAP(3,J4)=D(I)*F*0.5*T(I)*V2Z(I)
      DYM=0.0
      DO 100 I=1,17
  100 DYM=DYM+D(I)*YM(I)
      SIGM=(AM/SI)*(GR-DYM-0.5*F*DYTB)
      DO 15 I=1,85
      DO 15 K=1,3
   15 FO(I)=FO(I)+SHAP(K,I)*DAREA(K,1)*CG(IG)*CGZ(KG)*SIGM
  500 CONTINUE
      DO 16 I=1,85,5
      J=((I-1)/5)+1
   16 FX(J)=FO(I)
      DO 17 I=2,85,5
      J=((I-2)/5)+1
   17 FY(J)=FO(I)
      DO 18 I=3,85,5
      J=((I-3)/5)+1
   18 FZ(J)=FO(I)
      DO 19 I=4,85,5
      J=((I-4)/5)+1
   19 ALMOM(J)=FO(I)
      DO 20 I=5,85,5
      J=((I-5)/5)+1
   20 BEMOM(J)=FO(I)
C
C        GLOBAL COMPONENTS OF THE CALCULATED LOADS ARE TRANSFORMED INTO
C        LOCAL DIRECTIONS
C
      I=0
      N1=1
  491 I=I+1
      CRHS(1,I)=FX(N1)
      I=I+1
      CRHS(1,I)=FY(N1)
      I=I+1
      CRHS(1,I)=FZ(N1)
      I=I+1
      CRHS(1,I)=ALMOM(N1)
      I=I+1
```

```
      CRHS(1,I)=BEMOM(N1)
      N1=N1+1
      IF(N1.EQ.18) GO TO 492
      GO TO 491
  492 CONTINUE
      DO 496 I=1,17
      I1=5*I-4
      I2=5*I-3
      I3=5*I-2
      I4=5*I-1
      I5=5*I
      RHSRED(1,I1)=TRIN(I,1,1)*CRHS(1,I1)+TRIN(I,1,2)*CRHS(1,I2)+
     1TRIN(I,1,3)*CRHS(1,I3)
      RHSRED(1,I2)=TRIN(I,2,1)*CRHS(1,I1)+TRIN(I,2,2)*CRHS(1,I2)+
     1TRIN(I,2,3)*CRHS(1,I3)
      RHSRED(1,I3)=TRIN(I,3,1)*CRHS(1,I1)+TRIN(I,3,2)*CRHS(1,I2)+
     1TRIN(I,3,3)*CRHS(1,I3)
      RHSRED(1,I4)=CRHS(1,I4)
      RHSRED(1,I5)=CRHS(1,I5)
  496 CONTINUE
      RETURN
      END
```

```
C*************************************************************************
C          SPECIMEN DATA FOR A 90 DEG- BEND WITH ENDS TERMINATED BY
C          TANGENTS
C*************************************************************************
     1    48
  .8611363  .3478549
  .3399810  .6521452
 -.3399810  .6521452
 -.8611363  .3478549
  .5773503  1.0
 -.5773503  1.0
   90 DEG BEND WITH ENDS TERMINATED BY TANGENTS
    17     4     4     4     4
   90.0     4.5          1.745       0.125       12.0
```

APPENDIX E

## Shape Functions For A Ring Element

Referring to Figure 4.16, the element has 10 nodes. The shape functions are given as

$$N_i \ (i = 1,5) = NS_j \ (j = 1,5) \ \left(\frac{1-\xi}{2}\right)$$
$$N_i \ (i = 6,10) = NS_j \ (j = 1,6) \ \left(\frac{1+\xi}{2}\right) \qquad \text{(E.1)}$$

where

$$NS_1 = \left(\cos\frac{2\pi}{5} - \cos\pi\eta\right)\left(\cos\frac{\pi}{5} + \cos\pi\eta\right) / \left(\cos\frac{2\pi}{5} - 1\right)\left(\cos\frac{\pi}{5} + 1\right)$$

$$NS_2 = \left\{(1-\cos\pi\eta)\left(\cos\frac{\pi}{5} + \cos\pi\eta\right) / 2\left(1-\cos\frac{2\pi}{5}\right)\left(\cos\frac{\pi}{5} + \cos\frac{2\pi}{5}\right)\right\} +$$
$$\left\{\sin\pi\eta\left(\cos\frac{\pi}{5} + \cos\pi\eta\right) / 2\sin\frac{2\pi}{5}\left(\cos\frac{\pi}{5} + \cos\frac{2\pi}{5}\right)\right\}$$

$$NS_3 = \left\{(1-\cos\pi\eta)\left(\cos\frac{2\pi}{5} - \cos\pi\eta\right) / 2\left(1+\cos\frac{\pi}{5}\right)\left(\cos\frac{2\pi}{5} + \cos\frac{\pi}{5}\right)\right\} +$$
$$\left\{\sin\pi\eta\left(\cos\frac{2\pi}{5} - \cos\pi\eta\right) / 2\sin\frac{\pi}{5}\left(\cos\frac{2\pi}{5} + \cos\frac{\pi}{5}\right)\right\} \qquad \text{(E.2)}$$

$$NS_4 = \left\{(1-\cos\pi\eta)\left(\cos\frac{2\pi}{5} - \cos\pi\eta\right) / 2\left(1+\cos\frac{\pi}{5}\right)\left(\cos\frac{2\pi}{5} + \cos\frac{\pi}{5}\right)\right\} -$$
$$\left\{\sin\pi\eta\left(\cos\frac{2\pi}{5} - \cos\pi\eta\right) / 2\sin\frac{\pi}{5}\left(\cos\frac{2\pi}{5} + \cos\frac{\pi}{5}\right)\right\}$$

$$NS_5 = \left\{(1-\cos\pi\eta)\left(\cos\frac{\pi}{5} + \cos\pi\eta\right) / 2\left(1-\cos\frac{2\pi}{5}\right)\left(\cos\frac{\pi}{5} + \cos\frac{2\pi}{5}\right)\right\} -$$
$$\left\{\sin\pi\eta\left(\cos\frac{\pi}{5} + \cos\pi\eta\right) / 2\sin\frac{2\pi}{5}\left(\cos\frac{\pi}{5} + \cos\frac{2\pi}{5}\right)\right\}$$

Shape Functions For Half Ring Element

Referring to Figure 4.17

$$N_{i\ (i=1,5)} = {}^{1}/16\ (1-\xi)(9\xi^2-1)\ NS_j\ (j=1,5)$$

$$N_{i\ (i=6,10)} = {}^{9}/16\ (1-\xi^2)(1-3\xi)\ NS_j\ (j=1,5)$$

$$N_{i\ (i=11,15)} = {}^{9}/16\ (1-\xi^2)(1+3\xi)\ NS_j\ (j=1,5) \qquad \text{(E.3)}$$

$$N_{i\ (i=16,20)} = {}^{1}/16\ (1+\xi)(9\xi^2-1)\ NS_j\ (j=1,5)$$

where

$$NS_1 = \{(\cos\pi + \cos\pi\eta)(\cos\tfrac{\pi}{2} + \cos\pi\eta) / 2(\cos\pi + \cos\pi)(\cos\tfrac{\pi}{2} + \cos\pi)\}$$
$$-\{\sin\tfrac{\pi}{2}\eta(\cos\tfrac{\pi}{2} + \cos\pi\eta) / 2\sin\tfrac{\pi}{2}(\cos\tfrac{\pi}{2} + \cos\pi)\}$$

$$NS_2 = \{(\cos\pi + \cos\pi\eta)(1+\cos\pi\eta) / 2(\cos\pi + \cos\tfrac{\pi}{2})(1+\cos\tfrac{\pi}{2})\}$$
$$-\{\sin\tfrac{\pi}{2}\eta(1+\cos\pi\eta) / 2\sin\tfrac{\pi}{4}(1+\cos\tfrac{\pi}{2})\}$$

$$NS_3 = (\cos\tfrac{\pi}{2} + \cos\pi\eta)(1+\cos\pi\eta) / (\cos\tfrac{\pi}{2} + 1)(2) \qquad \text{(E.4)}$$

$$NS_4 = \{(\cos\pi + \cos\pi\eta)(1+\cos\pi\eta) / 2(\cos\pi + \cos\tfrac{\pi}{2})(1 + \cos\tfrac{\pi}{2})\}$$
$$+ \{\sin\tfrac{\pi}{2}\eta(1+\cos\pi\eta) / 2\sin\tfrac{\pi}{4}(1+\cos\tfrac{\pi}{2})\}$$

$$NS_5 = \{(\cos\pi + \cos\pi\eta)(\cos\tfrac{\pi}{2} + \cos\pi\eta) / 2(\cos\pi + \cos\pi)(\cos\tfrac{\pi}{2} + \cos\pi)\}$$
$$+ \{\sin\tfrac{\pi}{2}\eta(\cos\tfrac{\pi}{2} + \cos\pi\eta) / 2\sin\tfrac{\pi}{2}(\cos\tfrac{\pi}{2} + \cos\pi)\}$$

# APPENDIX F

## Moment Calculation

If at any cross-section of the pipe, the nodal longitudinal stresses on the outside and inside surfaces are known, the applied moment can be calculated.

Let $M_e$ be the moment contribution by an element on the cross-section, to the total moment M. Referring to Figure 4.22

$$M_e = \int_{\theta_1}^{\theta_2} \int_{-\frac{t}{2}}^{\frac{t}{2}} [(b+\zeta) \cos \theta] \, \sigma_\psi [b+\zeta] \, d\theta \, d\zeta \qquad (F.1)$$

where $\sigma_\psi$ is the longitudinal stress at $r = b+\zeta$. Since this stress varies linearly with thickness

$$\sigma_\psi = \frac{N_\psi}{t} + \zeta \frac{M_\psi}{I} \qquad (F.2)$$

where

$N_\psi$ is the force per unit wall length

$M_\psi$ is the moment per unit wall length

I is the second moment of area of the wall cross-section (per unit length)

$$= \frac{2}{3} \left(\frac{t}{2}\right)^3$$

Integrating over the thickness

$$M_e = \int_{\theta_1}^{\theta_2} \left\{ \left[ \frac{SA + 2.MA.b}{3} \right] \frac{t^3}{4} + SA(b)^2 \, t \right\} \cos\theta \, d\theta$$

$$= \int_{\theta_1}^{\theta_2} F(\theta) \, d\theta \qquad (F.3)$$

where $$SA = \frac{1}{2}\left[\sigma_\psi\Big|_{\text{outside}} + \sigma_\psi\Big|_{\text{inside}}\right]$$

$$MA = \frac{1}{t}\left[\sigma_\psi\Big|_{\text{outside}} - \sigma_\psi\Big|_{\text{inside}}\right]$$

The integration over the angle $\theta$ is done using Simpson's rule, to obtain $M_e$. These calculations are repeated for all the elements lying on the cross-section, and added to get the total applied moment M. The subroutine MOMENT in Appendix D computes this applied moment.

APPENDIX G

## Calculation of Flexibility

From the computed deflections of centre line of the pipe system and with the assumption that this deflected shape obeys the simple theory of bending, the average flexibility of tangent pipes and bend are calculated.

In Figure 6.2, the original and the computed final shapes of centre line of the pipe system are shown. Knowing the slope and deflections of the centre line at the restrained end (Point 1) and the computed deflections at junction 2 (junction of curved pipe with the tangent pipe), the assumed deflected shape of the tangent is obtained by passing a circle through these two points. Knowing the radius of curvature of the circle $R_c$, the flexibility of the tangent pipe is calculated using

$$K_c = \ell EI/M.\ell.R_c \qquad (F.1)$$

where $\ell$ is the length of the tangent pipe and the other symbols have their usual meaning. The assumed deflected shape of the centre line of the curved pipe, which is again a segment of a circle, is obtained with the condition of slope and displacement continuity at junction 2 and the computed deflections at junction 3. If $R_B$ is the radius of curvature of the deflected shape of the bend its flexibility is calculated using

$$\frac{d\psi}{\psi} = K.Ma/EI$$

(or)
$$K_B = (EI/Ma)(a-R_B)/R_B \qquad (F.2)$$

Thus knowing the calculated slope of the centre line at point 3, and computed deflections at 4, another circle can be passed through these points and the flexibility of this tangent pipe calculated as before.

Table 3.1

Central And Peripheral Processor Time

| Type of Element | Number of Elements | Central Processor Time | | Peripheral Processor Time | |
|---|---|---|---|---|---|
| | | Stored Immediately | Block Storage | Stored Immediately | Block Storage |
| Quartic shell element | 8 | 227 secs | 200 secs | 269 secs | 80 secs |

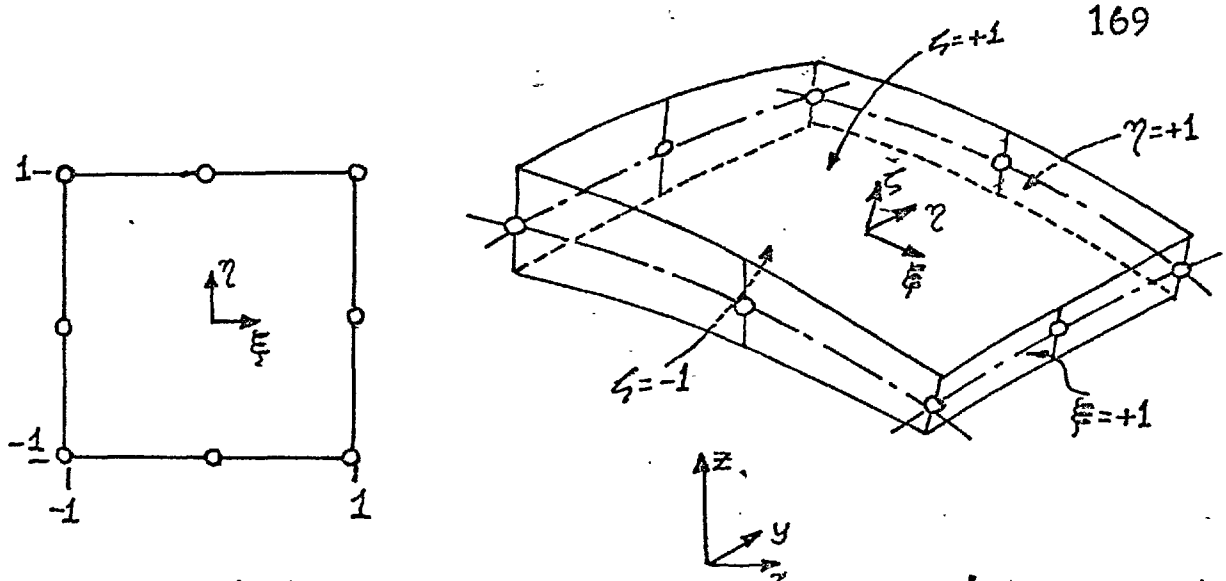
Table 3.2

Central Processor Time

| Number of elements per ring | Number of rings | Stiffness matrix calculated for all elements | Stiffness for elements in I ring only calculated |
|---|---|---|---|
| 8 | 8 | 676 secs | 569 secs |

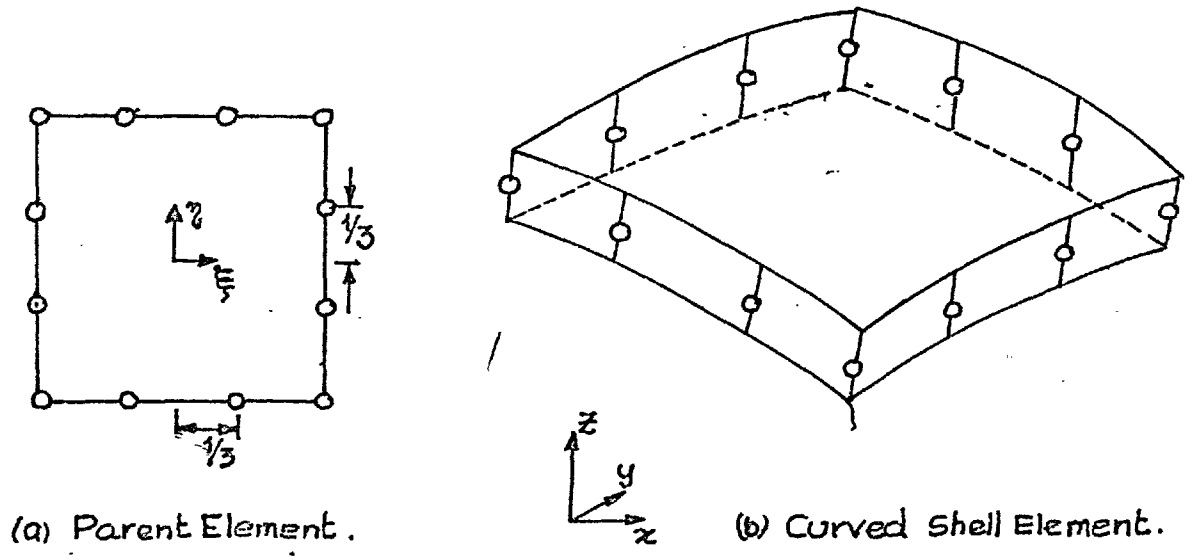
Table 6.1

| Bend radius a | Pipe bore radius b | Pipe wall thickness t | Pipe factor $\lambda = at/b^2$ | $\frac{1}{\gamma} = a/b$ |
|---|---|---|---|---|
| 10.0 | 5.0 | 0.125 | 0.05 | 2.0 |
| 18.0 | 6.0999 | 0.1875 | 0.0924 | 2.95 |
| 10.0 | 5.0 | 0.25 | 0.1 | 2.0 |
| 10.5 | 5.662 | 0.444 | 0.1458 | 1.86 |
| 10.0 | 5.0 | 0.5 | 0.2 | 2.0 |
| 10.0 | 5.0 | 0.75 | 0.3 | 2.0 |
| 19.0 | 3.1875 | 0.25 | 0.468 | 5.961 |



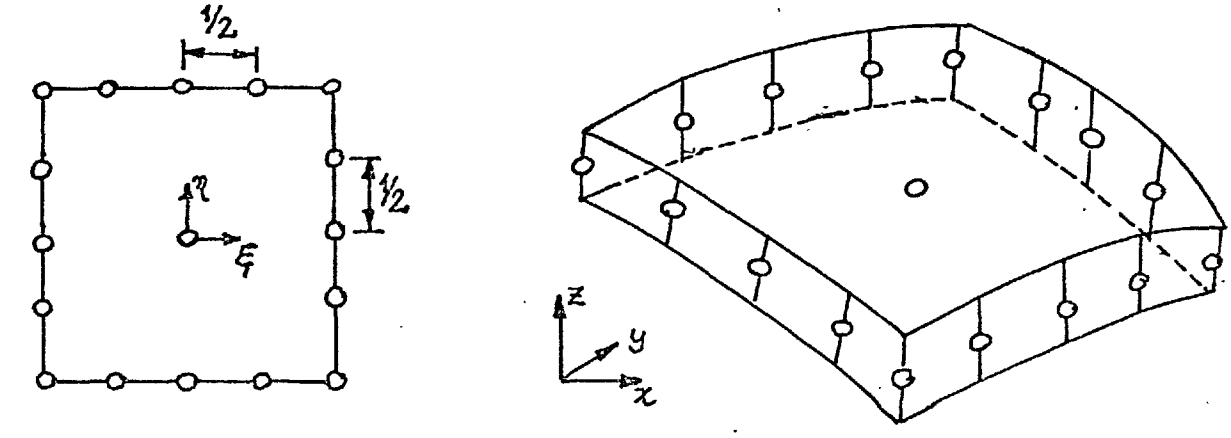

(a) Parent Element (b) Curved Shell Element.

FIG.2.1. QUADRATIC ELEMENT




(a) Parent Element. (b) Curved Shell Element.

FIG. 2.2. CUBIC ELEMENT




(a) Parent Element (b) Curved Shell Element

FIG.2.3. QUARTIC ELEMENT

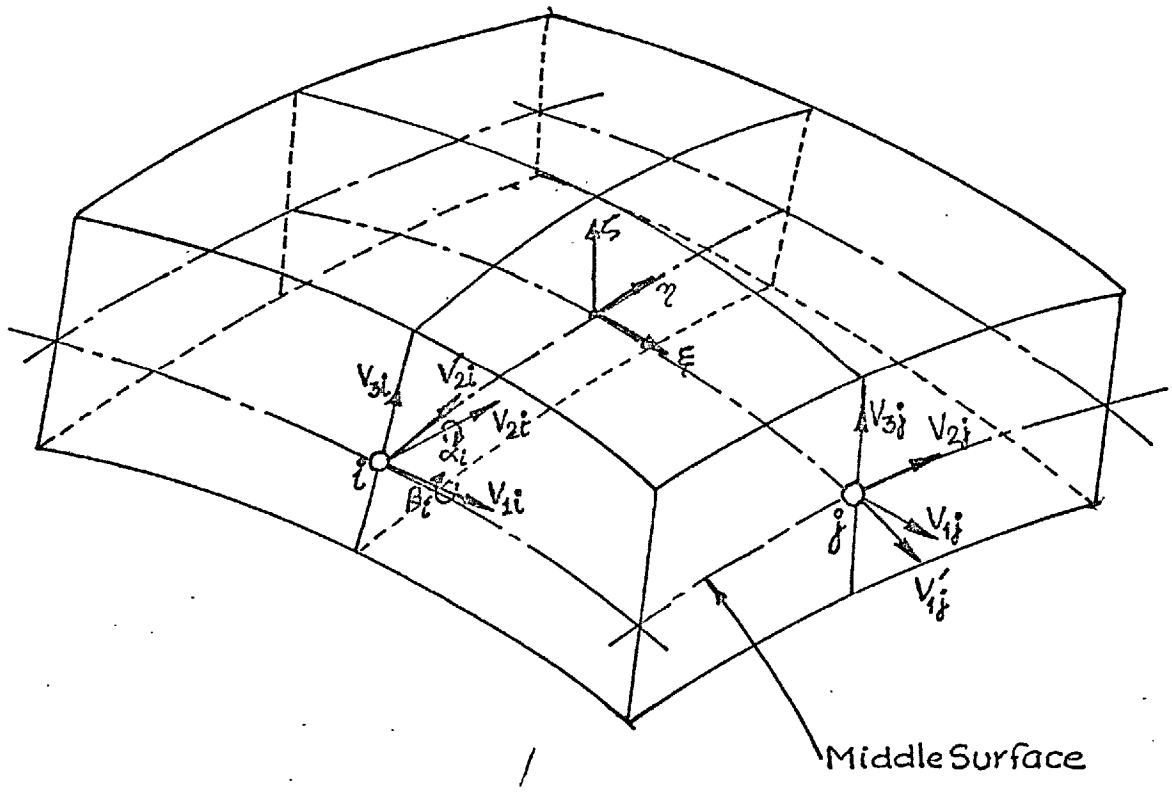
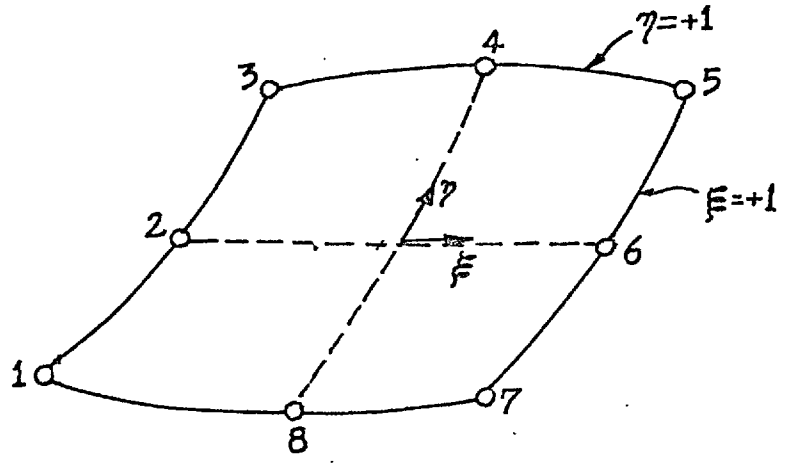
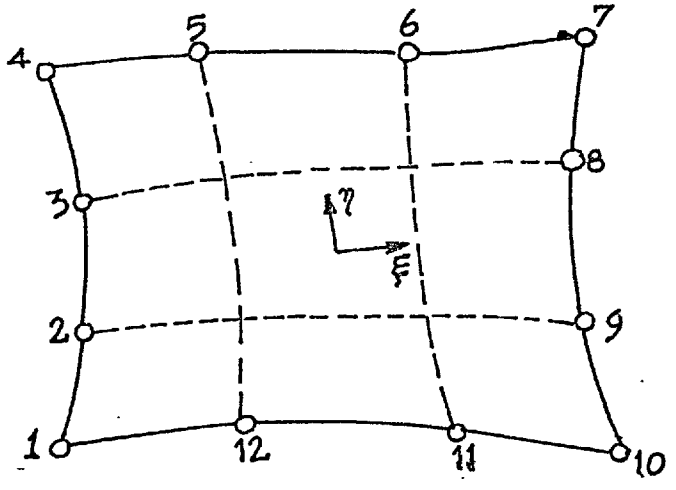


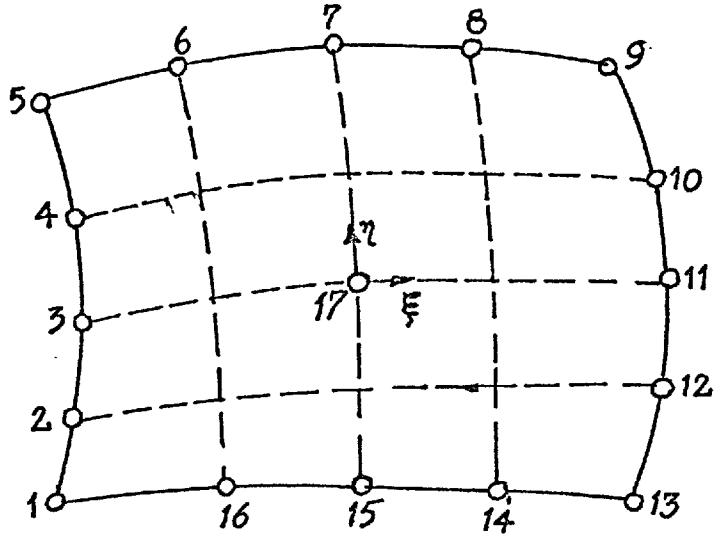

FIG-2.4. UNIQUE ORTHOGONAL VECTORS AT ANY NODE




(a)

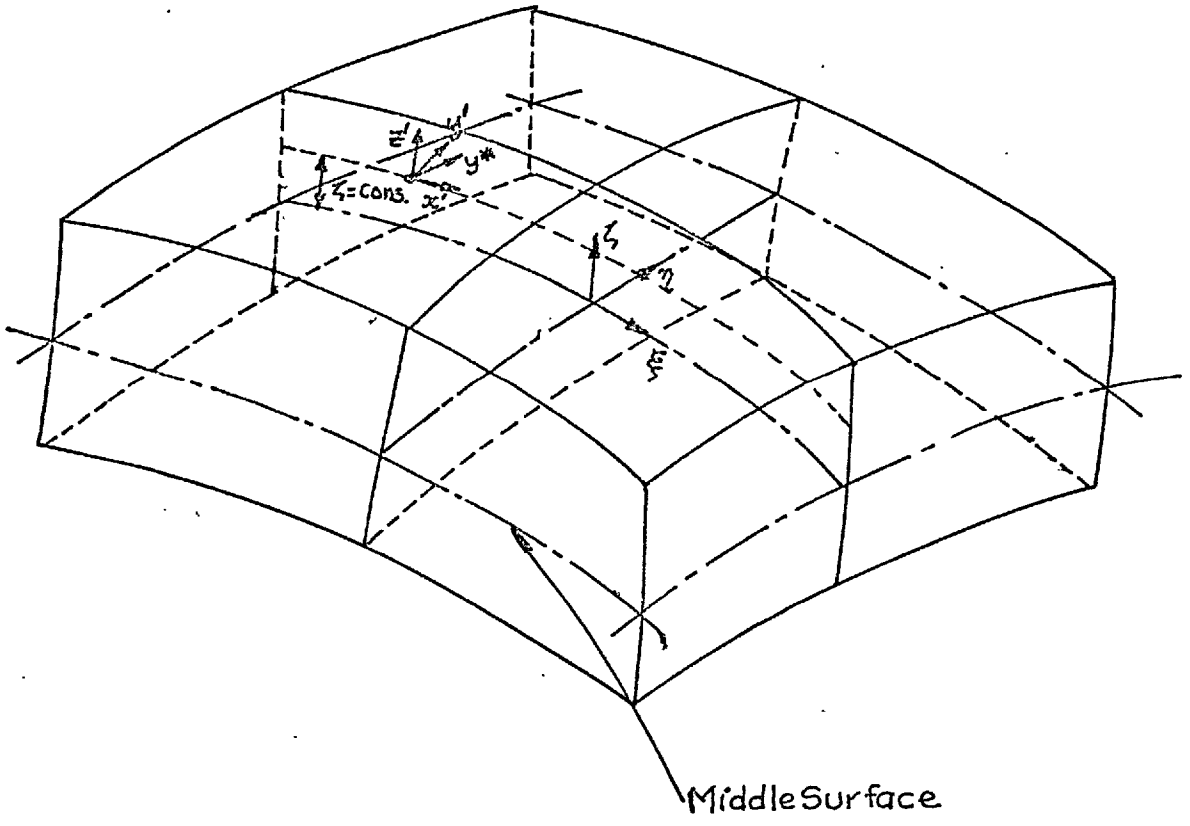



(b)




(c)

FIG.2.5. TWO DIMENSIONAL CURVED SPACES




FIG·2·6· LOCAL ORTHOGONAL AXES

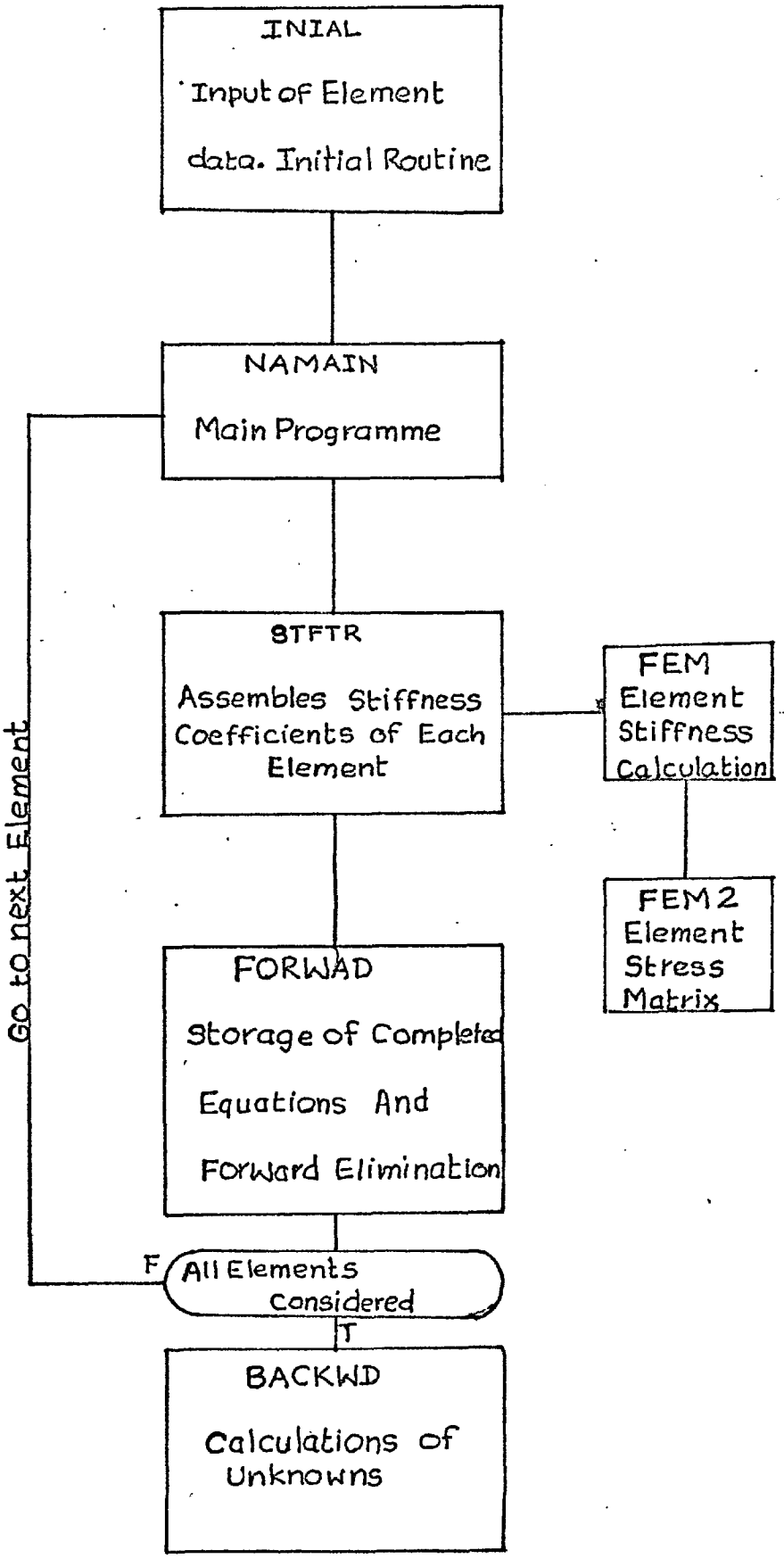



FIG-3-1. BLOCK DIAGRAM

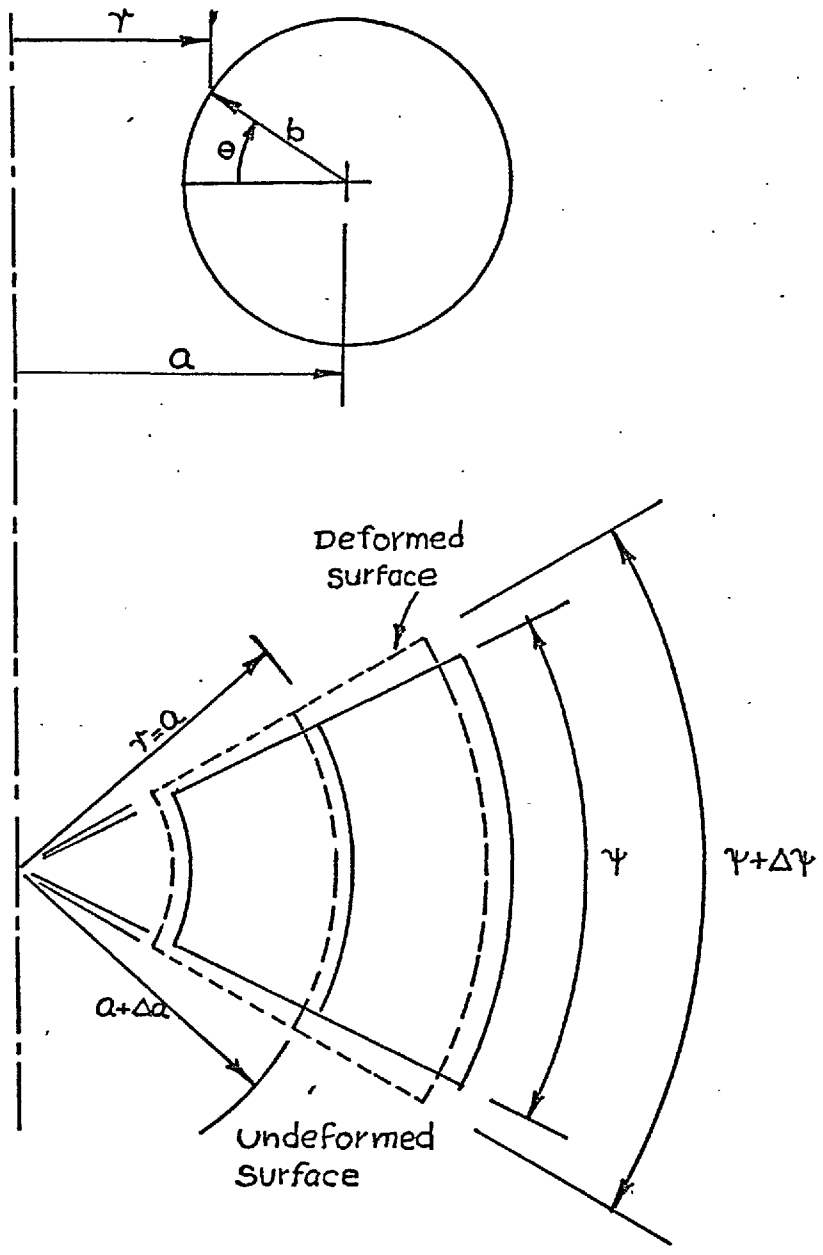
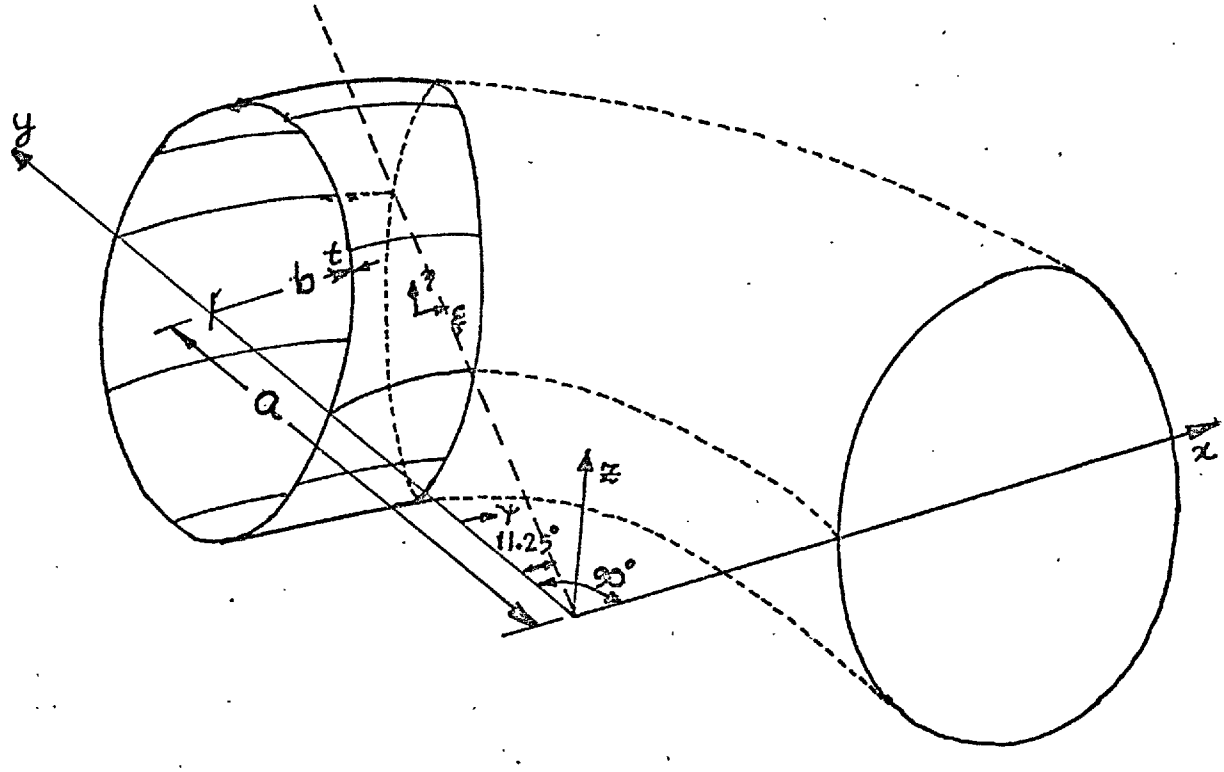



FIG. 4.1.




a = 10.5 inches
b = 5.662 inches
t = 0.444 inches
λ = 0.1458

FIG. 4-2. SECTOR OF A 90 DEG-BEND ANALYSED FOR IN-PLANE MOMENT

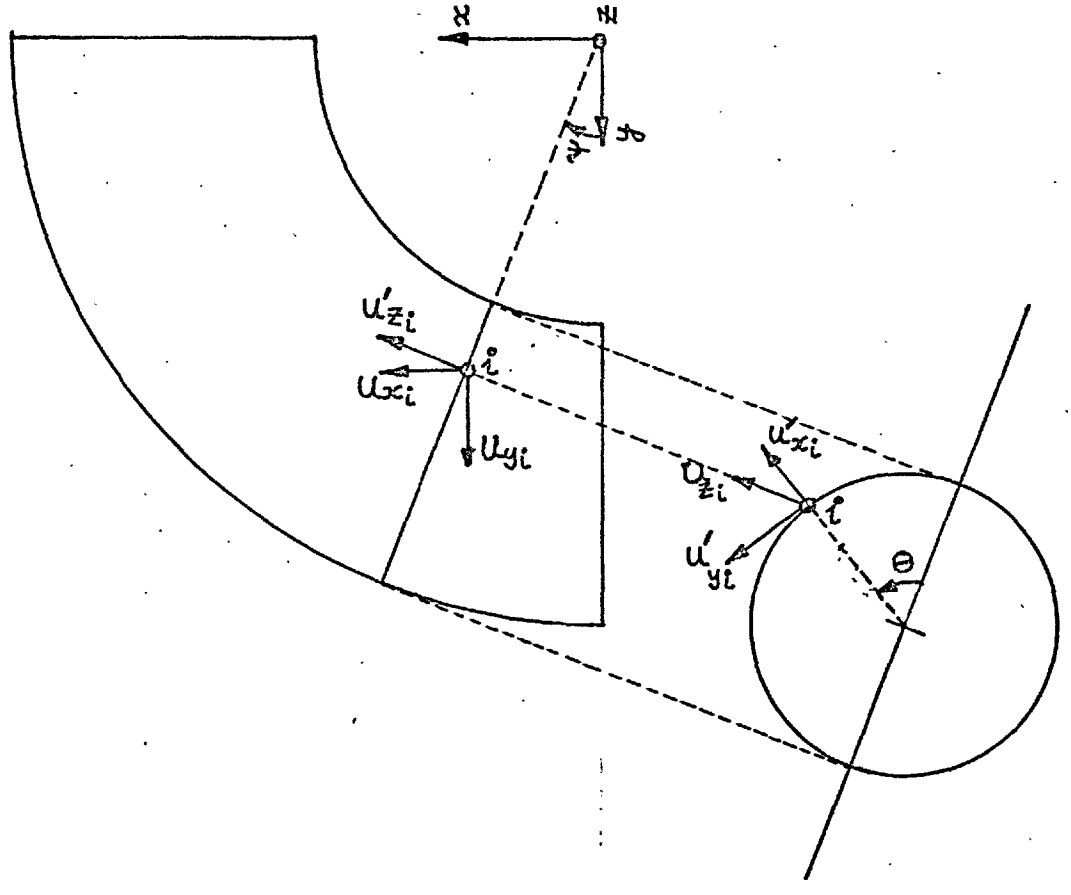



FIG. 4.3. DIRECTIONS OF LOCAL AND GLOBAL DISPLACEMENTS AT ANY POINT IN A PIPE BEND

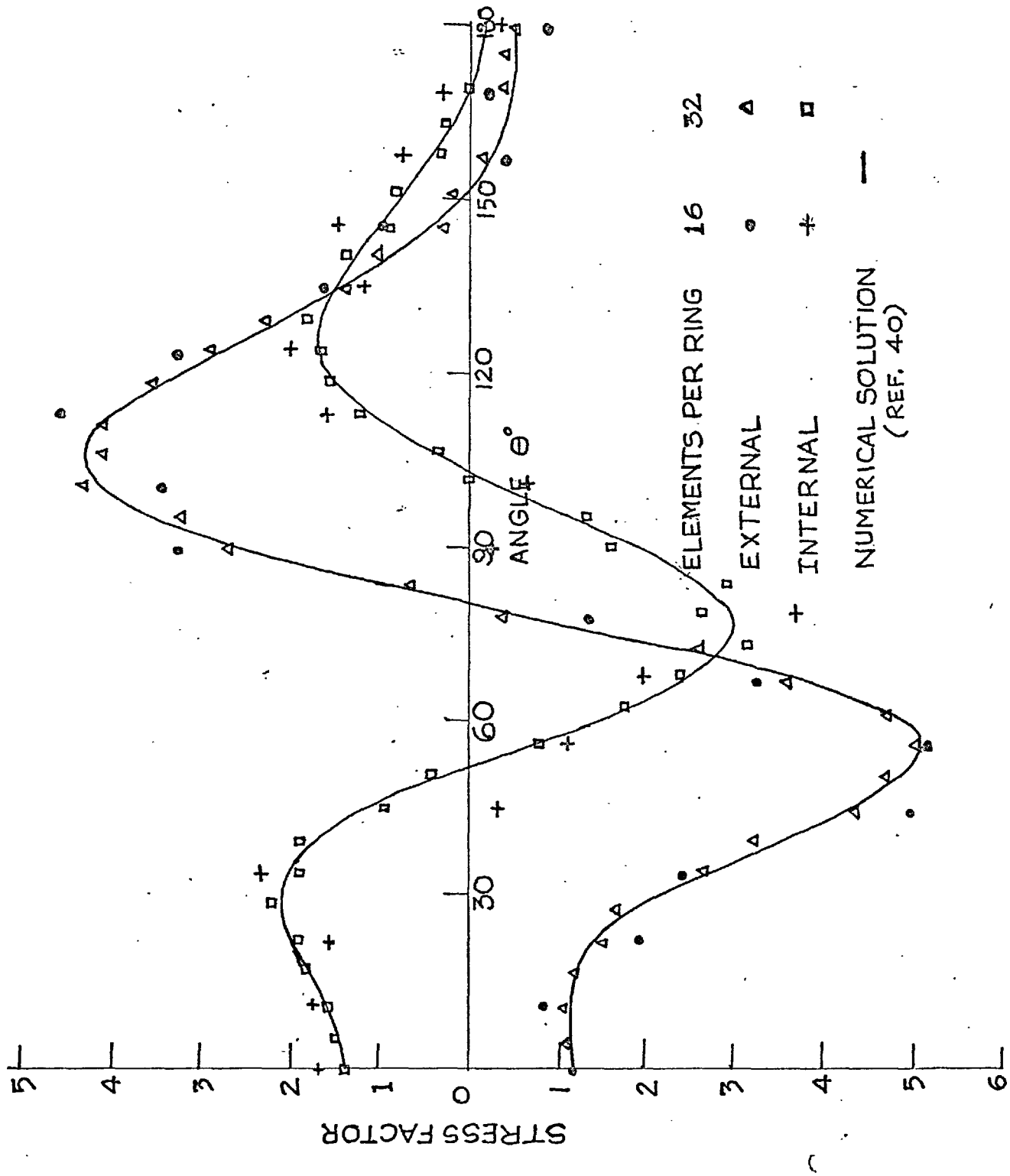



FIG.4.4. LONGITUDINAL STRESS FACTORS

QUADRATIC THREE DIMENSIONAL ELEMENTS

$\lambda = 0.1458$ , $\gamma = 0.538$

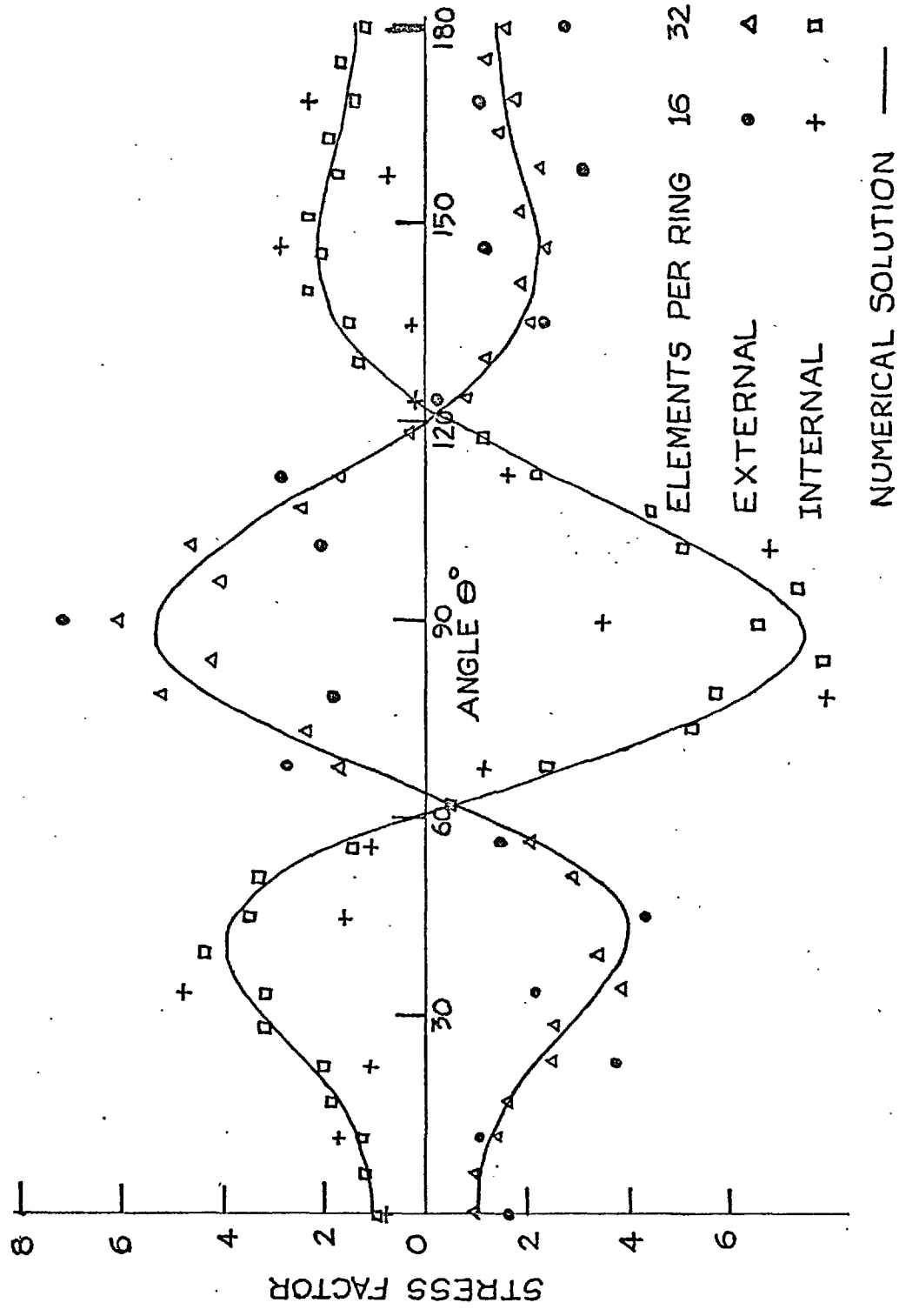



FIG.4.5. CIRCUMFERENTIAL STRESS FACTORS.

QUADRATIC THREE DIMENSIONAL ELEMENTS

$\lambda = 0.1458$ , $\gamma = 0.538$

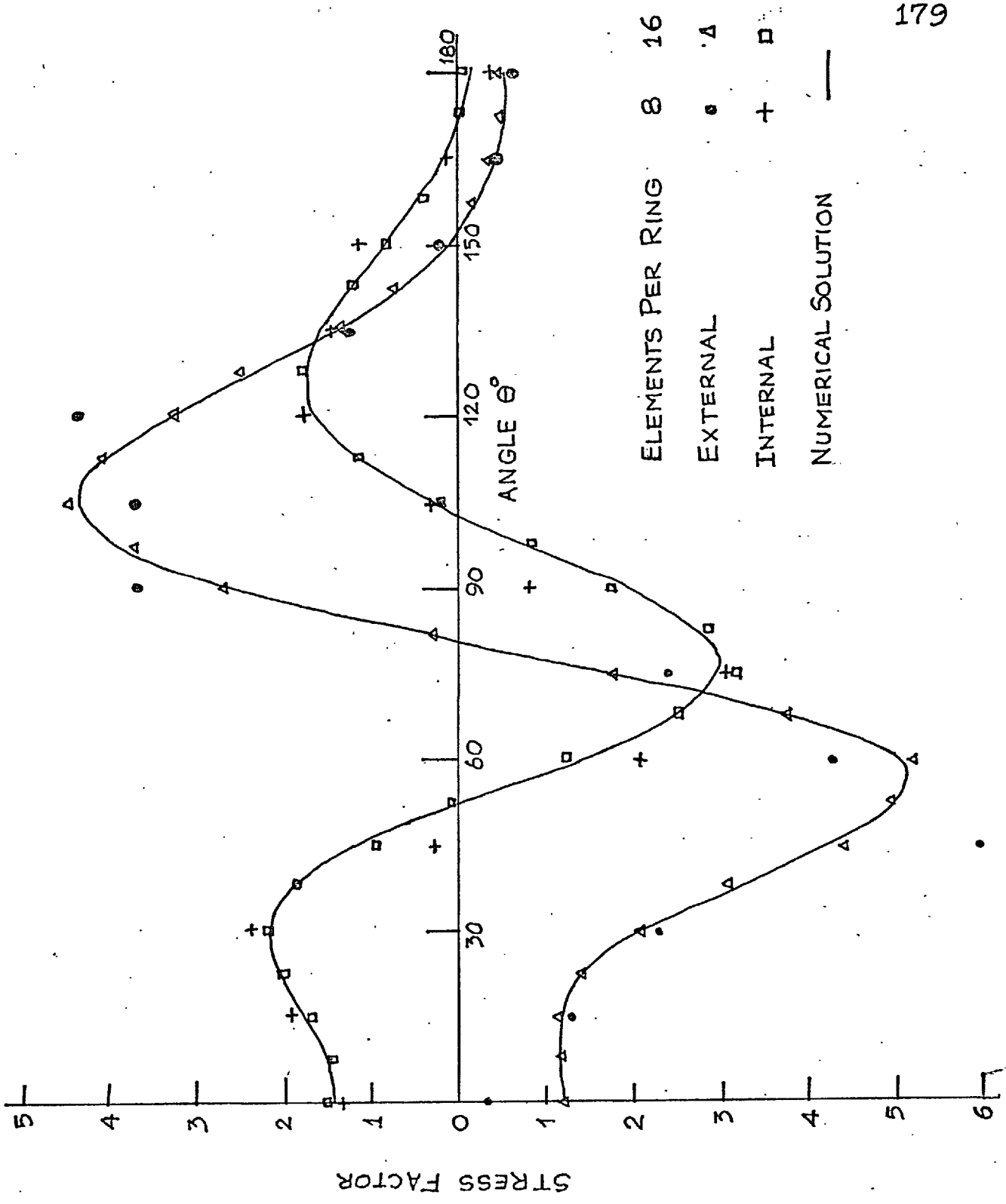



FIG.4-6. LONGITUDINAL STRESS FACTORS

CUBIC THREE DIMENSIONAL ELEMENTS

$\lambda = 0.1458$ , $\nu = 0.538$

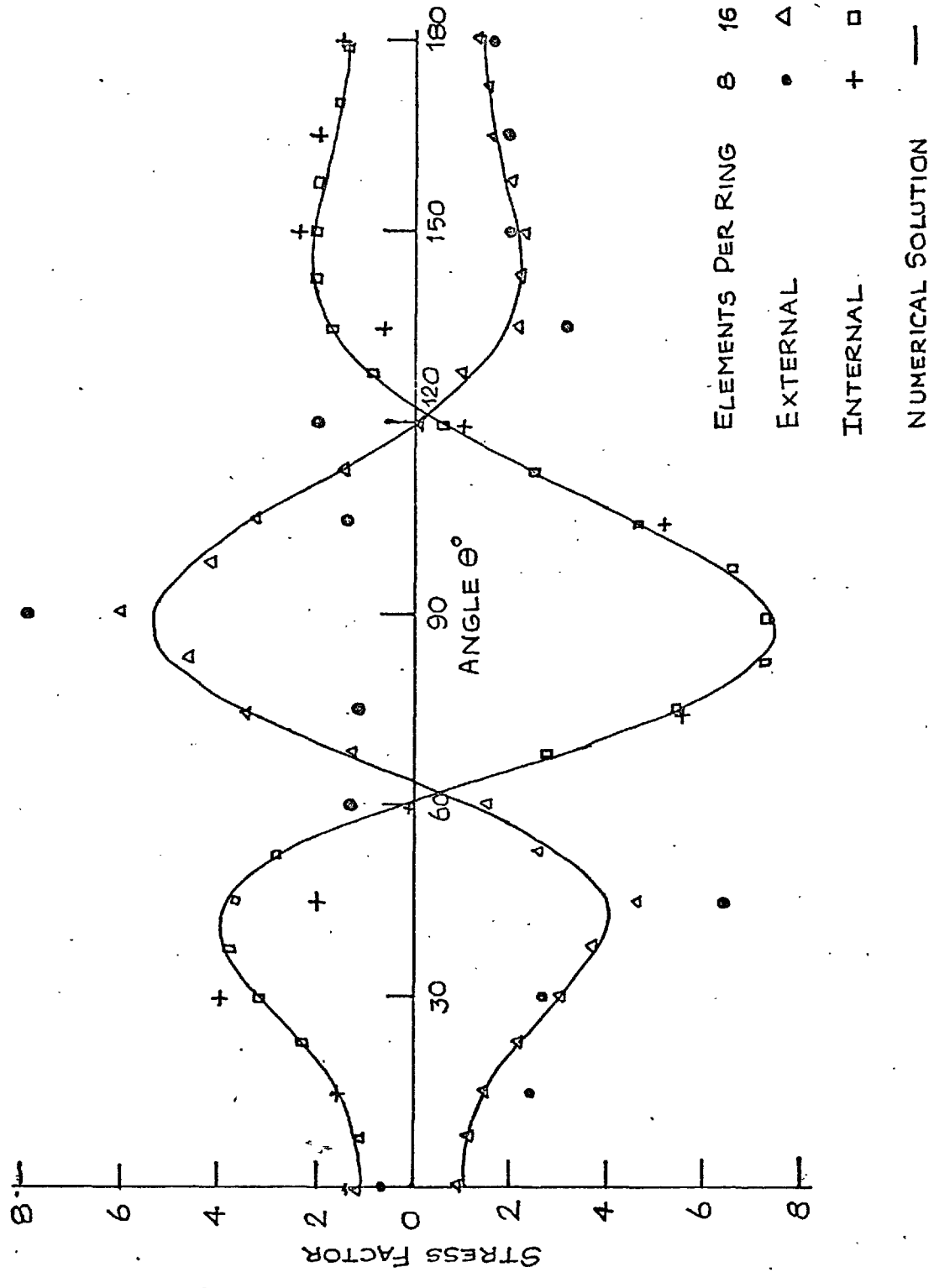



FIG. 4-7. CIRCUMFERENTIAL STRESS FACTORS
CUBIC THREE DIMENSIONAL ELEMENTS
$\lambda = 0.1458$ , $\gamma = 0.538$

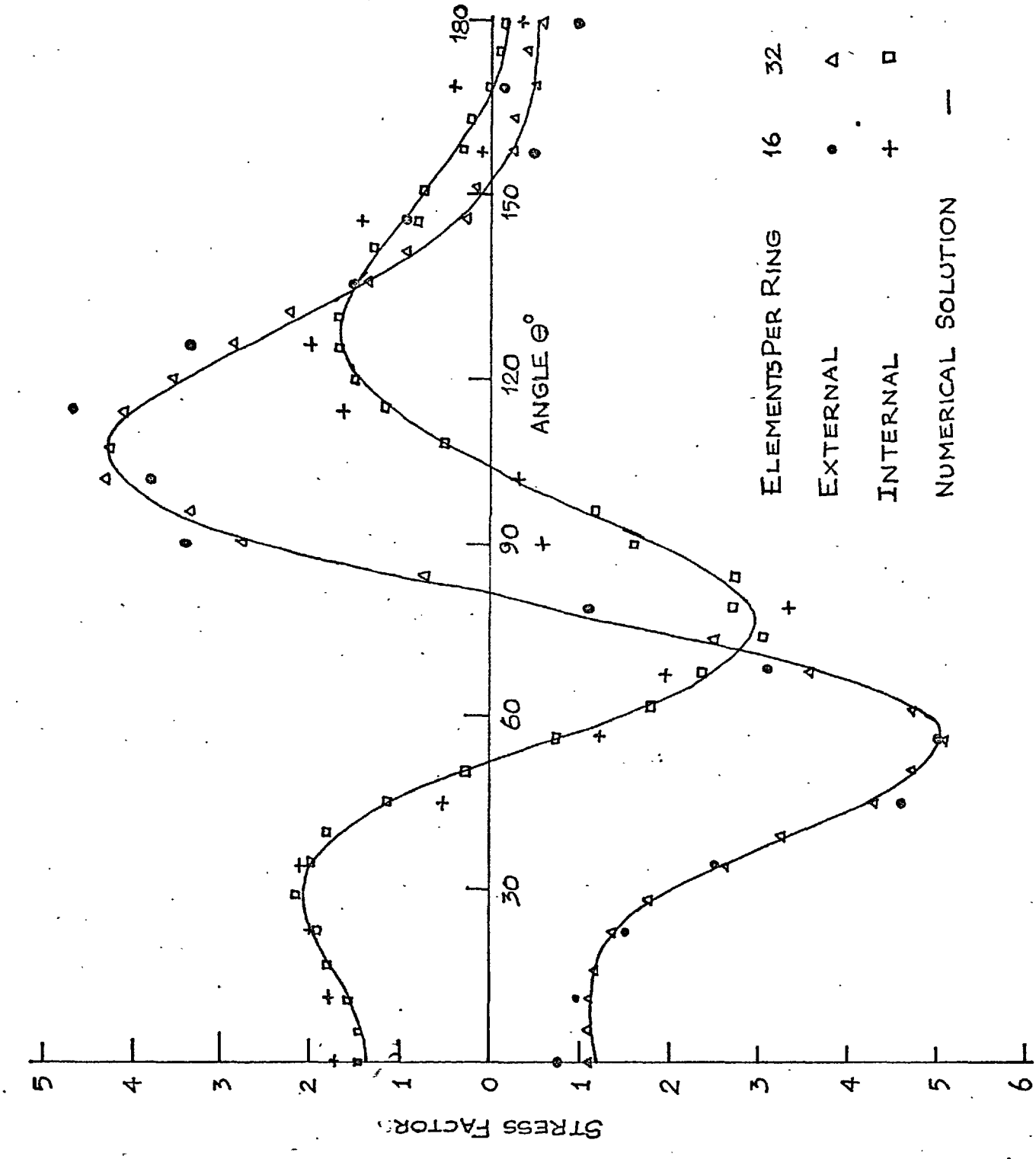



FIG. 4-8. LONGITUDINAL STRESS FACTORS

QUADRATIC SHELL ELEMENTS

$\lambda = 0.1458$ , $\gamma = 0.538$

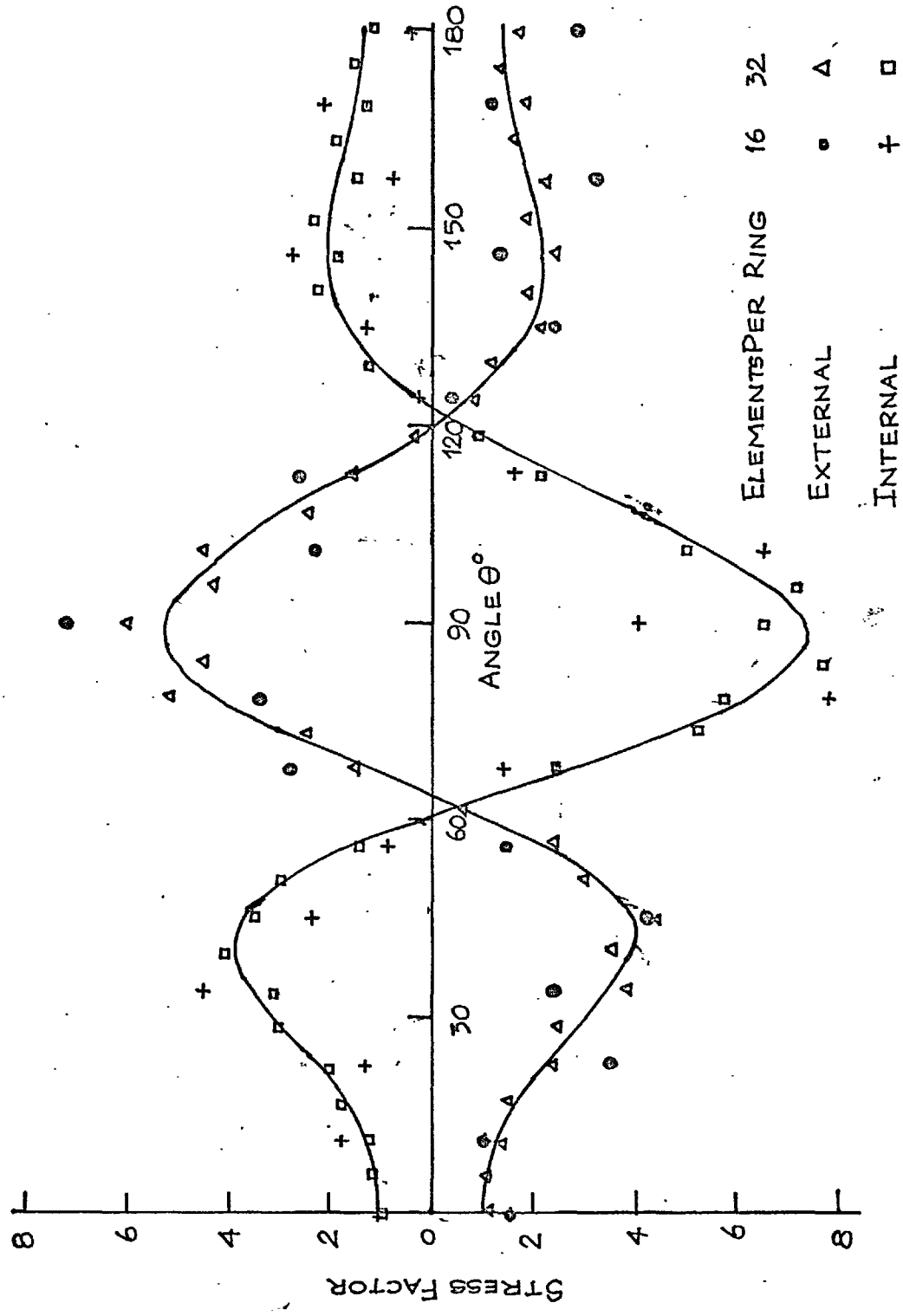



FIG. 4.9. CIRCUMFERENTIAL STRESS FACTORS

QUADRATIC SHELL ELEMENTS

$\lambda = 0.1458$ , $\gamma = 0.538$

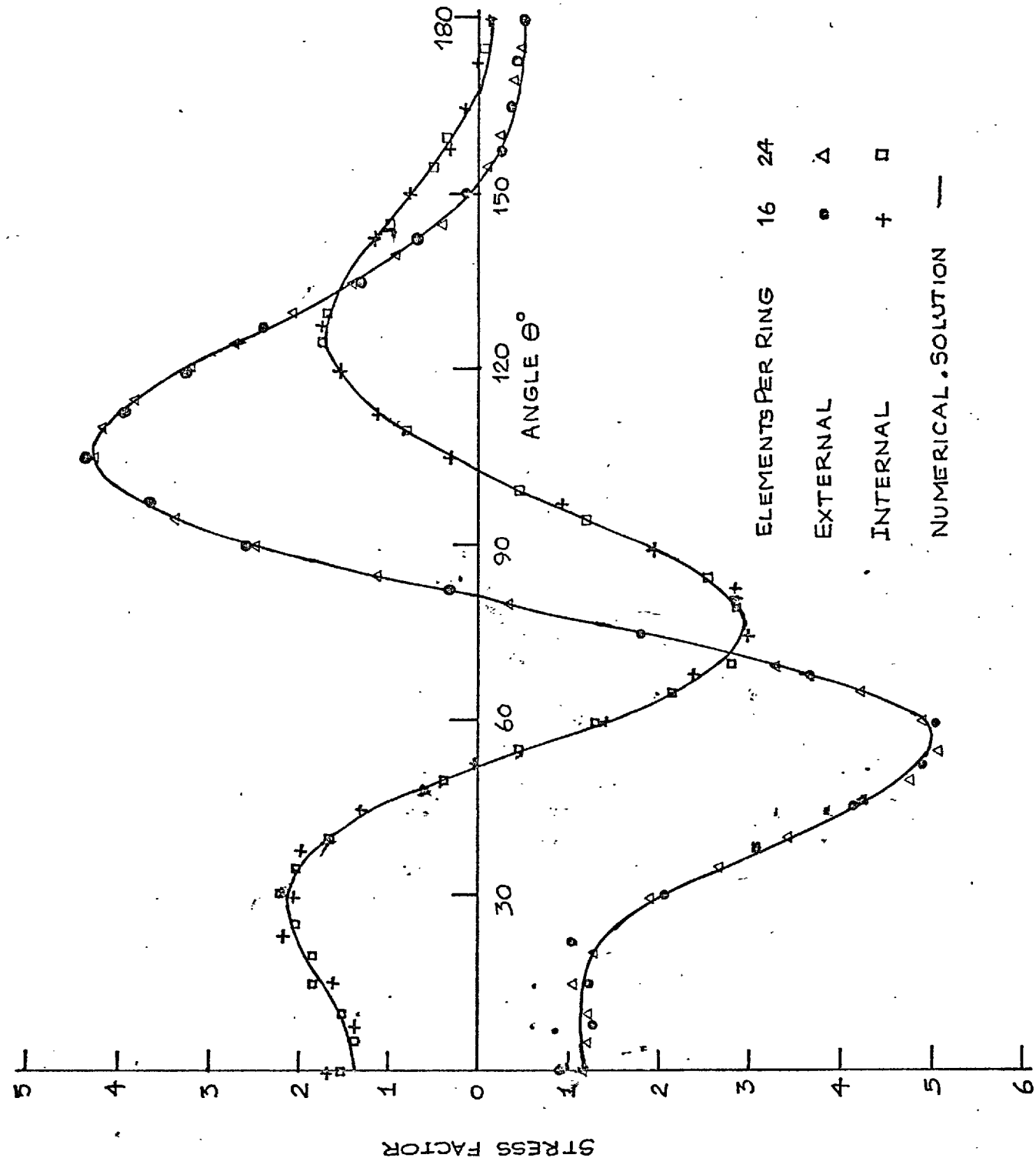



FIG.4.10. LONGITUDINAL STRESS FACTORS

CUBIC SHELL ELEMENTS

$\lambda = 0.1458$ , $\gamma = 0.538$

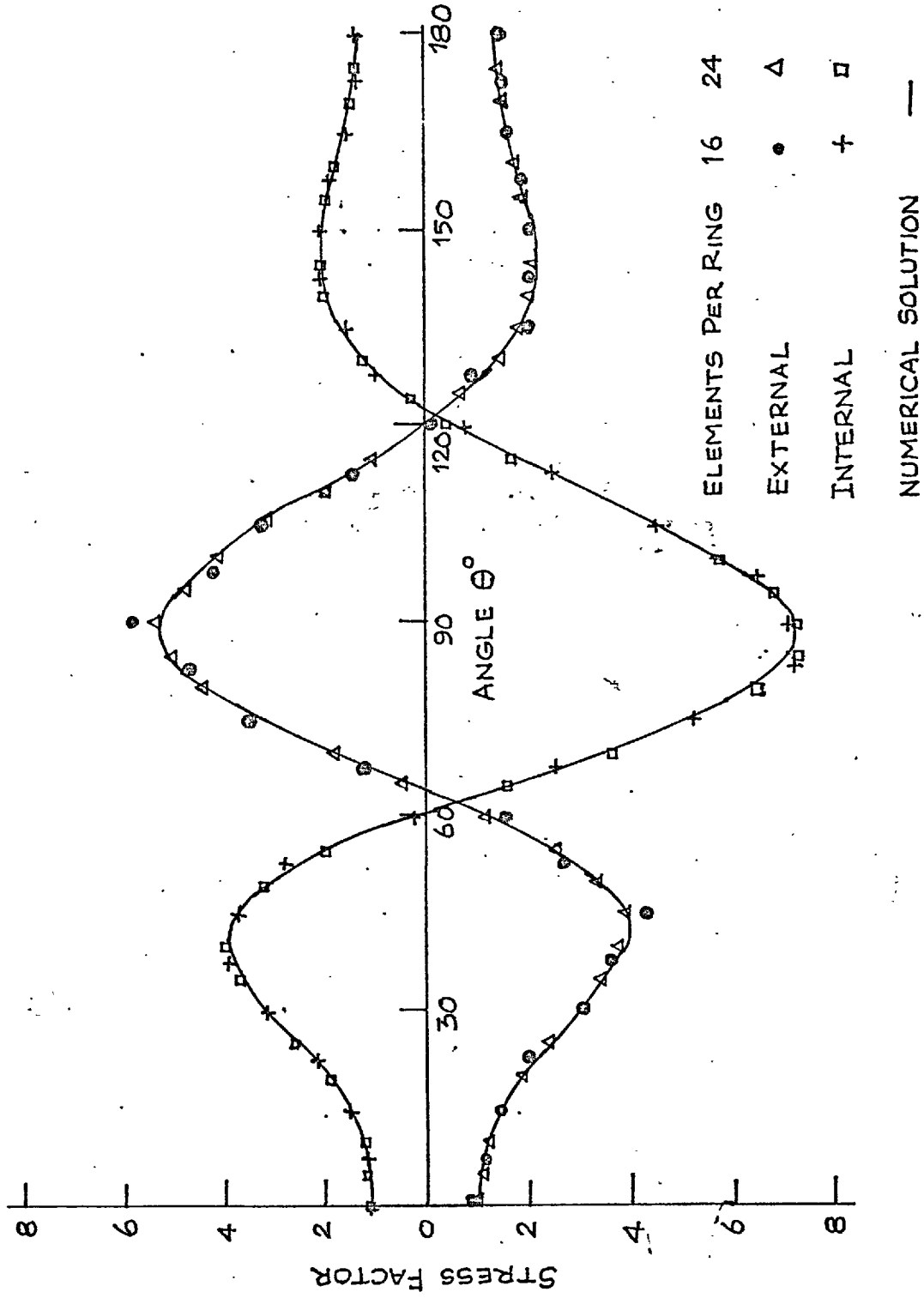



FIG. 4·11. CIRCUMFERENTIAL STRESS FACTORS

CUBIC SHELL ELEMENTS

$\lambda = 0.1458$ , $\gamma = 0.538$

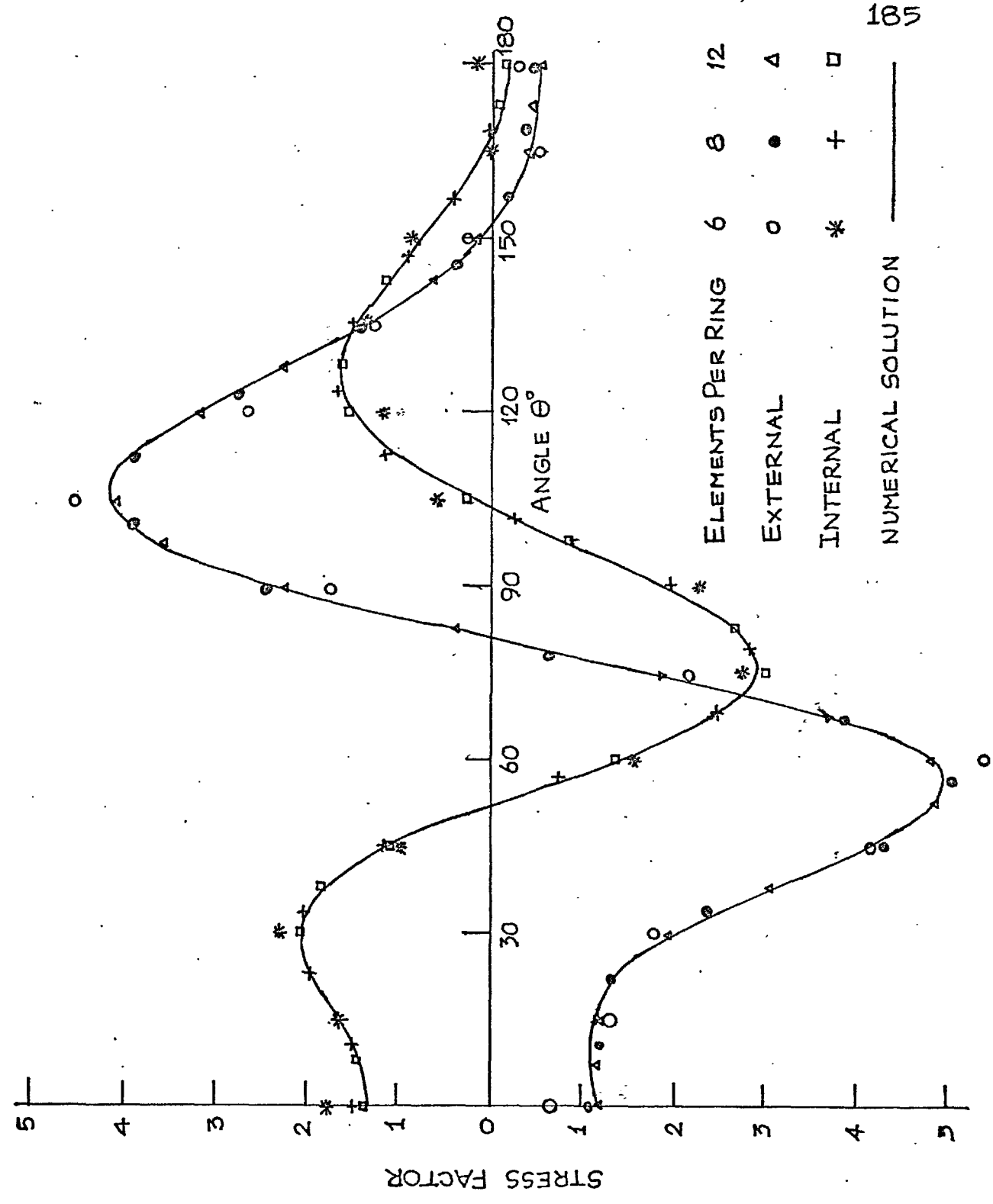



FIG. 4·12. LONGITUDINAL STRESS FACTORS

QUARTIC SHELL ELEMENTS

$\lambda = 0.1458$ , $\gamma = 0.538$

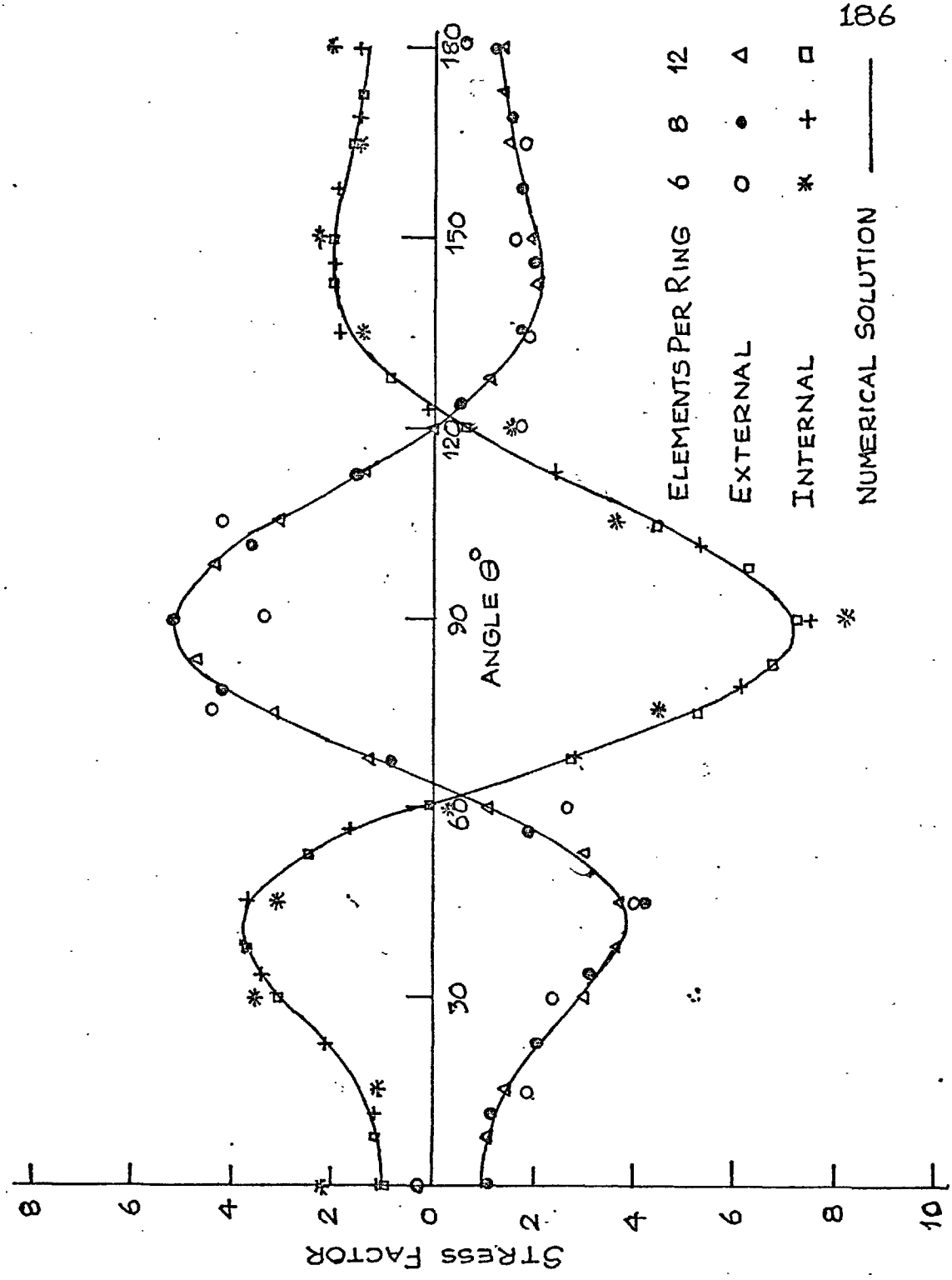



FIG 4·13. CIRCUMFERENTIAL STRESS FACTORS

QUARTIC SHELL ELEMENTS

$\lambda = 0.1458$ , $\nu = 0.538$

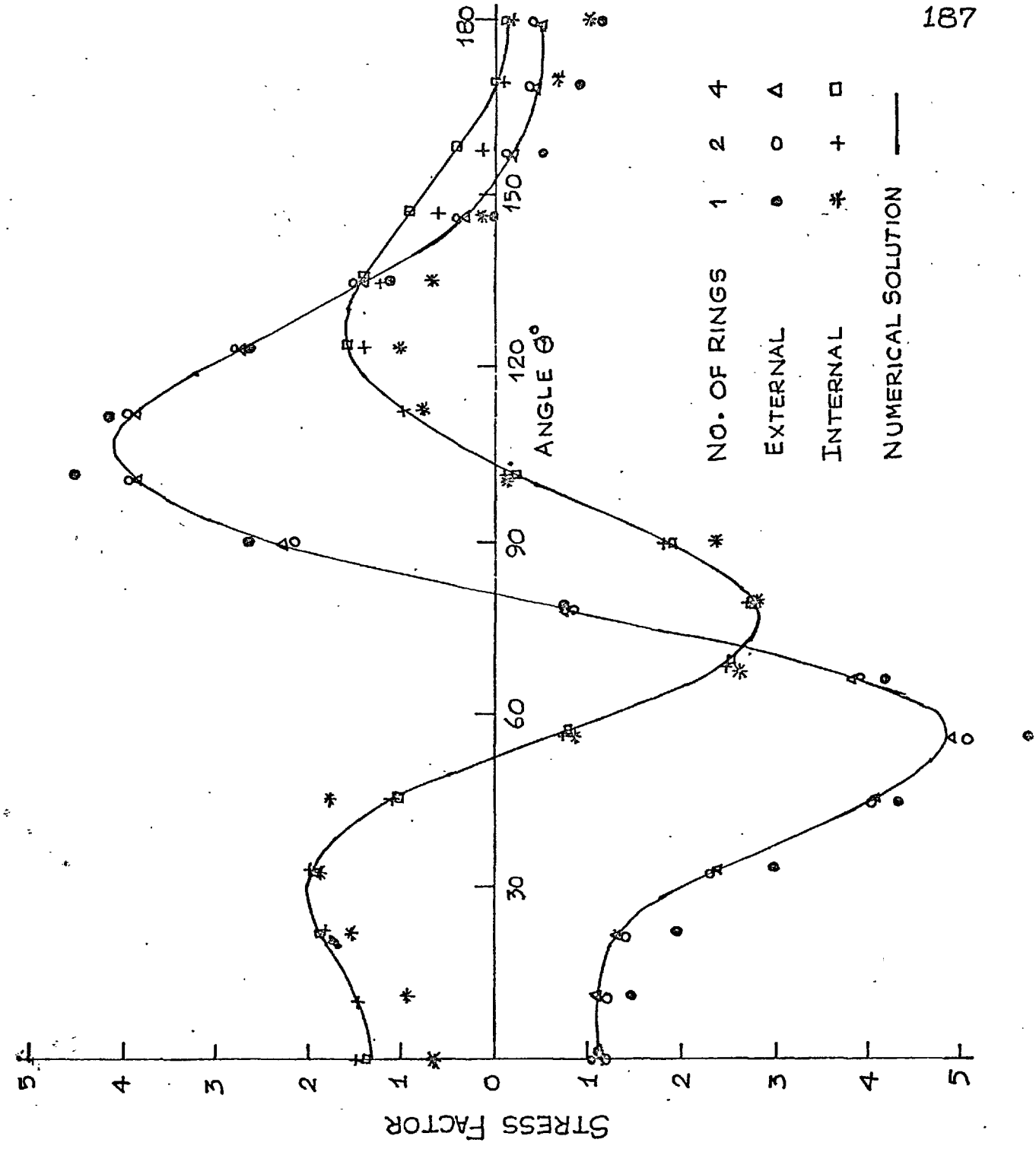



FIG. 4.14. LONGITUDINAL STRESS FACTORS
EIGHT QUARTIC ELEMENTS PER RING.
90° BEND $\lambda = 0.1458$, $\gamma = 0.538$

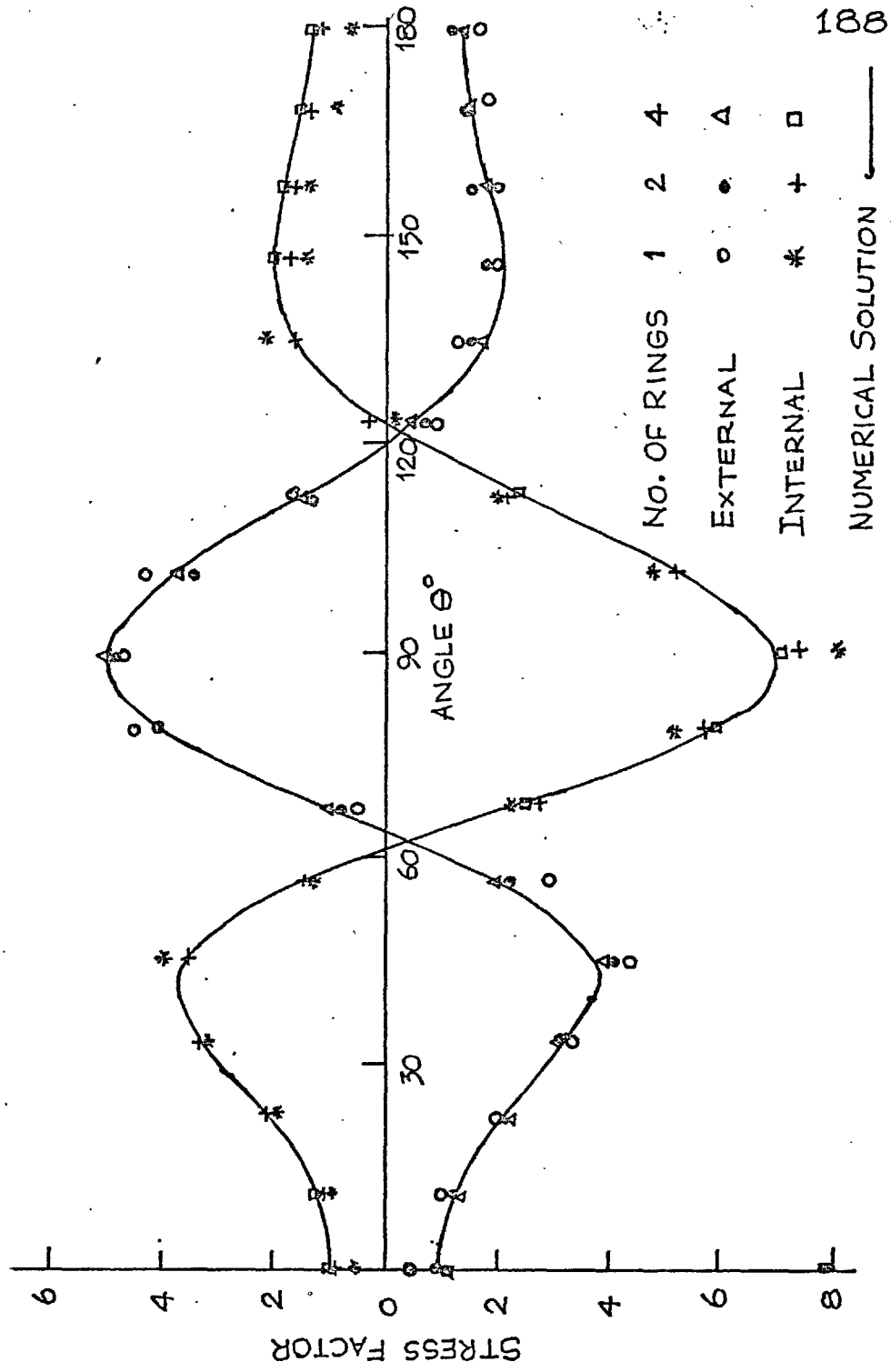



FIG. 4.15. CIRCUMFERENTIAL STRESS FACTORS
EIGHT QUARTIC ELEMENTS PER RING.
90° BEND, $\lambda = 0.1458$, $\gamma = 0.538$

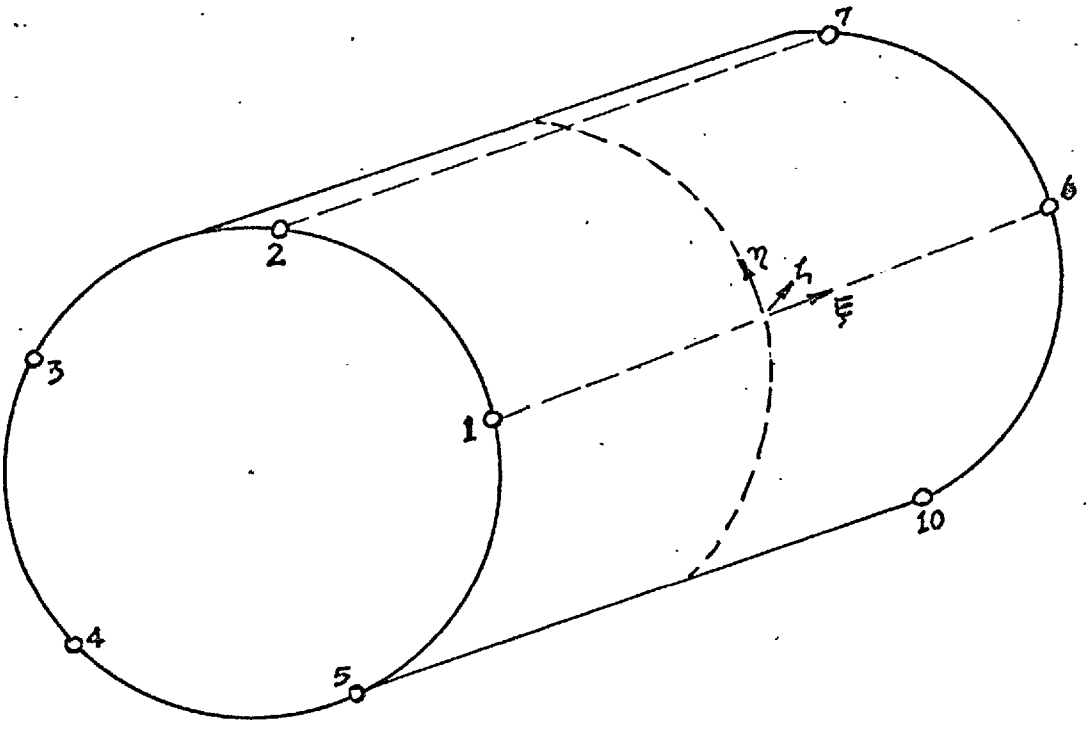



FIG 4-16 FULL RING ELEMENT

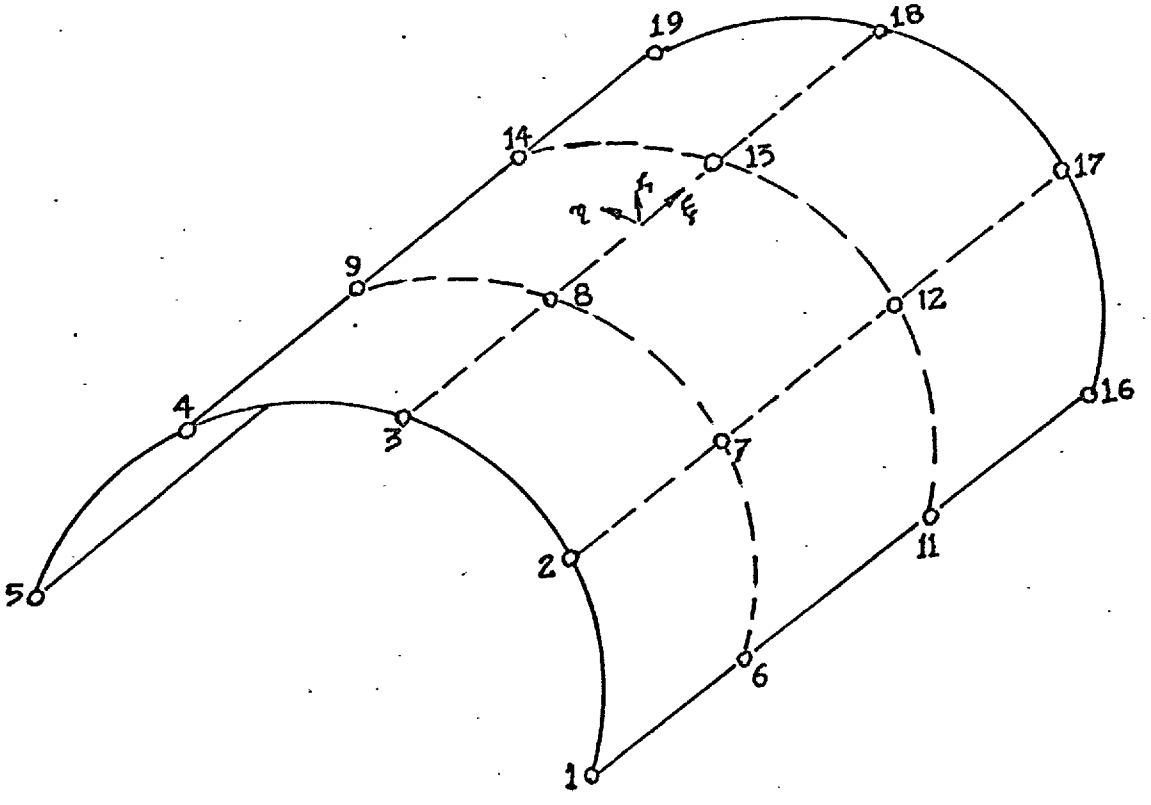



FIG 4-17 HALF RING ELEMENT

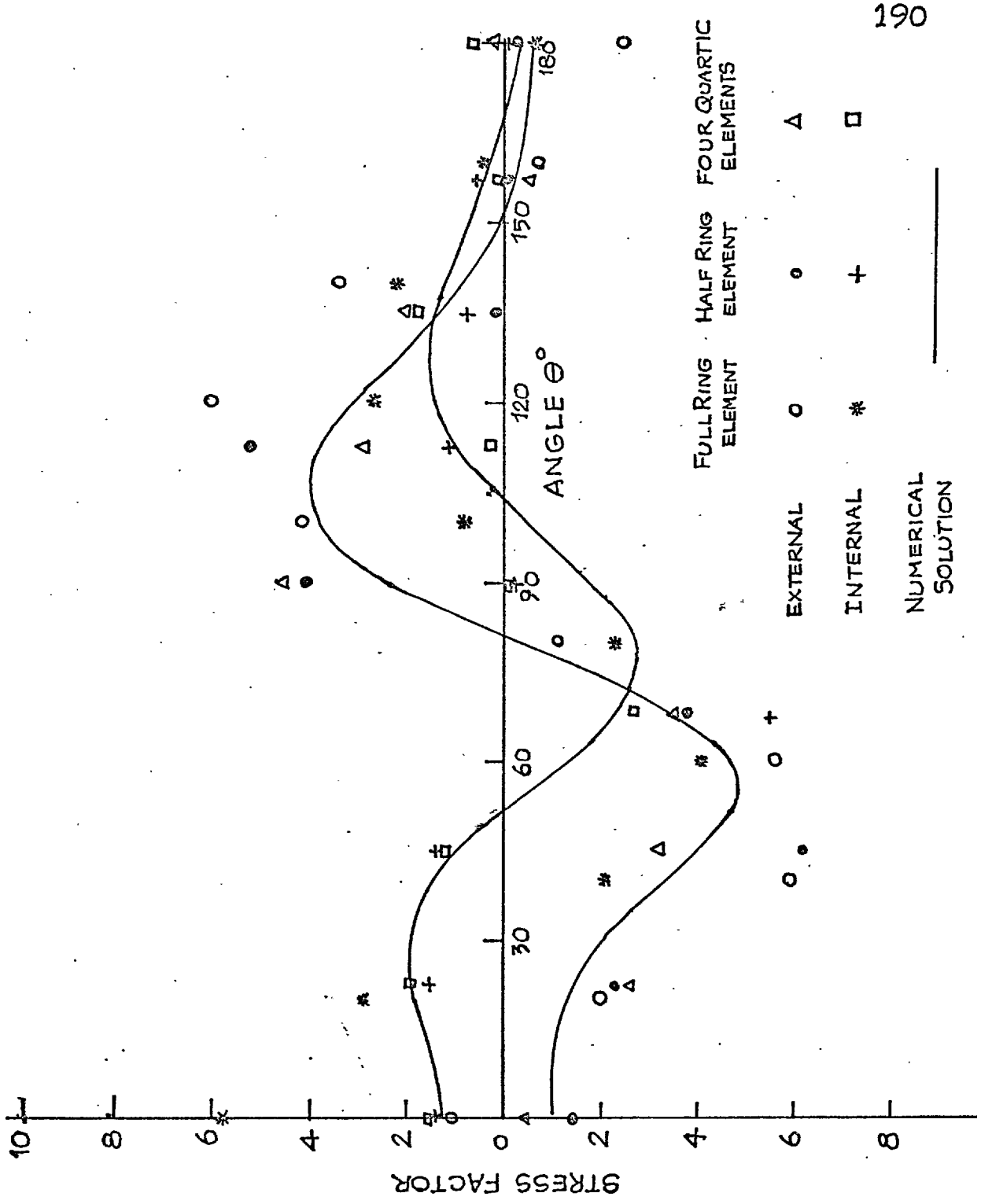



FIG. 4·18. LONGITUDINAL STRESS FACTORS
COMPARISON OF RING ELEMENTS
WITH QUARTIC ELEMENTS
$\lambda = 0.1458$, $\gamma = 0.538$

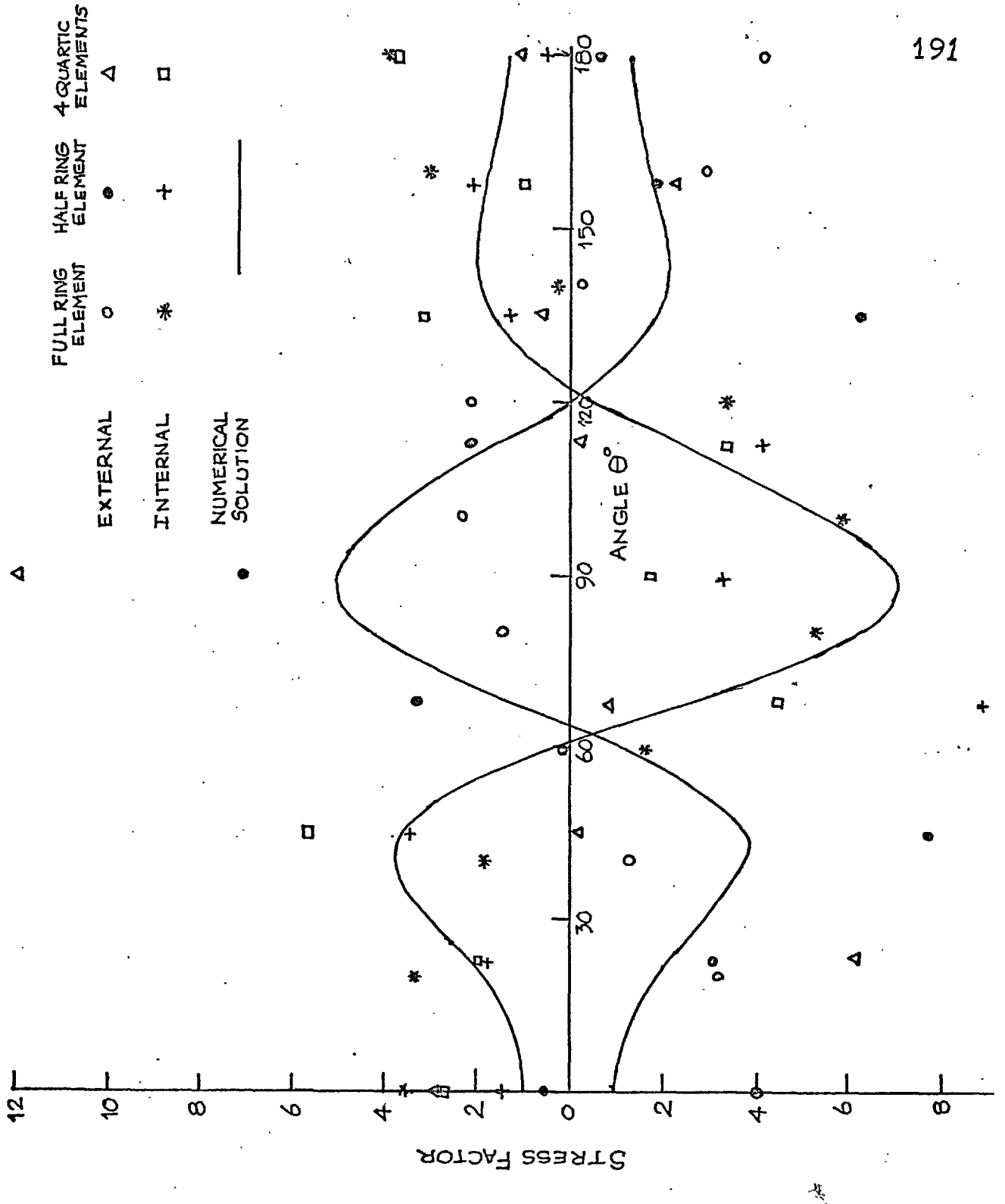



FIG. 4·19. CIRCUMFERENTIAL STRESS FACTORS
COMPARISON OF RING ELEMENTS
WITH QUARTIC ELEMENTS
$\lambda = 0.1458$ , $\gamma = 0.538$

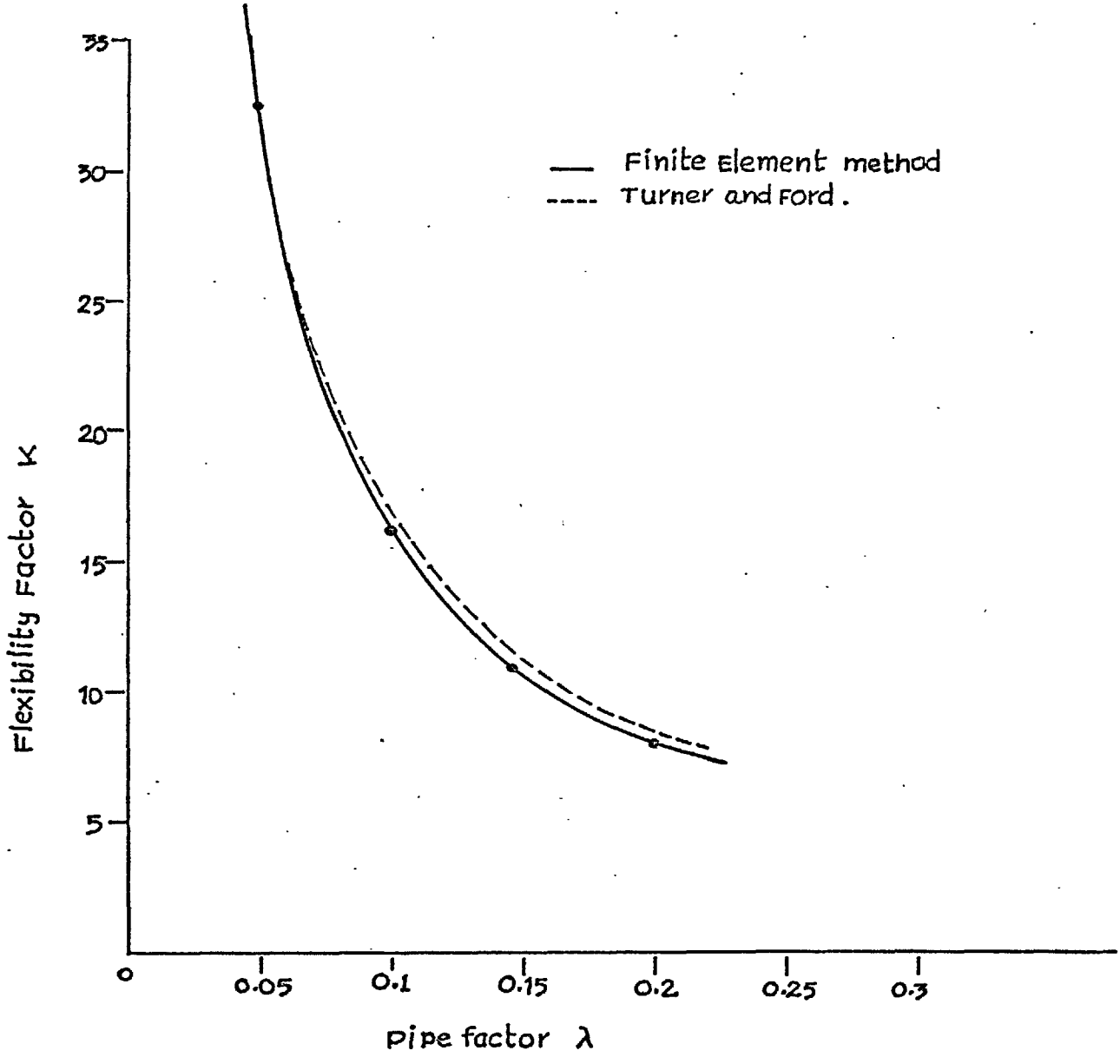



FIG. 4.20. FLEXIBILITY FACTORS OF 90 DEG-BENDS WITH THE ASSUMPTION OF PLANE SECTIONS REMAINING PLANE

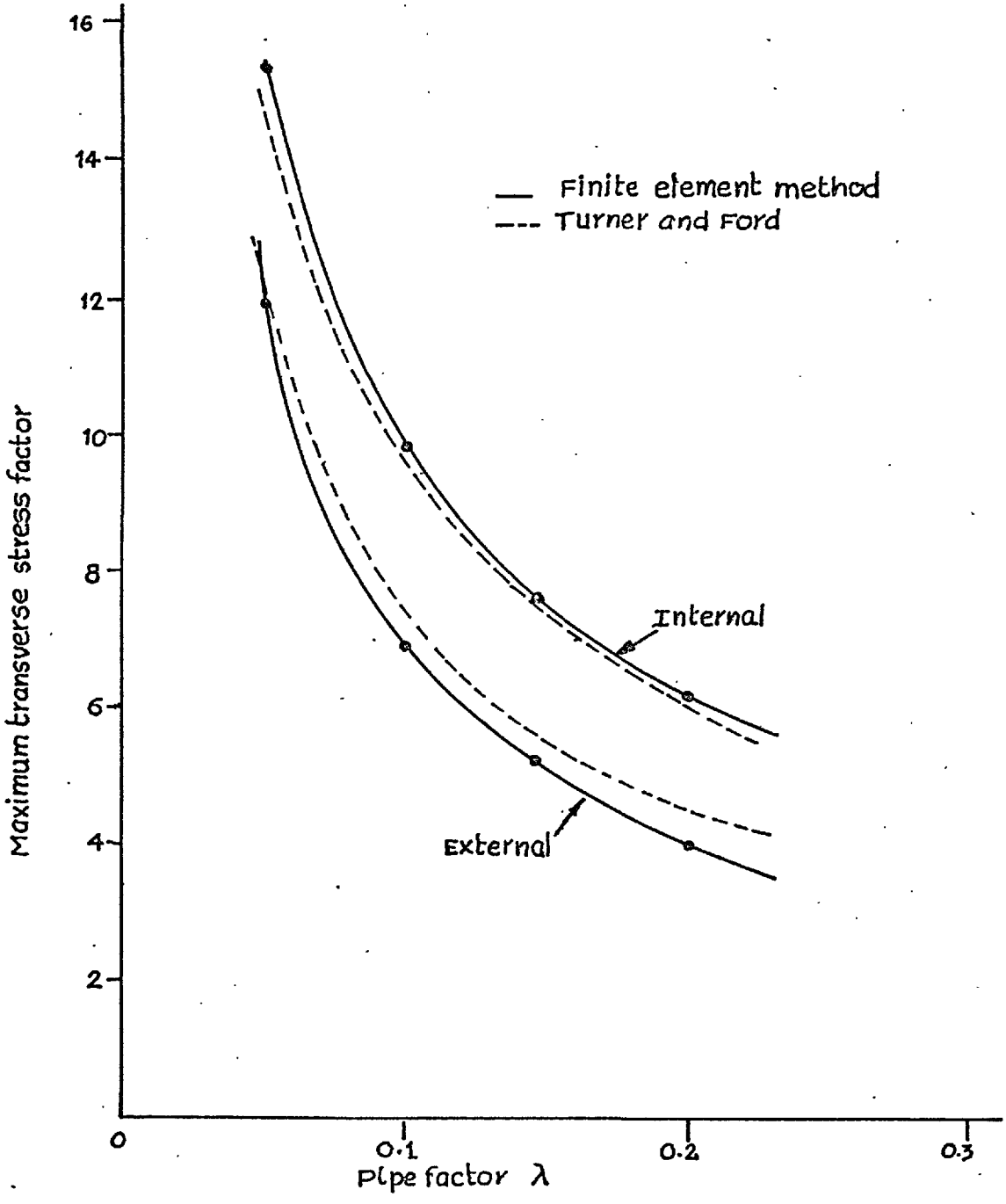



FIG. 4-21. MAXIMUM TRANSVERSE STRESS FACTORS OF 90 DEG-BENDS WITH THE ASSUMPTION OF PLANE SECTIONS REMAINING PLANE

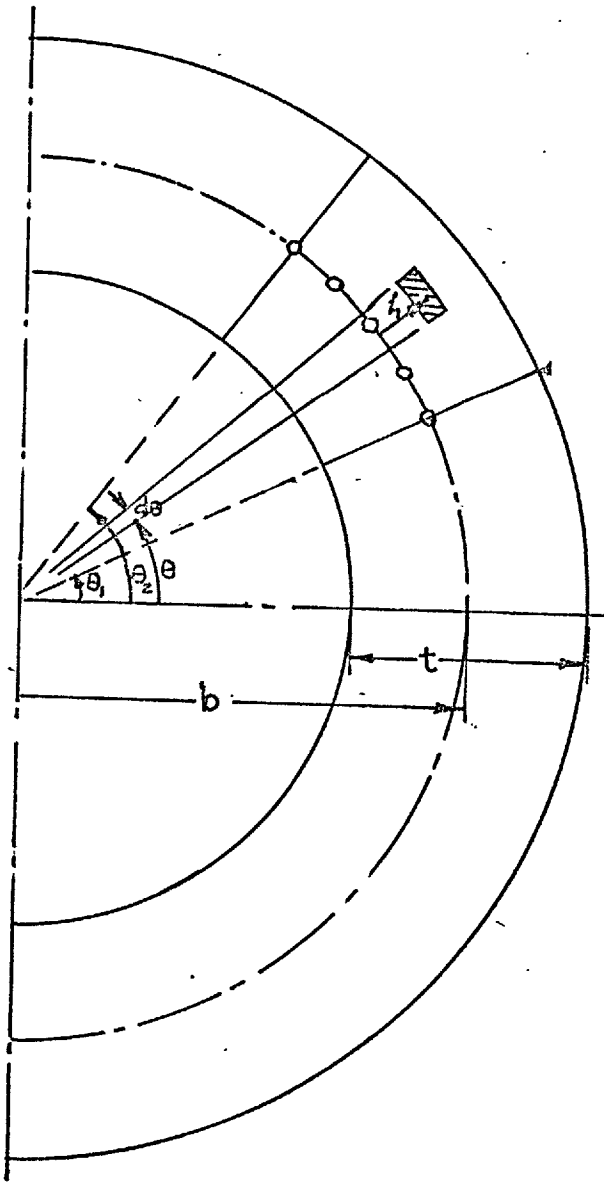
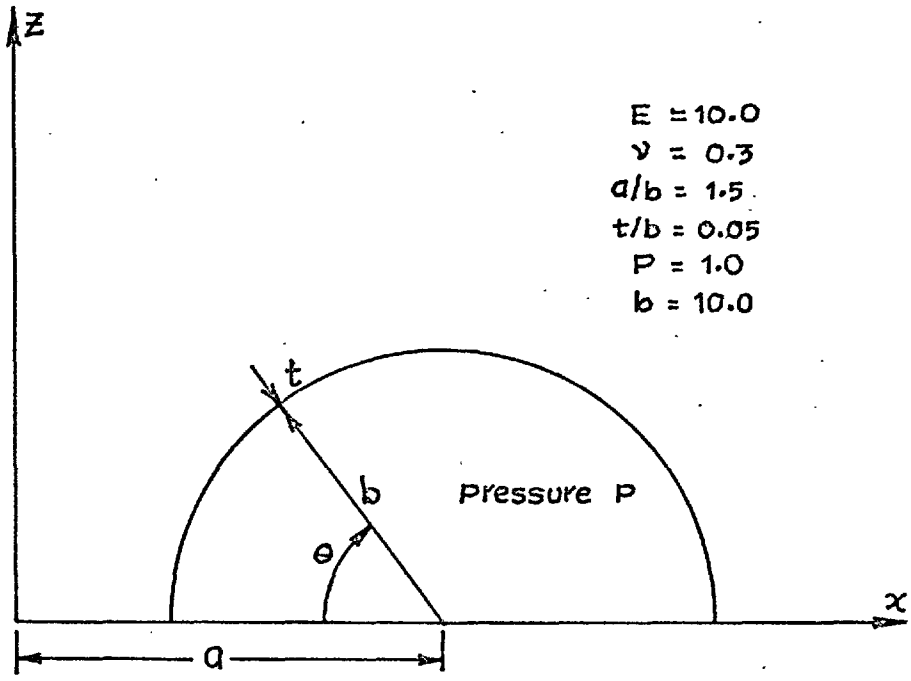
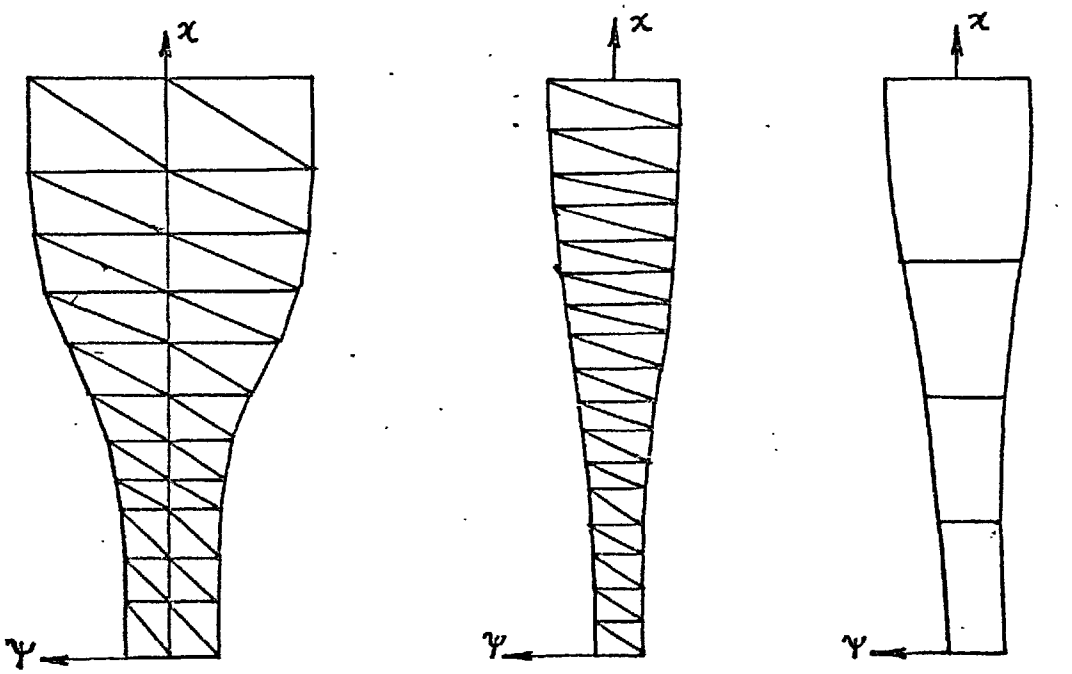



FIG. 4.22. CALCULATION OF APPLIED MOMENT




Cross-section of the torus




20° segment 10° segment 10° segment

Shallow Shell Quartic Shell

Element Subdivison — Plan view

FIG. 5.1. TORUS UNDER INTERNAL PRESSURE

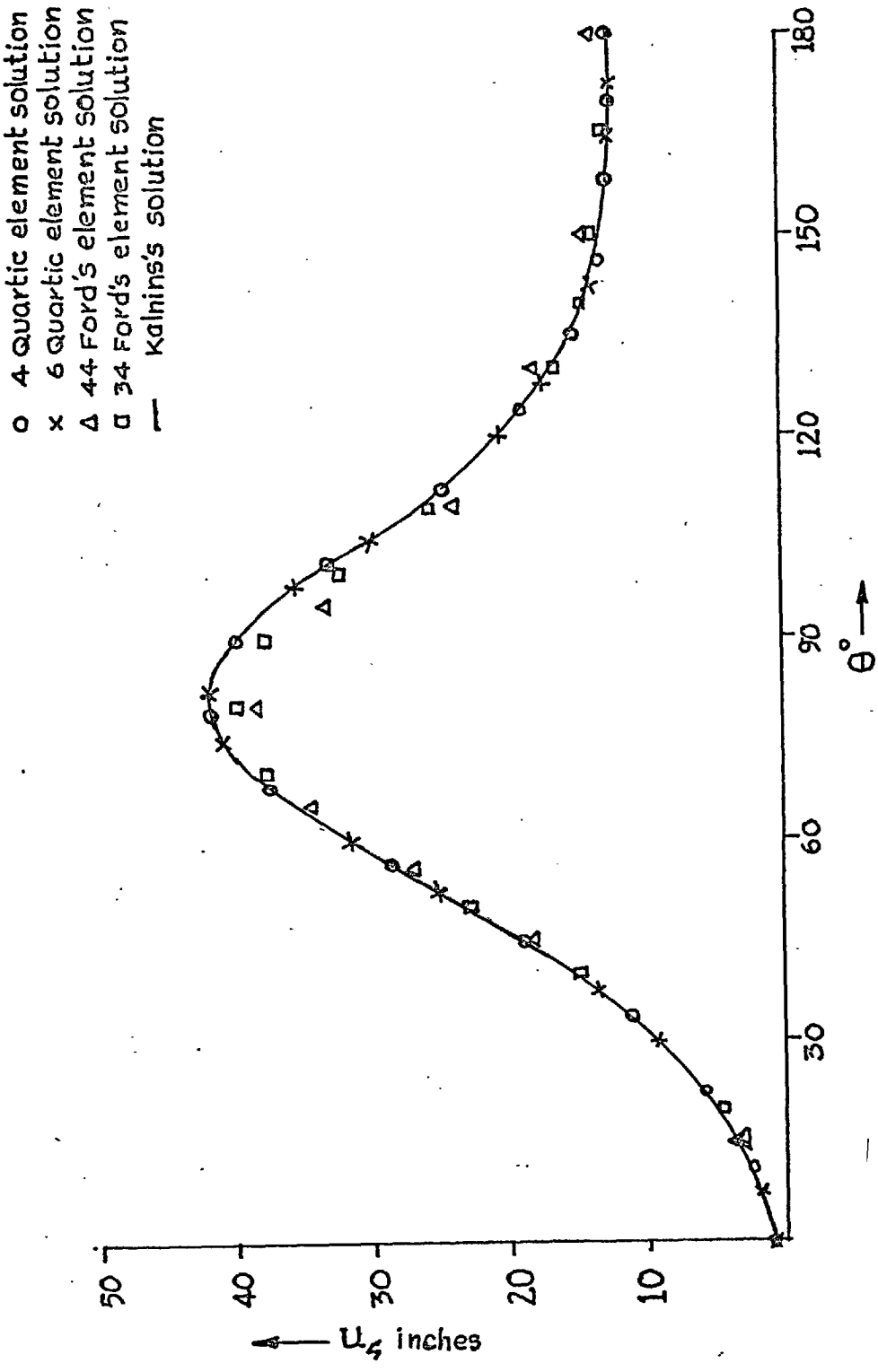



FIG.5.2. RADIAL DEFLECTION $u_\zeta$

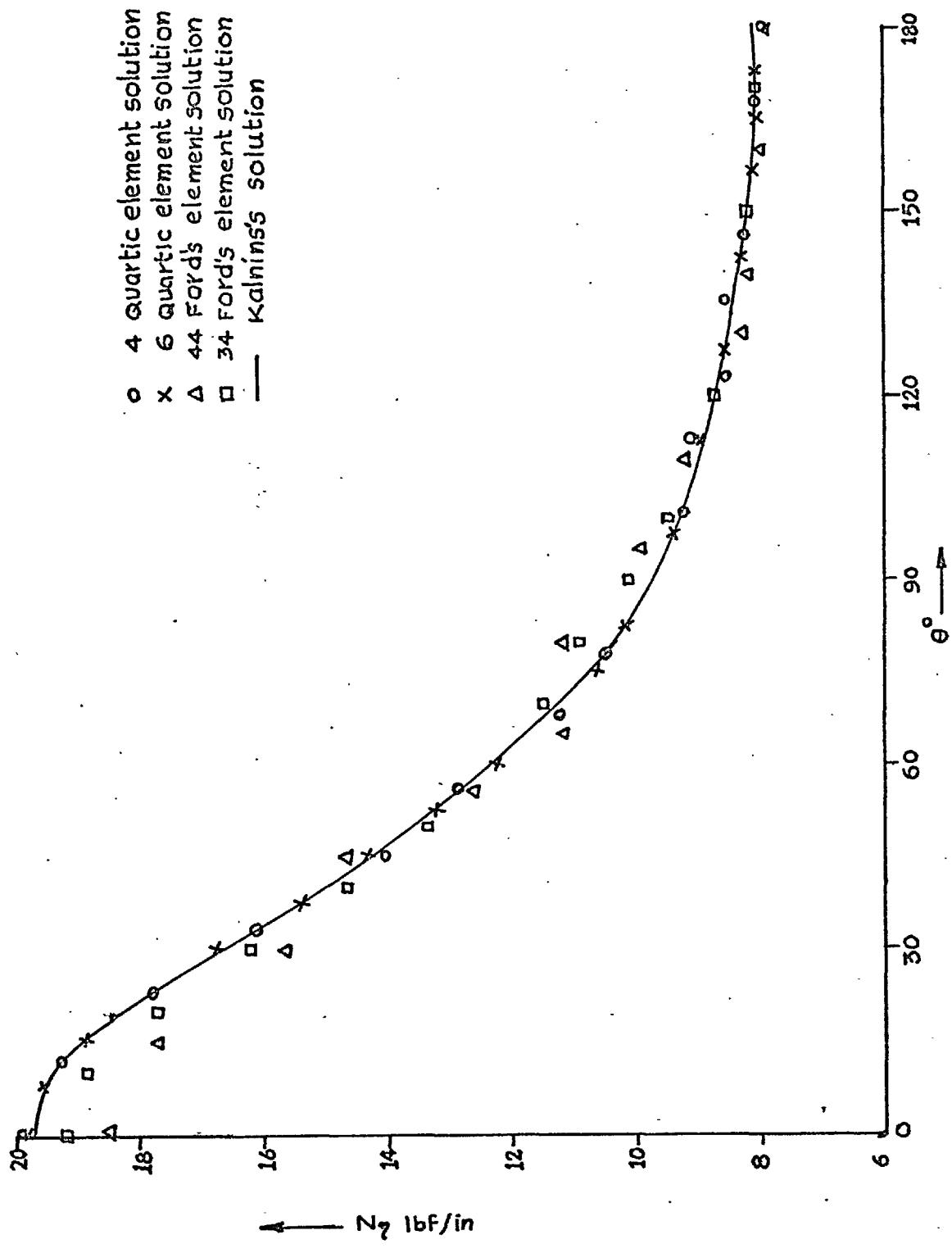



FIG.5.3. MERIDIONAL STRESS RESULTANT $N_\theta$

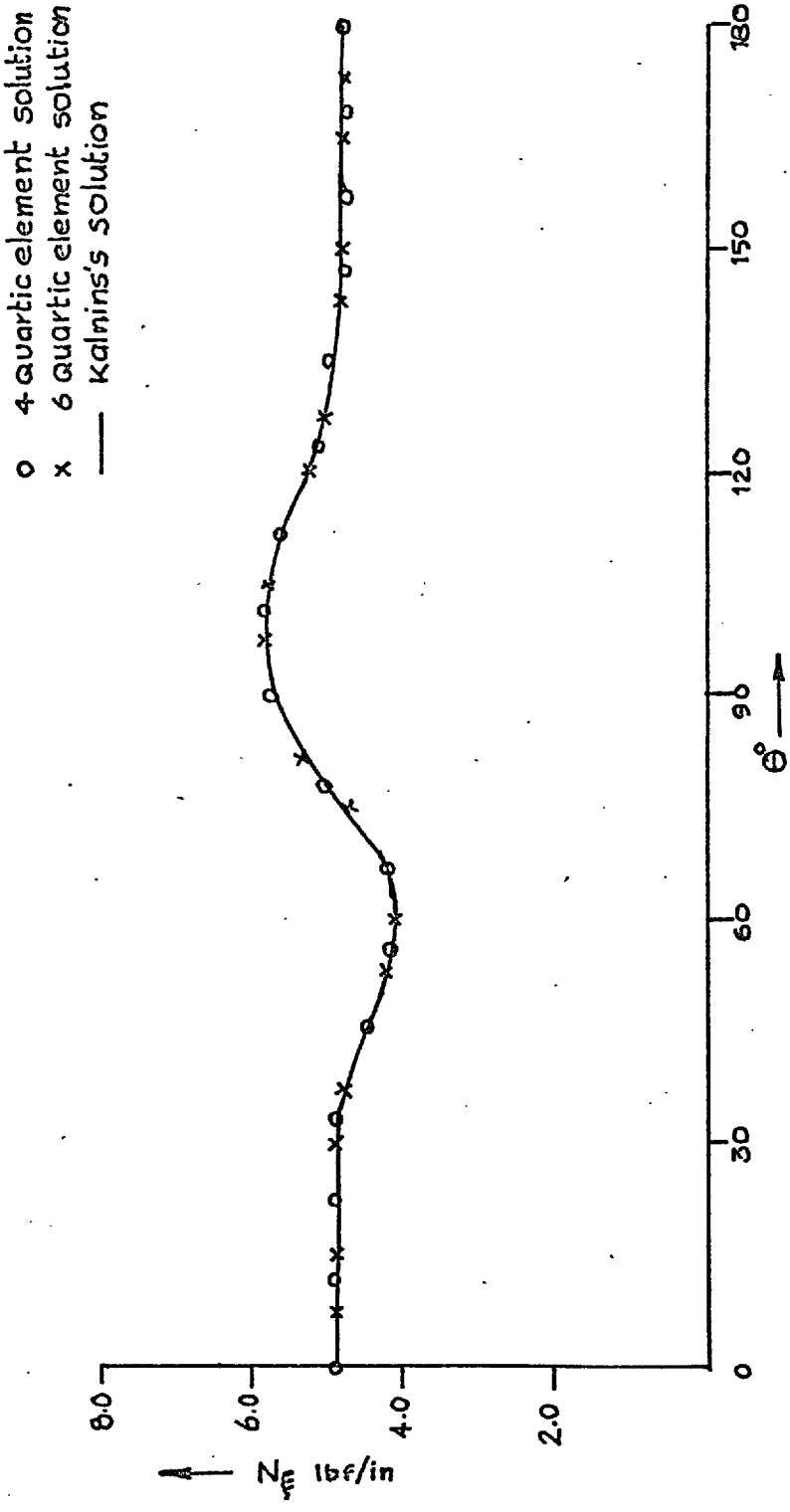
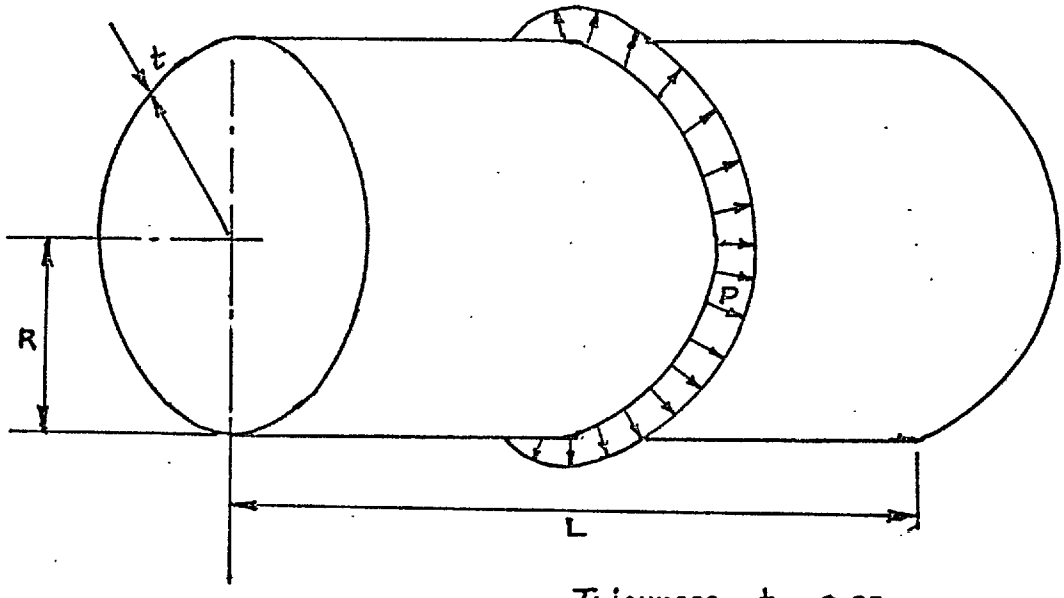
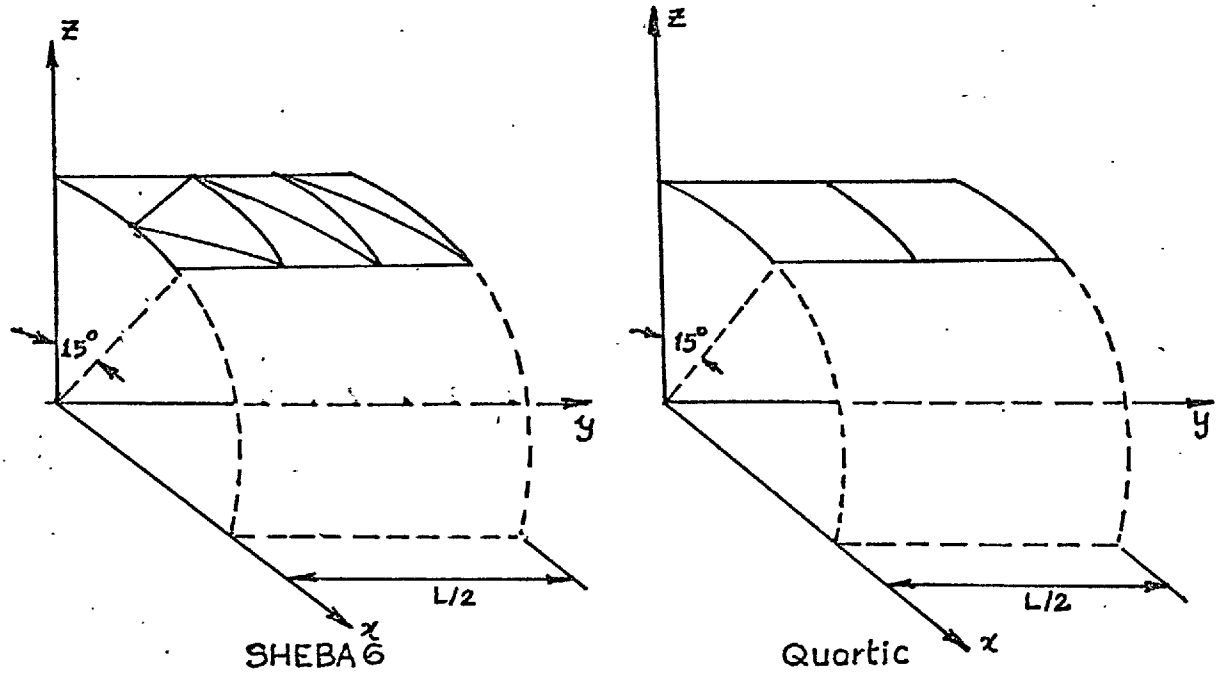



FIG. 5.4. LONGITUDINAL STRESS RESULTANT $N_\xi$




| | | |
|---|---|---|
| Thickness | t | = 0.05 |
| Radius | R | = 10.0 |
| Length | L | = 1.0 |
| | P | = 1.0 |
| | E | = 1.0 |
| | ν | = 0.3 |




Pattern of Elements

FIG. 5.5. CIRCULAR CYLINDER UNDER RADIAL RING LOAD

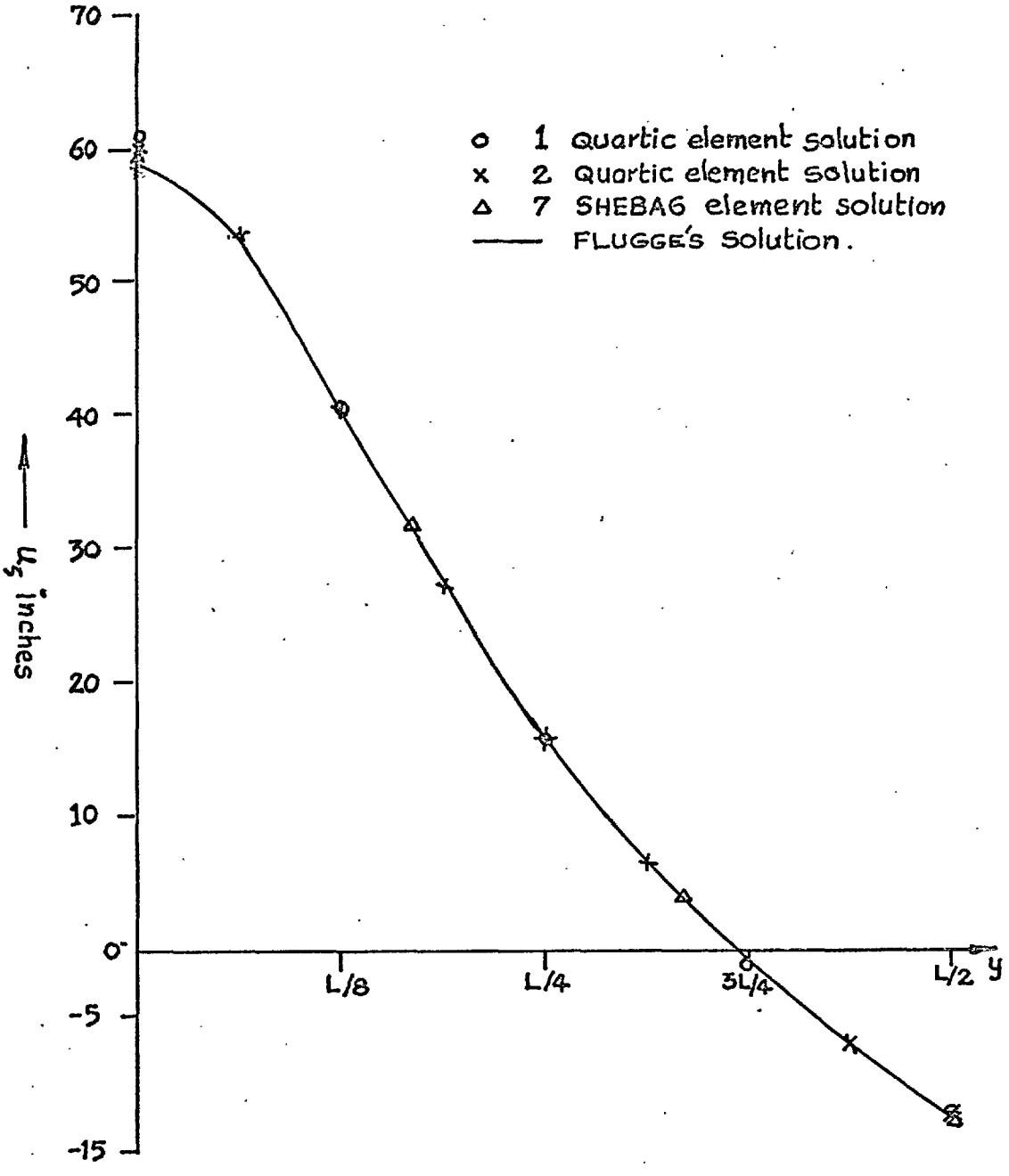



FIG. 5.6. RADIAL DISPLACEMENT $u_\zeta$

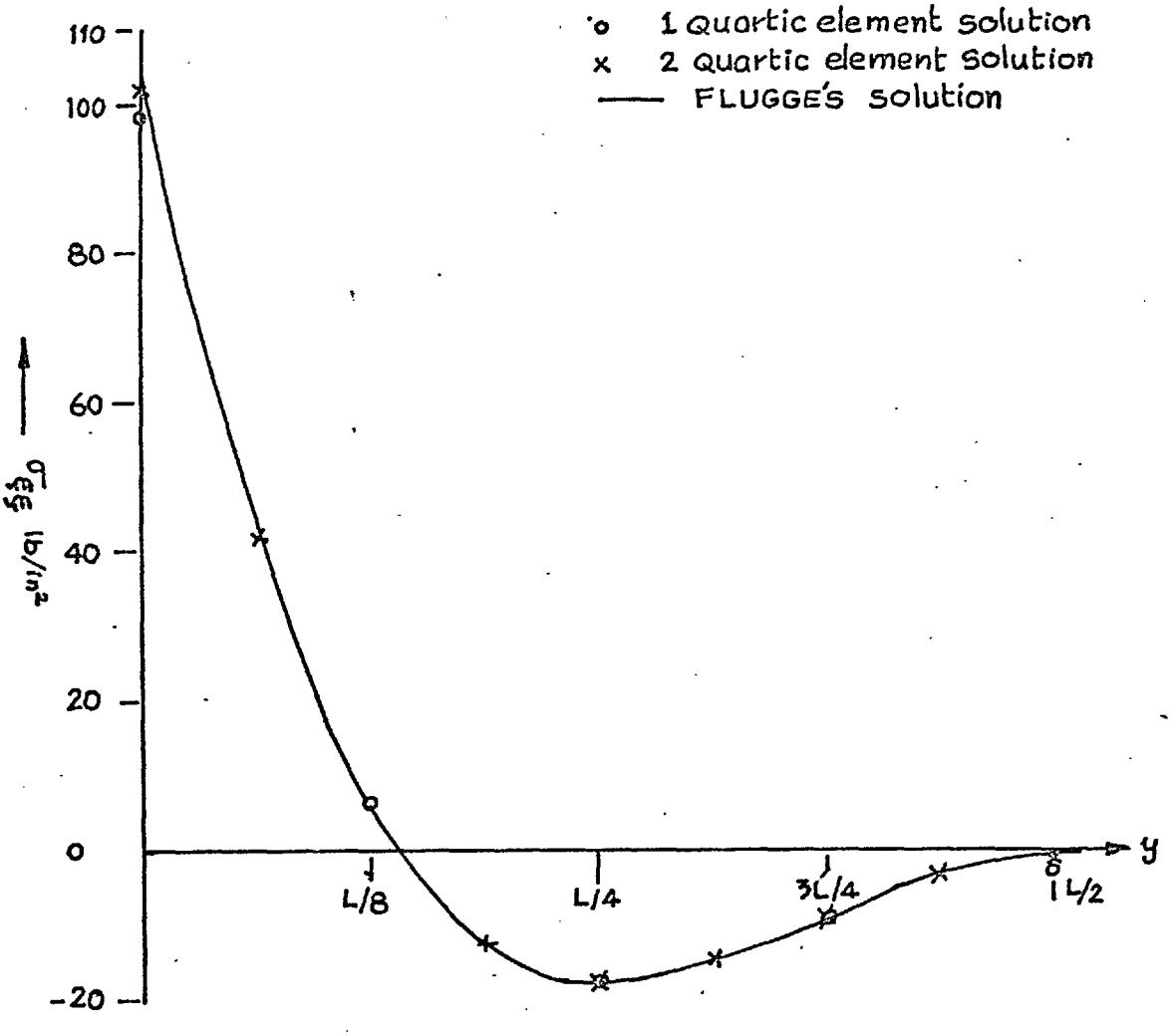



FIG. 5.7. LONGITUDINAL BENDING STRESS $\sigma_{ff}$

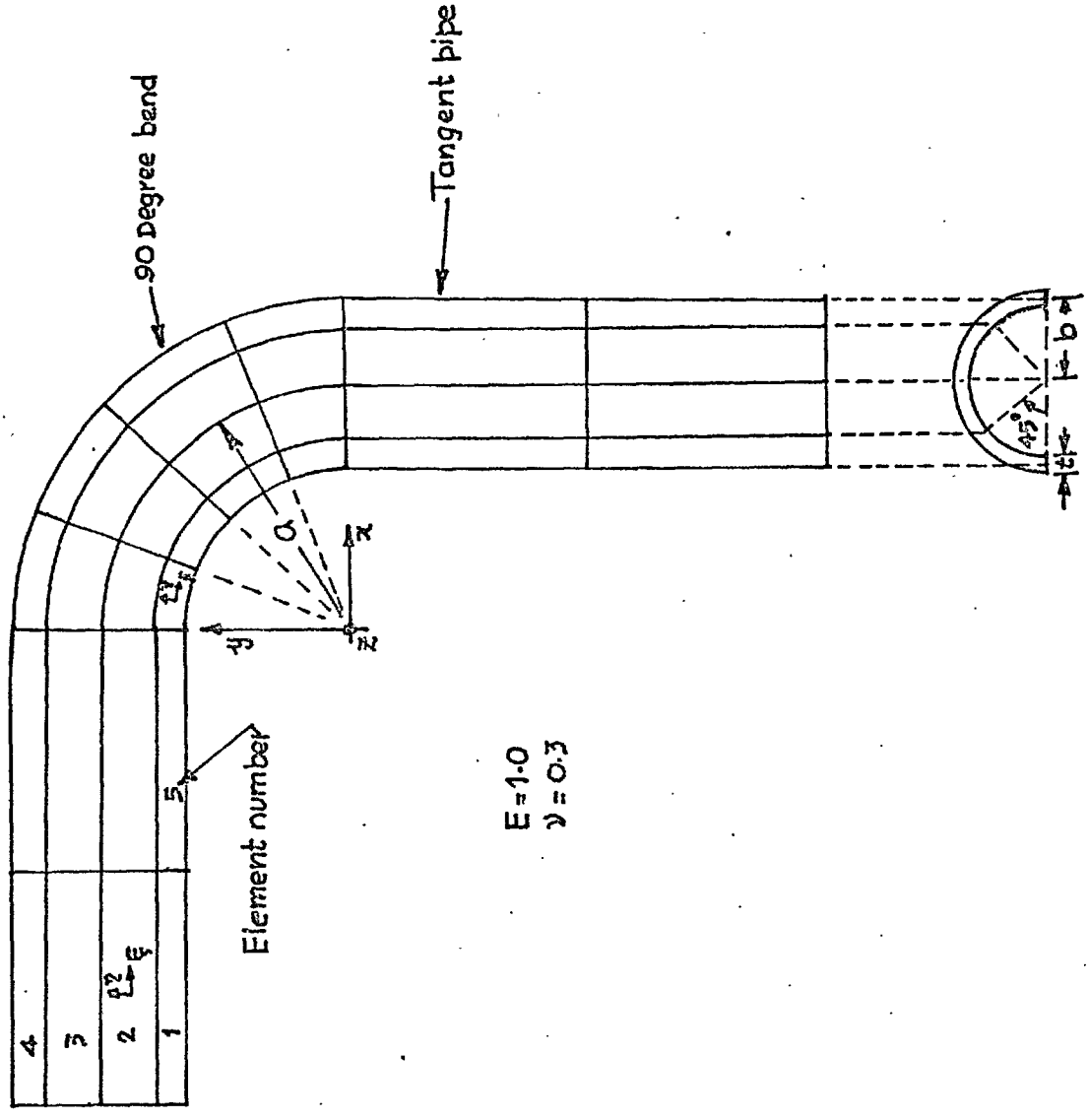
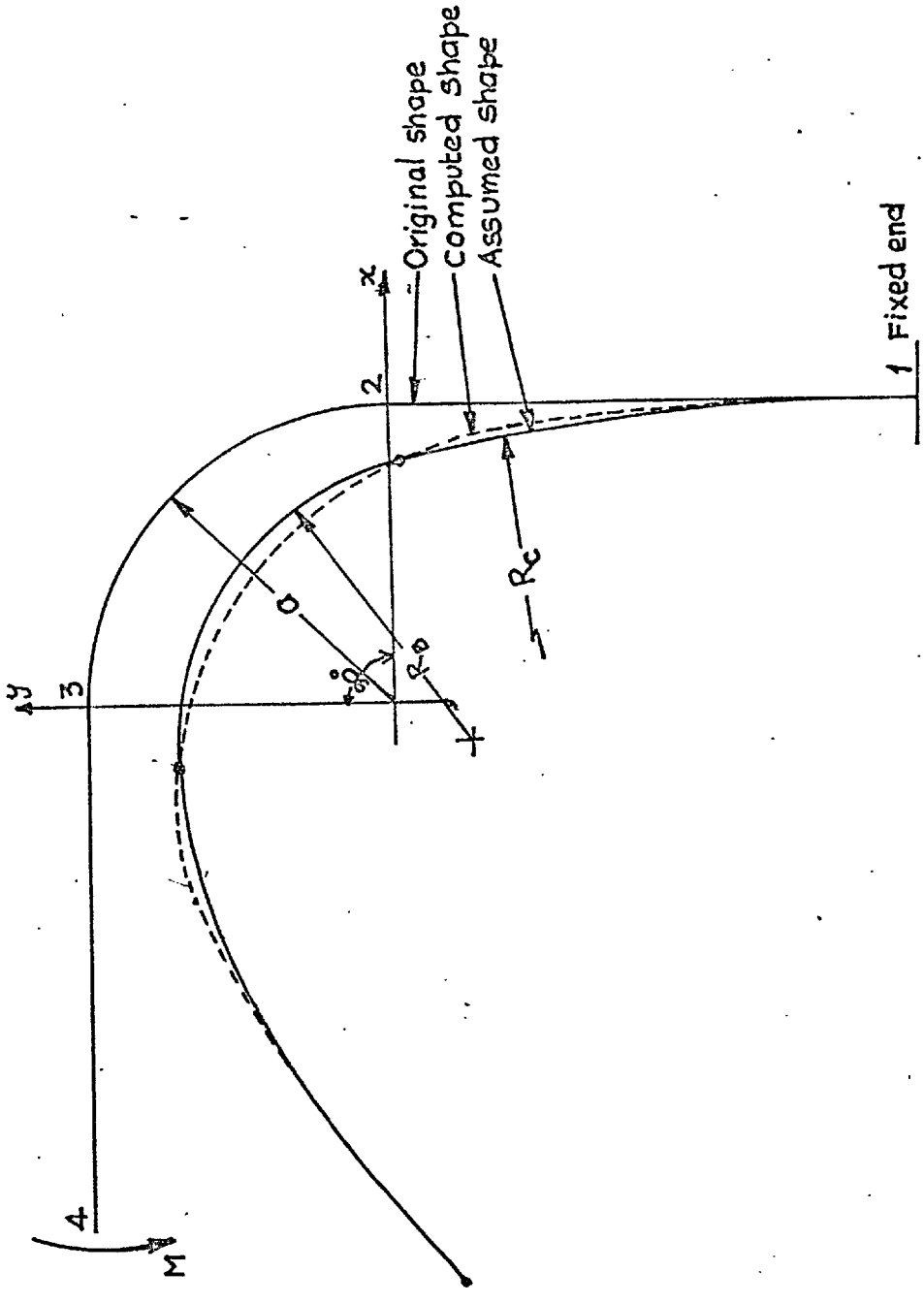



FIG. 6·1· FINITE ELEMENT IDEALISATION OF A PIPE STRUCTURE




FIG·6·2· DEFLECTED SHAPES OF THE PIPE STRUCTURE (NOT TO SCALE)

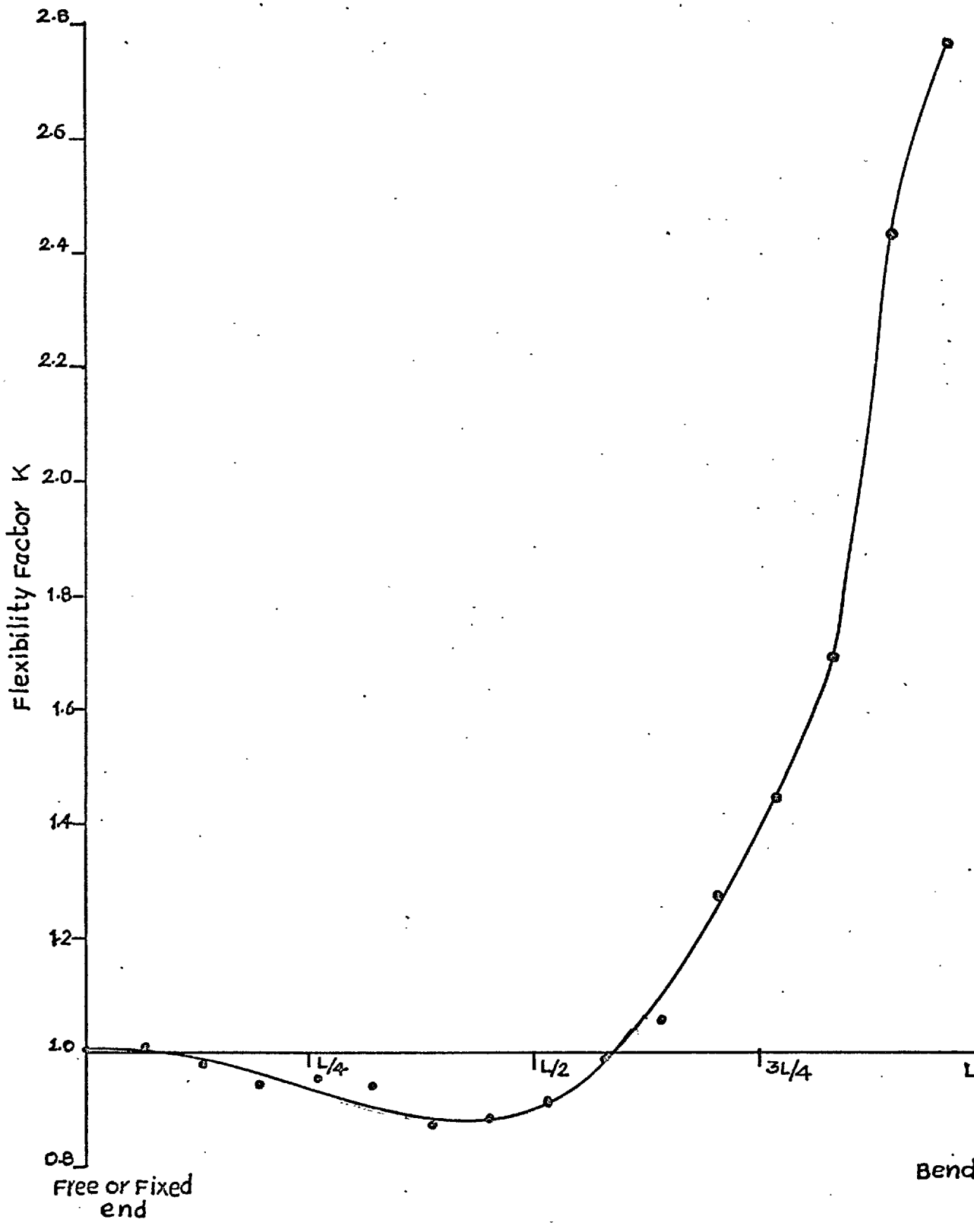



FIG. 6.3. VARIATION OF FLEXIBILITY FACTOR ALONG THE LENGTH OF A TANGENT PIPE

$\lambda = 0.1458$ , $\gamma = 0.538$ , $L = 32.0$

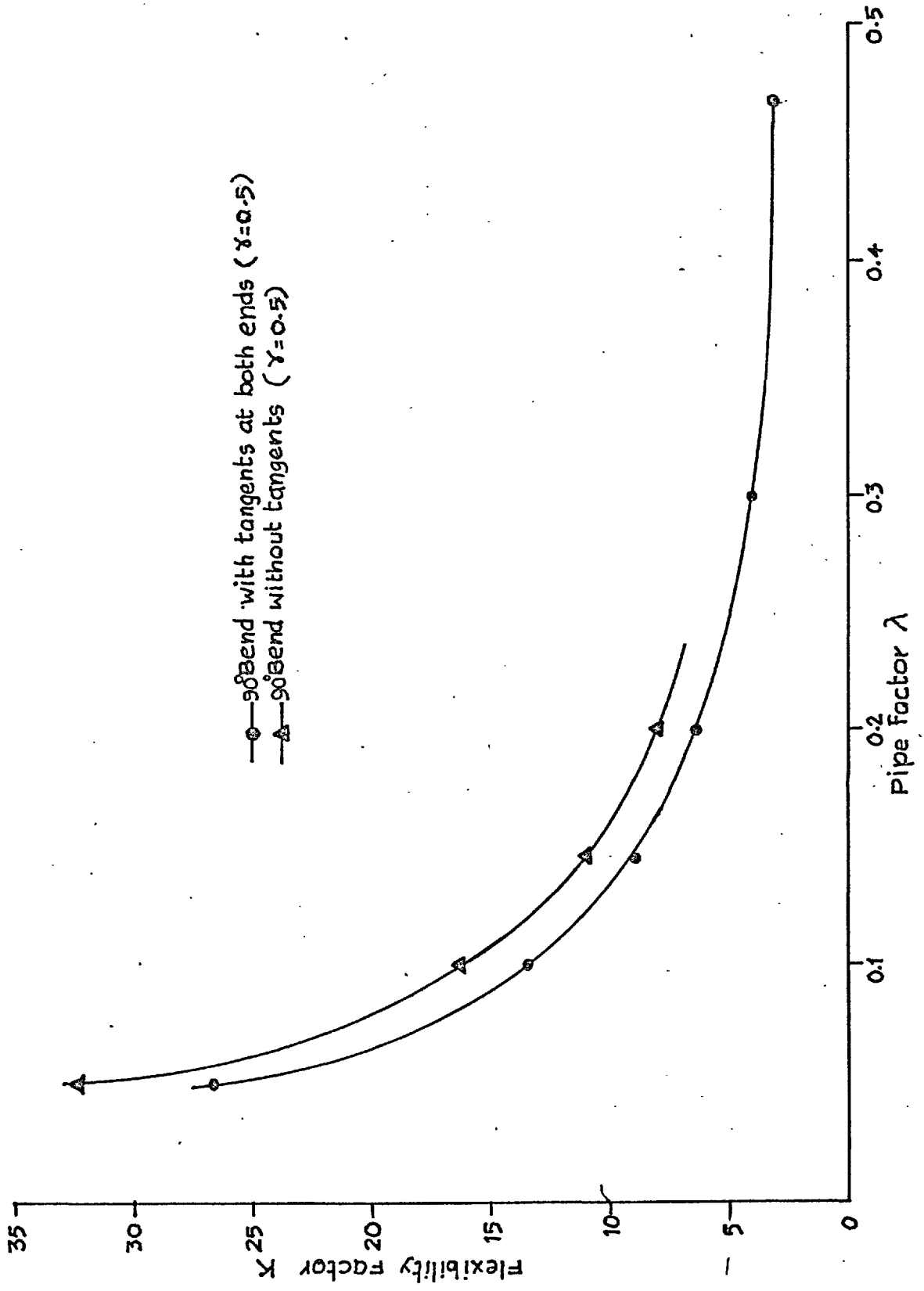



FIG. 6.4 · FLEXIBILITY FACTORS

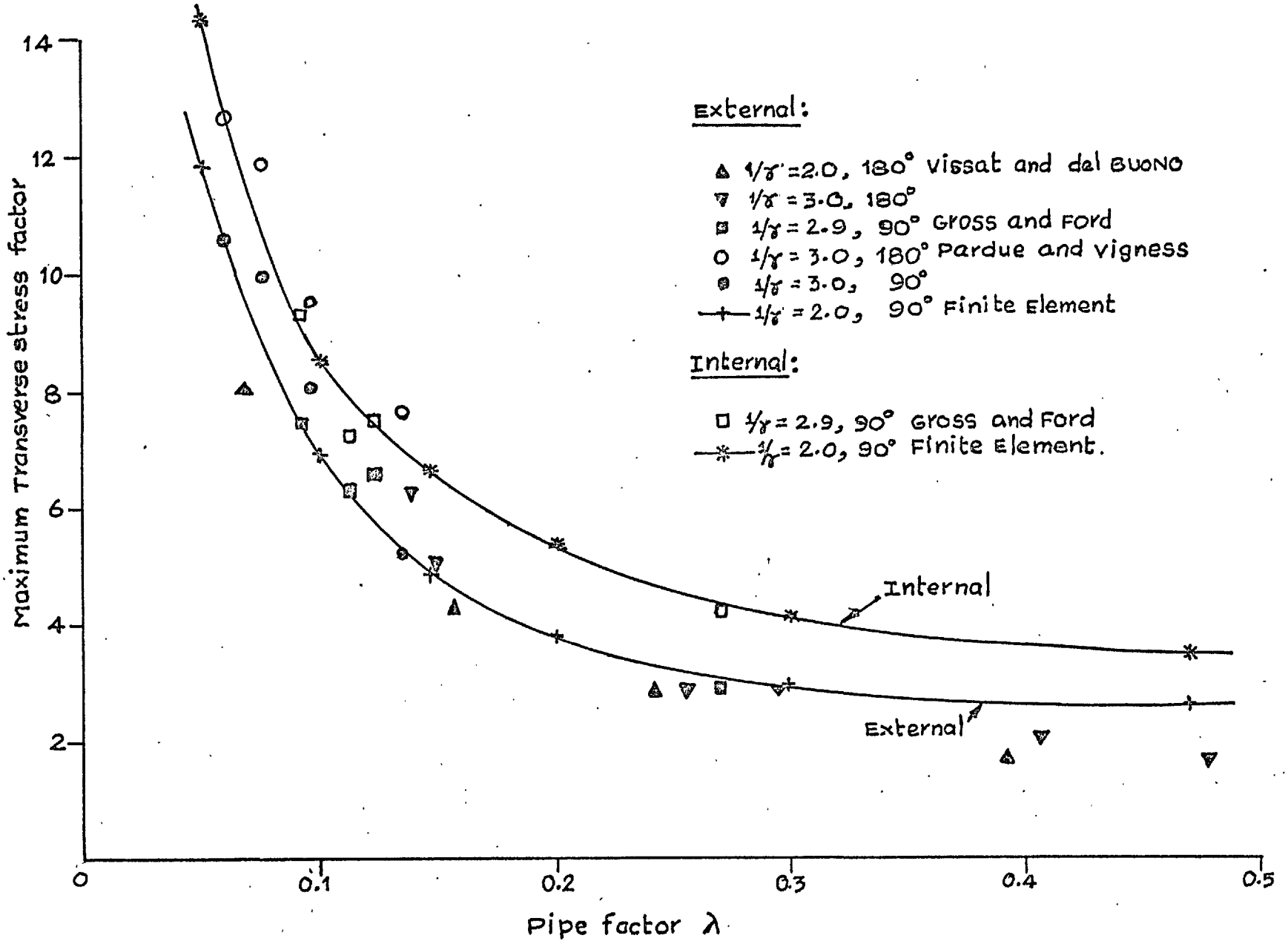



FIG. 6.5. MAXIMUM TRANSVERSE STRESS FACTORS

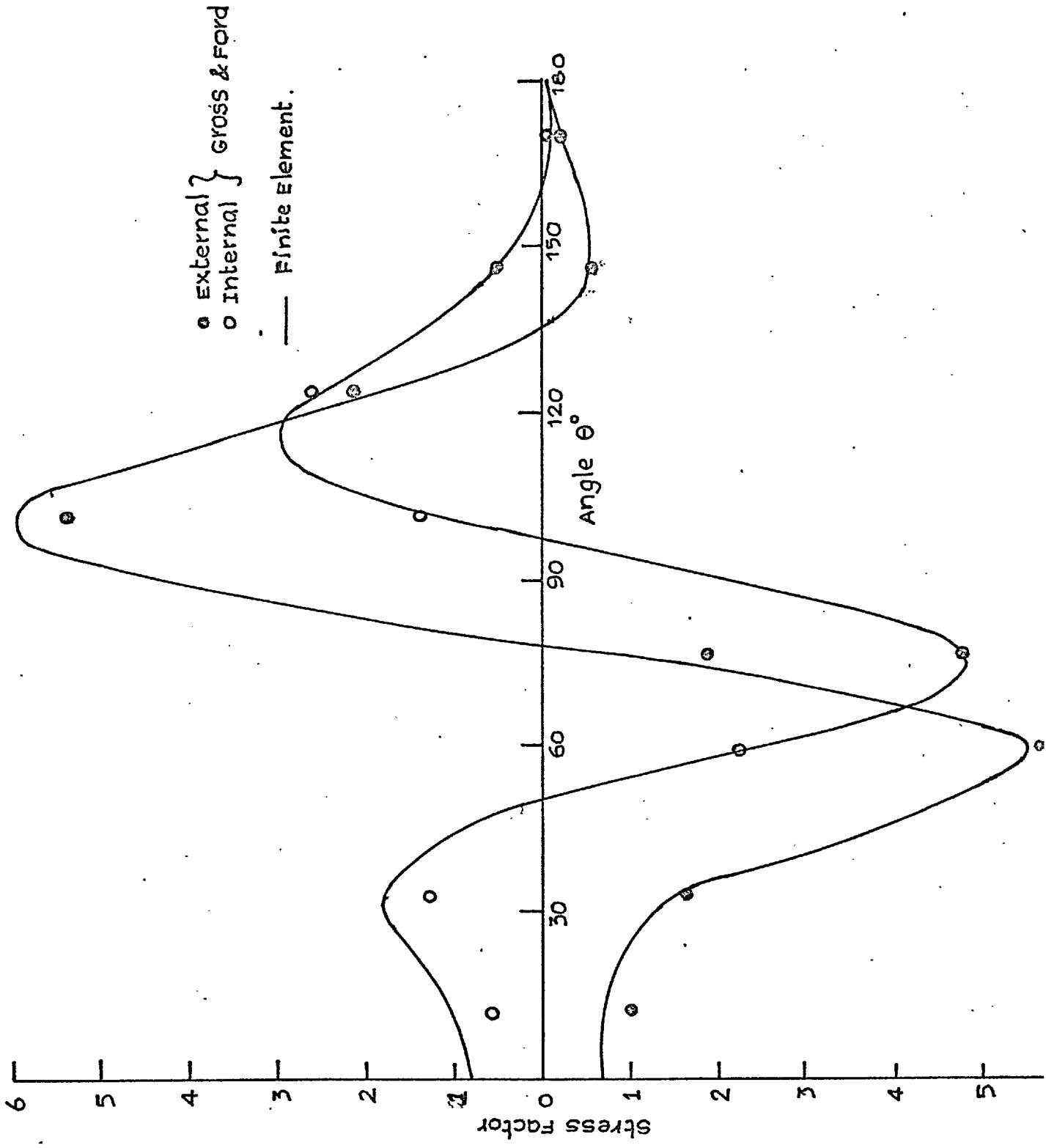



FIG. 6.6 - LONGITUDINAL STRESS FACTORS

$\lambda = 0.0924$ , $\gamma = 0.344$

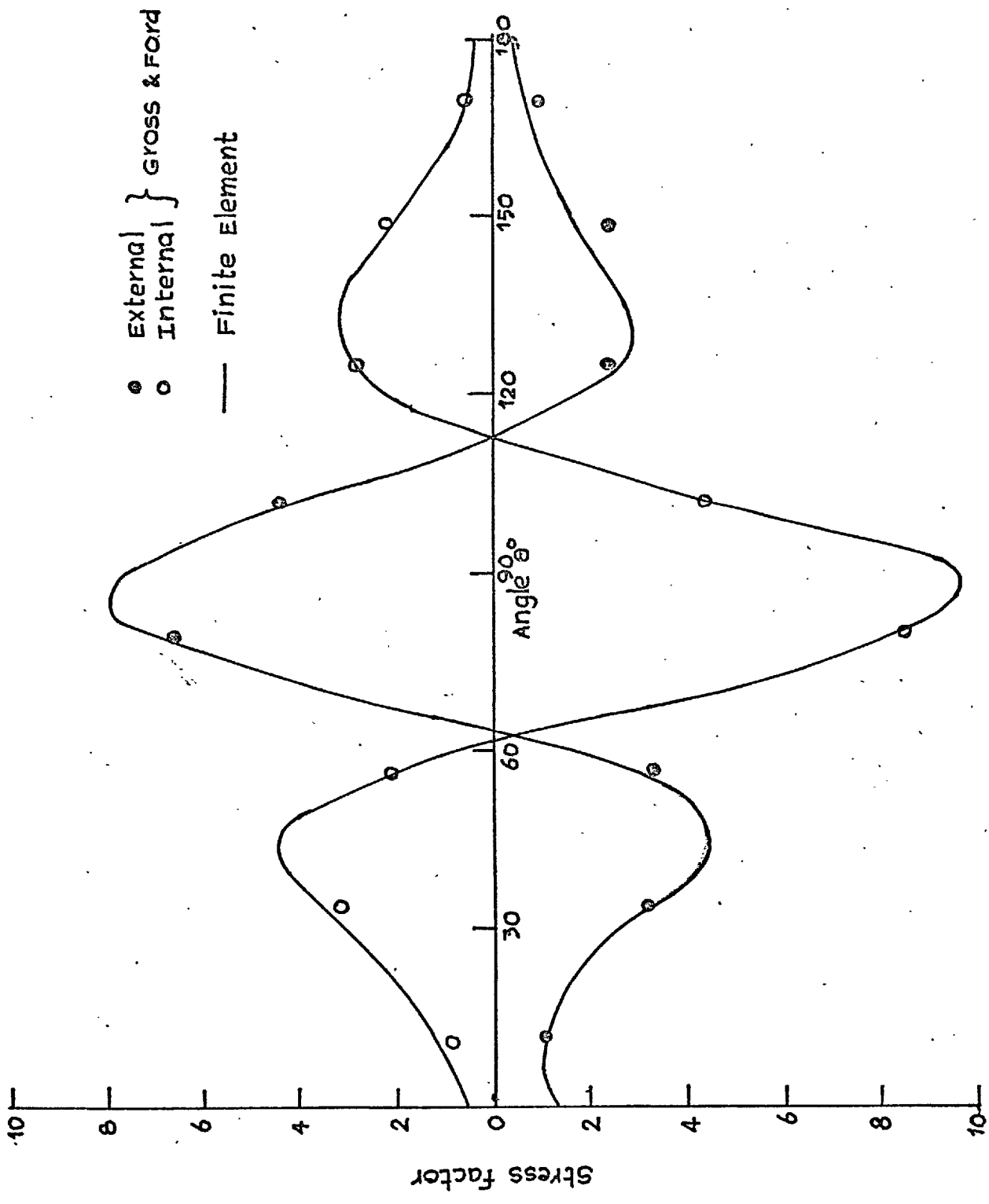



FIG. 6·7. CIRCUMFERENTIAL STRESS FACTORS

$\lambda = 0.0924$ , $\gamma = 0.344$

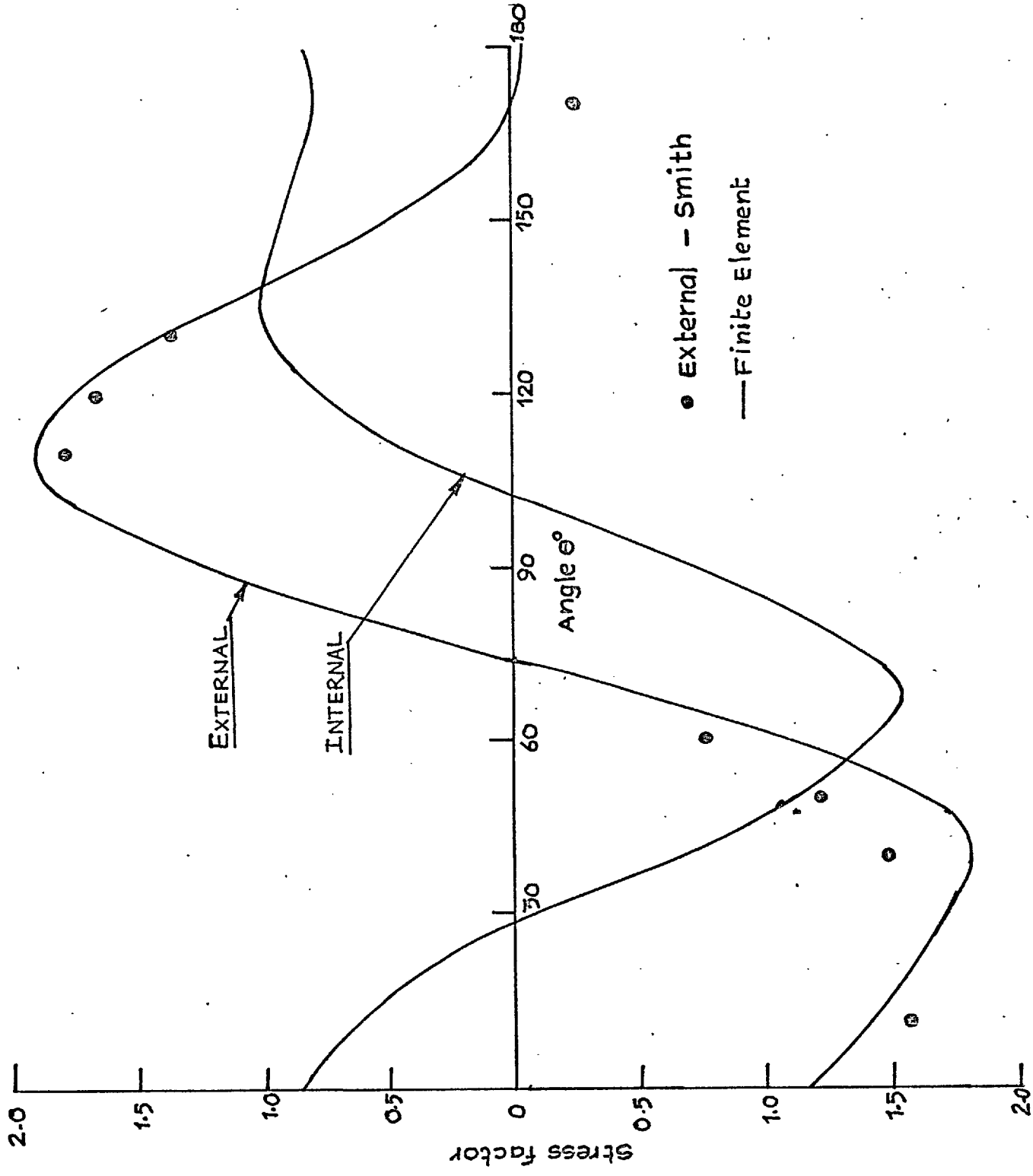



FIG. 6.8. LONGITUDINAL STRESS FACTORS

$\lambda = 0.468$, $\gamma = 0.168$

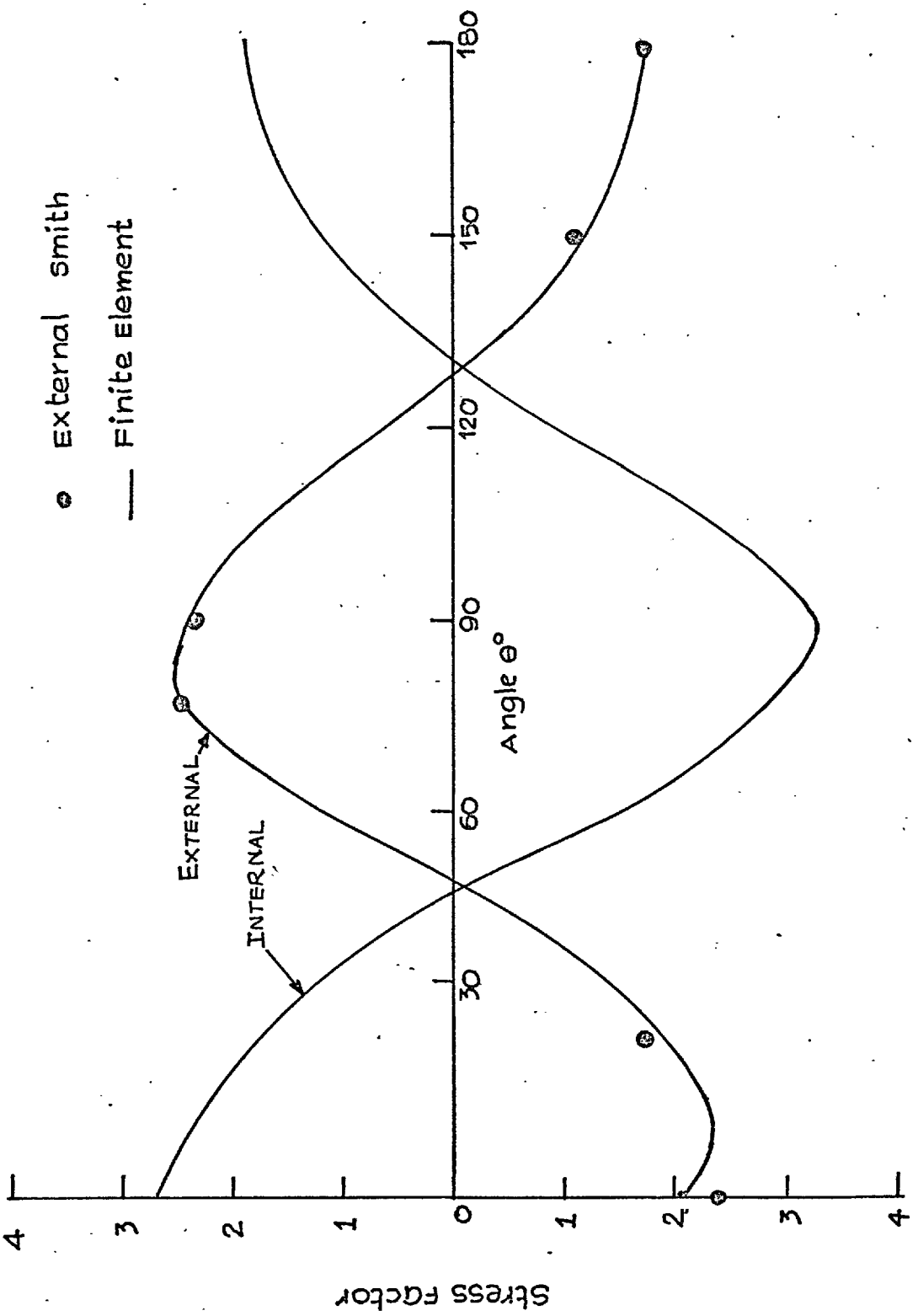



FIG. 6.9. CIRCUMFERENTIAL STRESS FACTORS

$\lambda = 0.468$, $\gamma = 0.168$

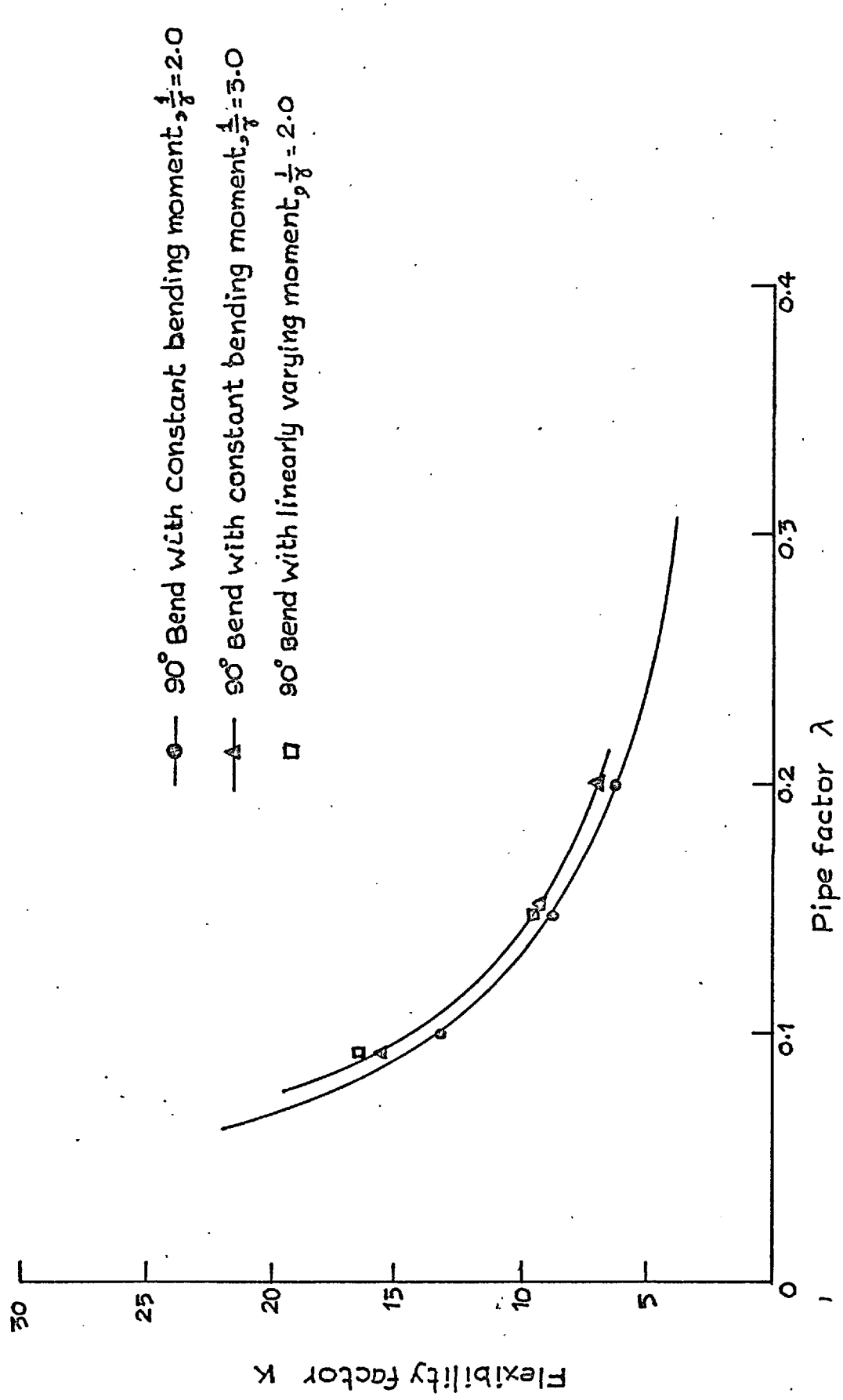



FIG. 6.10. FLEXIBILITY FACTORS

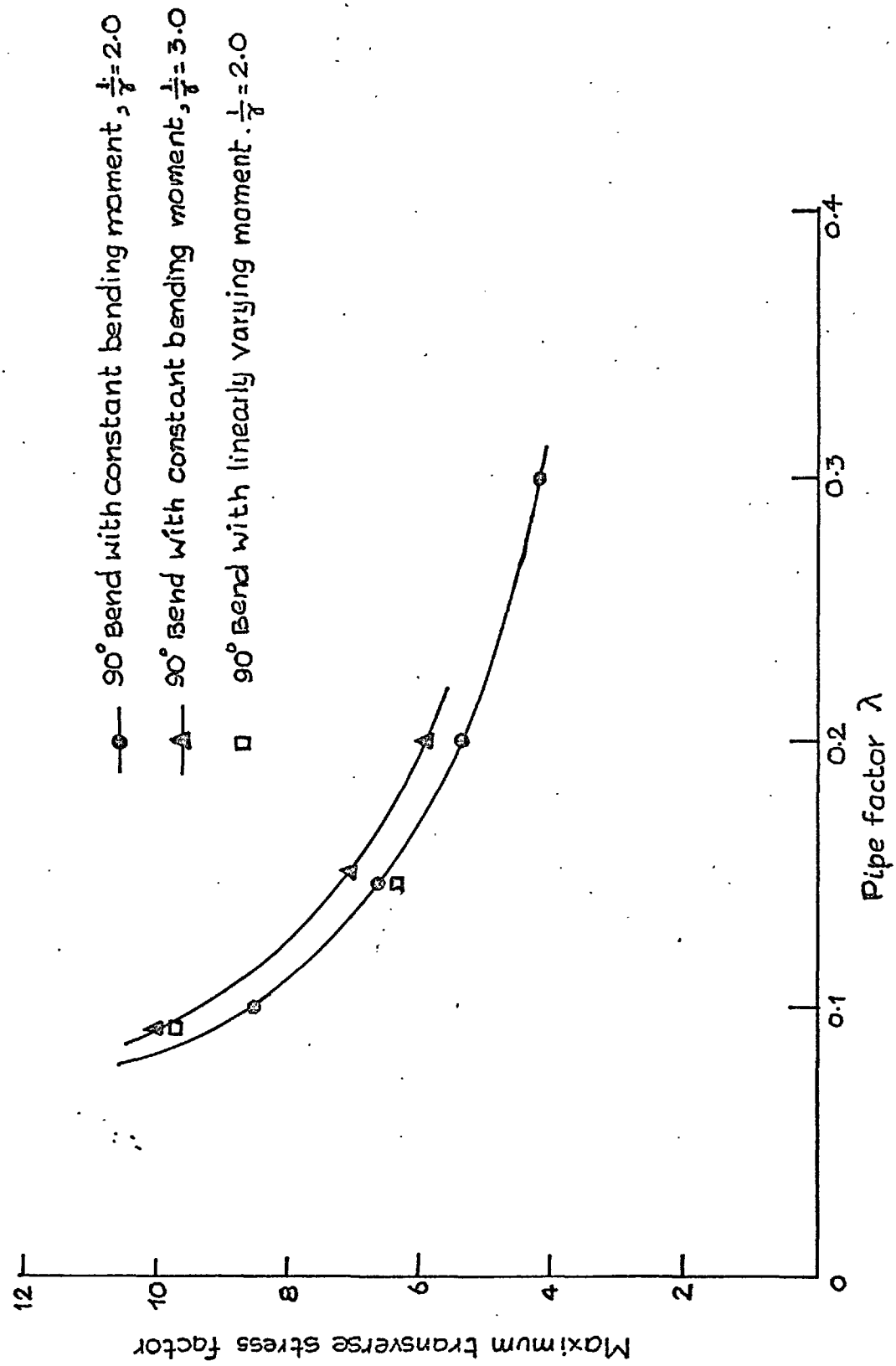



FIG. 6.11. MAXIMUM TRANSVERSE STRESS FACTORS

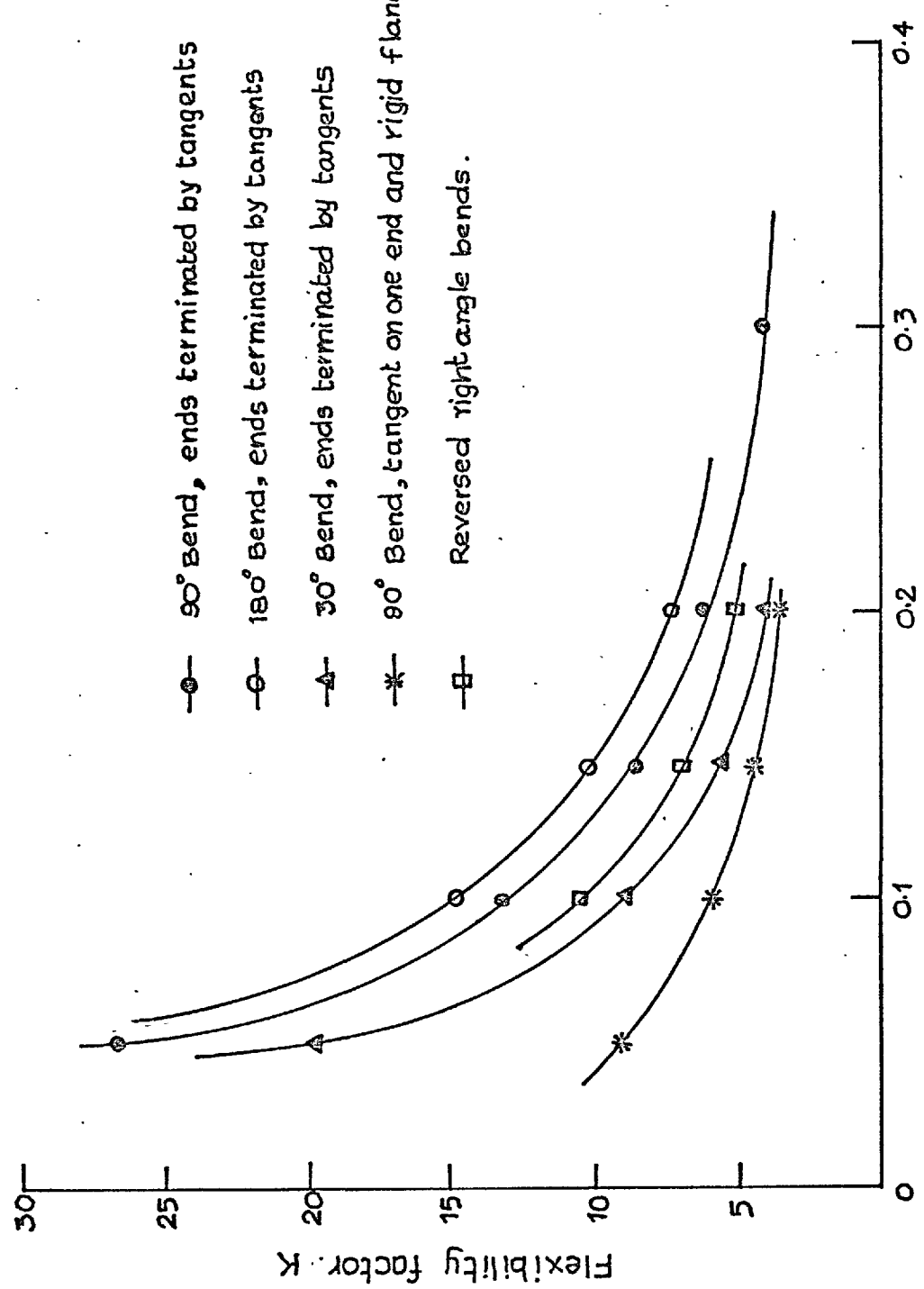



FIG. 6.12. FLEXIBILITY FACTORS

$\gamma = 0.5$

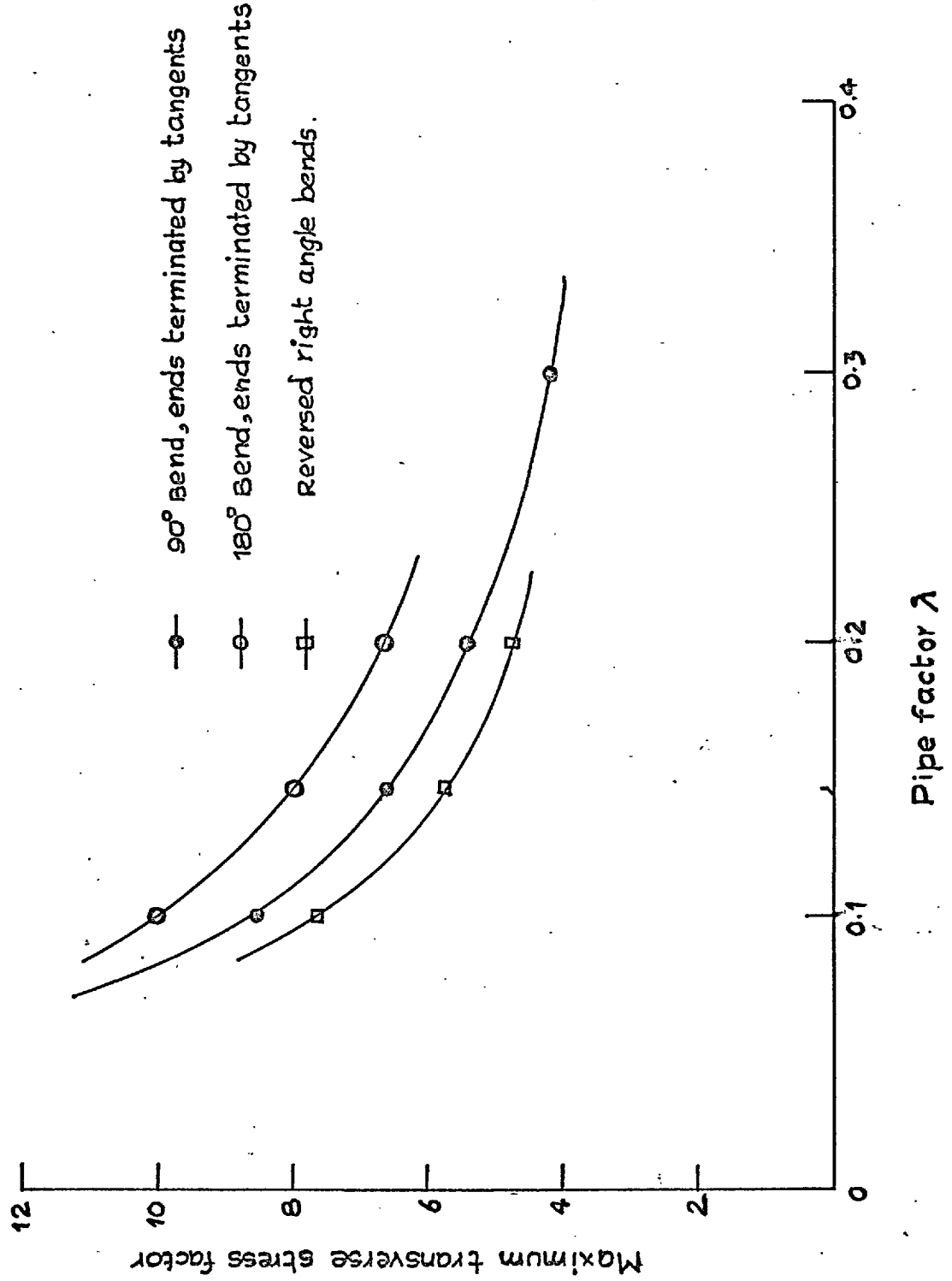



FIG. 6.13. MAXIMUM TRANSVERSE STRESS FACTORS

$\gamma = 0.5$

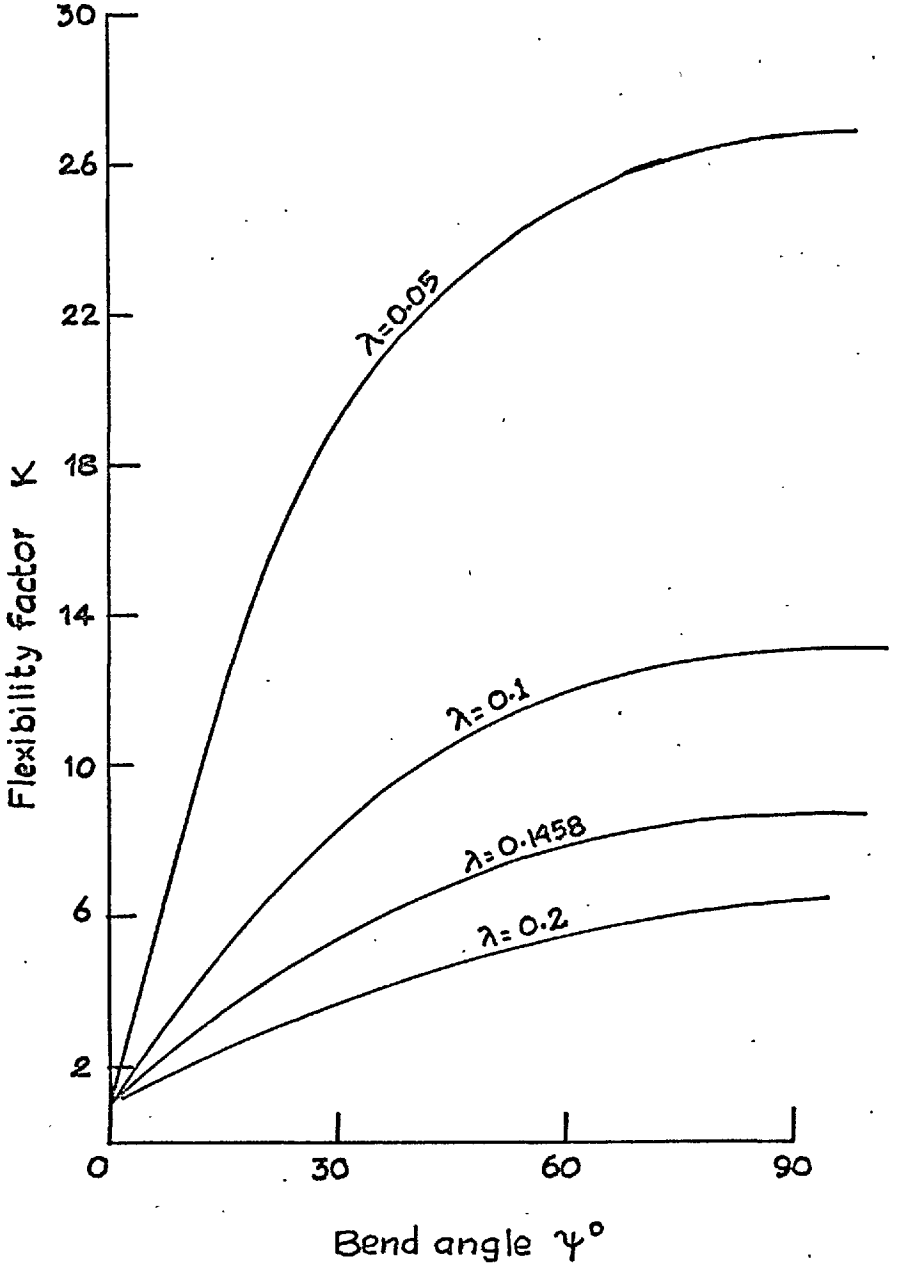



FIG. 6.14. FLEXIBILITY FACTORS

$\delta = 0.5$

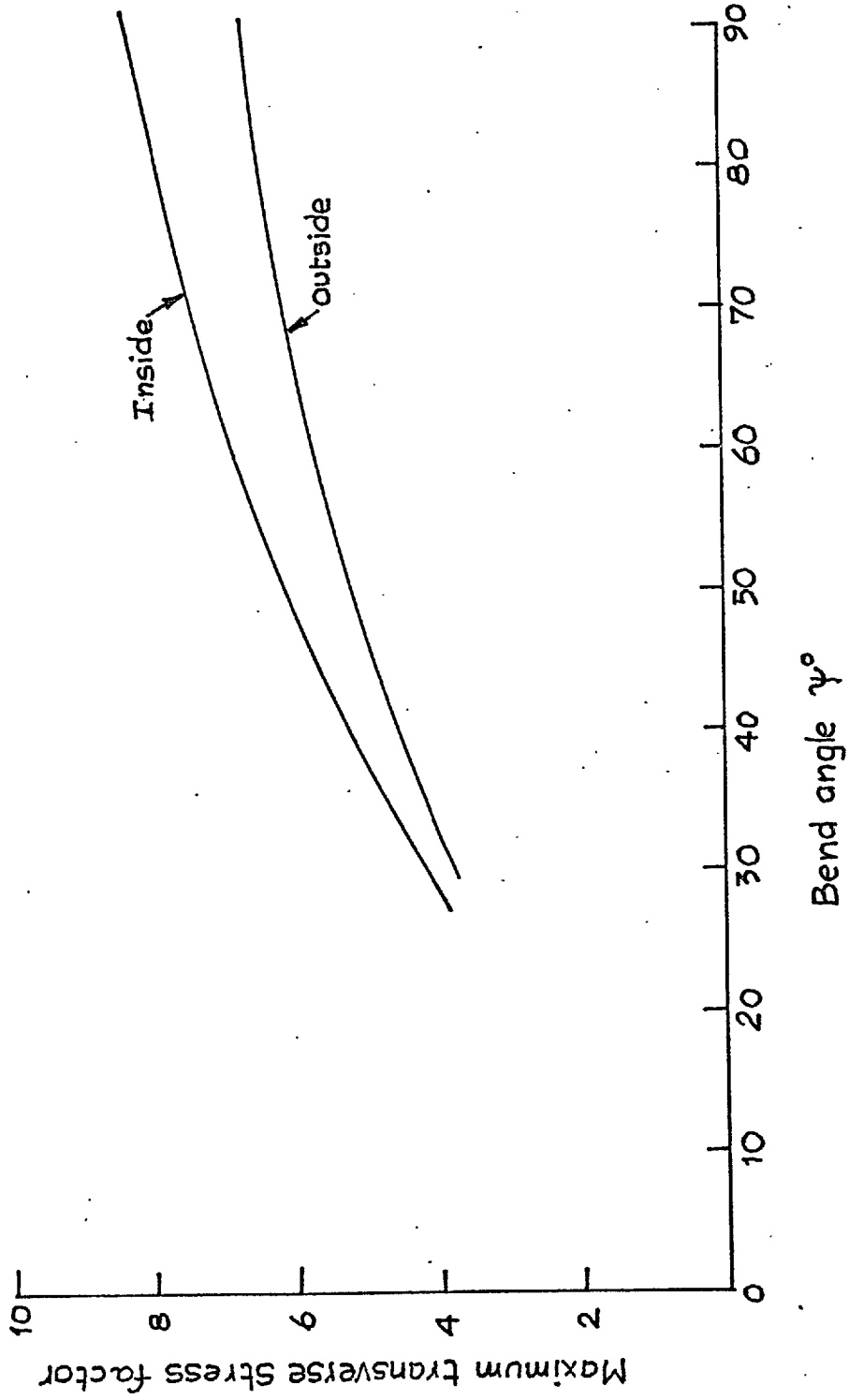



FIG. 6.15. MAXIMUM TRANSVERSE STRESS FACTORS

$\lambda = 0.1$, $\gamma = 0.5$

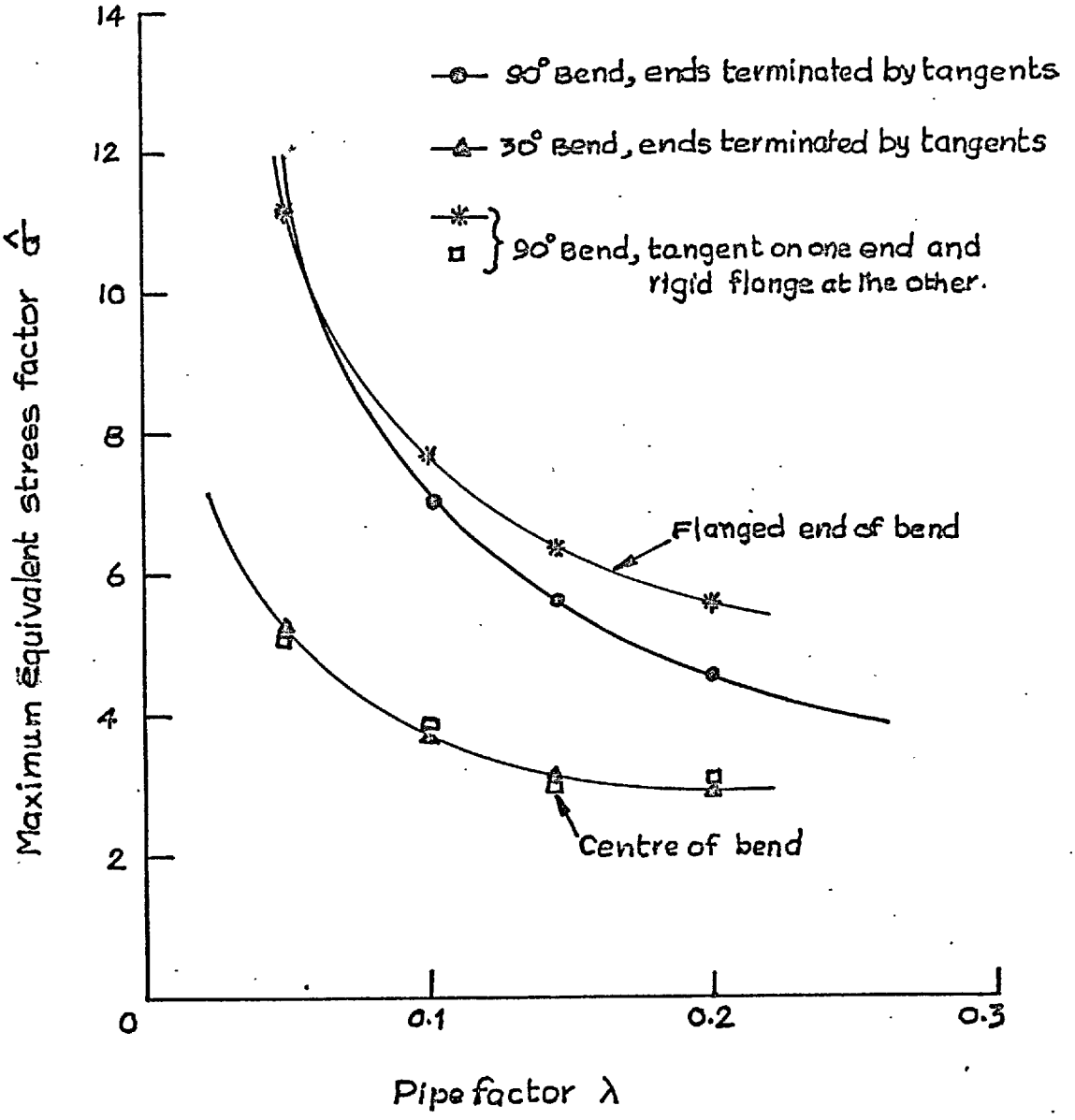



FIG. 6·16. MAXIMUM EQUIVALENT STRESS FACTORS

$\gamma = 0.5$

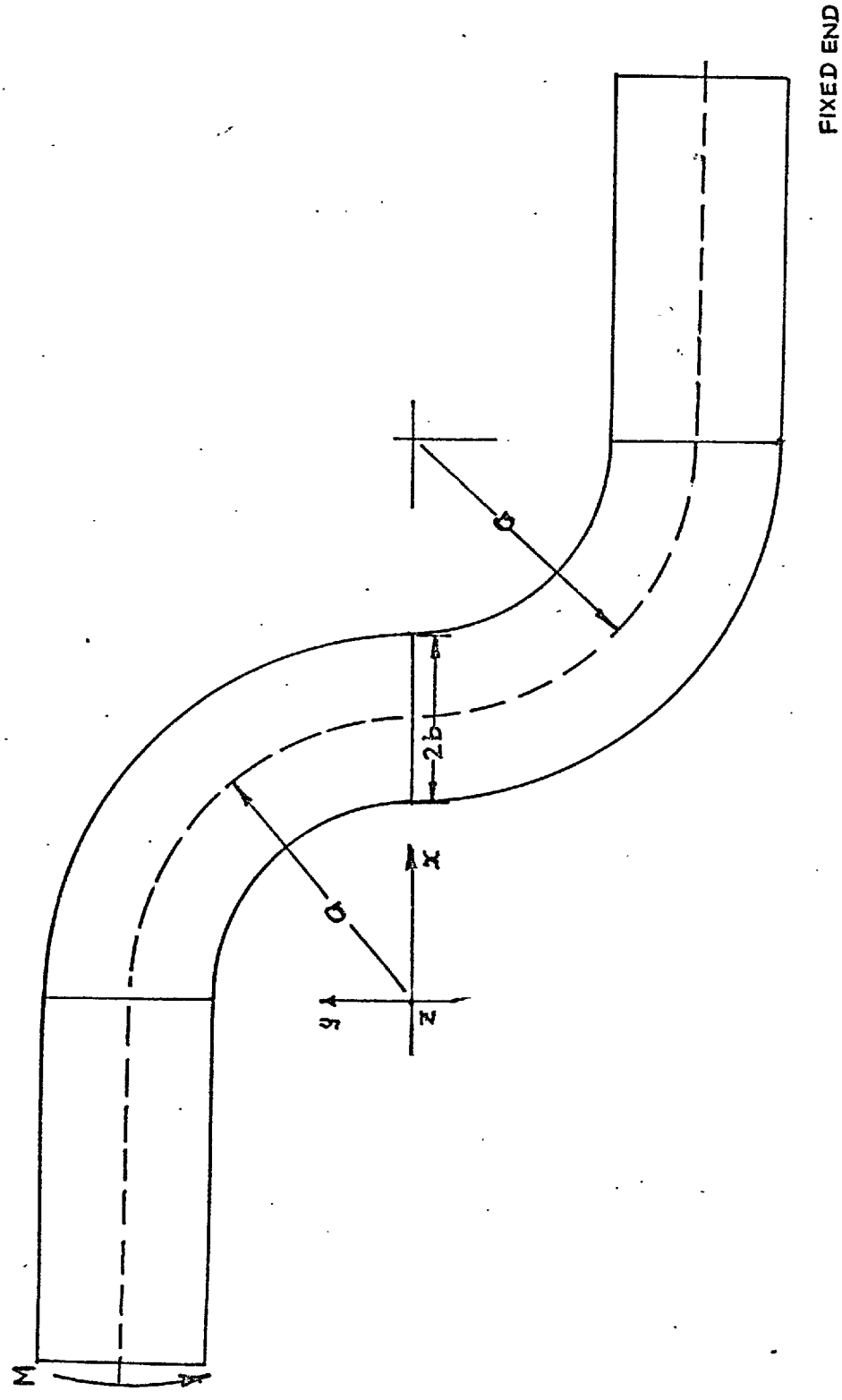



FIG. 6.17. REVERSED 90 DEG-BENDS

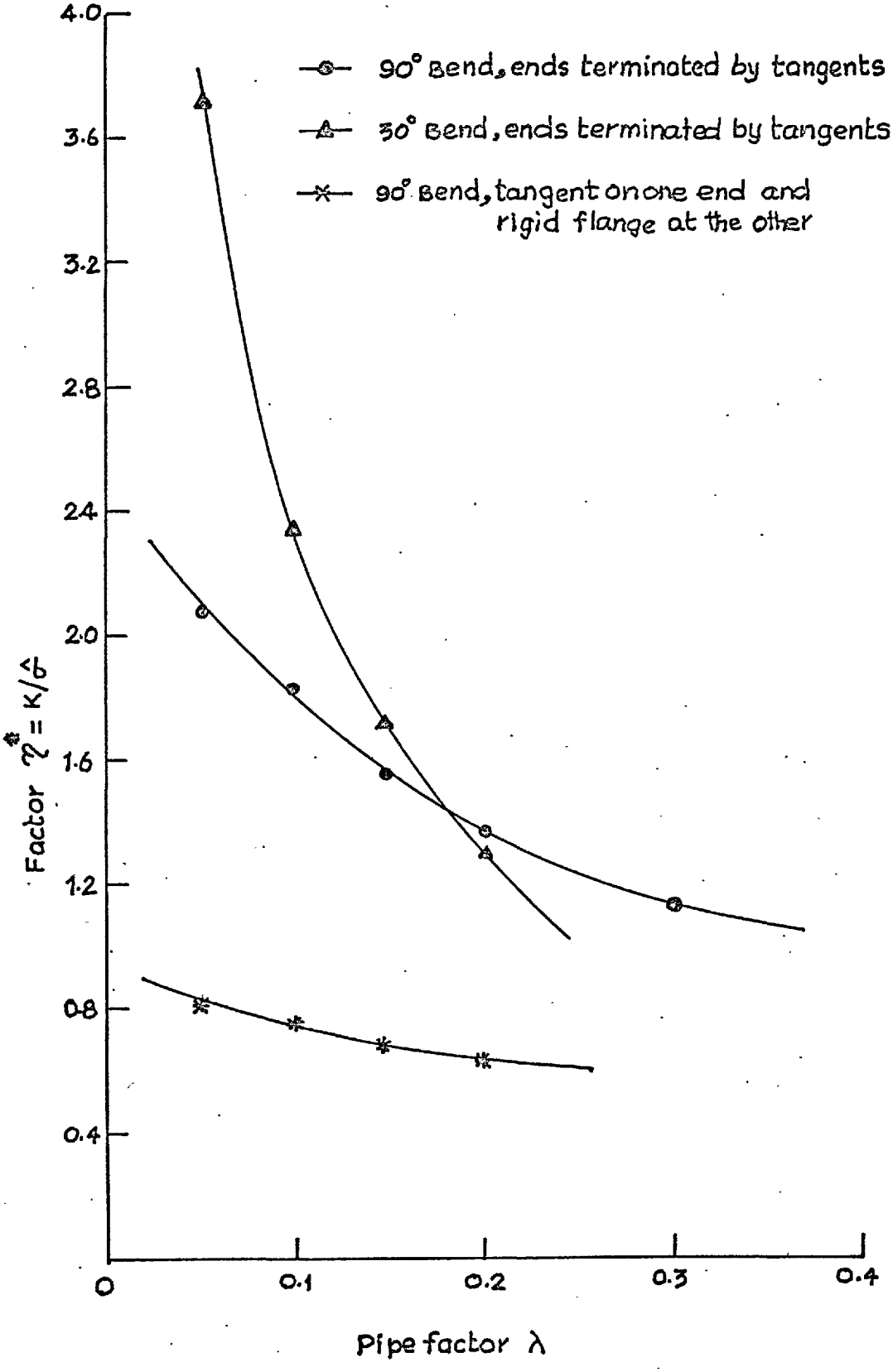
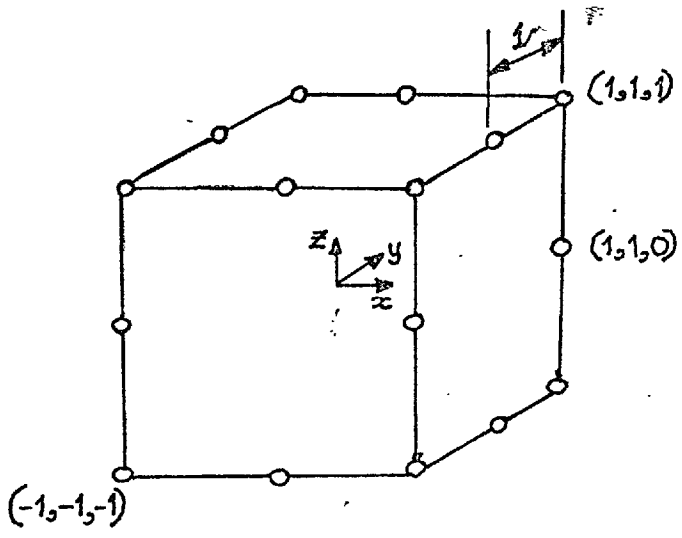
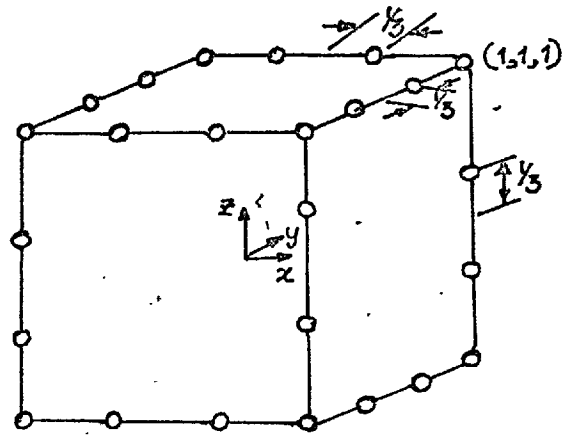



FIG. 6.18. $\eta^*$ FACTOR FOR PIPE BENDS

$\gamma = 0.5$

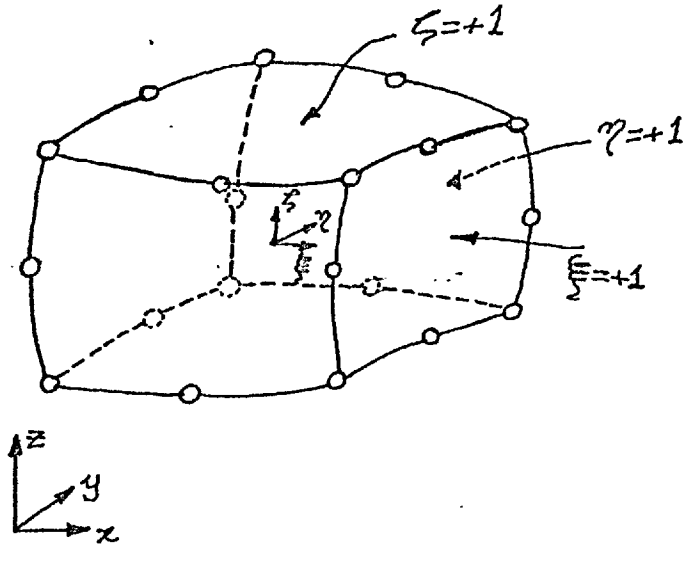



(a) Parabolic

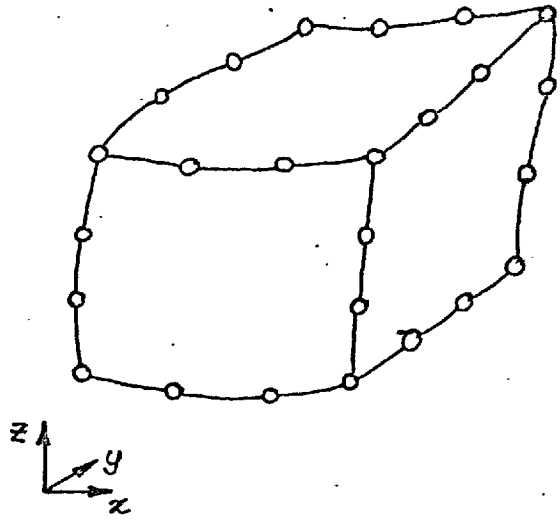



(b) Cubic

FIG. A1. PARENT THREE DIMENSIONAL ELEMENTS

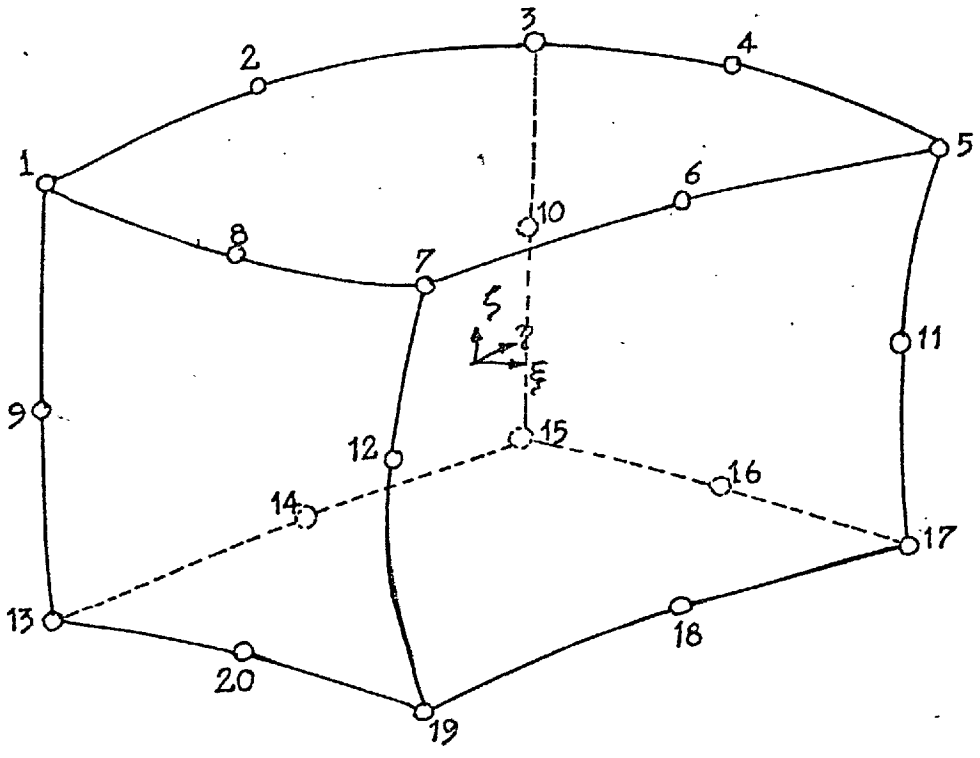



(a) Parabolic

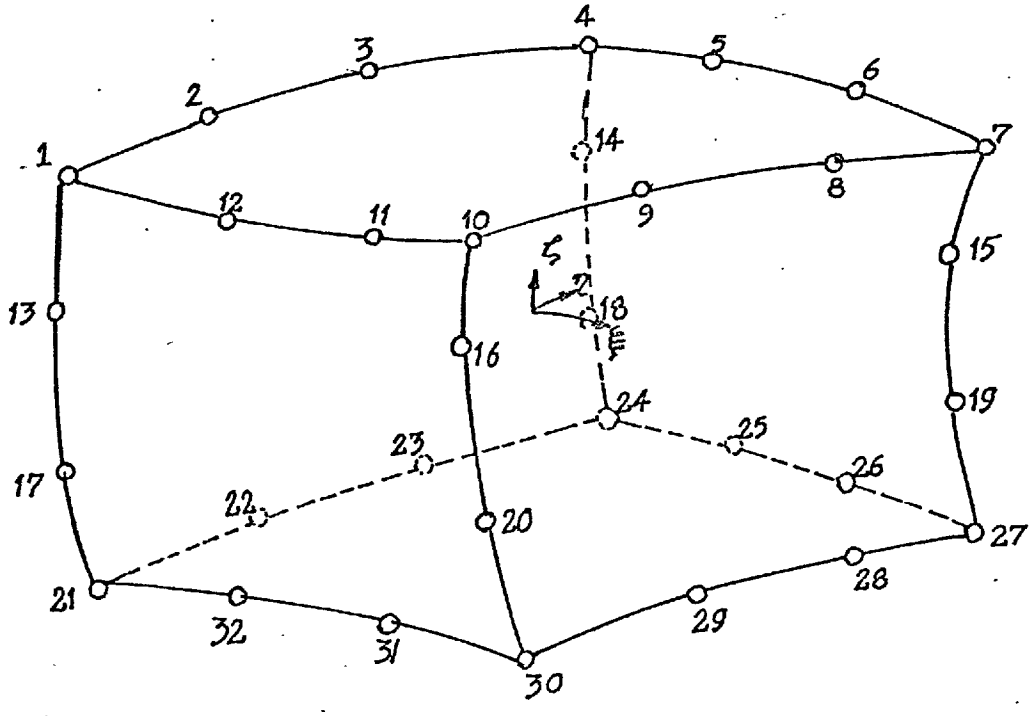



(b) Cubic

FIG. A2. CURVED THREE DIMENSIONAL ELEMENTS




Parabolic




CUBIC

FIG-A3. NUMBERING NODES OF THREE DIMENSIONAL ELEMENTS